

Published in Journals: Processes, Sustainability
and Toxics

Topic Reprint

Environmental and Health Issues and Solutions for Anticoccidials and other Emerging Pollutants of Special Concern

Edited by

Avelino Núñez-Delgado, Elza Bontempi, Yaoyu Zhou,
Esperanza Álvarez-Rodríguez, Maria Victoria López Ramón,
Mario Coccia, Zhien Zhang, Vanesa Santás-Miguel and Marco Race

mdpi.com/topics



Environmental and Health Issues and Solutions for Anticoccidials and other Emerging Pollutants of Special Concern

Environmental and Health Issues and Solutions for Anticoccidials and other Emerging Pollutants of Special Concern

Editors

Avelino Núñez-Delgado

Elza Bontempi

Yaoyu Zhou

Esperanza Álvarez-Rodríguez

Maria Victoria López Ramón

Mario Coccia

Zhien Zhang

Vanesa Santás-Miguel

Marco Race



Editors

Avelino Núñez-Delgado
University of Santiago de
Compostela
Lugo
Spain

Elza Bontempi
University of Brescia
Brescia
Italy

Yaoyu Zhou
Hunan Agricultural
University
Changsha
China

Esperanza Álvarez-Rodríguez
University of Santiago de
Compostela
Lugo
Spain

Maria Victoria López Ramón
University of Jaén
Jaén
Spain

Mario Coccia
National Research Council of
Italy (CNR)
Turin
Italy

Zhien Zhang
The Ohio State University
Columbus, OH
USA

Vanesa Santás-Miguel
University of Vigo
Vigo
Spain

Marco Race
University of Cassino and
Southern
Cassino
Italy

Editorial Office

MDPI AG
Grosspeteranlage 5
4052 Basel, Switzerland

This is a reprint of articles from the Topic published online in the open access journals *Processes* (ISSN 2227-9717), *Toxics* (ISSN 2305-6304), and *Sustainability* (ISSN 2071-1050) (available at: <https://www.mdpi.com/topics/O4L25D7LSD>).

For citation purposes, cite each article independently as indicated on the article page online and as indicated below:

Lastname, A.A.; Lastname, B.B. Article Title. <i>Journal Name</i> Year , <i>Volume Number</i> , Page Range.
--

ISBN 978-3-7258-2199-0 (Hbk)

ISBN 978-3-7258-2200-3 (PDF)

doi.org/10.3390/books978-3-7258-2200-3

© 2024 by the authors. Articles in this book are Open Access and distributed under the Creative Commons Attribution (CC BY) license. The book as a whole is distributed by MDPI under the terms and conditions of the Creative Commons Attribution-NonCommercial-NoDerivs (CC BY-NC-ND) license.

Contents

About the Editors vii

Avelino Núñez-Delgado, Elza Bontempi, Yaoyu Zhou, Esperanza Álvarez-Rodríguez, María Victoria López-Ramón, Mario Coccia, et al.
Editorial of the Topic “Environmental and Health Issues and Solutions for Anticoccidials and Other Emerging Pollutants of Special Concern”
Reprinted from: *Processes* **2024**, *12*, 1379, doi:10.3390/pr12071379 1

Samiha Hamdi, Manel Issaoui, Sonia Hammami, Ainoa Míguez-González, Raquel Cela-Dablanca, Ana Barreiro, et al.
Removal of the Highly Toxic Anticoccidial Monensin Using Six Different Low-Cost Bio-Adsorbents
Reprinted from: *Toxics* **2024**, *12*, 606, doi:10.3390/toxics12080606 4

Raquel Cela-Dablanca, Ainoa Míguez-González, Lucía Rodríguez-López, Ana Barreiro, Manuel Arias-Estévez, María J. Fernández-Sanjurjo, et al.
Removal of Cefuroxime from Soils Amended with Pine Bark, Mussel Shell and Oak Ash
Reprinted from: *Processes* **2024**, *12*, 1335, doi:10.3390/pr12071335 27

Xiaoming Zeng, Hao He, Liejiang Yuan, Haizhi Wu and Cong Zhou
Determination of 24 Trace Aromatic Substances in Rosemary Hydrosol by Dispersed Liquid–Liquid Microextraction–Gas Chromatography
Reprinted from: *Processes* **2024**, *12*, 498, doi:10.3390/pr12030498 43

Amer Al-Jokhadar, Yasmine Soudi, Suzanne Abdelmalek, Sarah R. Badran and Yasser Abuhashem
A Study on Sensitivity of Soil-Based Building Mixtures to Biodeterioration by Fungi: Towards Sustainable Earth Structures
Reprinted from: *Sustainability* **2024**, *16*, 1294, doi:10.3390/su16031294 58

Songsong Chen, Yuncai Wang and Limin Ma
Assessing Biodegradation Processes of Atrazine in Constructed Wetland Using Compound-Specific Stable Isotope Analysis
Reprinted from: *Processes* **2023**, *11*, 3252, doi:10.3390/pr11113252 74

Chaoqun Wang, Yongxiang Zhang, Lirong Deng, Mingtao Zhao, Meiqi Liang, Lien-Chieh Lee, et al.
Visualization Network Analysis of Studies on Agricultural Drainage Water Treatment
Reprinted from: *Processes* **2023**, *11*, 2952, doi:10.3390/pr11102952 89

Lingling Li, Yuanyuan Xue, Hengsheng Wang and Yansong Chen
Effects of Chlortetracycline on the Growth of Eggplant and Associated Rhizosphere Bacterial Communities
Reprinted from: *Sustainability* **2023**, *15*, 14593, doi:10.3390/su151914593 107

Jongho Kim, Sujin Kim and Jinwook Chung
Examining the Relationship between Pro-Environmental Attitudes, Self-Determination, and Sustained Intention in Eco-Friendly Sports Participation: A Study on Plogging Participants
Reprinted from: *Sustainability* **2023**, *15*, 11806, doi:10.3390/su151511806 122

Wei Li, Bin Yao, Yuguo Zheng, Guiqiang Zhang, Dan Zhi and Yaoyu Zhou
Efficient Degradation of Chlortetracycline by Graphene Supported Cobalt Oxide Activated Peroxydisulfate: Performances and Mechanisms
Reprinted from: *Processes* **2023**, *11*, 1381, doi:10.3390/pr11051381 **141**

Sanja Vasiljević, Maja Vujić, Jasmina Agbaba, Stefania Federici, Serena Ducoli, Radivoj Tomić and Aleksandra Tubić
Efficiency of Coagulation/Flocculation for the Removal of Complex Mixture of Textile Fibers from Water
Reprinted from: *Processes* **2023**, *11*, 820, doi:10.3390/pr11030820 **154**

About the Editors

Avelino Núñez-Delgado

Avelino Núñez-Delgado, Ph.D., was born in O Barco de Valdeorras (Ourense province, Galicia, Spain). He obtained his Ph.D. at the Department of Soil Science and Agricultural Chemistry, USC, in 1993. Between 1993 and 1996, he worked as a Post-doc Researcher in France (University of Montpellier) and Spain (USC), at the end of which he became a Professor in the Department of Soil Science and Agricultural Chemistry, Engineering Polytechnic School, Campus Lugo, University of Santiago de Compostela (USC), Spain, a position which he continues to hold to this day. He holds nine patents, has won several research awards, and has more than 400 publications to his name to date (July 2024), around 200 of which are in D1 and Q1 JCR journals. He has served as the principal investigator and/or a collaborator of more than 40 research projects. He is listed among the top 2% of world researchers by the Stanford ranking system and among the world's top researchers by Researchgate, Expertscape, Web of Sciences, Scopus, and other world research classifications. Currently, he is collaborating with a variety of research teams from various countries around the world. He is a Book Editor for Springer Nature, Elsevier, and other top scientific publishers. He is a Book Series Editor for Springer Nature, an Editor for various top research journals (covering roles such as Chief Editor, Associate Editor, Special Issue Editor, Managing Guest Editor, and Guest Editor), and a Reviewer for national and international research projects.

Elza Bontempi

Elza Bontempi holds a permanent position at the University of Brescia, where she is currently a Full Professor teaching courses on the Fundamentals of Chemistry for Technology. She is responsible for the research line concerning eco-materials at the Chemistry for Technologies Laboratory. She has been responsible for several national and international research projects developing new technologies and sustainable materials from waste and by-products. In recent years, her scientific activity has focused on the recovery of critical raw materials from exhausted batteries, such as lithium and cobalt, in the context of the circular economy. She is the author of more than 300 peer-reviewed papers and several patents in the field of material recovery. She is included in the list of Unstoppable Women (the 1000 women who are changing Italy) and Top Italian Scientists in the field of natural and environmental sciences, as well as in the list of 100 female STEM (Science, Technology, Engineering and Mathematics) experts.

Yaoyu Zhou

Dr. Yaoyu Zhou is a Full Professor at the College of Environment and Ecology at Hunan Agricultural University, Changsha, Hunan province, China.

Prof. Zhou's academic background covers waste management and the decontamination of aqueous effluents. Prof. Zhou also has experience in fundamental soil science and the remediation of various contaminants in soils and sediments. Prof. Zhou is listed on Stanford's list of the top 2% of scientists in the world (2020). Together with some of his graduate students and colleagues, Prof. Zhou has published more than 220 academic papers, 23 of which were ranked as ESI top papers (17 nominated as "Highly Cited Papers" and 8 nominated as "Hot Papers"). After being supported by the Hong Kong Scholar Program, Prof. Zhou worked at the Hong Kong Polytechnic University from 2018 to 2020. He also holds some international positions: he is a Member of the Editorial Board of *Environmental Technology*, *Carbon Research*, and *Biochar* and a Guest Editor of the *Journal of*

Environmental Management (JCR Q1, New Research on Soil Degradation and Restoration) and *Science of the Total Environment* (JCR Q1, Antibiotics and Heavy Metal; JCR Q1, BEEM conference 2019).

Esperanza Álvarez-Rodríguez

Esperanza Álvarez-Rodríguez is a Full Professor in the Department of Soil Science and Agricultural Chemistry at the University of Santiago de Compostela. She is the leader of the research group Sustainable Environmental and Forest Management Unit (UXAFORES). Her research focuses on the study of aluminum toxicity, the recovery of mine tailings, contamination by heavy metals, contamination by antibiotics used in human and veterinary medicine, and the use of waste materials as bioadsorbents for these contaminants. He has served as the principal investigator and/or a collaborator of more than 50 research projects, 17 of which are international, and more than 90 contracts with companies. She has published more than 300 articles, 165 of which are included in the JCR, and several book chapters. She was one of the editors of the book *The Environment in Galicia: A Book of Images*, Springer; Guest Editor of the journals *Environmental Science and Pollution Research* and the *Spanish Journal Soil Science*; and Associate Editor of this latter journal. She collaborates with various international research groups and is currently supervising six doctoral theses with these international teams.

Maria Victoria López Ramón

María Victoria López Ramón is a Full Professor at the Department of Inorganic and Organic Chemistry at the University of Jaén (Spain). She has served as a postdoctoral researcher at the University of Cambridge (UK) and a visiting professor at the Université de Neuchâtel (Switzerland). She is the leader of the Researcher Group in Carbon Materials and Environmental Applications RNM366. To date, she has participated in 17 research projects and has served as the principal investigator of eight of them. She has more than 80 publications to her name in journals with the highest Impact Factor in this area, six book chapters, and one book, as well as numerous communications at international and national conferences and meetings. Her research background is focused on the chemistry of solid surfaces and interfaces, carbon materials as adsorbents, and the environmental remediation of water using different advanced oxidation processes. She is currently an evaluator of scientific works in numerous international journals and an evaluator of national and international research projects. She has served as the Guest Editor of special issues for the journals *Catalyst*, *Nanomaterials*, *Environmental Research*, and *Processes*. She currently holds the position of Vice-President of the Spanish Adsorption Society.

Mario Coccia

Mario Coccia is a social scientist acting as the Research Director of the National Research Council of Italy and as a visiting scholar at Arizona State University (USA). He has served as a researcher at the Max Planck Institute of Economics and a visiting professor at the Polytechnic University of Torino and the University of Piemonte Orientale (Italy). He has carried out scientific research at the Georgia Institute of Technology, Yale University, UNU—Maastricht Economic and Social Research Institute on Innovation and Technology (United Nations University—MERIT), RAND Corporation (Washington D.C.), University of Maryland (College Park), Bureau d'Économie Théorique et Appliquée (Strasbourg, France), Munk School of Global Affairs (University of Toronto, Canada), and the Institute for Science and Technology Studies (University of Bielefeld, Germany). He conducts his investigations via statistical analyses, models, experiments, and observational studies with an interdisciplinary scientific perspective in order to explain the evolutionary properties of

science and technology in society, emerging research fields, and related scientific development, new technological trajectories, processes of coevolution between technologies, and the measurement of scientific and technological advances over time and space. He is a member of the editorial board of many international journals, and his research publications include more than 350 international papers covering several disciplines.

Zhien Zhang

Zhien Zhang is currently a Visiting Scientist at the University of Cincinnati. Prior to this position, he was a Research Assistant Professor at West Virginia University and a Senior Researcher at Ohio State University. His research interests are in the following areas: carbon capture, utilization, and storage (cCuS); gas separation; absorption; membranes; gas hydrate; process modeling and simulation; and optimization. To date, he has published more than 120 peer-reviewed journal articles, 20 journal editorials, two books, and six book chapters (h-index of 53) and has been invited to and delivered more than 30 talks and seminars. He is an Editor of journals such as *Applied Energy*, *Environmental Chemistry Letters*, *Gas Science and Engineering*, and *Chemical Papers* and serves as a committee member of several international conferences. He was recognized as a Highly Cited Researcher by Clarivate in 2021 and 2022.

Vanessa Santás-Miguel

Vanessa Santás-Miguel graduated in Environmental Sciences at Vigo University. In 2022, she obtained her PhD with a thesis entitled "Impact of tetracyclines on microbial communities in agricultural soils". Since 2022, she has worked as a postdoctoral researcher for Vigo University (Spain) and is currently visiting Lund University. Her research interests include the following areas: microbial ecology, soil pollution, antibiotics, heavy metals, and bioremediation. She has been an editorial board member of the *Spanish Journal of Soil Science* since 2022 and served as an editorial board member of the *International Journal of Environmental Research and Public Health* from 2022 to 2023. In addition, she has served as a Guest Editor of *Materials* (Green Biosorbents: Synthesis, Characterization and Application for the Removal of Contaminants from Water and Soil), and at present, she serves as a Guest Editor of *Agriculture* (Soil Amendment and Pollution Remediation: Creating a Better Soil Environment for Future Agricultural Sustainable Production). To date, she has published 40 articles in peer-reviewed journals and four book chapters (h-index of 13).

Marco Race

Marco Race was born in Napoli, Italy, graduated with an M.Sc. in Environmental Engineering at the Università degli Studi di Napoli Federico II in May 2012, and obtained his Ph.D. in Environmental Systems Analysis at UNINA in 2016. Since 2022, he has been an Associate Professor at the University of Cassino. His main research fields concern the treatment of waste or wastewater treatment, the remediation of soil and groundwater, novel contaminant (bio)monitoring and risk assessment approaches, and trace metals and organics in biogeochemical cycles. He is the author of more than 100 papers published in international journals, conference proceedings, and books chapters. He obtained an international award for his work on soil reclamation.

Editorial

Editorial of the Topic “Environmental and Health Issues and Solutions for Anticoccidials and Other Emerging Pollutants of Special Concern”

Avelino Núñez-Delgado ^{1,*}, Elza Bontempi ², Yaoyu Zhou ³, Esperanza Álvarez-Rodríguez ¹,
María Victoria López-Ramón ⁴, Mario Coccia ⁵, Zhien Zhang ⁶, Vanesa Santás-Miguel ⁷ and Marco Race ⁸

- ¹ Department of Soil Science and Agricultural Chemistry, Engineering Polytechnic School, University Santiago de Compostela, 27002 Lugo, Spain; esperanza.alvarez@usc.es
- ² INSTM (National Interuniversity Consortium of Materials Science and Technology) and Department of Mechanical and Industrial Engineering, University of Brescia, Via Branze, 38, 25123 Brescia, Italy; elza.bontempi@unibs.it
- ³ College of Resources and Environment, Hunan Agricultural University, Changsha 410128, China; zhouyy@hunau.edu.cn
- ⁴ Department of Inorganic and Organic Chemistry, Faculty of Experimental Science, University of Jaén, 23071 Jaen, Spain; mvlro@ujaen.es
- ⁵ Research Institute on Sustainable Economic Growth, National Research Council of Italy (CNR), Turin Research Area of the CNR, 10135 Torino, Italy; mario.coccia@cnr.it
- ⁶ Department of Geosciences and Environmental Engineering, University of Cincinnati, Cincinnati, OH 45221, USA; zhienzhang@hotmail.com
- ⁷ Department of Plant Biology and Soil Sciences, University of Vigo, 36310 Vigo, Spain; vsantas@uvigo.gal
- ⁸ Department of Civil and Mechanical Engineering, University of Cassino and Southern Lazio, Via Di Biasio 43, 03043 Cassino, Italy; marco.race@unicas.it
- * Correspondence: avelino.nunez@usc.es

Citation: Núñez-Delgado, A.; Bontempi, E.; Zhou, Y.; Álvarez-Rodríguez, E.; López-Ramón, M.V.; Coccia, M.; Zhang, Z.; Santás-Miguel, V.; Race, M. Editorial of the Topic “Environmental and Health Issues and Solutions for Anticoccidials and Other Emerging Pollutants of Special Concern”. *Processes* **2024**, *12*, 1379. <https://doi.org/10.3390/pr12071379>

Received: 24 June 2024

Accepted: 1 July 2024

Published: 2 July 2024



Copyright: © 2024 by the authors. Licensee MDPI, Basel, Switzerland. This article is an open access article distributed under the terms and conditions of the Creative Commons Attribution (CC BY) license (<https://creativecommons.org/licenses/by/4.0/>).

The editors of this Topic, entitled “Environmental and Health Issues and Solutions for Anticoccidials and other Emerging Pollutants of Special Concern”, proposed it with the knowledge that emerging pollutants continue to be of crucial importance. In addition, at the time of starting the Topic, it was suggested that the field of anticoccidial antibiotics could need special focus.

Various journals were involved in this Topical Issue, and of the submissions that were finally accepted following peer-review, six papers were published from the journal *Processes*, and three from *Sustainability*.

Chronologically, the first two papers accepted and included were “Efficiency of Coagulation/Flocculation for the Removal of Complex Mixture of Textile Fibers from Water” [1] and “Efficient Degradation of Chlortetracycline by Graphene Supported Cobalt Oxide Activated Peroxydisulfate: Performances and Mechanisms” [2], both from the journal *Processes*.

The third and fourth manuscripts accepted for this Topic were “Examining the Relationship between Pro-Environmental Attitudes, Self-Determination, and Sustained Intention in Eco-Friendly Sports Participation: A Study on Plogging Participants” [3] and “Effects of Chlortetracycline on the Growth of Eggplant and Associated Rhizosphere Bacterial Communities.” [4], both published in the journal *Sustainability*.

The fifth and sixth works were published in *Processes*, with the titles “Visualization Network Analysis of Studies on Agricultural Drainage Water Treatment.” [5] and “Assessing Biodegradation Processes of Atrazine in Constructed Wetland Using Compound-Specific Stable Isotope Analysis” [6].

The last manuscripts accepted were “A Study on Sensitivity of Soil-Based Building Mixtures to Biodeterioration by Fungi: Towards Sustainable Earth Structures” [7], published in *Sustainability*, “Determination of 24 Trace Aromatic Substances in Rosemary Hydrosol by

Dispersed Liquid-Liquid Microextraction-Gas Chromatography” [8], published in *Processes*, and “Removal of cefuroxime from soils by means of the bio-adsorbents pine bark, mussel shell and oak ash” [9], published in *Processes*.

This Topic is now closed to new submissions, with an acceptance rate near 50%. Further available data indicate that, to date, the current number of citations to individual published papers is four, while the number of views per single paper is in the range of 4038 to 667.

Finally, the editors of this Topic view it as a complement to a previous Topical Issue which had a general focus on emerging pollutants [10,11], with the current Issue including new high-quality and relevant contributions to this field of research. Looking forward, the quantification of existing and eventual new emerging pollutants will continue to be a matter of concern, as well as facing these challenges by proposing and assessing viable alternatives. In addition, it is clear that specific research dealing with anticoccidials as environmental pollutants is needed, as indicated in a recent publication [12].

Author Contributions: All authors contributed equally to all aspects of this Topical Issue. All authors have read and agreed to the published version of the manuscript.

Funding: This research was funded by the Spanish State Investigation Agency (*Agencia Estatal de Investigación*); grant number PID2021-122920OB-C21 (specifically, Avelino Núñez-Delgado and Esperanza Álvarez-Rodríguez received funding for research related to this Topic).

Data Availability Statement: Not applicable.

Conflicts of Interest: The authors declare no conflicts of interest. The funders had no role in the design of the study; in the collection, analyses, or interpretation of data; in the writing of the manuscript; or in the decision to publish the results.

References

1. Vasiljević, S.; Vujić, M.; Agbaba, J.; Federici, S.; Ducoli, S.; Tomić, R.; Tubić, A. Efficiency of Coagulation/Flocculation for the Removal of Complex Mixture of Textile Fibers from Water. *Processes* **2023**, *11*, 820. [CrossRef]
2. Li, W.; Yao, B.; Zheng, Y.; Zhang, G.; Zhi, D.; Zhou, Y. Efficient Degradation of Chlortetracycline by Graphene Supported Cobalt Oxide Activated Peroxydisulfate: Performances and Mechanisms. *Processes* **2023**, *11*, 1381. [CrossRef]
3. Kim, J.; Kim, S.; Chung, J. Examining the Relationship between Pro-Environmental Attitudes, Self-Determination, and Sustained Intention in Eco-Friendly Sports Participation: A Study on Plogging Participants. *Sustainability* **2023**, *15*, 11806. [CrossRef]
4. Li, L.; Xue, Y.; Wang, H.; Chen, Y. Effects of Chlortetracycline on the Growth of Eggplant and Associated Rhizosphere Bacterial Communities. *Sustainability* **2023**, *15*, 14593. [CrossRef]
5. Wang, C.; Zhang, Y.; Deng, L.; Zhao, M.; Liang, M.; Lee, L.-C.; Chicaiza-Ortiz, C.; Yang, L.; He, T. Visualization Network Analysis of Studies on Agricultural Drainage Water Treatment. *Processes* **2023**, *11*, 2952. [CrossRef]
6. Chen, S.; Wang, Y.; Ma, L. Assessing Biodegradation Processes of Atrazine in Constructed Wetland Using Compound-Specific Stable Isotope Analysis. *Processes* **2023**, *11*, 3252. [CrossRef]
7. Al-Jokhadar, A.; Soudi, Y.; Abdelmalek, S.; Badran, S.R.; Abuhashem, Y. A Study on Sensitivity of Soil-Based Building Mixtures to Biodeterioration by Fungi: Towards Sustainable Earth Structures. *Sustainability* **2024**, *16*, 1294. [CrossRef]
8. Zeng, X.; He, H.; Yuan, L.; Wu, H.; Zhou, C. Determination of 24 Trace Aromatic Substances in Rosemary Hydrosol by Dispersed Liquid-Liquid Microextraction-Gas Chromatography. *Processes* **2024**, *12*, 498. [CrossRef]
9. Cela-Dablanca, R.; Míguez-González, A.; Rodríguez-López, L.; Barreiro, A.; Arias-Estevez, M.; Fernández-Sanjurjo, M.J.; Álvarez-Rodríguez, E.; Núñez Delgado, A. Removal of cefuroxime from soils by means of the bio-adsorbents pine bark, mussel shell and oak ash. *Processes* **2024**, *12*, 1335. [CrossRef]
10. Núñez-Delgado, A.; Zhang, Z.; Bontempi, E.; Coccia, M.; Race, M.; Zhou, Y. Editorial on the Topic “New Research on Detection and Removal of Emerging Pollutants”. *Materials* **2023**, *16*, 725. [CrossRef] [PubMed]

11. Delgado, A.N. Our Environment: Everything Is Natural on Earth, but ... Editorial Piece on Current and Future Soil and Environmental Research. *Processes* **2023**, *11*, 6. [CrossRef]
12. Míguez-González, A.; Cela-Dablanca, R.; Barreiro, A.; Castillo-Ramos, V.; Sánchez-Polo, M.; López-Ramón, M.V.; Fernández-Sanjurjo, M.J.; Álvarez-Rodríguez, E.; Núñez-Delgado, A. Current Data on Environmental Problems Due to Ionophore Antibiotics Used as Anticoccidial Drugs in Animal Production, and Proposal of New Research to Control Pollution by Means of Bio-Adsorbents and Nanotechnology. In *Planet Earth: Scientific Proposals to Solve Urgent Issues*, 1st ed.; Núñez-Delgado, A., Ed.; Springer-Nature: Cham, Switzerland, 2024; pp. 241–261.

Disclaimer/Publisher’s Note: The statements, opinions and data contained in all publications are solely those of the individual author(s) and contributor(s) and not of MDPI and/or the editor(s). MDPI and/or the editor(s) disclaim responsibility for any injury to people or property resulting from any ideas, methods, instructions or products referred to in the content.

Article

Removal of the Highly Toxic Anticoccidial Monensin Using Six Different Low-Cost Bio-Adsorbents

Samiha Hamdi ^{1,2,3}, Manel Issaoui ^{1,3}, Sonia Hammami ³, Ainoa Míguez-González ², Raquel Cela-Dablanca ², Ana Barreiro ^{2,*}, Avelino Núñez-Delgado ², Esperanza Álvarez-Rodríguez ² and María J. Fernández-Sanjurjo ²

¹ Department of Biotechnology, Faculty of Science and Technology of Sidi Bouzid, University of Kairouan, Sidi Bouzid 9100, Tunisia; samihahamdi2020@gmail.com (S.H.); manelissaoui80@gmail.com (M.I.)

² Department of Soil Science and Agricultural Chemistry, Engineering Polytechnic School, University of Santiago de Compostela, 27002 Lugo, Spain; ainoa.miguez@rai.usc.es (A.M.-G.); raquel.dablanca@usc.es (R.C.-D.); avelino.nunez@usc.es (A.N.-D.); esperanza.alvarez@usc.es (E.Á.-R.); mf.sanjurjo@usc.es (M.J.F.-S.)

³ Laboratory of Nutrition–Functional Foods and Health (NAFS)-LR12ES05, Faculty of Medicine, University of Monastir, Avenue Avicenne, Monastir 5019, Tunisia; sonia.hammami@fmm.rnu.tn

* Correspondence: ana.barreiro.bujan@usc.es

Abstract: The anticoccidial monensin (MON) is a high-concern emerging pollutant. This research focused on six low-cost bio-adsorbents (alfa, cactus, and palm fibers, and acacia, eucalyptus, and zein oak barks), assessing their potential for MON removal. Batch adsorption/desorption tests were carried out, and the results were fitted to the Freundlich, Langmuir, Linear, Sips, and Temkin models. The concentrations adsorbed by the six materials were very similar when low doses of antibiotic were added, while they differed when adding MON concentrations higher than 20 $\mu\text{mol L}^{-1}$ (adsorption ranging 256.98–1123.98 $\mu\text{mol kg}^{-1}$). The highest adsorption corresponded to the sorbents with the most acidic pH (<5.5) and the highest organic matter and effective cation exchange capacity values (eucalyptus bark and acacia bark, reaching 92.3% and 87.8%), whereas cactus and palm fibers showed the lowest values (18.3% and 10.17%). MON desorption was below 8.5%, except for cactus and palm fibers. Temkin was the model showing the best adjustment to the experimental data, followed by the Langmuir and the Sips models. The overall results indicate that eucalyptus bark, alfa fiber, and acacia bark are efficient bio-adsorbents with potential for MON removal, retaining it when spread in environmental compartments, reducing related risks for human and environmental health.

Keywords: bio-adsorbents; ionophore antibiotics; monensin; natural barks; natural fibers

Citation: Hamdi, S.; Issaoui, M.; Hammami, S.; Míguez-González, A.; Cela-Dablanca, R.; Barreiro, A.; Núñez-Delgado, A.; Álvarez-Rodríguez, E.; Fernández-Sanjurjo, M.J. Removal of the Highly Toxic Anticoccidial Monensin Using Six Different Low-Cost Bio-Adsorbents. *Toxics* **2024**, *12*, 606. <https://doi.org/10.3390/toxics12080606>

Academic Editor: Xin-Gui Li

Received: 18 July 2024

Revised: 16 August 2024

Accepted: 18 August 2024

Published: 19 August 2024



Copyright: © 2024 by the authors. Licensee MDPI, Basel, Switzerland. This article is an open access article distributed under the terms and conditions of the Creative Commons Attribution (CC BY) license (<https://creativecommons.org/licenses/by/4.0/>).

1. Introduction

The global overconsumption of antibiotics has led to worldwide issues such as antibiotic resistance, underscoring the need for strict regulations and responsible medical practices [1–3]. Numerous classes of antibiotics used in animal husbandry are very similar or identical to those prescribed for human use [4], while others (such as the ionophore anticoccidials monensin, salinomycin, narasin, and lasalocid) are employed strictly in veterinary, as feed additives to promote growth and prevent diseases in livestock, particularly coccidiosis [5]. All these ionophores have been reported to exhibit higher toxicity than other antibiotics [6,7]. However, ionophore antibiotics have been extensively employed in farm animals, which has accounted for at least 50% of antibiotic use in the United States [8]. Consequently, several concerns related to the widespread use of these substances in cattle and poultry farming can be taken into account, raising worries due to their potential impact on human health and the environment.

After its administration, residues of the ionophore antibiotics are excreted in animal feces and urines, which are further used as fertilizer for soils [9]. In addition to animal manure/slurry, ionophores can reach soils via contaminated water and treated wastewater

used for crop irrigation and through the spreading of sludge resulting from wastewater treatment that are used as fertilizers [10]. Upon reaching the soil, these emerging pollutants can impact soil bacterial communities, generating anti-microbial resistance [11].

In the case of the ionophore antibiotic monensin (MON), due to its wide use, its potential high toxicity, and the limited knowledge with regards to its environmental repercussions, it has been classified as a high-priority environmental contaminant [12]. MON is a monocarboxylic polyether [13,14], primarily produced by the bacterium *Streptomyces cinnamomensis* [15], with its specific chemical structure shown in Figure 1.

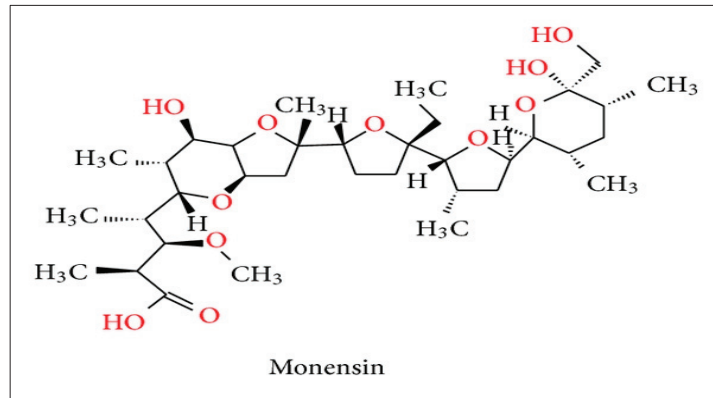


Figure 1. Chemical structure of monensin (MON) [13].

Adsorption to soils can potentially mitigate the health risks related to the transfer of MON to crops from the soil solution [16], although limited research has been conducted in this regard. In addition, it would be needed to carry out research focused on alternatives to prevent soil and water pollution caused by this very toxic antibiotic, as well as on techniques to remediate it in already contaminated areas.

Regarding wastewater treatment, different techniques are used to remove antibiotics, like membrane separation, filtration, and advanced oxidation [17–19]. However, these approaches are associated with high costs and substantial waste production [20–22], with their application often resulting in significant energy consumption and depletion of non-renewable resources, thereby contributing to ecological impacts. Adsorption methods offer an alternative to conventional techniques for depollution, providing pollutant-removal efficiency, cost-efficiency, simplicity, and versatility [23,24], making it a promising method for pollution-remediation applications such as antibiotic remediation, especially in water. Previous studies have encouraged the use of low-cost and eco-friendly materials to adsorb antibiotics like sulfonamides present in edaphic environments [25] or tetracyclines in water [26], as they are capable of increasing the adsorption of soils with low retention capacity or to be effective in water decontamination. However, there is a lack of studies investigating the potential of eco-friendly bio-adsorbents for the removal of ionophores from water and soils. In this regard, Míguez-González et al. [27] suggested the need to perform additional research in this area, particularly focusing on advancements in the retention/removal of ionophore anticoccidials from environmental compartments, using both raw and modified bio-adsorbents as well as nanomaterials.

Natural and/or modified fiber-based materials have previously been used to remove various emerging pollutants from water systems. In this context, a study outlined by Ben Rebah and Siddeeg [28] reviewed the high efficiency of cactus fiber in removing a wide array of heavy metals, such as copper (Cu (II)) and cadmium (Cd (II)), as well as dyes like methylene blue (MB) and eriochrome black T (EBT). This aligns with data obtained in earlier research on the use of cactus fiber-based adsorbents for these purposes [29–31]. Prodromou and Pashalidis [32] investigated the removal of chromium (Cr (II)) using phosphorylated

(with 1.5 M H_3PO_4) and MnO_2 -coated cactus fiber samples, comparing them to untreated cactus fiber. Additionally, recent studies have focused on using fiber materials, such as palm and alfa fibers, to remove pollutants like metals from aqueous solutions and wastewater effluents [33,34]. Other studies have explored the potential use of natural barks, such as eucalyptus and acacia barks, in water remediation. One early study evaluated a eucalyptus (*Eucalyptus camaldulensis*) bark-based composite, as new efficient adsorbent for the removal of basic blue 41 dye from aqueous solutions, showing a high level of adsorption [35]. A similar study used *Acacia raddiana* bark for the biosorption of copper cations from aqueous solutions, reporting a maximum copper biosorption capacity of 82.63 mg g^{-1} at pH 5 and a temperature of around 25–30 °C [36]. To be noted, studies on the adsorption properties of *Acacia salicina* bark are scarce, making it of interest for investigation.

With the above background, the present research was conceived as the first study simultaneously assessing alfa, cactus, and palm fibers, as well as acacia, eucalyptus, and zean oak barks, with regards to their potential for removing MON molecules from aqueous solutions. The results of this investigation could be of value in relation to controlling contamination episodes caused by this emerging pollutant, and at the same time could promote the recycling of low-cost by-products as bio-adsorbents, thus favoring sustainability, public health, and environmental protection.

2. Materials and Methods

2.1. Chemicals

MON was provided by Sigma-Aldrich (Madrid, Spain). The main physicochemical properties of this antibiotic are listed in Table S1 (Supplementary Material). Acetonitrile (purity $\geq 99.9\%$), and phosphoric acid (85% extra pure) were from Fisher Scientific (Madrid, Spain), while 95% pure $CaCl_2$ was from Panreac (Barcelona, Spain). In addition, optima-grade reagents methanol, $CaCl_2$, acetic acid, Trichloroacetic (TCA), and 2,4-Dinitrophenol (DNP) acids were purchased from Sigma-Aldrich (Madrid, Spain). For HPLC analyses, all necessary solutions were prepared with milliQ water obtained from Millipore (Madrid, Spain).

2.2. Bio-Adsorbent Materials

Six bio-adsorbents were used: (i) three natural fibers: alfa fiber (derived from *Stipa tenacissima*, a plant frequently distributed in central and southern Tunisia), which was sampled from the Hadej region (Menzel Bouzaiane, Sidi Bouzid, Central Tunisia); palm fiber (*Phoenix dactylifera* L.), which was sampled from the Midass region (Tozeur, southern Tunisia); and cactus fiber (*Opuntia ficus-indica*), from the Tala region (Kasserine, North-central Tunisia); (ii) three natural barks: two of them were acacia and eucalyptus barks, which were from the tree species *Acacia salicina* and *Eucalyptus camaldulensis*, respectively, both commonly found in arid and semi-arid regions of Tunisia, and that for this study were obtained from the Maknessy region in Sidi Bouzid, central Tunisia; and the third bark sample was derived from the zean oak tree (*Quercus canariensis* Willd), collected from the Tabarka region in northwestern Tunisia, where it is commonly distributed.

The sampling of the bio-adsorbent materials was done in March 2023 from different Tunisian locations, and they were subsequently transferred to the laboratory for preparation and physicochemical analyses. Before further processing, the bio-adsorbent samples were washed and dried (in an oven at 60 °C for 24 h), then crushed using an automatic grinder (SCP SCIENCE SP-2000 Swing Mill Grinder). After crushing, the bio-adsorbents used in the experiment were sieved through a 100- μm mesh.

2.3. Characterization of the Bio-Adsorbents

The six bio-adsorbents were characterized before performing adsorption-desorption tests. The physicochemical parameters that were assessed were pH and electrical conductivity (pH_w and EC, respectively) measured in water, pH in 0.1 M KCl solution (pH_{KCl}), pH of the point of zero charge (pH_{PZC}), humidity (H%), bulk density (D, expressed in $g\ cm^{-3}$),

swelling index (SI%), porosity (P%), ash (As) content, organic matter content, exchangeable cations (Ca_e , Mg_e , Na_e , K_e , and Al_e , expressed in $cmol_c\ kg^{-1}$), and effective cation exchange capacity (eCEC, also expressed in $cmol_c\ kg^{-1}$). The methods employed for the characterization of the bio-adsorbents are detailed in the Supplementary Material, where references to the methods presented in Fox and Kamprath [37], Lopes et al. [38], Nebot et al. [39], Peech [40], and Rodríguez-López et al. [41] are included.

2.4. Experimental Design

2.4.1. Influence of Environmental Factors

The main factors considered were adsorbent weight, contact time, and MON concentration. These factors were selected taking into consideration previous kinetic studies on ionophore antibiotics such as monensin and lasalocid [6], as well as non-ionophore antibiotics such as amoxicillin [42], when adsorbed onto soils and different bio-adsorbents, which had indicated that 48 h were sufficient to achieve equilibrium in the adsorption process. Additionally, the bio-adsorbent mass was fixed as 0.5 g, which were added to 10 mL of the MON solutions, with the samples being shaken under dark conditions to prevent photodegradation, particularly under ultraviolet (UV) light, which can impact the stability of MON molecules.

All the experiments were conducted at room temperature ($25 \pm 2\ ^\circ C$) without adjusting the pH, which is relevant to many real-world sorption applications, especially in environmental remediation. In addition, standard calibration procedures were performed before measuring with the pH-meter and atomic absorption spectrophotometer.

2.4.2. Experiments on Adsorption and Desorption (Batch Tests)

Batch experiments were employed to conduct adsorption and desorption investigations across the entire array of bio-adsorbents, following the procedure detailed in the Supplementary Material. Moreover, details about the experimental conditions for the adsorption-desorption tests were briefly mentioned in the Supplementary Material. Adsorption and desorption studies were executed through batch experiments, wherein 0.5 g of adsorbent were immersed in 10 mL of MON solutions using six concentrations, ranging from 5 to $100\ \mu mol\ L^{-1}$ in 0.005 M $CaCl_2$ solutions, as done previously in studies for tetracycline and sulfadiazine antibiotics in natural and modified clays [43,44] and onto forest bio-adsorbents like pine bark and oak ash [45]. $CaCl_2$ was used as a background electrolyte to maintain constant ionic strength. The shaking time was 48 h, which was found to be a sufficient duration to achieve equilibrium, as determined in previous unpublished kinetic studies. The desorption tests involved the addition of 10 mL of 0.005 M $CaCl_2$ solutions, followed by the application of the same procedure as employed in the adsorption tests. All these experiments were conducted in triplicate.

2.4.3. Quantification of MON

Prior to the quantification analysis, certain procedural steps were considered necessary to enhance the detectability of the MON antibiotic (details are provided in the Supplementary Material). MON quantification for adsorption and desorption phases was performed in triplicate, at room temperature ($25 \pm 2\ ^\circ C$), and with unmodified pH, using an UltiMate 3000 HPLC liquid chromatograph (Thermo Fisher Scientific, Madrid, Spain). During the quantification process, all HPLC samples from the adsorption-desorption steps were run with an isocratic method, with a single phase composed of methanol (88.5%), water (10%), and acetic acid (1.5%), with a flow rate set at $1\ mL\ min^{-1}$. Subsequently, the obtained data were analyzed using Chromeleon software version 7 (Thermo Fisher Scientific, Madrid, Spain). Further details concerning the HPLC equipment are outlined in the Supplementary Material. For the separation of MON, the following conditions were used: the injection volume for analysis was 200 μL , the total analysis time was 35 min, with a wavelength of 392 nm. The MON peak appeared divided into three peaks at times: 6.9 min, 7.2 min, and 8.4 min. Then, the areas of these three peaks were summed up. It is stressed to

note that between each measurement, the syringe was rinsed with the running solution. Figure S1 (Supplementary Material) presents some example chromatograms. Finally, taking into account the MON concentrations added, minus the equilibrium concentrations (C_{eq} ; $\mu\text{mol L}^{-1}$), allows the calculation of the amounts of MON adsorbed.

2.5. Calculation and Statistical Treatment

The experimental data obtained in the batch adsorption tests were adjusted to the Freundlich (Equation (1)), Langmuir (Equation (2)), Linear (Equation (3)), Sips (Equation (4)), and Temkin (Equation (5)) models:

$$q_a = K_F * C_{eq}^n, \tag{1}$$

$$q_a = (q_m K_L * C_{eq}) / (1 + K_L * C_{eq}), \tag{2}$$

$$q_a = K_d * C_{eq}, \tag{3}$$

$$q_a = q_m * ((K_S * C_{eq})^n / (1 + (K_S * C_{eq})^n)), \tag{4}$$

$$q_a = \beta \ln K_T + \beta \ln C_{eq}, \tag{5}$$

where q_a ($\mu\text{mol kg}^{-1}$) is the quantity of antibiotic retained by the different bio-adsorbents at equilibrium, the concentration of antibiotic present in the solution at equilibrium is denoted as C_{eq} ($\mu\text{mol L}^{-1}$); K_F is the Freundlich parameter associated with adsorption capacity ($\text{L}^n \mu\text{mol}^{1-n} \text{kg}^{-1}$); n (dimensionless) is the Freundlich linearity index, K_L is the Langmuir adsorption constant ($\text{L } \mu\text{mol}^{-1}$), while q_m is the maximum adsorption capacity according to the Langmuir model ($\mu\text{mol kg}^{-1}$). K_d (L kg^{-1}) is the distribution coefficient in the linear model; K_S represents the Sips adsorption constant, indicating the affinity of the adsorbate for the surface ($\text{L } \mu\text{mol}^{-1}$), while n (dimensionless) reflects the heterogeneity of the equilibrium system. In the Temkin model, $\beta = RT/bt$, bt is the Temkin constant associated with sorption (J/mol), R is the universal gas constant [46,47], and T denotes the temperature at 25 °C ($K = 298$ °C). Additionally, K_T represents the Temkin isotherm equilibrium binding constant (L g^{-1}).

In the current work, the hysteresis index (HI) (Equation (6)) was calculated using the formula established in prior literature [41]:

$$HI = (q_a^D - q_a^S) / q_a^S, \tag{6}$$

where q_a^S represents the adsorption concentrations of MON in the studied bio-adsorbents and q_a^D denotes the final concentration after the desorption experiments.

The adjustment of adsorption experiments to the different statistical models, along with one way-ANOVA analysis, was conducted using IBM SPSS Statistics version 21 software (New York, NY, USA).

In order to achieve more comprehensive information about the affinity of binding sites and to analyze the results of adsorption modeling, the Scatchard plot analysis [48], a widely used technique, also known as the independent-site oriented model, was applied to the experimental data. Compared to other mathematical transformations of the classical Langmuir equation, awareness about the equilibrium concentration ranges where the Langmuir model shows good fit to the experimental data can be acquired more easily through the Scatchard equation, which is represented as follows:

$$q_a / C_{eq} = Q_m^S K_b - q_a K_b, \tag{7}$$

where q_a and C_{eq} have the same meaning as mentioned above, and Q_m^S and K_b are the Scatchard parameters, with Q_m^S (expressed in $\mu\text{mol kg}^{-1}$) being the theoretical saturation

capacity (also known as a parameter related to the number of binding sites involved in a particular sorption process), whereas K_b is considered as a constant related to the affinity between sorbent and sorbate (also known as binding constant). Additionally, the Scatchard model was used to analyze adsorption data by plotting q_a/C_{eq} against q_a , creating a Scatchard plot (Figure S2, Supplementary Material). The shape of the plots obtained indicates: (i) a straight line reveals uniform adsorption sites; (ii) a nonlinear curve suggests nonspecific or multiple interactions; and (iii) concave curves denote negative cooperative effects or heterogeneous sites, while convex curves imply positive cooperative effects [44,49]. Deviations from linearity (as determined by R^2 values) can signal non-specific or multi-type interactions between adsorbents and adsorbates [50].

All the above indicated methods suppose the first steps included in a wide research program, with a series of subsequent phases to be accomplished with regards to empirical and computational tasks, according to previously defined protocols [51,52].

3. Results

3.1. Bio-Adsorbents Characteristics

Table 1 shows the values corresponding to the physicochemical parameters determined for the six bio-adsorbents studied.

Table 1. Chemical characteristics of the different bio-adsorbents, with average values ($n = 3$) and coefficients of variation always $<5\%$. EC: electrical conductivity (in $dS\ m^{-1}$); (H%): Moisture content (in percentage); DM: Dry matter content (%); P: Porosity (in percentage); As: Ash content (%); VM: Volatile matter content (%); BD: Bulk density (in $g\ cm^{-3}$); RD: Real density (in $g\ cm^{-3}$); SI: Swelling Index (in percentage); OM: organic matter content (%); OC%: Organic carbon content (in percentage); X_e : exchangeable cations (Al, Ca, K, Mg, and Na, expressed in $cmol_c\ kg^{-1}$); eCEC: effective cation exchange capacity (expressed in $cmol_c\ kg^{-1}$).

	Alfa Fiber	Cactus Fiber	Palm Fiber	Acacia Bark	Eucalyptus Bark	Zeal Oak Bark
pH _w	5.1	7.4	5.5	4.9	5.4	5.7
pH _{KCl}	4.7	7.6	6.9	4.2	5.1	4.8
pH _{PZC}	6.6	6.2	4.3	7.1	7.4	5.8
EC	21	204	818	19.7	4.2	5.9
H%	9.3	6.2	5.4	10.7	11.5	7.0
DM	90.7	93.8	94.6	89.3	88.5	93.0
P	86.6	48.0	41.6	62.8	65.7	57.5
As	2.45	3.34	4.36	1.22	1.42	1.91
VM	97.55	96.66	95.64	98.58	98.58	98.09
BD	1.28	0.96	0.81	1.42	1.53	1.1
RD	1.65	1.23	1.14	1.86	1.97	1.43
SI	2.56	1.43	1.08	2.82	2.96	1.84
OM	40.72	21.76	18.84	49.21	50.25	29.85
OC%	19.54	10.44	9.04	23.62	24.12	14.32
Al _e	0.11	0.05	0.05	0.18	0.11	0.09
Ca _e	6.74	2.04	1.97	7.44	7.98	4.22
K _e	2.22	3.04	2.96	2.02	2.07	2.79
Mg _e	1.57	3.06	2.99	1.03	0.86	2.81
Na _e	2.32	1.05	0.96	3.77	4.04	1.12
eCEC	13.97	9.26	8.55	14.45	15.08	11.04
Paricle size (%)						
0.075–0.1 mm	86.17	52.28	66.71	26.14	31.30	39.70
0.05–0.075 mm	11.68	30.61	15.77	68.43	65.45	53.40
0.05–0.02 mm	2.15	10.73	13.47	4.16	3.25	6.78
<0.02 mm	--	6.38	4.05	1.27	--	1.20

As shown in Table 1, the pH values (in water) ranged between 5.1 and 7.4 for the fibers, while the range was 4.9–5.7 for the bark samples. These values were higher than those of pH_{KCl} for alfa fiber, as well as for acacia and eucalyptus barks, which ranged from 4.2 to

5.1. Conversely, the pH_w values were lower than the pH_{KCl} values for cactus and palm fibers, as well as for zeon oak bark, which ranged from 4.8 to 7.6. The pH_{PZC} values shown in Table 1 were estimated from the intersection between the bisector line and the graphical representation of pH_{final} versus $pH_{initial}$ (see details in the Supplementary Material) as shown in Figure S1 (Supplementary Material). The pH_{PZC} values of the different bio-adsorbents here studied were in the range of 4.3–7.4, as indicated in Table 1 and Figure S3 (Supplementary Material). It is crucial to bear in mind that at $pH < pH_{PZC}$, the adsorbent surface is positively charged, and the adsorption of anions is consequently favored (as observed for acacia and eucalyptus barks, and also for alfa fiber), whereas, at $pH > pH_{PZC}$, the biosorbent surface is negatively charged, and biosorption of cations is favored (as noted for cactus and palm fibers along with zeon oak bark) [53–55]. The fibers had the highest EC levels (ranging 21–818 $dS\ m^{-1}$), being lower for the barks (4.2–19.7 $dS\ m^{-1}$). The moisture content (H%) values were typically higher (ranging 9.3–11.5%) for alfa fiber and eucalyptus and acacia barks, compared to those observed for cactus and palm fibers, as well as for zeon oak bark (ranging 5.4–7.0%) (Table 1). Thus, the highest values for dry matter (DM) content were observed for samples with lower H% scores, specifically cactus (93.8%) and palm (94.6%) fibers, as well as oak bark (93.0%) (Table 1).

Concerning the bio-adsorbent's porosity, their values oscillated between 41.6% and 86.6% for alfa fiber and palm fiber, respectively. The bark samples presented low levels of ash (As) content (1.22, 1.42, and 1.91% for acacia, eucalyptus, and zeon oak bark, respectively) and similar volatile matter (VM%) content (Table 1).

The bulk density (BD) values of the studied bio-adsorbents varied between 0.81 $g\ cm^{-3}$ of cactus fiber and 1.53 $g\ cm^{-3}$ of acacia bark, which were lower than the real density (RD) scores (ranging 1.14–1.97 $g\ cm^{-3}$) (Table 1).

Regarding the swelling indices (SI), acacia and eucalyptus barks and alfa fiber had the highest swelling power, compared to the other adsorbent materials, and are also the ones with the highest density (Table 1).

The organic matter content (OM) also shows a marked variability, oscillating between 18.84% (palm fiber) and 50.25% (eucalyptus bark). In the current study, eucalyptus and acacia barks, together with alfa fiber, present the highest OM values (>40%), whereas it is below 30% for the other bio-adsorbents. Similarly, eucalyptus and acacia barks, along with alfa fiber, exhibited the highest organic carbon (OC%) values, oscillating between 24.12% (acacia bark) and 19.54% (alfa fiber), while the OC% values for the other adsorbent materials did not exceed 14.32%. Among the exchangeable cations, Ca_e was predominant in alfa fiber and in the three barks, while Mg_e predominated in cactus and palm fibers. The highest Na_e values were observed in eucalyptus and acacia barks, together with alfa fiber. Conversely, Al_e showed low levels for all the bio-adsorbents (ranging between 0.05 and 0.18 $cmol_c\ kg^{-1}$), with its highest values associated with acacia and eucalyptus barks, and with alfa fiber, coinciding with its lower pH. Furthermore, both eucalyptus and acacia barks, as well as alfa fiber, showed the highest eCEC scores. Note that the three bio-adsorbents with the lowest OM contents (palm fiber, cactus fiber, and zeon oak bark) are those with the lowest eECE values, which is indicative of the importance of OM in the generation of electrical charges.

The wet sieving analysis indicated that the studied bio-adsorbents had particle sizes mostly ranging from 75 to 100 μm (0.075 to 0.1 mm) for fiber samples and from 50 to 75 μm (0.05 to 0.075 mm) for bark samples. All samples were well-homogenized before being used in this investigation.

3.2. MON Adsorption

Figure 2 shows adsorption curves, plotting the amount of antibiotic adsorbed (q_a , in $\mu mol\ kg^{-1}$) versus its concentration in the equilibrium solution (C_{eq} , in $\mu mol\ L^{-1}$). As depicted in Figure 2, the adsorbed amounts increase with the rise in equilibrium concentration (C_{eq}), while the slopes gradually decrease, with the most pronounced decrease being for cactus and palm fibers.

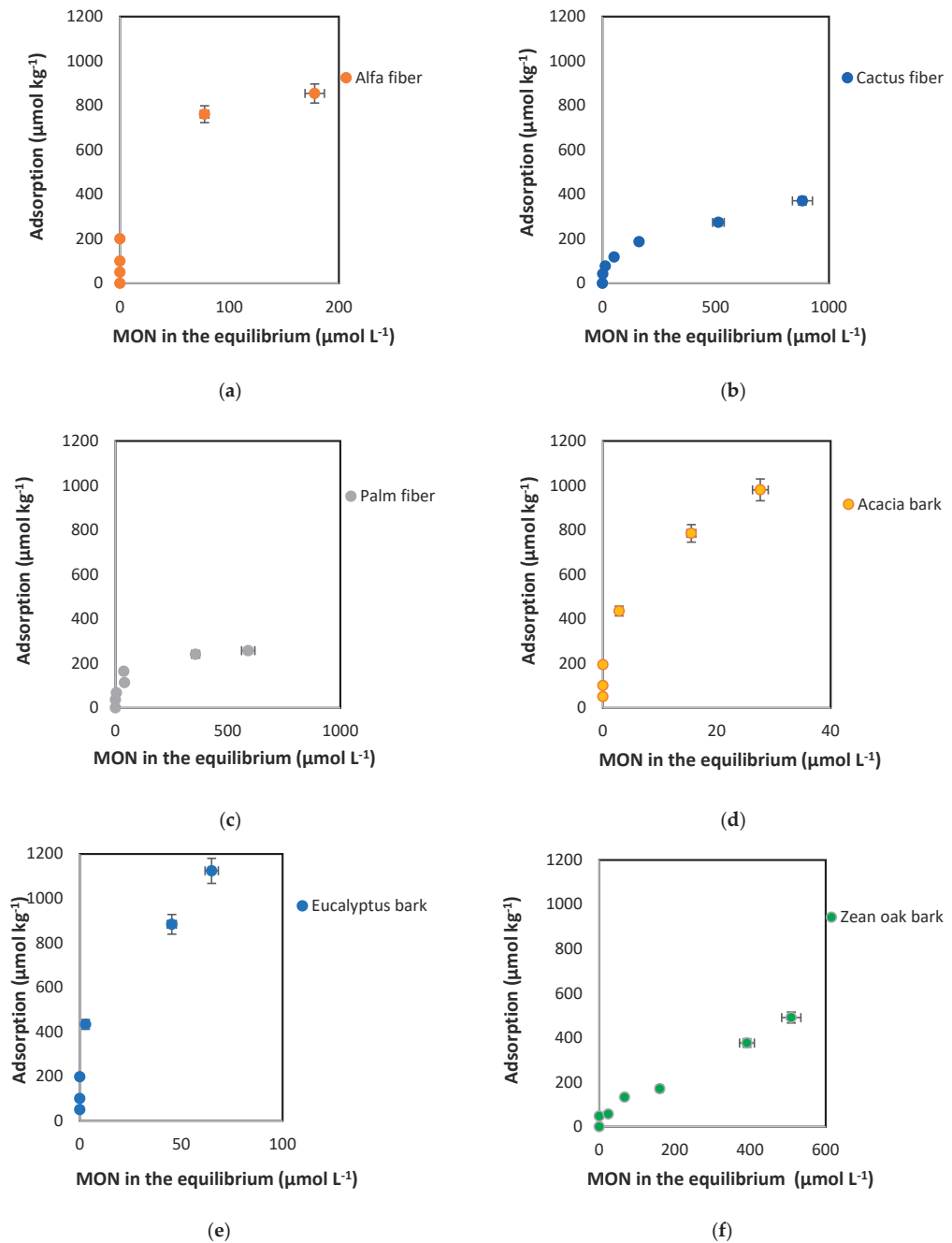
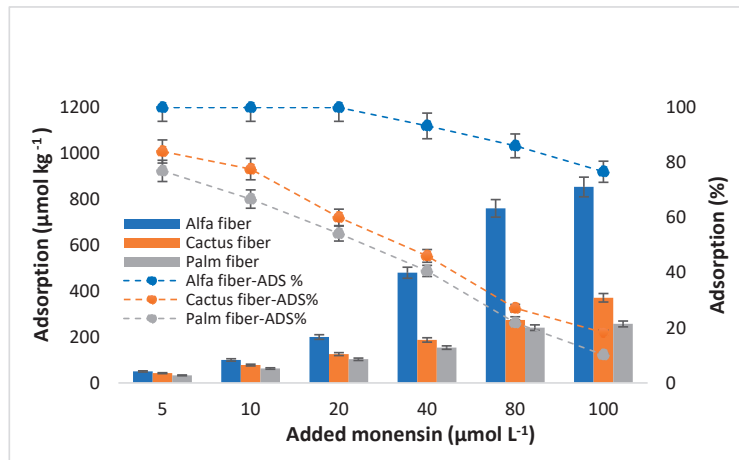
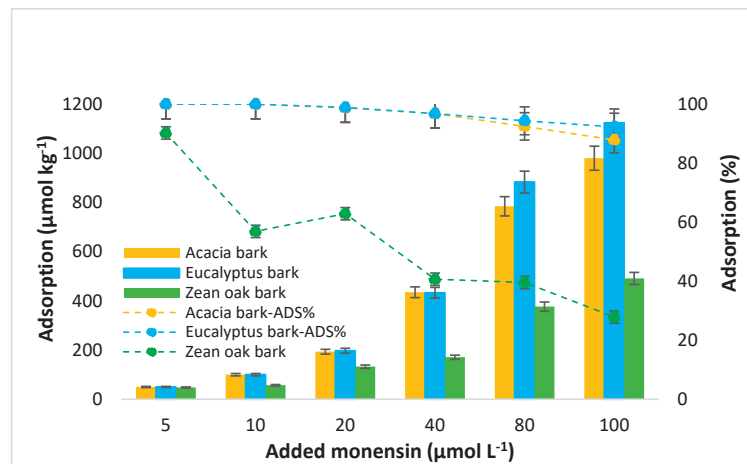


Figure 2. Adsorption curves for MON corresponding to the different bio-adsorbents used: natural fibers (a–c) and barks (d–f). Average values ($n = 3$), with coefficients of variation always $<5\%$. When the error bars are not visible, it means that they are smaller than the symbols. Adsorption tests conditions: 0.5 g of adsorbent with 10 mL of 0.005 M CaCl_2 solutions containing from 5 to 100 $\mu\text{mol L}^{-1}$ of MON, shaking for 48 h at 50 rpm in the dark and at $25 \pm 2^\circ\text{C}$, then centrifuging ($4000 \times g$) and filtering by 0.45 μm before HPLC quantification.

Additionally, the adsorption capacities of the studied bio-adsorbents, expressed in $\mu\text{mol kg}^{-1}$ and as a percentage, are shown in Figure 3. According to these data, the maximum adsorption corresponded to eucalyptus bark, followed by acacia bark and alfa fiber. Specifically, for the highest concentration of MON added ($100 \mu\text{mol L}^{-1}$), the adsorbent amounts were $1123.98, 930.34,$ and $853.98 \mu\text{mol kg}^{-1}$, for eucalyptus and acacia barks, and for alfa fiber, respectively. Contrary, for the same added concentration the minimum adsorption amounts were observed for palm fiber ($256.98 \mu\text{mol kg}^{-1}$), followed by cactus fiber ($370.98 \mu\text{mol kg}^{-1}$), and then zean oak bark ($491.18 \mu\text{mol kg}^{-1}$).



(a)



(b)

Figure 3. Monensin (MON) adsorption of (in $\mu\text{mol kg}^{-1}$ and %) onto natural fibers (a) and barks (b), as a function of the concentration of the antibiotic added ($\mu\text{mol L}^{-1}$). Average values ($n = 3$), with coefficients of variation always $<5\%$. When the error bars are not visible, it means that they are smaller than the symbols.

Considering the adsorption data presented in Figure 3, it is crucial to note that the amounts of MON adsorbed increase as a function of the concentration of antibiotic added, contrary to the adsorption percentages, which decrease with the rise of the MON concentration added, especially in case of palm and cactus fiber, and of zean oak bark. Adsorption

percentages are close or equal to 100% for eucalyptus and acacia barks, as well as for alfa fiber, when the MON concentrations added ranged between 5 and 20 $\mu\text{mol L}^{-1}$, while the scores decreased for cactus and palm fibers and for zean oak bark, going from 84.0 to 47.8% (Figure 3).

3.3. Fitting of Experimental Data to Adsorption Models

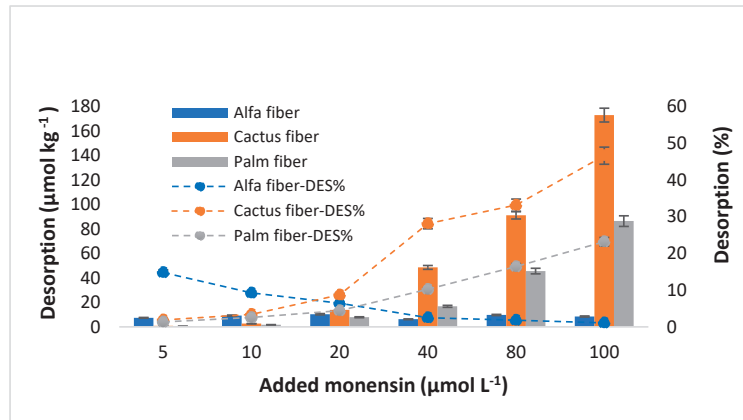
The details corresponding to the fitting of MON adsorption experimental data to the Freundlich, Langmuir, Linear, Sips and Temkin models are presented in Table 2.

Table 2. Values corresponding to the fitting of the experimental data (referred to MON adsorption onto the six bio-adsorbents) to the parameters of the Freundlich, Langmuir, Linear, Sips, and Temkin models. K_F ($L^n \mu\text{mol}^{1-n} \text{kg}^{-1}$); K_L ($L \text{kg}^{-1}$); q_m ($\mu\text{mol kg}^{-1}$); K_d ($L \text{kg}^{-1}$); K_s ($L \text{kg}^{-1}$); K_t ($L \text{g}^{-1}$); b_t (J/mol). R^2 : coefficient of determination; -: error too high for fitting.

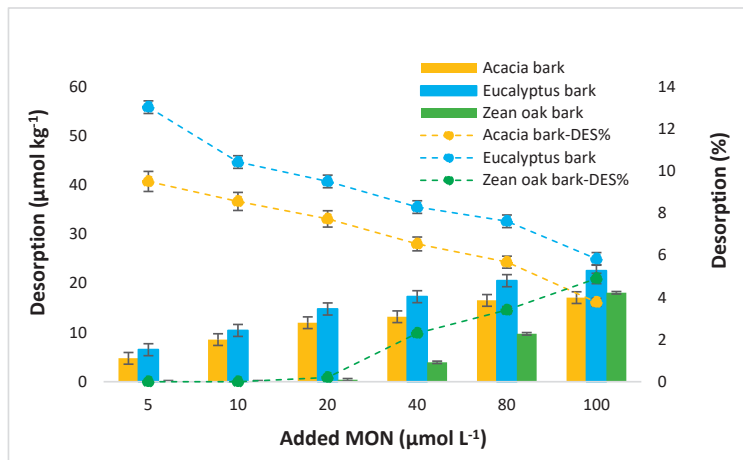
		Alfa Fiber	Cactus Fiber	Palm Fiber	Acacia Bark	Eucalyptus Bark	Zeaoak Bark
Freundlich model	K_F	227.7	116.1	57.4	331.1	470.4	195.5
	Error	40.1	9.8	19.1	93.1	101.2	6.4
	n	1.415	0.212	0.236	2.484	2.685	0.458
	Error	0.05	0.03	0.01	0.11	0.28	0.09
	R^2	0.762	0.826	0.817	0.723	0.741	0.842
Langmuir model	K_L	0.14	0.06	0.04	0.27	0.31	0.08
	Error	0.01	0.00	0.01	0.02	0.03	0.00
	q_m	957.9	835.8	809.9	987.2	1046.1	527.9
	Error	97.4	80.7	60.6	107.5	140.3	37.48
	R^2	0.997	0.962	0.995	0.972	0.989	0.934
Linear model	K_d	28.85	5.04	2.29	114.9	167.8	6.46
	Error	5.52	0.49	0.28	30.4	34.9	0.3
	R^2	0.634	0.622	0.611	0.631	0.578	0.601
Sips model	K_s	3.21	1.00	0.18	4.77	6.2	1.85
	Error	0.13	0.01	0.00	0.93	1.1	0.05
	n	1.523	0.270	0.173	2.137	2.754	0.441
	Error	0.13	0.1	0.007	0.24	0.22	0.02
	q_m	925.6	474.5	336.1	969.3	925.6	704.6
	Error	10.3	32.1	23.3	47.8	35.1	15.5
R^2	0.944	0.873	0.869	0.925	0.932	0.884	
Temkin model	K_t	2.71	0.64	-	3.84	4.21	-
	Error	0.004	0.00	-	0.34	0.001	-
	b_t	4.772	0.344	0.231	5.022	6.765	2.522
	Error	0.8	0.05	0.09	0.00	1.33	1.53
	R^2	0.989	0.979	0.968	1.00	1.00	0.982

3.4. MON Desorption

Figure 4 presents the amounts of MON desorbed from the different bio-adsorbents, as well as the desorption percentages, versus the initial MON concentrations added ($\mu\text{mol L}^{-1}$). When the MON concentrations added are lower than 20 $\mu\text{mol L}^{-1}$, the amounts desorbed are generally low (<10%) and similar for all the bio-adsorbents. At higher concentrations added, clearly higher desorption scores are observed for cactus fiber and palm fiber (Figure 4).



(a)



(b)

Figure 4. Desorption of monensin (MON) (in $\mu\text{mol kg}^{-1}$ and %) from natural fibers (a) and barks (b), as a function of the concentration of the antibiotic added ($\mu\text{mol L}^{-1}$). Average values ($n = 3$), with coefficients of variation always $<5\%$. When the error bars are not visible, it means that they are smaller than the symbols.

For cactus fiber the desorbed quantities reach $173 \mu\text{mol kg}^{-1}$ when the added concentration is $100 \mu\text{mol L}^{-1}$, which corresponds to almost 47% of the added antibiotic. As for palm fiber, the maximum desorption value was $84.4 \mu\text{mol kg}^{-1}$ (23.2%), also associated with the highest dose added. It is important to note that, at the three lowest MON concentrations added (5, 10, and $20 \mu\text{mol L}^{-1}$), the desorption percentages observed for both cactus and palm fibers did not exceed 9% and 5%, respectively. Alfa fiber exhibited the lowest desorption of MON ($8.45 \mu\text{mol kg}^{-1}$), representing 1.1% of the added antibiotic, at a MON concentration added of $100 \mu\text{mol L}^{-1}$ (Figure 4). The desorbed amounts never exceed $23 \mu\text{mol kg}^{-1}$ for eucalyptus and acacia barks, remaining below 10% across the four highest concentrations of antibiotic added (from 20 to $100 \mu\text{mol L}^{-1}$). Regarding zean oak bark, it did not desorb MON at the three lowest concentrations added, while it began to desorb when the initial concentration reached $40 \mu\text{mol L}^{-1}$, although it did not exceed 5% in any case (Figure 4). Thus, the desorption sequence for the three highest concentrations

of antibiotic added was: alfa fiber < zean oak bark < acacia bark < eucalyptus bark < palm fiber < cactus fiber.

The MON desorption percentages obtained for most of the here-studied sorbent materials demonstrate the low reversibility of the adsorption process. The calculation of the hysteresis index (HI) supports this idea, obtaining values greater than 0.906 in most samples, except in cactus and palm fibers, with average values around 0.235 and 0.429, respectively (Table 3).

Table 3. Hysteresis index (HI) corresponding to the desorption of MON from the six bio-adsorbents, and for each of the initial concentrations of the antibiotic added.

MON Concentration Added ($\mu\text{mol L}^{-1}$)	Hysteresis Index (HI)					
	Alfa Fiber	Cactus Fiber	Palm Fiber	Acacia Bark	Eucalyptus Bark	Zeal Oak Bark
5	0.852	0.977	0.982	0.904	0.869	1
10	0.907	0.956	0.961	0.914	0.895	1
20	0.935	0.855	0.918	0.921	0.903	0.996
40	0.973	0.390	0.748	0.932	0.914	0.943
80	0.979	-0.221	-0.248	0.938	0.919	0.914
100	0.985	-1.546	-1.281	0.957	0.936	0.824
Average values	0.938	0.235	0.429	0.928	0.906	0.946

Table 4 shows that, as happened regarding the fitting of the adsorption data, the desorption experimental results were well-described by both the Temkin model (with R^2 values ranging from 0.984 to 1.00) and the Sips model (R^2 ranging from 0.918 to 0.995).

Table 4. Values corresponding to the fitting of the experimental data (referred to MON desorption from the six bio-adsorbents) to the parameters of the Freundlich, Langmuir, Linear, Sips, and Temkin models. K_F ($L^n \mu\text{mol}^{1-n} \text{kg}^{-1}$); K_L ($L \text{kg}^{-1}$); q_m ($\mu\text{mol kg}^{-1}$); K_d ($L \text{kg}^{-1}$); K_s ($L \text{kg}^{-1}$); K_t ($L \text{g}^{-1}$); b_t (J/mol). R^2 : coefficient of determination; -: error too high for fitting.

		Alfa Fiber	Cactus Fiber	Palm Fiber	Acacia Bark	Eucalyptus Bark	Zeal Oak Bark
Freundlich model	K_F	0.627	-	17.638	2.685	-	-
	Error	0.263	-	2.143	0.519	-	-
	n	0.144	-	0.045	2.732	3.112	0.769
	Error	0.021	-	0.015	0.331	0.301	0.180
	R^2	0.737	-	0.892	0.719	0.741	0.868
Langmuir model	K_L	0.204	0.009	0.049	0.06	0.121	0.070
	Error	0.001	0.00	0.022	0.03	0.042	0.001
	q_m	281.36	443.21	324.65	270.58	254.36	178.12
	Error	32.02	97.46	65.13	104.70	123.23	54.82
	R^2	0.653	0.573	0.465	0.705	0.713	0.745
Linear model	K_d	0.641	6.210	0.955	0.423	0.418	0.162
	Error	0.182	0.521	0.026	0.072	0.068	0.029
	R^2	0.625	0.752	0.832	0.721	0.789	0.727
Sips model	K_s	0.875	-	-	-	-	0.052
	Error	0.00	-	-	-	-	0.0021
	n	0.872	0.445	1.972	0.582	0.673	0.341
	Error	0.00	0.012	0.052	0.00	0.00	0.001
	q_m	59.60	64.211	175.73	25.195	28.012	6.055
	Error	11.00	15.022	23.06	19.540	10.332	2.013
R^2	0.918	0.950	0.934	0.932	0.987	0.995	
Temkin model	K_t	0.381	1.292	2.887	1.022	1.307	0.077
	Error	0.049	0.011	0.153	0.142	0.062	0.010
	b_t	0.405	0.532	0.112	0.311	0.285	0.028
	Error	0.155	0.213	0.003	0.101	0.031	0.00
	R^2	0.998	0.989	0.984	1.00	1.00	0.993

4. Discussion

4.1. MON Adsorption

Most of the adsorption curves included in Figure 2 are L-type, according to Giles et al. [56], while those obtained for alfa fiber and, especially, for eucalyptus bark and acacia bark, can be considered type H, which are a special case of L-type curves, indicating that the adsorbent surface has a high affinity for the solute [57]. A decreasing slope with increasing concentration is indicative of this type of curve and is explained by the decrease in adsorption sites available on the adsorbent [58]. Generally, these curves exhibit non-linearity and concavity, suggesting that at low C_{eq} values there is a strong affinity for the bio-adsorbents, resulting in most of the pollutant being adsorbed in almost all the samples. It is important to note that in the case of zeon oak bark adsorption curves have a higher tendency to linearity, although they can also be considered type L, but with a much lower slope compared to those of alfa fiber and both acacia and eucalyptus barks.

As shown in Figure 3, for added concentrations ranging from 40 to 100 $\mu\text{mol L}^{-1}$, a decrease in the adsorption percentages is evidenced, which would be due to the adsorption sites in the bio-adsorbents gradually becoming saturated as higher concentrations of antibiotic are added [59]. Note that the percentages remain high (>90%) for acacia and eucalyptus barks, and for alfa fiber (>76.6%). These adsorption percentages indicate the strong affinity of the antibiotic for acacia and eucalyptus barks, and for alfa fiber, at all the concentrations added (with mean values of 92.6%, 95.9%, and 97.0%, respectively), while the other bio-adsorbents show percentages lower than 40% from 40 $\mu\text{mol L}^{-1}$ of antibiotic added. In relation to previous studies dealing with MON adsorption, Sassman and Lee [6] indicated that MON has the potential to be adsorbed on soils of varying physicochemical composition, with and without manure amendment, and the analysis of drainage water indicated that soil attenuation post-land application would significantly decrease the amount of MON entering the surface water.

From a structural perspective, carboxylic ionophores such as MON are aliphatic chains that bear five cyclic ether rings, with a carboxylic group on one end and with one or more hydroxyl groups on the other end [60] (Figure 1). Overall, the specific adsorption behavior of this ionophore antibiotic is influenced by the type and arrangement of these functional groups within its chemical structure, as well as by the properties of the adsorbent surface. According to the literature, it is assumed that ionophores are generally found in different environmental compartments (soil, water, and sediment), at a wide range of concentrations [16,61,62]. Several authors have found MON in surface waters, such as Bak and Björklund [16], who reported mean concentrations around 20 ng L^{-1} , or in streams of the southern Pampas, Argentina [62]. Hussain et al. [15] indicate that the persistence of MON in surface water was primarily dependent on the pH values in the affected environment and on its acidic pK_a values. Hafner et al. [11] reported the transport of MON to shallow groundwater after irrigation with dairy lagoon water. Bak and Björklund [16] detected the presence of MON molecules in soils at a concentration of 8 $\mu\text{g kg}^{-1}$. Although there are few studies on the uptake of this antibiotic by crops, Hilaire et al. [63] reported it for grassland species. This contaminant can further pass through the food chain to animals and humans.

Soil parameters such as pH, organic matter, or eCEC have been indicated to be of fundamental relevance in the behavior and fate of antibiotics once they are released into the environment [64,65]. Furthermore, the high values of porosity, moisture content, and swelling indices can enhance the adsorption capacities of materials used as antibiotic adsorbents [43,66]. In the current work, the highest adsorption efficiency corresponded to the sorbents that had a lower pH (Figure S4, Supplementary Material) and ash content (Table 1), higher OM, porosity, SI, H%, and eCEC levels, and more exchangeable Ca and Na (alfa fiber, acacia bark, and eucalyptus bark) (Table 1). The OM present at high percentages in all the studied bio-adsorbents, at the pH values of these materials (between 4.9 and 7.4), will mainly present a negative charge, mostly in their carboxylic groups, that have an acidic pK_a , which can ionize, forming carboxylate ions (RCOO^-) in aqueous solutions. In relation

to the electrical charge of MON, most of the experiments that have been carried out dealing with pK_a calculation have been performed in organic solvents or in solvent/water mixtures, giving a $pK_a = 6.4\text{--}6.7$, but these results would be difficult to apply to aqueous media [60]; in this sense, the authors of the latter research obtained a pK_a value = 4.5 in water, and, considering this pH and those of the bio-adsorbents (all above 4.5), MON would tend to become negatively charged, with which it could join the organic radicals of the positively charged bio-adsorbents; however, the binding to carboxylic groups would be carried out through a cationic bridge, which could be a frequent mode of interaction between MON and organic groups, as noted by Hansima et al. [67]. In relation to this, Ca^{2+} is known for its implication in the adsorption process where it can act as a bridge between the adsorbent surface and adsorbates such as antibiotics [68]. In addition to that commented for Ca^{2+} , several authors have indicated that MON has a high affinity for Na^+ [6,69]. Sun et al. [60] confirmed that the complexation of MON with Na^+ (Figure S5, Supplementary Material) is approximately one order of magnitude more favorable than with potassium ions, both in water and in methanol. The higher exchangeable Na^+ (and Ca^{2+}) contents of some of the sorbents used in the current research (alfa fiber, acacia bark, and eucalyptus bark) would contribute to justify their sorption capacity.

In view of the above, MON adsorption onto the studied bio-adsorbents could take place through different mechanisms, which could act simultaneously. One of the mechanisms is electrostatic attraction between the negative charges generated on the surface of the antibiotic at $pH > pK_a$ and the positive ones that appear in certain protonated amine groups ($-NH_3^+$) of the abundant organic matter present in all the bio-adsorbents under study. In fact, positive charges would be more relevant in those bio-adsorbents having higher organic matter contents and lower pH values, such as acacia and eucalyptus bark, and alfa fibers (Table 1). These three bio-adsorbents also show the highest acidity considering the pH in the equilibrium solution of the adsorption process (Table S2, Supplementary Material).

Another adsorption mechanism would make use of a cationic bridge (especially using Na^+ and Ca^{2+}) between the negative charges of the antibiotic and the negative charges that appear at pH values above 5 in certain organic functional groups such as carboxylic acids ($-COO^-$). All this justifies that the three bio-adsorbents with more acidic pH, more organic matter and eCEC levels, and more exchangeable Na^+ and Ca^{2+} (and less K^+ and Mg^{2+}) are the most effective at retaining MON, specifically adsorbing more than 76.5% of the amount added, even when using the highest antibiotic concentrations. In addition, Hansima et al. [67] indicate that MON has a hydrophobic nature and a great tendency to form colloidal bonds (considering soil environments), the main adsorption mechanisms being cation bridging, metal complexation, and hydrophobic interactions with OM.

Regarding the current research, other types of interactions that are possible involve hydrogen bonds between different oxygen-bearing functional groups, such as the ether groups ($-O-$) of MON and phenolic or carboxylic functional groups of bio-adsorbents.

The scarcity of previous research on MON adsorption onto biomaterials like forest bio-adsorbents complicates comparisons with the current study. Alternatively, and dealing with edaphic environments, Hussain and Prasher [70] assessed MON adsorption on sandy clay loam, and sandy soils, under varying pH conditions and organic matter contents, also finding greater MON affinity for soils with lower pH and higher organic matter content. Furthermore, several studies that used bio-adsorbents and different pollutants, such as eucalyptus bark powder for dyes [71] or palm fiber for cephalixin [72], mentioned the role of aromatic compounds on their adsorption capacities toward contaminants. Additionally, tannins present in bio-adsorbents derived from trees and plants can be important for the adsorption process, helping in establishing bindings between pollutants and adsorbent surfaces [73].

4.2. Fitting to Adsorption Models

In the current research, for all the tested bio-adsorbents, the Temkin and Langmuir models fit well the experimental adsorption data (with $R^2 \geq 0.968$ and ≥ 0.934 , respectively),

while the Sips model shows a somehow poorer fit ($R^2 \geq 0.869$). In the case of the Freundlich model the value was $R^2 \geq 0.723$ is obtained, whereas the worst corresponded to the Linear model ($0.578 \leq R^2 \leq 0.634$) (Table 2).

The fact that the Temkin model gives the best fitting for all the bio-adsorbents here studied would suggest that adsorption is taking place mainly by means of electrostatic attractions between charges of different signs of the antibiotic and the bio-adsorbents [2], which underscores the significance of chemisorption processes [74]. Moreover, Table 2 shows that the highest Kt values (oscillating between 0.223 and 4.219 L g⁻¹) and bt values (ranging between 0.231 and 6.765 J/mol), corresponded to eucalyptus and acacia barks, followed by alfa fiber, which imply a more efficient adsorption process and a stronger affinity between these bio-adsorbents and the pollutant (adsorption energetically favorable). However, the lower Kt and bt values observed for both cactus and palm fibers, which have the lowest adsorption, compared to the other bio-adsorbents, suggest lower interaction between the adsorbate molecules and these adsorbents. Generally, the fitting of adsorption data to the Temkin model shows a linear decrease in adsorption energy with surface occupation, which is related to adsorbent-adsorbate interactions [75].

Regarding the Langmuir model, the maximum adsorption capacity (q_m) was 1046.1 $\mu\text{mol kg}^{-1}$ (for eucalyptus bark) (Table 2), which was in agreement with the measured data (1123.9 $\mu\text{mol kg}^{-1}$ for eucalyptus bark) (Figures 2 and 3). Acacia bark and alfa fiber also show high q_m scores ($>950 \mu\text{mol kg}^{-1}$), with the lowest value obtained for zean oak bark (527.9 $\mu\text{mol kg}^{-1}$), in agreement with the amounts adsorbed in the experiment. With regards to K_L (the constant related to the affinity of the binding sites and energy of adsorption [76]), its highest values were associated to eucalyptus and acacia barks, as well as to alfa fiber (0.319, 0.276, and 0.149 L kg⁻¹, respectively) (Table 2), suggesting that there is a high affinity between these bio-adsorbents and MON. In this regard, the K_L values for these materials were higher than those reported in a previous investigation conducted by Mirizadeh et al. [77], who studied the adsorption of other antibiotics like tetracycline and ciprofloxacin using raw palm waste as adsorbent. In the current research, both cactus and palm fibers, along with zean oak bark, had lower K_L values, around 0.069, 0.043, and 0.082 L kg⁻¹, which are consistent with those obtained for oak ash and pine bark referred to other antibiotics like ciprofloxacin ($K_L = 0.05 \text{ L kg}^{-1}$) and trimethoprim ($K_L = 0.03 \text{ L kg}^{-1}$) [78]. Existing a good fit of experimental data to the Langmuir model, in such cases the adsorption process appears to be dominated by chemical and monolayer adsorption on a surface, featuring a finite number of identical and energetically equal sites, which would explain the decrease in the adsorption percentage as the added concentration increases [79,80], being a chemical adsorption mechanism primarily influenced by strong π - π interactions through electrostatic attraction and physical retention [81] and leading to more effective MON adsorption onto the bio-adsorbents.

Concerning the Sips model, the values of the Sips adsorption constant (K_S), which is related to the affinity of the adsorbate towards the adsorbent surface [49], ranged from 0.187 to 6.201 L kg⁻¹, with the highest scores found for eucalyptus bark, acacia bark, and alfa fiber (Table 2). The n parameter of the Sips model typically indicates the degree of heterogeneity in the adsorption system. When n is equal to 1, the Sips isotherm returns to the Langmuir isotherm, predicting homogeneous adsorption. On the other hand, the deviation of the n value from 1 approximates the fit to a Freundlich isotherm, indicating interactions with heterogeneous surfaces [49,82]. In the current research, n ranged between 0.173 and 2.754, with the highest values (greater than 1) corresponding, again, to eucalyptus bark, acacia bark, and alfa fiber. Values of n greater than 1 would indicate that the adsorbed molecules have a strong affinity towards adsorbent sites [83], and this would coincide with the greater adsorption capacity of these three bio-adsorbents.

In the Freundlich model, the linearity index (n) can be seen as indicative of the reactivity of the active sites in the adsorbent [84]. Values of n greater than 1 would correspond to sites of high adsorption energy, with high accessibility of the antibiotic to the surface of the adsorbent [84,85]. It is shown that $n > 1$ for eucalyptus bark, acacia bark, and alfa

fiber (2.68, 2.48, and 1.41, respectively). However, for the rest of the materials (cactus fiber, palm fiber, and zein oak bark), the values of n are clearly lower than 1 (0.21 to 0.45), which would indicate that there is a limitation in the specific adsorption sites available on the surface of the sorbents. This would be related to a non-linear and concave adsorption curve (Figure 2), evidencing the greater difficulty in adsorption as the antibiotic concentration increases, because the high-energy sites are those that are occupied first [86,87]. On the other hand, the Freundlich constant, K_F , related to the degree of interaction between the antibiotic and the adsorbents (the higher this value, the higher the adsorption intensity) [88], presents the following sequence: eucalyptus bark > acacia bark > alfa fiber > zein oak bark > cactus fiber > palm fiber. This sequence agrees with the adsorption results obtained for the different bio-adsorbents (Figure 3).

4.3. Scatchard Plots Analysis

Considering the sorption of antibiotic molecules onto various adsorbents, it is well-known that bio-adsorbent materials can interact with antibiotic molecules through multiple mechanisms, such as ion exchange, hydrogen bonding, and complex formation. Table S3 (Supplementary Material) shows the results of Scatchard parameters and plots. Also, the Scatchard plots obtained for the six bio-adsorbents under investigation are shown in Figure S2 (Supplementary Material). These kinds of plots are typically used to assess receptor affinity for ligands, identify the number of binding sites, and calculate binding constants (K_b) [50]. R^2 values across the data range may indicate nonspecific or multi-type interactions between adsorbate molecules and surface sites. The overall R^2 values were used to discuss the results, with R^2 (L) and R^2 (H) values noted on the Scatchard plots (Figure S2, Supplementary Material). In the current work, the R^2 values calculated were always higher than 0.805 (except for the cactus and palm fibers, with R^2 equal to 0.7 and 0.61, respectively), which indicates that the presence of nonspecific interactions is higher for most of the sorbent materials than for the cactus and palm fibers, being the highest the ones obtained for eucalyptus and acacia barks (0.968 and 0.960, respectively) and for alfa fiber (0.952). In addition, the Scatchard plots obtained for cactus and palm fibers, as well as for zein oak bark, can be considered as concave curves that are associated with a negative cooperative adsorption phenomenon, as well as to surface heterogeneity [89,90]. In contrast, for acacia and eucalyptus barks, and alfa fiber, the showed curves were considered as convex, indicating positive cooperative phenomena, meaning that initial adsorption occurs with low affinity, but the adsorbate becomes a likely site for subsequent adsorption.

Note that the observed deviations from the linearity in the Scatchard plots of MON adsorption onto the six bio-adsorbents here studied are attributed to different affinities of the binding sites toward MON molecules. Consequently (although needing complementary studies, such as FTIR analyses to make it evident), it could be considered that the carboxyl groups (which had relatively low pK_a values) of adsorbent materials (both fibers and barks), especially those adsorbing more MON, and exhibiting suitable conformations for antibiotic binding, may potentially intervene in the main high-affinity (strong) binding sites, whereas phenolic groups exhibiting relatively high pK_a values are assumed to be the main low-affinity (weak) binding sites (Figure S2, Supplementary Material).

Furthermore, as shown in Table S3 (Supplementary Material), the values of the binding constants (K_b) and the maximum capacities (Q_m^S) of high- and low- affinity levels were separately calculated. According to Table S3 (Supplementary Material), it can be seen that the obtained K_b and Q_m^S values were very close to those calculated for the Langmuir model (except for cactus and palm fibers). Based on these results, the adsorption of MON onto the three natural barks and alfa fiber was primarily attributed to the high-affinity binding sites. Conversely, the interactions between the MON molecules and the cactus/palm fibers were governed by the low-affinity binding sites, and it was believed that the binding involving the complex formations had actually occurred through complex formation [50]. Thus, the low-affinity binding is caused by the complex formation, whereas the high-affinity binding

is associated with the ion exchange mechanism in the MON adsorption onto natural barks and alfa fiber along with the other mechanisms cited above.

4.4. MON Desorption

Regarding the results shown in Figure 4, the MON desorption values obtained for the three barks were lower than those reported in a previous study for clarithromycin using pine bark as sorbent, where percentages of 15% were reached when adding $100 \mu\text{mol L}^{-1}$ [91].

The influence of the increase in the initial MON concentration added on rising desorption was clearly observed for the bio-adsorbents with the lowest removal efficiency (cactus and palm fiber), while the relation was less marked in the case of zean oak bark (Figure 4). However, for the most efficient bio-adsorbents (both eucalyptus and acacia barks, and alfa fiber), this is not the case, as a slight decrease in the desorption percentage is observed when the antibiotic dose is increased. The lower desorption scores of the latter bio-adsorbents may be related to some of their physicochemical characteristics, especially their pH and OM content, which would facilitate dissociation of organic functional groups, allowing a strong binding of the antibiotic that hinders its desorption. Similar conclusions were reported by Hu et al. [92] when studying sulfadiazine and sulfamethoxazole in different agricultural soils. Additionally, Jeong et al. [93] indicated that adding softwood and hardwood biochar as low-cost adsorbents to soils considerably decreased the desorption of the macrolide antibiotic tylosin. In the current research, we found lower desorption percentages for the three barks and alfa fiber compared to those previously reported for cefuroxime desorption from eucalyptus leaves and pine bark [59] or compared to sulfonamides from different agricultural soils [25]. This would encourage additional in-depth studies focused on using the bio-adsorbents here investigated as soil amendments.

Considering the hysteresis values (HI, Table 3), the scores were relatively high for most of the bio-adsorbents here studied, reflecting a slow desorption process [86,94], except for cactus and palm fibers.

In relation to fitting of the desorption experimental data to different models (Table 4), in the Temkin equation the $bt_{(\text{des})}$ values (which were in the range 0.028–0.532) were consistently lower than those of the $bt_{(\text{ads})}$ parameter (0.231–6.765), except for both palm and cactus fibers, suggesting the low reversibility of the bonds [95]. This fact complements the information derived from Sips's $K_{S(\text{des})}$ values, which were typically lower than those of $K_{S(\text{ads})}$ (Table 2). Meanwhile, the q_m values obtained from the Sips model (ranging between 6.0 and $175.7 \mu\text{mol kg}^{-1}$) were consistent with those observed for the real desorption data (oscillating between 9.4 and $172.9 \mu\text{mol kg}^{-1}$) obtained in the current study (Figure 4). In contrast, the q_m values of the Langmuir model (oscillating between 178.1 and $443.2 \mu\text{mol kg}^{-1}$) were clearly higher than those observed for the real desorption data (Table 4). In fact, a good fit was not found for this model, with R^2 not exceeding values of 0.745 in all cases (Table 4). In the same way, the desorption data did not fit either the Freundlich model or the Linear model. Additional research in this field, as well as in other related aspects of soil and environment sciences, would be a must for environmental and public health protection, and also for promoting recycling, crop sustainability, and the circular economy [96,97].

Further in-depth research is required to clarify the specific mechanisms involved in both the MON adsorption and desorption processes on the studied sorbent materials. This research is planned for the near future and will involve complementary analytical techniques, such as FTIR analysis of samples before and after adsorption and desorption, as well as other specialized analyses currently being refined and implemented. Additionally, super-computational modeling will be employed to investigate the interactions between the pollutants and the sorbents across a range of environmental conditions [51].

5. Conclusions

Eucalyptus and acacia barks, along with alfa fiber, were the most efficient bio-adsorbents among those tested in the current research for MON retention (with adsorption always >76.6%). These three bio-adsorbents have the lowest pH values, as well as the highest organic matter contents and eCEC scores, with higher levels of exchangeable Na and Ca (and less exchangeable K and Mg). The Temkin model was the most appropriate for explaining MON adsorption onto the six bio-adsorbents ($R^2 \geq 0.968$), indicating the relevance of chemisorption processes based on strong electrostatic interactions between positive and negative charges. Furthermore, the good fit of the Langmuir model to the adsorption experimental data ($R^2 \geq 0.934$) suggests the dominance of chemical and monolayer adsorption on surfaces with finite, energetically equal sites, as evidenced by the significant decrease in adsorption efficiency observed at higher MON concentrations added. The bio-adsorbents that present the highest MON adsorption (the three barks and alfa fiber), desorb a low proportion of the previously retained antibiotic, indicating a low reversibility for the process. In relation to this, the values of the hysteresis index for these bio-adsorbents were clearly lower than those obtained for the rest of the materials, with a greater tendency towards desorption of the antibiotic by cactus and palm fibers. Valorizing both eucalyptus and acacia barks, along with alfa fiber, would lead to a more efficient use of these by-products, potentially offering environmental and economic benefits with regards to environmental remediation in MON-polluted compartments. For the future, it would be interesting to perform more in-depth studies, in a variety of experimental and environmental conditions, focused on the removal of MON and other anticoccidials, as well as of other emerging pollutants, using the low-cost bio-adsorbents here assessed, which could be raw or modified when justified. This would be in line with the promotion of recycling and sustainability, as well as with environmental and public health protection.

Supplementary Materials: The following supporting information can be downloaded at: <https://www.mdpi.com/article/10.3390/toxics12080606/s1>, Table S1: Main physicochemical characteristics of monensin (MON). K_{oc} : organic carbon partition coefficient; K_{ow} : octanol-water coefficient of partition; K_c : equilibrium constant. Table S2: Variation of pH values in aqueous media containing MON and the studied bio-adsorbents. Table S3: Scatchard parameters for monensin adsorption onto the six studied bio-adsorbents. Figure S1: HPLC example chromatograms. Figure S2: Scatchard plots derived for adsorption data obtained at natural pH for the six studied biomaterials. Figure S3: pH_{PZC} of the six bio-adsorbents ($T = 25 \pm 2$ °C). Figure S4: Effect of the initial pH on MON adsorption onto the bio-adsorbents used. Figure S5: Illustration of the pseudo-cyclic conformation of the MON-Na complex (adapted from [38]). References [98–104] are cited in the supplementary materials.

Author Contributions: Conceptualization, E.Á.-R., A.N.-D., M.J.F.-S., M.I. and S.H. (Sonia Hamami); methodology, E.Á.-R., A.N.-D., M.J.F.-S., A.B. and M.I.; software, S.H. (Samiha Hamdi), A.M.-G., R.C.-D. and A.B.; validation, E.Á.-R., A.N.-D., M.J.F.-S., A.B. and M.I.; formal analysis, S.H. (Samiha Hamdi), A.M.-G., R.C.-D. and A.B.; investigation, S.H. (Samiha Hamdi), A.M.-G., R.C.-D. and A.B.; resources, E.Á.-R., A.N.-D., M.J.F.-S. and M.I.; data curation, E.Á.-R., A.N.-D., M.J.F.-S., A.B. and M.I.; writing—original draft preparation, E.Á.-R., A.N.-D., M.J.F.-S., A.B. and M.I.; writing—review and editing, A.N.-D.; visualization, E.Á.-R., A.N.-D., M.J.F.-S., A.B. and M.I.; supervision, E.Á.-R., A.N.-D., M.J.F.-S. and M.I.; project administration, E.Á.-R. and A.N.-D.; funding acquisition, E.Á.-R. and A.N.-D. All authors have read and agreed to the published version of the manuscript.

Funding: This research was funded by Spanish “Agencia Estatal de Investigación” (State Investigation Agency) [grant number PID2021-122920OB-C21] and the Tunisian Ministry of Higher Education and Scientific Research.

Institutional Review Board Statement: Not applicable.

Informed Consent Statement: Not applicable.

Data Availability Statement: Experimental data could be provided after specific request and after receiving authorization from the funding agency.

Acknowledgments: The authors wish to express their gratitude to the members of the university of Kairouan (Tunisia), which supported part of this work (work-study scholarship), as well as of the members of the Department of Soil Science and Agricultural Chemistry, Engineering Polytechnic School, University of Santiago de Compostela (Spain), and the members of FST Sidi Bouzid (Tunisia) also collaborating and supporting this work.

Conflicts of Interest: The authors declare no conflicts of interest. The funders had no role in the design of the study; in the collection, analyses, or interpretation of data; in the writing of the manuscript; or in the decision to publish the results.

References

1. Chee-Sanford, J.C.; Mackie, R.I.; Koike, S.; Krapac, I.G.; Lin, Y.F.; Yannarell, A.C.; Maxwell, S.; Aminov, R.I. Fate and transport of antibiotic residues and antibiotic resistance genes following land application of manure waste. *J. Environ. Qual.* **2009**, *38*, 1086–1108. [CrossRef]
2. Gao, Y.; Li, Y.; Zhang, L.; Huang, H.; Hu, J.; Shah, S.M.; Su, X. Adsorption and removal of tetracycline antibiotics from aqueous solution by graphene oxide. *J. Colloid. Interface Sci.* **2012**, *368*, 540–546. [CrossRef] [PubMed]
3. Walsh, T.R.; Gales, A.C.; Laxminarayan, R.; Dodd, P.C. Antimicrobial Resistance: Addressing a global threat to humanity. *PLoS Med.* **2023**, *20*, e1004264. [CrossRef]
4. Kumar, K.; Gupta, S.C.; Chander, Y.; Singh, A.K. Antibiotic use in agriculture and its impact on the terrestrial environment. *Adv. Agron.* **2005**, *87*, 1–54. [CrossRef]
5. Ghasemi-Sadabadi, M.; Ebrahimnezhad, Y.; Shaddel-Tili, A.; Bannapour-Ghaffari, V.; Saemi Peste-Bigelow, S. Comparison of using ionophore and non-ionophore coccidiostats on performance, carcass characteristics, blood biochemical parameters and gut microbial flora in broiler chickens. *Iran. J. Appl. Anim. Sci.* **2020**, *10*, 693–704.
6. Sassman, S.A.; Lee, L.S. Sorption and degradation in soils of veterinary ionophore antibiotics: Monensin and lasalocid. *Environ. Toxicol. Chem.* **2007**, *26*, 1614–1621. [CrossRef]
7. Ekinci, I.B.; Chłódowska, A.; Olejnik, M. Ionophore toxicity in animals: A review of clinical and molecular aspects. *Int. J. Mol. Sci.* **2023**, *24*, 1696–1710. [CrossRef]
8. Food and Drug Administration. New Animal Drugs; Monensin. Federal Register 69, 68783–68784. Available online: <http://www.fda.gov/ohrms/dockets/98fr/04-26091.pdf> (accessed on 1 June 2024).
9. Furtula, V.; Huang, L.; Chambers, P.A. Determination of veterinary pharmaceuticals in poultry litter and soil by methanol extraction and liquid chromatography-tandem mass spectrometry. *J. Environ. Sci. Health* **2009**, *44*, 717–723. [CrossRef] [PubMed]
10. Sun, P.; Barmaz, D.; Cabrera, M.L.; Pavlostathis, S.G.; Huang, C.H. Detection and quantification of ionophore antibiotics in runoff, soil and poultry litter. *J. Chromatogr. A* **2013**, *1312*, 10–17. [CrossRef]
11. Hafner, S.C.; Harter, T.; Parikh, S.J. Evaluation of monensin transport to shallow groundwater after irrigation with dairy lagoon water. *J. Environ. Qual.* **2016**, *45*, 480–487. [CrossRef]
12. Capleton, A.C.; Courage, C.; Rumsby, P.; Holmes, P.; Stutt, E.; Boxall, A.B.A.; Levy, L.S. Prioritizing veterinary medicines according to their potential indirect human exposure and toxicity profile. *Toxicol. Lett.* **2006**, *163*, 213–223. [CrossRef]
13. Rokka, M.; Jestoi, M.; Peltonen, K. Trace level determination of polyther ionophores in feed. *BioMed Res. Int. J.* **2013**, *2013*, 151363. [CrossRef]
14. El Sayed, E.M.; Prasher, S.O. Fate and transport of monensin in the presence of nonionic surfactant Brij35 in soil. *Sci. Total Environ.* **2014**, *490*, 629–638. [CrossRef] [PubMed]
15. Hussain, S.A.; Prasher, S.O.; Patel, R.M. Removal of ionophoric antibiotics in free water surface constructed wetlands. *Ecol. Eng.* **2012**, *41*, 13–21. [CrossRef]
16. Bak, S.A.; Björklund, E. Occurrence of ionophores in the Danish environment. *Antibiotics* **2014**, *3*, 564–571. [CrossRef]
17. Nath, K. *Membrane Separation Processes*, 2nd ed.; Raj Press: New Delhi, India, 2017.
18. Omufere, L.O.; Maseko, R.; Olowoyo, J.O. Occurrence of antibiotics in wastewater from hospital and conventional wastewater treatment plants and their impact on the effluent receiving rivers: Current knowledge between 2010 and 2019. *Environ. Monit. Assess.* **2022**, *194*, 306–320. [CrossRef]
19. Ajala, O.A.; Akinawo, S.O.; Bamişay, A.; Adedipe, D.T.; Adesina, M.O.; Okon-Akan, O.A.; Adebuseyi, T.A.; Ojedokun, A.T.; Adegoke, K.A.; Bello, O.S. Adsorptive removal of antibiotic pollutants from wastewater using biomass/biochar-based adsorbents. *Royal Soc. Chem. Adv.* **2023**, *13*, 4678–4712. [CrossRef]
20. Ding, H.; Wu, Y.; Zou, B.; Lou, Q.; Zhang, W.; Zhong, J.; Lu, L.; Dai, G. Simultaneous removal and degradation characteristics of sulfonamide, tetracycline, and quinolone antibiotics by laccase-mediated oxidation coupled with soil adsorption. *J. Hazard. Mater.* **2016**, *307*, 350–358. [CrossRef]
21. Russell, J.N.; Yost, C.K. Alternative, environmentally conscious approaches for removing antibiotics from wastewater treatment systems. *Chemosphere* **2021**, *263*, 128177–128189. [CrossRef]
22. Juela, D.M. Promising adsorptive materials derived from agricultural and industrial wastes for antibiotic removal: A comprehensive review. *Separ. Purif. Technol.* **2022**, *284*, 120286–120296. [CrossRef]

23. Errais, E.; Duplay, J.; Darragi, F. Textile dye removal by natural clay—Case study of Fouchana Tunisian clay. *Environ. Technol.* **2010**, *31*, 373–380. [CrossRef] [PubMed]
24. Tran, V.S.; Nguyen, K.M.; Nguyen, H.T.; Stefanakis, A.I.; Nguyen, P.M. Food processing wastes as a potential source of adsorbent for toxicant removal from water. *Circul Econ. Sustain.* **2022**, *2*, 491–507. [CrossRef]
25. Conde-Cid, M.; Fernández-Calviño, D.; Núñez-Delgado, A.; Fernández-Sanjurjo, M.J.; Arias-Estévez, M.; Álvarez-Rodríguez, E. Influence of mussel shell, oak ash, and pine bark on the adsorption and desorption of sulfonamides in agricultural soils. *J. Environ. Manag.* **2020**, *261*, 110221–110233. [CrossRef] [PubMed]
26. Zhang, F.; Wang, J.; Tian, Y.; Liu, C.; Zhang, L.; Cao, L.; Zhou, Y.; Zhang, S. Effective removal of tetracycline antibiotics from water by magnetic functionalized biochar derived from rice waste. *Environ. Pollut.* **2023**, *330*, 121681–121693. [CrossRef]
27. Míguez-González, A.; Cela-Dablanca, R.; Barreiro, A.; Castillo-Ramos, V.; Sánchez-Polo, M.; López-Ramón, M.V.; Fernández-Sanjurjo, M.J.; Álvarez-Rodríguez, E.; Núñez-Delgado, A. Current Data on Environmental Problems due to Ionophore Antibiotics Used as Anticoccidial Drugs in Animal Production, and Proposal of New Research to Control Pollution by Means of Bio-Adsorbents and Nanotechnology. In *Planet Earth: Scientific Proposals to Solve Urgent Issues*, 1st ed.; Núñez-Delgado, A., Ed.; Springer: Cham, Switzerland, 2024; pp. 241–261. [CrossRef]
28. Ben Rebah, F.; Siddeeg, S.M. Cactus an eco-friendly material for wastewater treatment: A review. *J. Mater. Environ. Sci.* **2017**, *8*, 1770–1782.
29. Hadjittofi, L.; Prodromou, M.; Pashalidis, I. Activated biochar derived from cactus fibres—Preparation, characterization and application on Cu(II) removal from aqueous solutions. *J. Bioresour. Technol.* **2014**, *159*, 460–464. [CrossRef]
30. Barka, N.; Abdennouri, M.; El Makhfouk, M.; Qourzal, S. Biosorption characteristics of cadmium and lead onto eco-friendly dried cactus (*Opuntia ficus indica*) clado des. *J. Environ. Chem. Eng.* **2013**, *1*, 144–149. [CrossRef]
31. Barka, N.; Ouzaoit, K.; Abdennouri, M.; El Makhfouk, M. Dried prickly pear cactus (*Opuntia ficus indica*) cladodes as a low-cost and eco-friendly biosorbent for dyes removal from aqueous solutions. *J. Taiwan Inst. Chem. Eng.* **2013**, *44*, 52–60. [CrossRef]
32. Prodromou, M.; Pashalidis, I. Copper(II) removal from aqueous solutions by adsorption on non-treated and chemically modified cactus fibres. *Water Sci. Technol.* **2013**, *68*, 2497–2504. [CrossRef]
33. Bennacer, L.; Benmammour, D.; Ahfir, N.D.; Alem, A.; Mignot, M.; Pantet, M. Potential of using Alfa grass fibers (*Stipa Tenacissima* L.) to remove Pb²⁺, Cu²⁺, and Zn²⁺ from an aqueous solution. *Environ. Technol.* **2022**, *104*, 1. [CrossRef]
34. Melliti, A.; Srivastava, V.; Kheriji, J.; Sillanpää, M.; Hamrouni, B. Date Palm Fiber as a novel precursor for porous activated carbon: Optimization, characterization and its application as Tylosin antibiotic scavenger from aqueous solution. *Surf. Interfaces* **2021**, *24*, 101047. [CrossRef]
35. Zafar, L.; Khan, A.; Kamran, U.; Park, S.J.; Bhatti, H.N. Eucalyptus (*camaldulensis*) bark-based composites for efficient Basic Blue 41 dye biosorption from aqueous stream: Kinetics, isothermal, and thermodynamic studies. *Surf. Interfaces* **2022**, *31*, 101897. [CrossRef]
36. Talhi, M.F.; Cheriti, A.; Belboukhari, N.; Agha, L.; Roussel, C. Biosorption of copper ions from aqueous solutions using the desert tree *Acacia raddiana*. *Desalination Water Treat.* **2010**, *21*, 323–327. [CrossRef]
37. Fox, R.L.; Kamprath, E.J. Phosphate sorption isotherms for evaluating the phosphate requirements of soils. *Soil. Sci. Soc. Am. J.* **1970**, *34*, 902–907. [CrossRef]
38. Lopes, N.P.; Stark, C.B.; Gates, P.J.; Staunton, J. Fragmentation studies on monensin A by sequential electrospray mass spectrometry. *Analyst* **2002**, *127*, 503–506. [CrossRef] [PubMed]
39. Nebot, C.; Iglesias, A.; Regal, P.; Miranda, J.M.; Fente, C.; Cepeda, A. A sensitive and validated HPLC–MS/MS method for simultaneous determination of seven coccidiostats in bovine whole milk. *Food Control* **2011**, *27*, 29–36. [CrossRef]
40. Peech, M. Methods of soil analysis for soil-fertility investigations. *US Dept Agr. Circ.* **1947**, *757*, 7–11.
41. Rodríguez-López, L.; Santás-Miguel, V.; Cela-Dablanca, R.; Núñez-Delgado, A.; Álvarez-Rodríguez, E.; Pérez-Rodríguez, P.; Arias-Estévez, M. Ciprofloxacin and Trimethoprim Adsorption/Desorption in Agricultural Soils. *Int. J. Environ. Res. Public Health* **2022**, *19*, 8426. [CrossRef] [PubMed]
42. Cela-Dablanca, R.; Barreiro, A.; Rodríguez-López, L.; Santás-Miguel, V.; Arias-Estévez, M.; Fernández-Sanjurjo, M.J.; Álvarez-Rodríguez, E.; Núñez-Delgado, A. Amoxicillin retention/release in agricultural soils amended with different bio-adsorbent materials. *Materials* **2022**, *15*, 3200. [CrossRef]
43. Hamdi, S.; Gharbi-Khelifi, H.; Barreiro, A.; Mosbahi, M.; Cela-Dablanca, R.; Brahmi, J.; Fernández-Sanjurjo, M.J.; Núñez-Delgado, A.; Issaoui, M.; Álvarez-Rodríguez, E. Tetracycline adsorption/desorption by raw and activated Tunisian clays. *Environ. Res.* **2024**, *242*, 117536–117548. [CrossRef]
44. Hamdi, S.; Mosbahi, M.; Issaoui, M.; Barreiro, A.; Cela-Dablanca, R.; Brahmi, J.; Tlili, A.; Jamoussi, F.; Fernández-Sanjurjo, M.J.; Núñez-Delgado, A.; et al. Experimental data and modeling of sulfadiazine adsorption onto raw and modified clays from Tunisia. *Environ. Res.* **2024**, *248*, 118309–118321. [CrossRef] [PubMed]
45. Conde-Cid, M.; Ferreira-Coelho, G.; Arias-Estévez, M.; Álvarez-Esmoris, C.; Carlos Nóvoa- Muñoz, J.; Núñez-Delgado, A.; Fernández-Sanjurjo, M.J.; Álvarez-Rodríguez, E. Competitive adsorption/desorption of tetracycline, oxytetracycline, and chlortetracycline on pine bark, oak ash, and mussel shell. *J. Environ. Manag.* **2019**, *250*, 109509–109519. [CrossRef] [PubMed]
46. Meng, Q.; Zhang, Y.; Meng, D.; Liu, X.; Zhang, Z.; Gao, P.; Lin, A.; Hou, L. Removal of sulfadiazine from aqueous solution by in-situ activated biochar derived from cotton shell. *Environ. Res.* **2020**, *191*, 110104–110111. [CrossRef]

47. Conde-Cid, M.; Ferreira-Coelho, G.; Fernández-Calviño, D.; Núñez-Delgado, A.; Fernández-Sanjurjo, M.J.; Arias-Estévez, M.; Álvarez-Rodríguez, E. Experimental data and model prediction of tetracycline adsorption and desorption in agricultural soils. *Environ. Res.* **2019**, *177*, 108607–108620. [CrossRef]
48. Scatchard, G. The attractions of proteins for small molecules and ions. *Ann. N. Y. Acad. Sci.* **1949**, *51*, 660. [CrossRef]
49. Roca Jalil, M.E.; Baschini, M.; Sapag, K. Removal of ciprofloxacin from aqueous solutions using pillared clays. *Materials* **2017**, *10*, 1345. [CrossRef]
50. Anirudhan, T.S.; Suchithra, P.S. Equilibrium, kinetic and thermodynamic modeling for the adsorption of heavy metals onto chemically modified hydrotalcite. *Indian J. Chem. Technol.* **2010**, *17*, 247–259.
51. Núñez-Delgado, A. Research on environmental aspects of retention/release of pollutants in soils and sorbents. What should be next? *Environ. Res.* **2024**, *251*, 118593. [CrossRef]
52. Núñez-Delgado, A. Avoiding basic mistakes when programming the use of artificial intelligence in soil and environmental science research. *Sci. Total Environ.* **2024**, *934*, 173310. [CrossRef]
53. Yaneva, Z.; Georgieva, N. Insights into Congo Red adsorption on agro-industrial materials—Spectral, equilibrium, kinetic, thermodynamic, dynamic and desorption studies. A review. *Int. Rev. Chem. Eng.* **2012**, *4*, 127–146.
54. Bonetto, L.R.; Ferrarini, F.; De Marco, C.; Crespoa, S.; Guéanb, R.; Giovanelaa, M. Removal of methyl violet 2B dye from aqueous solution using a magnetic composite as an adsorbent. *J. Water Process Eng.* **2015**, *6*, 11–20. [CrossRef]
55. Karoui, S.; Ben Arfi, R.; Fernández-Sanjurjo, M.J.; Núñez-Delgado, A.; Ghorbal, A.; Álvarez-Rodríguez, E. Optimization of synergistic biosorption of oxytetracycline and cadmium from binary mixtures on reed-based beads: Modeling study using Brouers-Sotolongo models. *Environ. Sci. Pollut. Res.* **2021**, *28*, 46431–46447. [CrossRef]
56. Giles, C.H.; Smith, D.; Huitson, A. A general treatment and classification of the solute adsorption isotherm I. *Theoretical. J. Colloid. Interface Sci.* **1974**, *47*, 755–765. [CrossRef]
57. Nazari, G.; Abolghasemi, H.; Esmaili, M. Batch adsorption of cephalixin antibiotic from aqueous solution by walnut shell-based activated carbon. *J. Taiwan. Inst. Chem. Eng.* **2016**, *58*, 357–365. [CrossRef]
58. Sipos, P. Searching for optimum adsorption curve for metal sorption on soils: Comparison of various isotherm models fitted by different error functions. *SN Appl. Sci.* **2021**, *3*, 387–400. [CrossRef]
59. Cela-Dablanca, R.; Nebot, C.; Rodríguez López, L.; Fernández-Calvino, D.; Arias-Estévez, M.; Núñez-Delgado, A.; Fernández-Sanjurjo, M.J.; Álvarez-Rodríguez, E. Efficacy of different waste and by-products from forest and food industries in the removal/retention of the antibiotic cefuroxime. *Processes* **2021**, *9*, 1151–1163. [CrossRef]
60. Sun, P.; Pavlostathis, S.G.; Huang, C.H. Estimation of environmentally relevant chemical properties of veterinary ionophore antibiotics. *Environ. Sci. Pollut. Res.* **2016**, *23*, 18353–18361. [CrossRef] [PubMed]
61. D’Alessio, M.; Durso, L.M.; Miller, D.N.; Woodbury, B.; Ray, C.; Snow, D.D. Environmental fate and microbial effects of MON, lincomycin, and sulfamethazine residues in soil. *Environ. Pollut.* **2019**, *246*, 60–68. [CrossRef]
62. Pérez, D.J.; Okada, E.; Iturburu, F.G.; De Gerónimo, E.; Cantón, G.; Aparicio, V.C.; Costa, J.L.; Menone, M.L. Monensin occurrence in surface water and its impact on aquatic biota in a stream of the southeast Pampas, Argentina. *Environ. Sci. Pollut. Res. J.* **2021**, *28*, 8530–8538. [CrossRef]
63. Hilaire, S.S.; Bellows, B.; Brady, J.A.; Muir, J.P. Oxytetracycline and monensin uptake by tifton 85 bermudagrass from dairy manure-applied soil. *Agronomy* **2020**, *10*, 468–484. [CrossRef]
64. Sassman, S.A.; Lee, L.S. Sorption of three tetracyclines by several soils: Assessing the role of pH and cation exchange. *Environ. Sci. Technol.* **2005**, *39*, 7452–7459. [CrossRef]
65. Albero, B.; Tadeo, J.L.; Escario, M.; Miguel, E.; Pérez, R.A. Persistence and availability of veterinary antibiotics in soil and soil-manure systems. *Sci. Total Environ.* **2018**, *643*, 1562–1570. [CrossRef] [PubMed]
66. Della, K.D.; Henini, G.; Laidani, Y. A biosorbent material from brahea edulis palm leaves—Application to amoxicillin adsorption. *Cellul. Chem. Technol.* **2023**, *57*, 903–910. [CrossRef]
67. Hansima, M.A.C.K.; Zvomuya, F.; Amarakoon, I. Fate of veterinary antimicrobials in Canadian prairie soils—a critical review. *Sci. Total Environ.* **2023**, *892*, 164387–164399. [CrossRef] [PubMed]
68. Parolo, M.E.; Avena, M.J.; Pettinari, G.R.; Baschini, M.T. Influence of Ca²⁺ on tetracycline adsorption on montmorillonite. *J. Colloid Interf. Sci.* **2012**, *368*, 420–426. [CrossRef]
69. Cox, B.G.; Truong, N.g.V.; Rzeszotarska, V.; Schneider, H. Rates and equilibria of alkali metal and silver ion complex formation with monensin in ethanol. *J. Amer Chem. Soc.* **1984**, *106*, 5965–5969. [CrossRef]
70. Hussain, S.A.; Prasher, S.O. Understanding the sorption of ionophoric pharmaceuticals in a treatment wetland. *Wetlands* **2011**, *31*, 563–571. [CrossRef]
71. Srivastava, R.; Rupainwar, D.C. Eucalyptus bark powder as an effective adsorbent: Evaluation of adsorptive characteristics for various dyes. *Desalin Water Treat.* **2009**, *11*, 302–313. [CrossRef]
72. Acelas, N.; Lopera, S.M.; Porras, J.; Torres-Palma, R.A. Evaluating the removal of the antibiotic cephalixin from aqueous solutions using an adsorbent obtained from palm oil fiber. *Molecules* **2021**, *26*, 3340–3356. [CrossRef]
73. Paksamut, J.; Boonsong, P. Removal of copper (II) ions in aqueous solutions using tannin-rich plants as natural bio-adsorbents. *IOP Conf. Series. Mat. Sci. Eng.* **2018**, *317*, 012058–012064. [CrossRef]
74. Biswas, K.; Saha, S.K.; Ghosh, U.C. Adsorption of fluoride from aqueous solution by a synthetic iron (III)–aluminum (III) mixed oxide. *Indust Eng. Chem. Res.* **2007**, *46*, 5346–5356. [CrossRef]

75. Boparai, H.K.; Joseph, M.; O'Carroll, D.M. Kinetics and thermodynamics of cadmium ion removal by adsorption onto nano zerovalent iron particles. *J. Hazard Mater.* **2011**, *186*, 458–465. [CrossRef]
76. Ahmadi, S.; Igwegbe, C.A. Removal of methylene blue on zinc oxide nanoparticles: Nonlinear and linear adsorption isotherms and kinetics study. *Sigma J. Eng. Nat. Sci.* **2020**, *38*, 289–303.
77. Mirzadeh, S.; Al Arni, S.; Elwaheidi, M.; Salih, A.A.M.; Converti, A.; Alberto Casazza, A. Adsorption of tetracycline and ciprofloxacin from aqueous solution on raw date palm waste. *Process Eng. (MMPE)* **2023**, *46*, 1957–1964. [CrossRef]
78. Míguez-González, A.; Cela-Dablanca, R.; Barreiro, A.; Rodríguez-López, L.; Rodríguez-Seijo, A.; Arias-Estévez, M.; Núñez-Delgado, A.; Fernández-Sanjurjo, M.J.; Castillo-Ramos, V.; Álvarez-Rodríguez, E. Adsorption of antibiotics on bio-adsorbents derived from the forestry and agro-food industries. *Environ. Res.* **2023**, *233*, 116360–116368. [CrossRef]
79. Nwakonobi, T.U.; Onoja, S.B.; Ogbaje, H. Removal of certain heavy metals from brewery wastewater using date palm seeds activated carbon. *Appl. Eng. Agric.* **2018**, *34*, 233–238. [CrossRef]
80. Wang, J.; Guo, X. Adsorption isotherm models: Classification, physical meaning, application and solving method. *Chemosphere* **2020**, *258*, 127279. [CrossRef]
81. Agboola, O.D.; Benson, N.U. Physisorption and chemisorption mechanisms influencing micro (nano) plastics-organic chemical contaminants interactions: A review. *Front. Environ. Sci.* **2021**, *9*, 678574. [CrossRef]
82. Nethaji, S.; Sivasamy, A.; Mandal, A.B. Adsorption isotherms, kinetics and mechanism for the adsorption of cationic and anionic dyes onto carbonaceous particles prepared from Juglans regia shell biomass. *Int. J. Environ. Sci. Technol.* **2013**, *10*, 231–242. [CrossRef]
83. Toth, J. *Adsorption*, 1st ed.; CRC Press: Boca Raton, FL, USA, 2002.
84. Conde-Cid, M.; Ferreira-Coelho, G.; Núñez-Delgado, A.; Fernández-Calviño, D.; Arias-Estévez, M.; Álvarez-Rodríguez, E.; Fernández-Sanjurjo, M.J. Competitive adsorption of tetracycline, oxytetracycline and chlortetracycline on soils with different pH value and organic matter content. *Environ. Res.* **2019**, *178*, 108669–108681. [CrossRef] [PubMed]
85. Bezerra, W.F.D.P.; Dognani, G.; Alencar, D.L.N.; Silva Parizi, M.P.; Boina, R.F.; Cabrera, F.C.; Job, A.E. Chemical treatment of sugarcane bagasse and its influence on glyphosate adsorption. *Matéria (Rio Jan.)* **2022**, *27*, e13142. [CrossRef]
86. Sukul, P.; Lamshöft, M.; Zühlke, S.; Spittler, M. Sorption and desorption of sulfadiazine in soil and soil-manure systems. *Chemosphere* **2008**, *73*, 1344–1350. [CrossRef]
87. Conde-Cid, M.; Fernández-Calviño, D.; Núñez-Delgado, A.; Fernández-Sanjurjo, M.J.; Arias-Estévez, M.; Álvarez-Rodríguez, E. Estimation of adsorption/desorption Freundlich's affinity coefficients for oxytetracycline and chlortetracycline from soil properties: Experimental data and pedotransfer functions. *Ecotox Environ. Safe* **2020**, *196*, 110584–110596. [CrossRef] [PubMed]
88. Kakaei, S.; Sattarzadeh Khameneh, E.; Rezazadeh, F.; Hosseini, M.H. Heavy metal removing by modified bentonite and study of catalytic activity. *J. Mol. Struct.* **2020**, *1199*, 126989–127011. [CrossRef]
89. Dahlquist, F.W. *The Meaning of Scatchard and Hill Plots, Methods of Enzymology*, Hirs, C.H.W., Timasheff, S.N., Eds.; Academic Press: New York, NY, USA, 1978; Volume 48, 270–299. [CrossRef]
90. Gerente, C.; Couespel du Mesnil, P.; Andrès, Y.; Thibault, J.F.; Le Cloirec, P. Removal of metal ions from aqueous solution on low cost natural polysaccharides Sorption mechanism approach. *React. Funct. Polym.* **2000**, *46*, 135–144. [CrossRef]
91. Rodríguez-López, L.; Santás-Miguel, V.; Cela-Dablanca, R.; Pérez-Rodríguez, P.; Núñez-Delgado, A.; Álvarez Rodríguez, E.; Rodríguez-Seijo, A.; Arias-Estévez, M. Valorization of forest by-products as bio-adsorbents for emerging contaminants. *J. Environ. Chem. Eng.* **2023**, *11*, 111437–111448. [CrossRef]
92. Hu, S.; Zhang, Y.; Shen, G.; Zhang, H.; Yuan, Z.; Zhang, W. Adsorption/desorption behavior and mechanisms of sulfadiazine and sulfamethoxazole in agricultural soil systems. *Soil. Til. Res.* **2019**, *186*, 233–241. [CrossRef]
93. Jeong, C.Y.; Wang, J.J.; Dodla, S.K.; Eberhardt, T.L.; Groom, L. Effect of biochar amendment on tylosin adsorption-desorption and transport in two different soils. *J. Environ. Qual.* **2012**, *41*, 1185–1192. [CrossRef]
94. Li, Y.; Pan, T.; Miao, D.; Chen, Z.; Tao, Y. Sorption-desorption of typical tetracyclines on different soils: Environment hazards analysis with partition coefficients and hysteresis index. *Environ. Eng. Sci.* **2015**, *32*, 865–871. [CrossRef]
95. Vega, F.A.; Covelo, E.F.; Couce, M.L.A. Applying Freundlich, Langmuir and Temkin Models in Cu and Pb soil sorption experiments. *Span. J. Soil. Sci.* **2011**, *1*, 20–37. [CrossRef]
96. Núñez-Delgado, A.; Otero-Pérez, X.L.; Álvarez-Rodríguez, E. Editorial: Current Research on Soil Science and Related Aspects of Environmental Sciences in Galicia. *Span. J. Soil. Sci.* **2023**, *13*, 11485. [CrossRef]
97. Roy, R.; Núñez-Delgado, A.; Sultana, S.; Wang, J.; Munir, A.; Battaglia, M.L.; Sarker, T.; Seleiman, M.F.; Barmon, M.; Zhang, R. Additions of optimum water, spent mushroom compost and wood biochar to improve the growth performance of *Althaea rosea* in drought-prone coal-mined spoils. *J. Environ. Manag.* **2021**, *295*, 113076. [CrossRef] [PubMed]
98. European Food Safety Authority (EFSA). Opinion of the Scientific Panel on Additives and Products or Substances used in Animal Feed on a request from the Commission on the safety and the efficacy of product “BIO-COX 120G” as feed additive in accordance with Council Directive 70/524/EEC. *EFSA J.* **2004**, *75*, 1–51.
99. Hamza, S.; Saad, H.; Charrier, B.; Ayed, N.; Charrier-El Bouhtoury, F. Physico-chemical characterization of Tunisian plant fibers and its utilization as reinforcement for plaster based composites. *Ind. Crops Prod.* **2013**, *49*, 357–365. [CrossRef]
100. Jaishankar, M.; Mathew, B.B.; Shah, M.S.; Murthy, T.P.K.; Gowda, K.R.S. Biosorption of Few Heavy Metal Ions Using Agricultural Wastes. *J. Environ. Pollut. Hum. Health* **2014**, *2*, 1–6. [CrossRef]

101. Larous, S.; Meniai, A.H. Adsorption of diclofenac from aqueous solution using activated carbon prepared from olive stones. *Int. J. Hydrog. Energy* **2016**, *41*, 10380–10390. [CrossRef]
102. Qlihaa, A.; Dhimni, S.; Melrhaka, F.; Hajjaji, N.; Srhiri, A. Physico chemical characterization of a Moroccan clay. *J. Mater. Environ. Sci.* **2016**, *7*, 1741–1750.
103. Riyajan, S.; Maneechay, S. Preparation and Properties of Natural Rubber Latex-GModified Cationic Polyacrylamide Copolymers and its Palm Oil Absorbent. *Rubber Compos.* **2014**, *43*, 264–270. [CrossRef]
104. Saramolee, P.; Lopattananon, N.; Sahakaro, K. Preparation and some properties of modified natural rubber bearing grafted poly(methyl methacrylate) and epoxide groups. *Eur. Polym. J.* **2014**, *56*, 1–10. [CrossRef]

Disclaimer/Publisher's Note: The statements, opinions and data contained in all publications are solely those of the individual author(s) and contributor(s) and not of MDPI and/or the editor(s). MDPI and/or the editor(s) disclaim responsibility for any injury to people or property resulting from any ideas, methods, instructions or products referred to in the content.

Article

Removal of Cefuroxime from Soils Amended with Pine Bark, Mussel Shell and Oak Ash

Raquel Cela-Dablanca ^{1,*}, Ainoa Míguez-González ¹, Lucía Rodríguez-López ², Ana Barreiro ¹, Manuel Arias-Estévez ², María J. Fernández-Sanjurjo ¹, Esperanza Álvarez-Rodríguez ¹ and Avelino Núñez-Delgado ¹

- ¹ Department of Soil Science and Agricultural Chemistry, Engineering Polytechnic School, University of Santiago de Compostela, Campus Univ. s/, 27002 Lugo, Spain; ainoa.miguez.gonzalez@usc.es (A.M.-G.); ana.barreiro.bujan@usc.es (A.B.); mf.sanjurjo@usc.es (M.J.F.-S.); esperanza.alvarez@usc.es (E.Á.-R.); avelino.nunez@usc.es (A.N.-D.)
- ² Soil Science and Agricultural Chemistry, Faculty of Sciences, University of Vigo, 32004 Ourense, Spain; lucia.rodriguez.lopez@uvigo.es (L.R.-L.); mastevez@uvigo.es (M.A.-E.)
- * Correspondence: raquel.dablanca@usc.es

Abstract: The global increase in antibiotics consumption has caused hazardous concentrations of these antimicrobials to be present in soils, mainly due to the spreading of sewage sludge (or manure or slurry) and wastewater, and they could enter the food chain, posing serious risks to the environment and human health. One of these substances of concern is cefuroxime (CFX). To face antibiotics-related environmental pollution, adsorption is one of the most widely used techniques, with cost-effective and environmentally friendly byproducts being of clear interest to retain pollutants and increase the adsorption capacity of soils. In light of this, in this work, three low-cost bioadsorbents (pine bark, oak ash, and mussel shell) were added to different soil samples (at doses of 12 and 48 t/ha) to study their effects on the adsorption of CFX. Specifically, batch experiments were carried out for mixtures of soils and bioadsorbents, adding a range of different antibiotic concentrations at a fixed ionic strength. The results showed that the addition of pine bark (with pH = 3.99) increased the adsorption to 100% in most cases, while oak ash (pH = 11.31) and mussel shell (pH = 9.39) caused a clearly lower increase in adsorption (which, in some cases, even decreased). The Freundlich and linear models showed rather good adjustment to the experimental data when the bioadsorbents were added at both doses, while the Langmuir model showed error values which were too high in many cases. Regarding desorption, it was lower than 6% for the soils without bioadsorbents, and there was no desorption when the soils received bioadsorbent amendments. These results show that the addition of appropriate low-cost bioadsorbents to soils can be effective for adsorbing CFX, helping in the prevention of environmental pollution due to this emerging contaminant, which is a result of clear relevance to environmental and human health.

Citation: Cela-Dablanca, R.; Míguez-González, A.; Rodríguez-López, L.; Barreiro, A.; Arias-Estévez, M.; Fernández-Sanjurjo, M.J.; Álvarez-Rodríguez, E.; Núñez-Delgado, A. Removal of Cefuroxime from Soils Amended with Pine Bark, Mussel Shell and Oak Ash. *Processes* **2024**, *12*, 1335. <https://doi.org/10.3390/pr12071335>

Academic Editor: Monika Wawrzekiewicz

Received: 27 May 2024

Revised: 20 June 2024

Accepted: 24 June 2024

Published: 27 June 2024



Copyright: © 2024 by the authors. Licensee MDPI, Basel, Switzerland. This article is an open access article distributed under the terms and conditions of the Creative Commons Attribution (CC BY) license (<https://creativecommons.org/licenses/by/4.0/>).

Keywords: adsorption; antibiotics; byproducts; desorption; soil

1. Introduction

Pharmaceuticals are broadly used worldwide, generating high concentrations of substances such as antibiotics in wastewaters, which can be released to different environmental compartments [1]. The massive use of antibiotics has caused their widespread presence in the environment, with derived pollution detected in soils, sediments, sludges, water, plants, and aquatic animals [2,3]. The time required for the degradation of antibiotics in the environment depends on many factors, such as the concentration and chemical structure of the pollutant, as well as the characteristics of the affected soils or sediments (including the humic acid content, humidity, pH, temperature, sorption capacity, presence of inorganic matter, and availability of oxygen and microorganisms that support the biodegradation

process) [4,5]. We note that between 20% and 97% of any dose of most antibiotics administered to humans and animals is excreted as active substances [6,7]. Specifically, the incomplete absorption of antibiotics by humans entails the discharge of large quantities of these pharmaceuticals in municipal wastewater treatment plants (WWTPs) [1] which, together with their inefficiency at removing antibiotics [8], is the main cause of this pollution problem. These WWTP coexist with and contact relevant amounts of microorganisms and antibiotic residues for prolonged periods of time, triggering the additional problem of increasing antibiotic resistance [9–11]. The increase in antibiotic-resistant bacteria (ARB) is a major problem for public health due to the fact that infections caused by these resistant microbes are difficult to treat, with COVID-19 deriving an additional rise in antibiotic consumption [12], also affecting the general levels of antimicrobial resistance (AMR) [13].

The removal of antibiotics in WWTPs by means of conventional treatments is limited to 50–80%, depending on the antibiotics' physicochemical properties [14–16]. In this regard, the antibiotic CFX has been detected in wastewater at $\mu\text{g/L}$ and ng/L levels [17] as well as in surface waters, with the highest concentration reaching 210 $\mu\text{g/L}$ for wastewater from the pharmaceutical industry and hospitals around the world [18,19]. A study carried out in multiple urban wastewaters in Germany showed CFX concentrations up to 6196 ng/L and 1957 ng/L in influent and effluent samples, respectively [20].

The spreading of wastewater and sewage sludge is a potential way to introduce pharmaceutical compounds into waterbodies and soils [21,22]. The use of reclaimed wastewater for the irrigation of crops is an important source of ARB and antibiotic resistant genes (ARGs) in agricultural soils [23]. Furthermore, it is quite common that annual fertilization with repeated applications of inappropriate doses of sewage sludge is carried out to provide soil nutrients and organic matter [24,25]. In Europe, for many years, more than 50% of produced sewage sludge is used in agriculture [26–29]. However, the application of sewage sludge to soils may pose a problem for the environment, due to their contents including a wide variety of toxic pollutants [29–32]. Furthermore, emerging pollutants pose an important risk if they are transferred to groundwater because it is a source of drinking water [33–35], and degradation will likely be extremely limited in these aquatic systems [36,37].

Antibiotic residues have different persistence times and transport types in agricultural soils, affected by factors such as adsorption, degradation, and lixiviation [38,39]. Their dissipation rates, expressed as half-lives, can range from 18.6 to 21.3 days for sulfonamide antibiotics, whereas for tetracyclines, they can be up to 1–2 months, and for enrofloxacin, they can be approximately 7–8 months [40]. Conde-Cid et al. [41] observed no degradation for three sulfonamides in the dark, while under simulated sunlight, after 2 h of exposure, sulfachloropyridazine and sulfadiazine degraded by 90%, and sulfamethazine degraded by 80% after 8 h. Rodríguez-López et al. [42] studied the degradation of clarithromycin, ciprofloxacin, and trimethoprim under different conditions, observing that after 1 h of exposure to light radiation, 85% of the ciprofloxacin degraded. They also reported that clarithromycin degradation was pH-dependent, obtaining the highest degradation percentage (30%) at $\text{pH} = 4$, whereas trimethoprim reached less than 5%. A study carried out in China's Xuanwu Lake found four cephalosporins degraded abiotically in the surface water in the dark, with half-lives between 2.7 and 18.7 days, while the time decreased by up to 2.2–5 days under exposure to simulated sunlight [43].

Adsorption is widely used to remove antibiotics due to its simple design and because it is environmentally friendly, economic, and versatile [44]. Its efficiency depends on the type of adsorbent, adsorbate properties, and waste stream (in the case of waste liquids) composition [45,46]. Depending on the pH of the medium and the pK_a of the pollutant, sorption is also affected by the charges of the molecular forms of the sorbates, (i.e., neutral, cationic, anionic, or zwitterionic) [47]. Furthermore, developing cost-effective and environmentally friendly treatment techniques for the remediation of specific contaminants (such as antibiotics) present in soils is imperative [48,49]. The need to deal with agricultural and industrial wastes or byproducts has drawn additional attention to the adsorption field,

due to the eco-friendly approach and advantages of using these materials, such as their easy access, high availability, and low cost compared with synthetic or other high-cost materials [50]. Some examples were shown by Ahmed et al. [51], whereas other specific previous studies showed that the addition of pine bark to soils increased the retention of three sulfonamides [52]. Also, in a previous work, we studied the effectiveness of the byproducts pine bark, oak ash, and mussel shell as bioadsorbents for the antibiotics amoxicillin, ciprofloxacin, and trimethoprim, with good results [53], and other studies focused on the retention of CFX in soils [54] and onto the same byproducts [55], although no research was performed dealing with the retention or release of CFX on or from soils amended with these sorbents.

In light of the above background, the objective of this work was to characterize the potential of three bioadsorbents (pine bark, oak ash, and mussel shell) to retain or remove the antibiotic cefuroxime (CFX) after the amendment of six different soils at two doses (12 and 48 t/ha). The results of the investigation could be of relevance regarding the management of soils contaminated with this emerging pollutant as well as the recycling of byproducts, potentially facilitating sustainability and a circular economy.

2. Materials and Methods

2.1. Soils and Bioadsorbents

To carry out this research, six different soil samples were selected, with all of them coming from different agricultural areas in Galicia (northwest Spain). These soils are devoted to vineyards (named VP1, VP2, and VO), and corn production (denoted as C1, C2, and C3). In a previous work [54], we studied CFX adsorption onto 23 different soils, and we selected among them the 6 soils with the lowest CFX adsorption capacities for use in the current research. The selected soils were amended with various bioadsorbents to assess the eventual modification of CFX adsorption onto these soils. The methods used for their characterization are presented in the Supplementary Materials, with the results shown in Table S1.

Three byproducts were used as bioadsorbents, with two of them coming from the forestry industry—pine bark, provided by Geolia (Madrid, Spain), and oak ash from a combustion boiler in Lugo (Spain)—while the third one was from the canning industry: mussel shell, provided by Abonomar S.L (Pontevedra, Spain).

Table 1 shows the results corresponding to the characterization of different parameters for the three bioadsorbents. The pH values were determined using a soil-to-liquid ratio of 1:2.5. The contact time for the pH in water was 10 min, while for the pH in KCl, it was 2 h [55]. The measurements were made with a CRISON pH meter, model 2001 (Crison, Barcelona, Spain). The available phosphorous was determined by the Olsen method [56]. To carry out this method, 2.5 grams of bioadsorbent was weighted, and 50 mL of the extracting solution (sodium bicarbonate at pH = 8.5) was added. This mixture was subjected to shaking for 30 min before utilizing visible spectrophotometry for P quantification. Determination of the total C and N was carried out using an elemental analysis method with a LECO TRUSPEC CHNS instrument (Leco, St. Joseph, MI, USA). The exchangeable cations (Ca_e , Mg_e , Na_e , Ke , and Al_e) were displaced using a 1 M NH_4Cl solution in a 1:10 sorbent:solution ratio, with subsequent quantification by means of atomic absorption spectrophotometry using a Perkin Elmer AAnalyst 200 apparatus (Perkin Elmer, Waltham, MA, USA). The total contents of the elements analyzed were determined through the EPA 3051 method using acid digestion with a 65% HNO_3 solution. The measurements were performed by means of an ICP-MS (Perkin-Elmer, USA). To determine the total non-crystalline Fe and Al contents, a specific type of extraction was performed using ammonium oxalate buffered at a pH level of 3, followed by stirring for 4 h in the dark, adding 5 drops of 0.25% superfloc to the resulting extract, centrifuging at 2000 rpm for 10 min, and filtering and diluting the supernatant to a 1:5 ratio. Finally, Fe and Al in non-crystalline form (Fe_o and Al_o) were quantified with atomic absorption spectrophotometry (Perkin-Elmer, USA).

Table 1. Characteristics of the bioadsorbent materials. Ca_e , Mg_e , Na_e , K_e , and Al_e = elements in the exchange complex; Sat. Al = Al saturation in the exchange complex; eCEC = effective cation exchange capacity; XT = total content of the element (X); and Al_o and Fe_o = non-crystalline Al and Fe, respectively. Average values ($n = 3$) with coefficients of variation always <5%.

Parameter	Unit	Pine Bark	Oak Ash	Mussel Shell
C	%	48.70	13.23	11.43
N	%	0.08	0.22	0.21
C/N		608.75	60.14	55.65
pH _{water}		3.99	11.31	9.39
pH _{KCl}		3.42	13.48	9.04
Ca_e	cmol _c kg ⁻¹	5.38	95.0	24.75
Mg_e	cmol _c kg ⁻¹	2.70	3.26	0.72
Na_e	cmol _c kg ⁻¹	0.46	12.17	4.37
K_e	cmol _c kg ⁻¹	4.60	250.65	0.38
Al_e	cmol _c kg ⁻¹	1.78	0.07	0.03
eCEC	cmol _c kg ⁻¹	14.92	361.15	30.25
Sat Al	%	11.93	0.02	0.10
Available P	mg kg ⁻¹	70.45	462.83	54.17
Na_T	mg kg ⁻¹	68.92	2950	5174.00
Mg_T	mg/kg	473.55	26,171	980.66
Al_T	mg kg ⁻¹	561.50	14,966	433.24
K_T	mg kg ⁻¹	737.84	99,515	202.07
Ca_T	mg kg ⁻¹	2318.81	136,044	280,168
Cr_T	mg kg ⁻¹	1.88	36.28	4.51
Mn_T	mg kg ⁻¹	30.19	10554	33.75
Fe_T	mg kg ⁻¹	169.78	12,081	3535
Co_T	mg kg ⁻¹	0.20	17.25	1.02
Ni_T	mg kg ⁻¹	1.86	69.25	8.16
Cu_T	mg kg ⁻¹	<LD	146.33	6.72
Zn_T	mg kg ⁻¹	6.98	853.00	7.66
As_T	mg kg ⁻¹	<LD	8.36	1.12
Cd_T	mg kg ⁻¹	0.13	19.93	0.07
Al_o	mg kg ⁻¹	315.0	8323	178.33
Fe_o	mg kg ⁻¹	74.0	4233	171.0

Other details related to additional previously published characteristics are provided in the Supplementary Materials.

These bioadsorbents were added to soil samples in doses of 12 and 48 t/ha. The mixtures reached the pH values that are shown in Table S2 (Supplementary Materials).

2.2. Chemicals and Reagents

The antibiotic cefuroxime (CFX) was provided by Sigma Aldrich (Barcelona, Spain) and was of >95% purity. Phosphoric acid (85% extra pure) was supplied by Acros Organics (Barcelona, Spain), acetonitrile (purity $\geq 99.9\%$) was supplied by Fisher Scientific (Madrid, Spain), and $CaCl_2$ (95% purity) was supplied by Panreac (Barcelona, Spain). All of the reagents needed for the quantification of antibiotics were of HPLC grade.

2.3. Adsorption and Desorption Experiments

Batch experiments were carried out to study the adsorption capacity of the mixtures of soil and bioadsorbents. To accomplish this, 5 mL of a 0.005 M $CaCl_2$ solution (which served as the background electrolyte to maintain a constant ionic strength) received the appropriate amount of antibiotics to achieve different specific CFX concentrations (0, 2.5, 5, 10, 20, 30, 40, and 50 $\mu\text{mol/L}$). Then, each of these solutions was added to 2 g of the corresponding mixtures of soil and bioadsorbent. Afterward, the samples were subjected to shaking for 48 h and centrifugated at 4000 rpm for 15 min, with the resulting supernatants being passed

through 0.45 μm nylon-type syringe filters. Previous kinetic studies demonstrated that 48 h is enough time to reach equilibrium.

Quantification of the antibiotic concentrations was performed using HPLC equipment, with all the details provided in the Supplementary Materials.

Figure S1 shows some select chromatograms corresponding to the quantification of CFX.

After the adsorption phase, the desorption experiments were carried out. For this, 5 mL of CaCl_2 was added to the remaining post-adsorption materials. The samples were shaken for 48 h, centrifugated, filtered, and analyzed in the same conditions as those during the adsorption process.

2.4. Modeling and Statistics

The experimental adsorption data were fitted to the Freundlich (Equation (1)), Langmuir (Equation (2)), and linear (Equation (3)) models [57]:

$$q_e = K_F C_{eq}^n \quad (1)$$

$$q_e = \frac{q_m K_L C_{eq}}{1 + K_L C_{eq}} \quad (2)$$

$$K_d = q_e / C_{eq} \quad (3)$$

where q_e is the amount of CFX retained (concentration added minus concentration in the equilibrium); C_{eq} is the CFX concentration in equilibrium; K_F is the Freundlich adsorption capacity parameter; n is a parameter related to heterogeneity in adsorption; K_L is the Langmuir adsorption constant; q_m is the Langmuir maximum adsorption capacity; and K_d is the linear model's partition coefficient.

All of the experimental determinations were made in triplicate.

The fitting of the experimental data to the Langmuir, Freundlich, and linear models was performed by means of SPSS Statistics 21 software.

The studies carried out for this research can be seen as the first steps within an overall broader strategy which will need further future works to be completed, both with classic and new scientific tools [58,59].

3. Results and Discussion

3.1. CFX Adsorption

Figures 1 and 2 show the adsorption curves corresponding to the different soils amended with doses of 12 and 48 t/ha of each of the three bioadsorbents.

Both figures show that, overall, mussel shell (pH = 9.39) was the sorbent with the greatest positive effect on the increase in CFX adsorption for any of the soils receiving both doses of the amendments. In fact, with this byproduct, the concentrations in the antibiotic's equilibrium (expressed in $\mu\text{mol/L}$) were the lowest, being associated with the highest adsorption levels (expressed in $\mu\text{mol/kg}$). In contrast, pine bark (pH = 3.99) showed the weakest effects as an amendment intended to increase CFX adsorption for the soils treated with the three byproducts.

Compared with previous studies [54,60] focused on retention of the same antibiotic on equivalent soils and byproducts but performed for soils and sorbents separately (not mixing the soils and sorbents, which was performed for the first time in the present study), the following comments can be presented. Regarding the adsorption of CFX onto the bioadsorbents (without soil), based on a previous publication by Cela-Dablanca et al. [60], the influence of the pH level was confirmed, with oak ash (pH = 11.31) showing the highest adsorption values (927.95 $\mu\text{mol/kg}$ when a concentration of 50 $\mu\text{mol/L}$ was added), followed by mussel shell (pH = 9.39), with maximum adsorption of 721.65 $\mu\text{mol/kg}$ when a concentration of 50 $\mu\text{mol/L}$ was added, and finally pine bark (pH = 3.99), which presented

the lowest adsorption ($551.62 \mu\text{mol kg}^{-1}$ when a concentration of $50 \mu\text{mol/L}$ was added). Furthermore, in another previous study [54] focused on CFX adsorption by soils (without bioadsorbents) with different pH values, the authors confirmed that soils with an alkaline pH presented the highest CFX adsorption, with scores oscillating between $74.86 \mu\text{mol kg}^{-1}$ (for soil with $\text{pH} = 5.7$) and $123.88 \mu\text{mol/kg}$ (for soil with $\text{pH} = 8.02$).

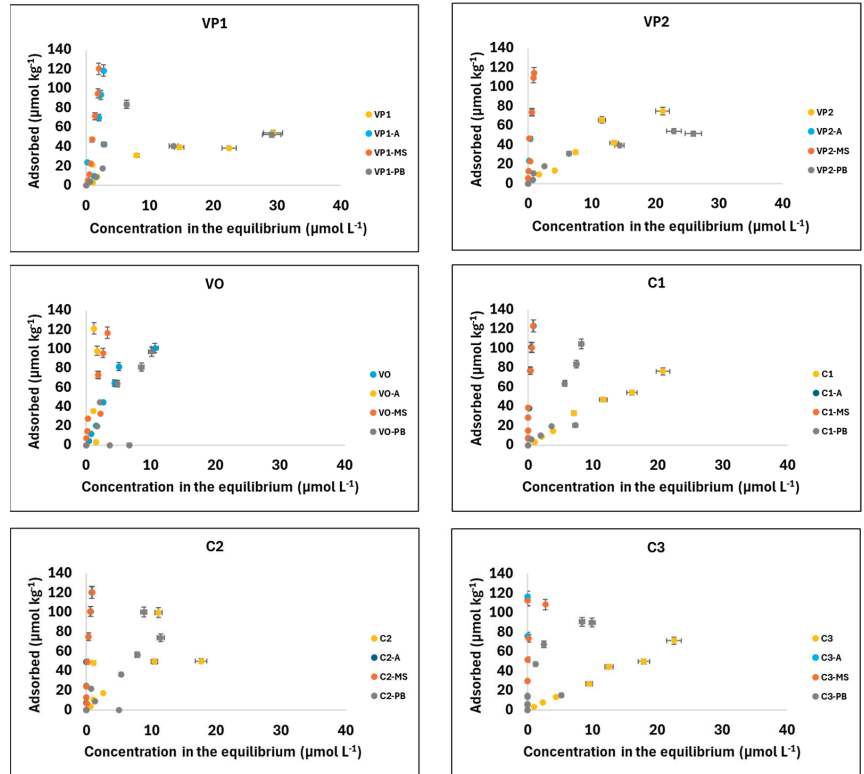


Figure 1. Adsorption curves for CFX corresponding to soils without and with bioadsorbents (amended with a dose of 12 t/ha). Average values ($n = 3$) are with coefficients of variation always lower than 5%. Bars indicate standard deviation. C = corn soils; VO and VP = vineyard soils; A = oak ash; MS = mussel shell; and PB = pine bark.

Figures 3 and 4 show the CFX adsorption (as a percentage) for the different antibiotic concentrations added to the soils (2.5 – $50 \mu\text{mol/L}$) without and with the amendment of the three bioadsorbents, which were applied in doses of 12 t/ha (Figure 3) and 48 t/ha (Figure 4).

As shown in Figure 3, when the bioadsorbents were added to soils at a dose of 12 t/ha, the behaviors were different as a function of the byproduct used. Specifically, the addition of mussel shell and oak ash generated an increase in CFX adsorption, reaching values of 100% retention in most cases. However, when pine bark was added to soils, the adsorption increase was significantly lower, and adsorption even decreased in some cases.

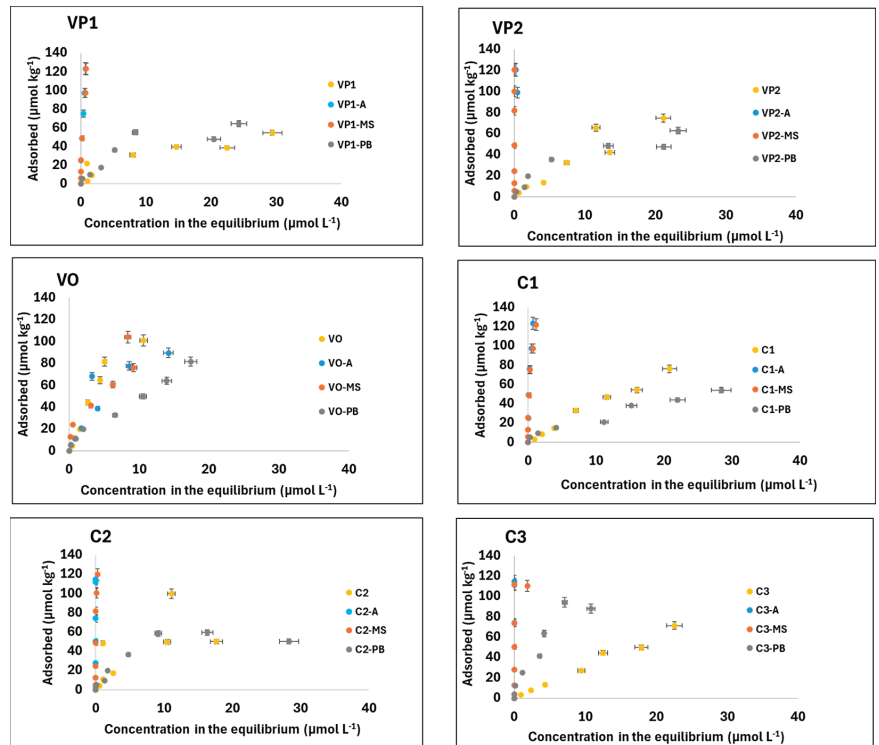


Figure 2. Adsorption curves for CFX corresponding to soils without and with bioadsorbents (amended at a dose of 48 t/ha). Average values ($n = 3$) are with coefficients of variation always lower than 5%. Bars indicate standard deviation. C = corn soils; VO and VP = vineyard soils; A = oak ash; MS = mussel shell; and PB = pine bark.

Despite this, in a previous work carried out for other antibiotics (three sulfonamides), Conde-Cid et al. [52] found that adding pine bark to soils increased the adsorption capacity to 99.6%. Once again, it should be noted that mussel shell and oak ash present alkaline pH values (9.39 and 11.31, respectively), while pine bark has a pH level of 3.99. This would suggest that CFX adsorption is pH-dependent. These results were confirmed by the abovementioned previous studies performed separately for soils and bioadsorbents [54,60]. We note that the dissociation constant (pK_a) is a parameter having marked relevance regarding the environmental fate of organic compounds [4]. In this sense, the pH level affects the behavior of antibiotics when they are cationic, anionic, or neutral molecules, and it also affects the activity of functional groups in a solution [61]. According to El-Shaboury et al. [62], Lin et al. [63], and Ribeiro and Schmidt [64], cephalosporin structures generally have two or more ionization centers. In the case of CFX, the dissociation constants are $pka_1 = 3.15$ and $pka_2 = 10.97$ [64]. At pH values below 3.15, CFX will be in its cationic form, and above pH 10.97, it will be in its anionic form. In the pH range 3.15–10.97 (in which our samples were placed), CFX would be zwitterionic. In this case, the positive charges of the antibiotic (NH_4^+) will bind to the negative charges of the sorbents due to electrostatic interactions, while the negative charges of CFX (COO^-) could make use of a cationic bridge with negative charges present on the surface of the sorbent materials [65]. Calcium was the predominant cation in most samples used in this study, and it would be the most probable binding element acting as a cationic bridge between the adsorbents and the adsorbate. Soils amended with the bioadsorbents used here generally reach a pH level above 5.5, with the highest values corresponding to amendments with mussel shell and the lowest ones

associated with pine bark (which has a pH lower than that of the used soils), particularly for those at doses of 48 t/ha (Table S2, Supplementary Materials). The variable charge components of the soils used in this study (mainly kaolinite, non-crystalline Al and Fe minerals, and organic matter) and non-crystalline minerals of the bioadsorbents (extremely abundant in the case of oak ash) would exhibit a negative charge at these pH values. This negative charge in the soil and bioadsorbent mixture would be greater for higher pH levels (soil with mussel shell and soil with oak ash), favoring electrostatic interactions between these negative charges and the positively charged groups of CFX, or through cationic bridges with the anionic groups of this antibiotic [65]. In contrast, the soils amended with pine bark showed lower CFX adsorption since the pH level was lower than those of the other mixtures, as the high amount of organic matter they provided would present few negative charges. Additionally, pine bark had a lower content of non-crystalline minerals, which provide a negative charge at $\text{pH} > 6$, and a lower Ca content to establish cationic bridges between CFX and the soils amended with this byproduct. All of this would explain why this bioadsorbent was less effective in CFX retention than the other two. Furthermore, in acidic conditions, free H^+ in the medium could contribute to the formation of hydrogen bonds between the adsorbent's surface and the antibiotic [66].

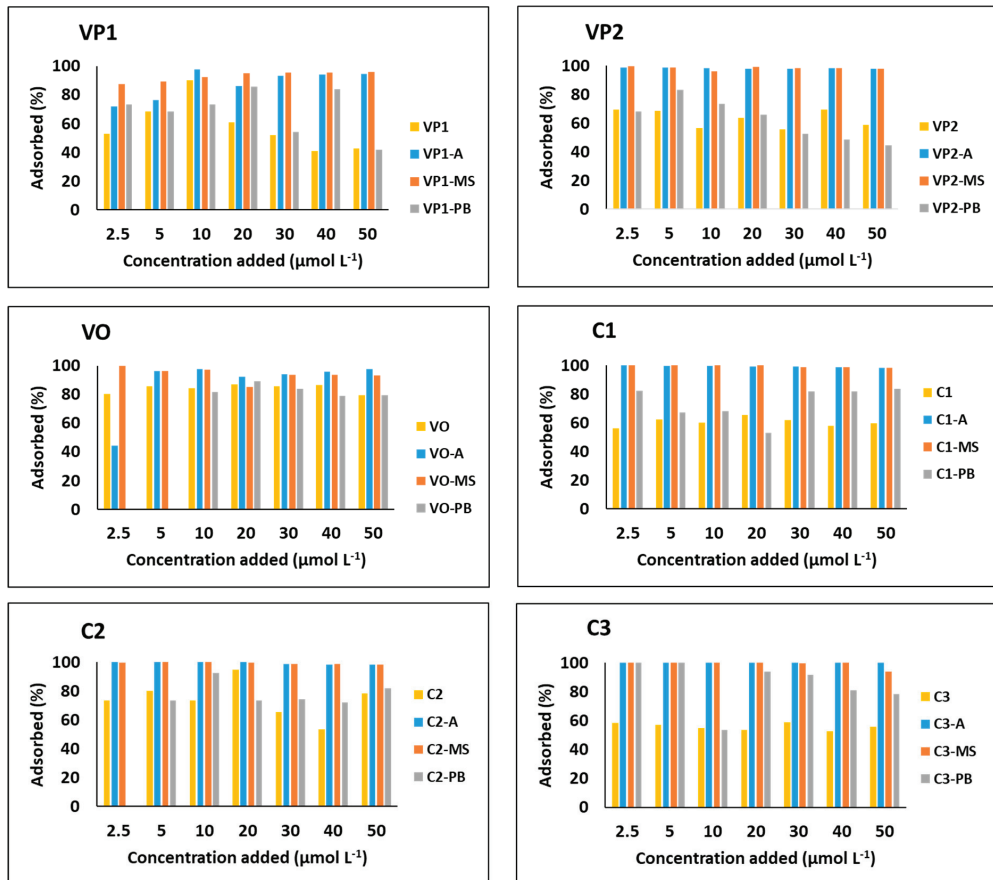


Figure 3. Adsorption of CFX (as a percentage) by soils without and with bioadsorbents amended at a dose of 12 t/ha as a function of the concentration of antibiotics added. Average values ($n = 3$) are with coefficients of variation always lower than 5%. C = corn soils; VO and VP = vineyard soils; A = oak ash; MS = mussel shell; and PB = pine bark.

Figure 4 shows the CFX adsorption by soils without bioadsorbents and amended with the three bioadsorbents at a dose of 48 t/ha.

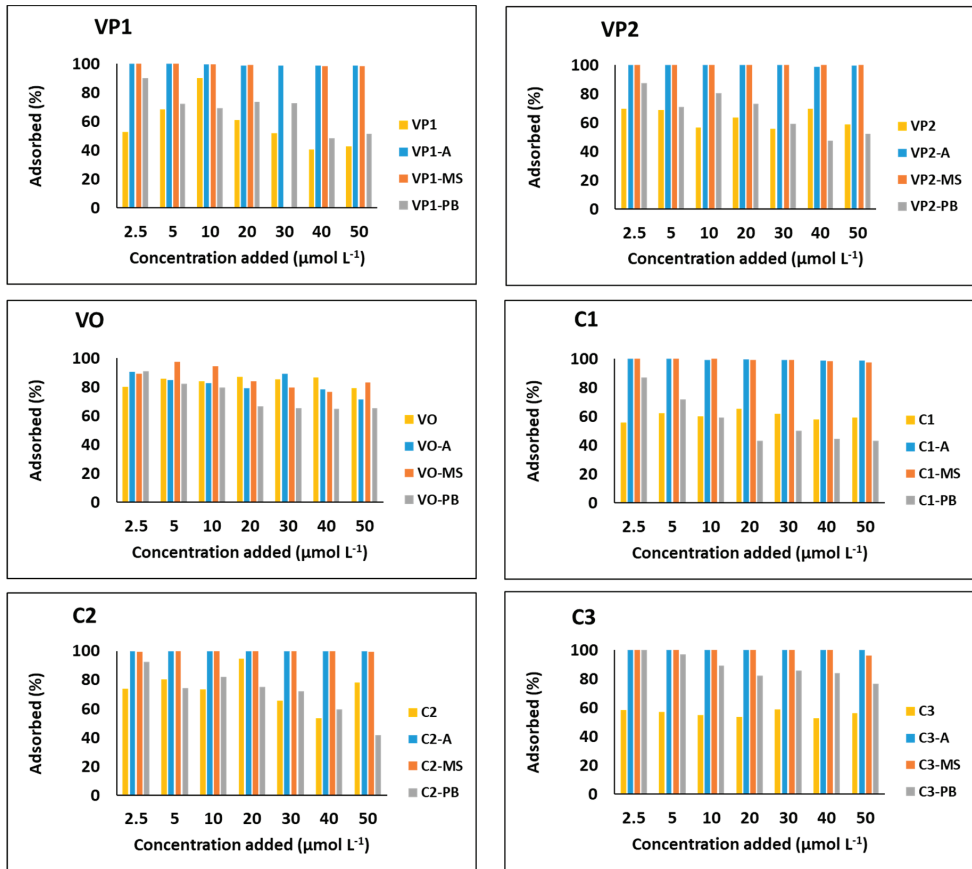


Figure 4. Adsorption of CFX (as a percentage) by soils without and with bioadsorbents amended at a dose of 48 t/ha as a function of the concentration of antibiotics added. Average values ($n = 3$) are with coefficients of variation always lower than 5%. C = corn soils; VO and VP = vineyard soils. A = oak ash; MS = mussel shell; and PB = pine bark.

The data obtained corresponding to the addition of the bioadsorbents to the six soils at a dose of 48 t/ha (Figure 4) confirmed an equivalent behavior to that found for the dose of 12 t/ha. The addition of bioadsorbents with alkaline pH levels (oak ash and mussel shell) was associated with the highest increase in adsorption, while the addition of pine bark (with an acidic pH) caused a lower increase (and decreased adsorption in several cases). These results would confirm that CFX adsorption onto these sorbents depends on the pH level. In this regard, a previous study dealing with the adsorption of one cephalosporin (cefixime) by a porous, aluminum-based metal–organic framework-aminoclay nanocomposite reported an increase in antibiotic adsorption when the pH oscillated from 3 to 7, obtaining the maximum adsorption at a pH level of seven [67]. To further evidence the potential relation, statistical analyses were performed, obtaining a significant and positive correlation between adsorption and pH ($r = 0.440$, $p < 0.05$). In a previous study in which the adsorption of amoxicillin by mixtures equivalent to those used here was studied, it was observed that the organic matter content also influenced the adsorption of the antibiotic [68]. Furthermore, previous studies focused on CFX adsorption for soils varying within a wide range of pH

level (4.62–8.02) and organic matter contents (1.09–16.87), showing a clear influence of these two parameters on retention of the antibiotic [54]. However, in the current research, all soil samples had a moderate organic matter content, with the pH level being the most influential characteristic affecting CFX adsorption for the mixtures of soil and bioadsorbent. In addition to the pH level, other properties of the bioadsorbent materials, such as the higher exchangeable Ca content in mussel shell and oak ash and the non-crystalline Al and Fe contents in oak ash, would contribute to explaining the higher increase in CFX adsorption caused by these two materials compared with pine bark [60].

3.2. Adsorption Isotherms for Soils and Mixtures of Soil and Bioadsorbents

The fitting of the experimental adsorption results to adsorption equations was evaluated for the Freundlich, Langmuir, and linear models. Table 2 shows the results of the parameters of the adjustments, considering soils without and with bioadsorbents added at a dose of 12 t/ha.

Table 2. Parameters of adsorption isotherms for cefuroxime in soils without and with bioadsorbents at a dose of 12 t/ha (K_F expressed in $L^n \text{ kg}^{-1} \mu\text{mol}^{1-n}$; n = dimensionless; K_L expressed in $L \mu\text{mol}^{-1}$; q_m expressed in $\mu\text{mol kg}^{-1}$; K_d expressed in $L \text{ kg}^{-1}$; - = error value too high for fitting). C = corn soils; VO and VP = vineyard soils; A = oak ash; MS = mussel shell; and PB = pine bark.

Sample	Freundlich					Langmuir					Linear Model		
	K_F	Error	n	Error	R^2	K_L	Error	q_m	Error	R^2	K_d	Error	R^2
VP1	10.877	3.319	0.458	0.104	0.895	0.15	0.095	58.473	11.744	0.876	2.018	0.266	0.693
VP1-A	22.781	17.403	1.345	0.826	0.661	-	-	-	-	-	30.783	5.082	0.648
VP1-MS	41.676	3.52	1.483	0.142	0.982	-	-	-	-	-	52.343	3.516	0.932
VP1-PB	22.04	10.863	0.308	0.195	0.49	-	-	65.554	20.877	0.608	-	-	-
VP2	6.365	3.11	0.815	0.18	0.907	-	-	225.213	188.987	0.912	3.838	0.323	0.892
VP2-A	120.162	2.58	0.909	0.048	0.996	0.129	0.118	1053.162	875.508	0.995	122.871	2.444	0.994
VP2-MS	122.858	12.836	0.959	0.235	0.916	-	-	-	-	-	124.267	9.223	0.916
VP2-PB	10.765	1.548	0.499	0.049	0.98	0.13	0.03	67.645	5.521	0.983	2.345	0.241	0.811
C1	5.135	0.958	0.881	0.068	0.988	0.013	0.008	341.167	174.058	0.989	3.699	0.122	0.983
C1-A	137.408	7.386	0.52	0.054	0.979	2.742	0.896	174.487	24.936	0.973	169.606	18.516	0.824
C1-MS	122.905	14.431	0.329	0.126	0.904	-	-	211.46	172.105	0.848	169.582	18.416	0.826
C1-PB	-	-	-	-	-	-	-	-	-	-	9.249	1.523	0.671
VO	21.681	4.085	0.685	0.096	0.948	0.113	0.037	193.42	37.656	0.975	11.48	1.085	0.863
VO-A	52.829	16.977	-	-	0.359	-	-	-	-	-	43.309	11.013	0.314
VO-MS	33.059	15.12	0.979	0.456	0.823	-	-	-	-	-	32.377	3.568	0.823
VO-PB	-	-	1.285	0.754	0.495	-	-	-	-	-	7.981	1.72	0.487
C2	22.027	11.843	0.410	0.225	0.57	-	-	80.688	28.959	0.6	4.735	1.169	0.328
C2-A	132.409	31.22	0.511	0.408	0.77	-	-	-	-	-	161.564	22	0.727
C2-MS	131.114	11.877	0.490	0.104	0.94	3.548	1.866	153.98	29.786	0.94	160.503	18.222	0.807
C2-PB	-	-	1.324	0.65	0.671	-	-	-	-	-	7.276	1.218	0.655
C3	3.219	0.817	0.985	0.088	0.985	-	-	-	-	-	3.084	0.095	0.985
C3-A	-	-	-	-	-	-	-	-	-	-	-	-	-
C3-MS	-	-	-	-	-	-	-	-	-	-	-	-	-
C3-PB	37.349	18.209	0.330	0.258	0.661	-	-	83.349	29.002	0.624	9.619	1.828	0.517

The results indicate that when the bioadsorbents were added at a dose of 12 t/ha, the Freundlich model showed the best adjustment, because 45% of the samples obtained an R^2 value > 0.9, whereas in the case of the Langmuir and linear models, the values decreased to 25% and 20%, respectively.

The Freundlich affinity coefficient (K_F) values ranged between 2.396 and 137.408 $L^n \text{ kg}^{-1} \mu\text{mol}^{1-n}$, while the n values oscillated between 0.308 and 1.693. Some authors postulated that when $n < 1$, adsorption is carried out in a heterogeneous matrix, with the highest energy sites being occupied first [69]. Meanwhile, when $n > 1$, a deviation from the Freundlich equation would occur, such as the eventual existence of irreversible reactions like precipitation [70] or cooperative adsorption [71]. The values of the distribution constant of the linear model (K_d) ranged between 2.018 and 169.606 $L \text{ kg}^{-1}$, whereas those of the Langmuir adsorption constant (K_L) were between 0.013 and 3.548 $L \mu\text{mol}^{-1}$.

Table 3 shows the results of the parameters of the adjustments to the adsorption models considering soils without and with bioadsorbents added at a dose of 48 t/ha. In this case, 62.5% of the samples obtained an R^2 value >0.9 when adjusted to the Langmuir model. This percentage decreased to 54% and 25% when adjusted to the Freundlich and linear models, respectively (Table 3). In this regard, Jafari et al. [72] studied the adsorption of two cephalosporins (cephalexin and cefixime) onto multi-walled carbon nanotubes and obtained a better adjustment to the Freundlich model for the adsorption of cefixime, while cephalixin adsorption fit better to the Langmuir equation.

Table 3. Parameters of adsorption isotherms for cefuroxime in soils without and with bioadsorbents at a dose of 48 t/ha (K_F expressed in $L^n \text{ kg}^{-1} \mu\text{mol}^{1-n}$; n = dimensionless; K_L expressed in $L \mu\text{mol}^{-1}$; q_m expressed in $\mu\text{mol kg}^{-1}$ K_d expressed in $L \text{ kg}^{-1}$; - = error value too high for fitting). C = corn soils; VO and VP = vineyard soils; A = oak ash; MS = mussel shell; and PB = pine bark.

	Freundlich					Langmuir					Linear Model		
	K_F	Error	n	Error	R^2	K_L	Error	q_m	Error	R^2	K_d	Error	R^2
VP1	10.877	3.319	0.458	0.104	0.895	0.150	0.095	58.473	11.744	0.876	2.018	0.266	0.693
VP1-A	148.757	10.363	0.714	0.094	0.979	0.848	0.567	308.951	140.343	0.972	174.349	9.055	0.958
VP1-MS	129.954	8.905	0.592	0.102	0.973	1.635	1.073	200.034	63.88	0.961	149.227	11.307	0.933
VP1-PB	14.658	4.505	0.455	0.112	0.879	0.157	0.071	76.091	12.693	0.918	2.922	0.463	0.606
VP2	6.365	3.11	0.815	0.18	0.907	-	-	-	-	-	3.838	0.323	0.892
VP2-A	-	-	-	-	-	-	-	-	-	-	-	-	-
VP2-MS	-	-	-	-	-	-	-	-	-	-	-	-	-
VP2-PB	13.248	2.902	0.473	0.078	0.947	0.169	0.056	70.367	7.659	0.962	2.79	0.334	0.754
C1	5.133	0.958	0.881	0.068	0.988	0.013	0.008	341.167	174.058	0.989	3.699	0.122	0.983
C1-A	140.678	12.98	0.511	0.091	0.951	3.499	1.444	161.637	27.525	0.949	183.897	20.641	0.814
C1-MS	112.159	8.731	0.414	0.107	0.935	2.905	1.403	151.631	26.71	0.935	116.45	15.809	0.737
C1-PB	5.254	1.399	0.691	0.088	0.972	0.023	0.015	134.903	61.572	0.961	2.036	0.121	0.937
VO	21.681	4.085	0.685	0.096	0.948	0.113	0.037	193.42	37.656	0.975	11.48	1.085	0.863
VO-A	22.164	5.979	0.550	0.123	0.887	0.169	0.089	128.494	30.869	0.909	7.728	1.082	0.71
VO-MS	23.636	6.952	0.591	0.147	0.918	-	-	162.823	89.866	0.9	10.285	0.928	0.872
VO-PB	8.756	1.668	0.764	0.073	0.986	0.018	0.016	326.384	235.677	0.976	4.728	0.196	0.971
C2	22.027	11.843	0.41	0.225	0.57	-	-	80.688	28.959	0.6	4.735	1.169	0.328
C2-A	-	-	-	-	-	-	-	-	-	-	-	-	-
C2-MS	53.205	27.298	-	-	0.402	-	-	-	-	-	571.086	153.561	0.229
C2-PB	18.948	5.349	0.361	0.104	0.84	0.261	0.107	67.821	8.438	0.93	2.675	0.593	0.304
C3	3.219	0.817	0.985	0.088	0.985	-	-	-	-	-	3.084	0.095	0.985
C3-A	-	-	-	-	-	-	-	-	-	-	-	-	-
C3-MS	-	-	-	-	-	-	-	-	-	-	-	-	-
C3-PB	26.541	5.886	0.544	0.112	0.94	0.158	0.085	150.68	40.312	0.944	10.352	1.104	0.824

The values of the K_F parameter ranged between 3.219 and 148.757 $L^n \text{ kg}^{-1} \mu\text{mol}^{1-n}$. These scores are similar to those previously obtained for another antibiotic (amoxicillin) in equivalent soil-bioadsorbent mixtures [68]. Focusing on the data, the K_F values were significantly higher when mussel shell or oak ash was added, indicating stronger adsorption when the soils were amended with these alkaline adsorbents. Regarding Freundlich's n values, they were lower than one in all cases, suggesting the presence of heterogeneous adsorption sites and a nonlinear and concave curve, which was frequently interpreted. This suggests that the sites with high adsorption energy are occupied first, indicating chemical adsorption [71,73]. The K_d values ranged between 2.018 and 571.086 $L \mu\text{mol}^{-1}$, while the Langmuir adsorption constant (K_L) ranged between 0.013 and 10.917 $L \text{ kg}^{-1}$. These values are lower than those previously obtained for amoxicillin in equivalent mixtures [68].

3.3. Comparison with Previously Studied Bioadsorbents

Other authors previously studied the capacity of different bioadsorbents to retain or remove CFX. Awwad et al. [74] used activated carbon and a micelle-clay complex to retain this antibiotic, achieving adsorption values of 26.31 mg g^{-1} and 31.25 mg g^{-1} , respectively, for a CFX-added concentration of 20 mg L^{-1} . Ma et al. [75] studied CFX adsorption with a cationic *Enteromorpha prolifera* polysaccharide-based hydrogel, obtaining adsorptions of 5 mg g^{-1} for a concentration of 50 mg L^{-1} and 25–30 mg g^{-1} for a concentration of

400 mg L⁻¹. In addition, different bioadsorbents have been previously studied regarding their adsorption of other antibiotics of the cephalosporins group. Among them, biochar derived from fiber residues of palm oil were used to remove cephalixin, obtaining adsorption values of 57.47 mg g⁻¹ [76]. Cephalixin adsorption was also studied for natural zeolite and zeolite coated with manganese oxide nanoparticles, reaching adsorption values of 16.1 and 24.5 mg g⁻¹, respectively [77]. When comparing these results with the data obtained in the current study, the bioadsorbents used here showed lower adsorption capacities in the specific experimental conditions of the present research (which are not identical to those of the other investigations). However, expressed as a percentage, adsorption was above 80% for the mussel shell and oak ash in most cases. We note that the adsorbent materials evaluated in the referred previous research are not low-cost materials. In light of this, in case of requiring better adsorption performance associated with the low-cost byproducts employed here, one might suggest assessing the effect of carrying out different chemical modifications in this regard. Table 4 shows the results corresponding to each of the compared bioadsorbents.

Table 4. Comparison of antibiotics' adsorption capacities for various bioadsorbents.

Bioadsorbent	Antibiotic	Initial Concentration	Adsorption (mg g ⁻¹)	Reference
Activated carbon	Cefuroxime	20 mg L ⁻¹	26.31	Awwad et al., 2015 [74]
Micelle-clay complex	Cefuroxime	20 ppm	31.25	Awwad et al., 2015 [74]
<i>Enteromorpha prolifera</i> polysaccharide-based hydrogel	Cefuroxime	50 mg L ⁻¹	5	Ma et al., 2022 [75]
<i>Enteromorpha prolifera</i> polysaccharide-based hydrogel	Cefuroxime	400 mg L ⁻¹	25–30	Ma et al., 2022 [75]
Fiber residues of palm oil	Cephalixin	20 mg L ⁻¹	57.47	Acelas et al., 2021 [76]
Natural zeolite	Cephalixin	10 mg L ⁻¹	16.1	Samarghandi, 2015 [77]
MnO zeolite	Cephalixin	10 mg L ⁻¹	24.5	Samarghandi, 2015 [77]
Pine bark	Cefuroxime	21 mg L ⁻¹	0.037	This study
Mussel shell	Cefuroxime	21 mg L ⁻¹	0.052	This study
Oak ash	Cefuroxime	21 mg L ⁻¹	0.052	This study

3.4. Desorption

Desorption was always lower than 10% for the soils without bioadsorbents and decreased to 0% when the bioadsorbents were added, indicating strong retention. Similar results were previously obtained for amoxicillin in equivalent mixtures, where desorption decreased from 17% to 6% after adding bioadsorbent amendments to the soils [68].

4. Conclusions

The two bioadsorbents we investigated which had alkaline pH levels (mussel shell and oak ash) were highly effective at increasing CFX adsorption after being applied to the studied soils, resulting in strong and practically irreversible retention. The bioadsorbent amendment at 12 t/ha was sufficient to achieve these effects and did not require higher doses. In contrast, the bioadsorbent having an acidic pH, pine bark, was less effective, in some cases (high CFX concentrations and a dose of 48 t/ha of the bioadsorbent) even causing a decrease in CFX adsorption compared with the unamended soil. These facts suggest that among the different characteristics of the soils and bioadsorbents studied here, the pH level would be the one with the highest influence on adsorption of the antibiotic CFX. These results could be useful to manage soils and other environmental compartments affected by pollution episodes due to the antibiotic CFX, which can clearly be seen as relevant. For future research, it would be interesting to carry out equivalent

experiments focusing on the efficacy of the bioadsorbents studied here and other low-cost bioadsorbents to retain combinations of different antibiotics simultaneously present in the medium. In addition, complementary studies to shed further light on the retention and release mechanisms would be of relevance, as well as investigating low-cost procedures to increase the efficacy of raw adsorbents in cases where they would be needed.

Supplementary Materials: The following supporting information can be downloaded at <https://www.mdpi.com/article/10.3390/pr12071335/s1>. Table S1: Values corresponding to the basic parameters determined in the soils. C = corn soils; VO = vineyard soils (Ourense province); and VP = vineyard soils (Pontevedra province). Average values (n = 3) with coefficients of variation always <5%. Table S2: pH values of soils amended with the bio-adsorbents in doses of 12 and 48 t/ha. C = corn soils; VO = vineyard soils (Ourense province); VP = vineyard soils (Pontevedra province); A = ash; MS = mussel shell; and PB = pine bark. Figure S1: Example chromatograms corresponding to CFX adsorption onto soils amended with bio-adsorbents.

Author Contributions: Conceptualization, E.Á.-R., M.J.F.-S., and A.N.-D.; methodology, E.Á.-R., M.J.F.-S., A.N.-D., M.A.-E., R.C.-D., and A.M.-G.; software, E.Á.-R. and R.C.-D.; validation, E.Á.-R., M.J.F.-S., A.N.-D., and A.B.; formal analysis, R.C.-D.; investigation, E.Á.-R., M.J.F.-S., R.C.-D., and A.M.-G.; resources, E.Á.-R., M.J.F.-S., and M.A.-E.; data curation, E.Á.-R., M.J.F.-S., A.N.-D., and A.B.; writing—original draft preparation, E.Á.-R., M.J.F.-S., A.M.-G., and R.C.-D.; writing—review and editing, A.N.-D.; visualization, E.Á.-R., M.J.F.-S., A.N.-D., R.C.-D., L.R.-L., A.M.-G., and A.B.; supervision, E.Á.-R., M.J.F.-S., A.B., and A.N.-D.; project administration, E.Á.-R., M.J.F.-S., and M.A.-E.; funding acquisition, E.Á.-R., M.J.F.-S., and M.A.-E. All authors have read and agreed to the published version of the manuscript.

Funding: This research was funded by the Spanish “Agencia Estatal de Investigación” (State Investigation Agency) (grant number PID2021-122920OB-C21). Cela-Dablanca R. received a predoctoral grant from Campus Terra (University of Santiago de Compostela).

Data Availability Statement: Data are contained within the article and Supplementary Materials.

Conflicts of Interest: The authors declare no conflicts of interest. The funders had no role in the design of the study; in the collection, analyses, or interpretation of data; in the writing of the manuscript; or in the decision to publish the results.

References

- Phoon, B.L.; Ong, C.C.; Shuaib, M.; Saheed, M.; Show, P.; Chang, J.; Ling, T.C.; Lam, S.S.; Juan, J.C. Conventional and emerging technologies for removal of antibiotics from wastewater. *J. Hazard. Mater.* **2020**, *400*, 122961–122988. [CrossRef]
- Gothwal, R.; Shashidhar, T. Antibiotic pollution in the environment: A review. *Clean Soil Air Water* **2015**, *43*, 479–489. [CrossRef]
- Yang, Q.; Gao, Y.; Ke, J.; Show, P.L.; Ge, Y.; Liu, Y.; Guo, R.; Chen, J. Antibiotics: An overview on the environmental occurrence, toxicity, degradation, and removal methods. *Bioengineered* **2021**, *12*, 7376–7416. [CrossRef]
- Kümmerer, K. The presence of pharmaceuticals in the environment due to human use—present knowledge and future challenges. *J. Environ. Manage.* **2009**, *90*, 2354–2366. [CrossRef] [PubMed]
- Löffler, P.; Escher, B.I.; Baduel, C.; Virta, M.P.; Lai, F.Y. Antimicrobial transformation products in the aquatic environment: Global occurrence, ecotoxicological risks, and potential of antibiotic resistance. *Environ. Sci. Tech.* **2023**, *57*, 9474–9494. [CrossRef]
- Jelic, A.; Rodriguez-Mozaz, S.; Barceló, O.; Gutierrez, O. Impact of in-sewer transformation on 43 pharmaceuticals in a pressurized sewer under anaerobic conditions. *Water Res.* **2015**, *68*, 98–108. [CrossRef]
- Quaik, S.; Embrandiri, A.; Ravindran, B.; Hossain, K.; Abdullah Al-Dhabi, N.; Valan Arasu, M.; Ignacimuthu, S.; Ismail, N. Veterinary antibiotics in animal manure and manure laden soil: Scenario and challenges in Asian countries. *J. King Saud Univ. Sci.* **2020**, *32*, 1300–1305. [CrossRef]
- Foroughi, M.; Khiadani, M.; Kakhki, S.; Kholghi, V.; Naderi, K.; Yektay, S. Effect of ozonation-based disinfection methods on the removal of antibiotic resistant bacteria and resistance genes (ARB/ARGs) in water and wastewater treatment: A systematic review. *Sci. Total Environ.* **2022**, *811*, 151404–151426. [CrossRef]
- Makowska, N.; Koczura, R.; Mokracka, J. Class 1 integrase, sulfonamide and tetracycline resistance genes in wastewater treatment plant and surface water. *Chemosphere* **2016**, *144*, 1665–1673. [CrossRef]
- Karkman, A.; Do, T.T.; Walsh, F.; Virta, M.P.J. Antibiotic-resistance genes in waste water. *Trends Microbiol.* **2018**, *26*, 220–228. [CrossRef]
- Larsson, D.G.J.; Flach, C.F.; Laxminarayan, R. Sewage surveillance of antibiotic resistance holds both opportunities and challenges. *Nat. Rev. Microbiol.* **2023**, *21*, 213–214. [CrossRef] [PubMed]

12. Rawson, T.M.; Ming, D.; Ahmad, R.; Moore, L.S.P.; Holmes, A.H. Antimicrobial use, drug-resistant infections and COVID-19. *Nat. Rev. Microbiol.* **2020**, *18*, 409–410. [CrossRef] [PubMed]
13. Hsu, J. How COVID-19 is accelerating the threat of antimicrobial resistance. *BMJ* **2020**, *369*, 1983–1984. [CrossRef] [PubMed]
14. Abegglen, C.; Joss, A.; McARDell, C.S.; Fink, G.; Schlüsener, M.P.; Ternes, T.A.; Siegrist, H. The fate of selected micropollutants in a single-house MBR. *Water Res.* **2009**, *43*, 2036–2046. [CrossRef] [PubMed]
15. Massé, D.I.; Saady, N.M.C.; Gilbert, Y. Potential of biological processes to eliminate antibiotics in livestock manure: An overview. *Animals* **2014**, *4*, 146–163. [CrossRef] [PubMed]
16. Moles, S.; Mosteo, R.; Gómez, J.; Szpunar, J.; Gozzo, S.; Castillo, J.R.; Ormad, M.P. Towards the removal of antibiotics detected in wastewaters in the POCTEFA territory: Occurrence and TiO₂ photocatalytic pilot-scale plant performance. *Water* **2020**, *12*, 1453. [CrossRef]
17. Solís, R.R.; Chávez, A.M.; Monago-Maraña, O.; Muñoz de la Peña, A.; Beltrán, F.J. Photo-assisted ozonation of cefuroxime with solar radiation in a CPC pilot plant. Kinetic parameters determination. *Sep. Purif. Technol.* **2021**, *266*, 118514. [CrossRef]
18. Oğuz, M.; Mihçioğur, H. Environmental risk assessment of selected pharmaceuticals in Turkey. *Environ. Toxicol. Pharmacol.* **2014**, *38*, 79–83. [CrossRef] [PubMed]
19. Yu, X.; Tang, X.; Zuo, J.; Zhang, M.; Chen, L.; Li, Z. Distribution and persistence of cephalosporins in cephalosporin producing wastewater using SPE and UPLC–MS/MS method. *Sci. Total Environ.* **2016**, *569–570*, 23–30. [CrossRef]
20. Rossmann, J.; Schubert, S.; Gurke, R.; Oertel, R.; Kirch, W. Simultaneous determination of most prescribed antibiotics in multiple urban wastewater by SPE-LC–MS/MS. *J. Chromatogr. B.* **2014**, *969*, 162–170. [CrossRef]
21. Kinney, C.A.; Furlong, E.T.; Werner, S.L.; Cahill, J.D. Presence and distribution of wastewater-derived pharmaceuticals in soil irrigated with reclaimed water. *Environ. Toxicol.* **2009**, *25*, 317–326. [CrossRef] [PubMed]
22. Styszko, K.; Durak, J.; Kończak, B.; Głodniok, M.; Borgulat, A. The impact of sewage sludge processing on the safety of its use. *Sci. Rep.* **2022**, *12*, 12227. [CrossRef] [PubMed]
23. Cerqueira, F.; Christou, A.; Fatta-Kassinos, D.; Vila-Costa, M.; Bayona, J.M.; Piña, B. Effects of prescription antibiotics on soil- and root-associated microbiomes and resistomes in an agricultural context. *J. Hazard. Mater.* **2020**, *400*, 123208–123219. [CrossRef]
24. Hamdi, H.; Hechmi, S.; Khelil, M.N.; Zoghalmi, I.R.; Benzarti, S.; Mokni-Tlili, S.; Hassen, A.; Jedidi, N. Repetitive land application of urban sewage sludge: Effect of amendment rates and soil texture on fertility and degradation parameters. *Catena* **2019**, *172*, 11–20. [CrossRef]
25. Urra, J.; Alkorta, I.; Mijangos, I.; Epelde, L.; Garbisu, C. Application of sewage sludge to agricultural soil increases the abundance of antibiotic resistance genes without altering the composition of prokaryotic communities. *Sci. Total Environ.* **2019**, *647*, 1410–1420. [CrossRef] [PubMed]
26. Kelessidis, A.; Stasinakis, A.S. Comparative study of the methods used for treatment and final disposal of sewage sludge in European countries. *Waste Manag.* **2012**, *32*, 1186–1195. [CrossRef] [PubMed]
27. Malmborg, J.; Magnér, J. Pharmaceutical residues in sewage sludge: Effect of sanitization and anaerobic digestion. *J. Environ. Manag.* **2015**, *153*, 1–10. [CrossRef]
28. Ezzariai, A.; Hafidi, M.; Khadra, A.; Aemig, Q.; Fels, L.E.; Barret, M.; Merlina, G.; Patureau, D.; Pinelli, E. Human and veterinary antibiotics during composting of sludge or manure: Global perspectives on persistence, degradation, and resistance genes. *J. Hazard. Mater.* **2018**, *359*, 465–481. [CrossRef]
29. Buta, M.; Hubeny, J.; Zieliński, W.; Harnisz, M.; Korzeniewska, E. Sewage sludge in agriculture—The effects of selected chemical pollutants and emerging genetic resistance determinants on the quality of soil and crops—A review. *Ecotoxicol. Environ. Saf.* **2021**, *214*, 112070. [CrossRef]
30. Roig, N.; Sierra, J.; Martí, E.; Nadal, M.; Schuhmacher, M.; Domingo, J.L. Long-term amendment of Spanish soils with sewage sludge: Effects on soil functioning. *Agr. Ecosyst. Environ.* **2012**, *158*, 41–48. [CrossRef]
31. Petrie, B.; Barden, R.; Kasprzyk-Hordern, B. A review on emerging contaminants in wastewaters and the environment: Current knowledge, understudied areas and recommendations for future monitoring. *Water Res.* **2014**, *72*, 3–27. [CrossRef] [PubMed]
32. Fijalkowski, K.; Rorat, A.; Grobelak, A.; Kacprzak, M.J. The presence of contaminations in sewage sludge—The current situation. *J. Environ. Manag.* **2017**, *203*, 1126–1136. [CrossRef] [PubMed]
33. Ma, L.; Li, B.; Jiang, X.T.; Wang, Y.L.; Xia, Y.; Li, A.D.; Zhang, T. Catalogue of antibiotic resistome and host-tracking in drinking water deciphered by a large scale survey. *Microbiome* **2017**, *5*, 154–165. [CrossRef] [PubMed]
34. Szekeres, E.; Chiriac, C.M.; Baricz, A.; Szóke-Nagy, T.; Lung, I.; Soran, M.L.; Rudi, K.; Dragos, N.; Coman, C. Investigating antibiotics, antibiotic resistance genes, and microbial contaminants in groundwater in relation to the proximity of urban areas. *Environ. Pollut.* **2018**, *236*, 734–744. [CrossRef] [PubMed]
35. Shi, J.; Dong, Y.; Shi, Y.; Yin, T.; He, W.; An, T.; Tang, Y.; Hou, X.; Chong, S.; Chen, D.; et al. Groundwater antibiotics and microplastics in a drinking-water source area, northern China: Occurrence, spatial distribution, risk assessment, and correlation. *Environ. Res.* **2022**, *210*, 112855. [CrossRef] [PubMed]
36. Vermillion Maier, M.L.; Tjeerdema, R.S. Azithromycin sorption and biodegradation in a simulated California river system. *Chemosphere* **2018**, *190*, 471–480. [CrossRef] [PubMed]
37. Zheng, S.; Wang, Y.; Chen, C.; Zhou, X.; Liu, Y.; Yang, J.; Geng, Q.; Chen, G.; Ding, Y.; Yang, F. Current Progress in Natural Degradation and Enhanced Removal Techniques of Antibiotics in the Environment: A Review. *Int. J. Environ. Res. Public Health* **2022**, *19*, 10919. [CrossRef] [PubMed]

38. Pan, M.; Chu, L.M. Fate of antibiotics in soil and their uptake by edible crops. *Sci. Total Environ.* **2017**, *599–600*, 500–512. [CrossRef] [PubMed]
39. Rietra, R.P.J.J.; Berendsen, B.J.A.; Mi-Gegotek, Y.; Römkens, P.F.A.M.; Pustjens, A.M. Prediction of the mobility and persistence of eight antibiotics based on soil characteristics. *Helijon* **2024**, *10*, e23718. [CrossRef]
40. Yang, L.; Wu, L.; Liu, W.; Huang, Y.; Luo, Y.; Christie, P. Dissipation of antibiotics in three different agricultural soils after repeated application of biosolids. *Environ. Sci. Pollut. Res.* **2018**, *25*, 104–114. [CrossRef]
41. Conde-Cid, M.; Fernández-Calviño, D.; Nóvoa-Muñoz, J.C.; Arias-Estévez, M.; Díaz-Raviña, M.; Núñez-Delgado, A.; Fernández-Sanjurjo, M.J.; Álvarez-Rodríguez, E. Degradation of sulfadiazine, sulfachloropyridazine and sulfamethazine in aqueous media. *J. Environ. Manag.* **2018**, *228*, 239–248. [CrossRef]
42. Rodríguez-López, L.; Cela-Dablanca, R.; Núñez-Delgado, A.; Álvarez-Rodríguez, E.; Fernández-Calviño, D.; Arias-Estévez, M. Photodegradation of Ciprofloxacin, Clarithromycin and Trimethoprim: Influence of pH and Humic Acids. *Molecules* **2021**, *26*, 3080. [CrossRef] [PubMed]
43. Jiang, M.; Wang, L.; Ji, R. Biotic and abiotic degradation of four cephalosporin antibiotics in a lake surface water and sediment. *Chemosphere* **2010**, *80*, 1399–1405. [CrossRef] [PubMed]
44. Cheng, N.; Wang, B.; Wu, P.; Lee, X.; Chen, M.; Gao, B. Adsorption of emerging contaminants from water and wastewater by modified biochar: A review. *Environ. Pollut.* **2021**, *273*, 116448–116461. [CrossRef]
45. Aksu, Z.; Tunç, Ö. Application of biosorption for penicillin G removal: Comparison with activated carbon. *Process Biochem.* **2005**, *40*, 831–847. [CrossRef]
46. Acevedo-García, V.; Rosales, E.; Puga, A.; Pazos, M.; Sanromán, M.A. Synthesis and use of efficient adsorbents under the principles of circular economy: Waste valorisation and electroadvanced oxidation process regeneration. *Sep. Purif. Technol.* **2020**, *242*, 116796. [CrossRef]
47. Schmidtová, Z.; Kodešová, R.; Grabicová, K.; Kočárek, M.; Fér, M.; Švecová, H.; Klement, A.; Nikodem, A.; Grabic, R. Competitive and synergic sorption of carbamazepine, citalopram, clindamycin, fexofenadine, irbesartan and sulfamethoxazole in seven soils. *J. Contam. Hydrol.* **2020**, *234*, 103680–103692. [CrossRef] [PubMed]
48. Jiang, C.; Cai, H.; Chen, L.; Chen, L.; Cai, T. Effect of forestry-waste biochars on adsorption of Pb(II) and antibiotic florfenicol in red soil. *Environ. Sci. Pollut. Res.* **2017**, *24*, 3861–3871. [CrossRef]
49. Nkoh, J.N.; Oderinde, O.; Etafo, N.O.; Kifle, G.A.; Okeke, E.S.; Ejeromedoghene, O.; Mgbachidinma, C.L.; Oke, E.A.; Raheem, S.A.; Bakare, O.C.; et al. Recent perspective of antibiotics remediation: A review of the principles, mechanisms, and chemistry controlling remediation from aqueous media. *Sci. Total Environ.* **2023**, *881*, 163469. [CrossRef]
50. Juela, D. Promising adsorptive materials derived from agricultural and industrial wastes for antibiotic removal: A comprehensive review. *Sep. Purif. Technol.* **2022**, *284*. [CrossRef]
51. Ahmed, M.; Mavukkandy, M.O.; Giwa, A.; Elektorowicz, M.; Katsou, E.; Khelifi, O.; Naddeo, V.; Hasan, S.W. Recent developments in hazardous pollutants removal from wastewater and water reuse within a circular economy. *NPJ Clean Water* **2022**, *5*, 12. [CrossRef]
52. Conde-Cid, M.; Fernández-Calviño, D.; Fernández-Sanjurjo, M.J.; Núñez-Delgado, A.; Álvarez-Rodríguez, E.; Arias-Estévez, M. Effects of pine bark amendment on the transport of sulfonamide antibiotics in soils. *Chemosphere* **2020**, *248*, 126041. [CrossRef]
53. Míguez-González, A.; Cela-Dablanca, R.; Barreiro, A.; Rodríguez-López, L.; Rodríguez-Seijo, A.; Arias-Estévez, M.; Núñez-Delgado, A.; Fernández-Sanjurjo, M.J.; Castillo-Ramos, V.; Álvarez-Rodríguez, E. Adsorption of antibiotics on bio-adsorbents derived from the forestry and agro-food industries. *Environ. Res.* **2023**, *233*, 116360. [CrossRef]
54. Cela-Dablanca, R.; Nebot, C.; Rodríguez-López, L.; Fernández-Calviño, D.; Arias-Estévez, M.; Núñez-Delgado, A.; Álvarez-Rodríguez, E.; Fernández-Sanjurjo, M.J. Retention of the Antibiotic Cefuroxime onto Agricultural and Forest Soils. *Appl. Sci.* **2021**, *11*, 4663. [CrossRef]
55. Guitián, F.; Carballas, T. *Técnicas de Análise de Solos (Soil Analysis Techniques)*; Editorial Pico Sacro: Santiago de Compostela, Spain, 1976.
56. Olsen, S.R.; Sommers, L.E. Phosphorus. In *Methods of Soil Analysis: Part 2 Chemical and Microbiological Properties*; Page, A.L., Miller, R.H., Keeney, D.R., Eds.; SSSA, Inc.: Madison, WI, USA, 1982.
57. Ayawei, N.; Ebelegi, A.N.; Wankasi, D. Modelling and Interpretation of Adsorption Isotherms. *J. Chem.* **2017**, *2017*, 11–23. [CrossRef]
58. Núñez-Delgado, A. Research on environmental aspects of retention/release of pollutants in soils and sorbents. What should be next? *Environ. Res.* **2024**, *251*, 118593. [CrossRef]
59. Núñez-Delgado, A. Avoiding basic mistakes when programming the use of artificial intelligence in soil and environmental science research. *Sci. Total Environ.* **2024**, *934*, 173310. [CrossRef] [PubMed]
60. Cela-Dablanca, R.; Nebot, C.; Rodríguez-López, L.; Fernández-Calviño, D.; Arias-Estévez, M.; Núñez-Delgado, A.; Fernández-Sanjurjo, M.J.; Álvarez-Rodríguez, E. Efficacy of Different Waste and By-Products from Forest and Food Industries in the Removal/Retention of the Antibiotic Cefuroxime. *Processes* **2021**, *9*, 1151. [CrossRef]
61. Pavlović, D.M.; Čop, K.T.; Barbir, V.; Gotovuša, M.; Lukač, I.; Lozančić, A.; Runje, M. Sorption of cefdinir, memantine, praziquantel and trimethoprim in sediment and soil samples. *Environ. Sci. Pollut. Res.* **2022**, *29*, 66841–66857. [CrossRef]
62. El-Shaboury, S.R.; Saleh, G.A.; Mohamed, F.A.; Rageh, A.H. Analysis of cephalosporin antibiotics. *J. Pharmaceut. Biomed. Anal.* **2007**, *45*, 1–19. [CrossRef]

63. Lin, C.E.; Chen, H.W.; Lin, E.C.; Lin, K.S.; Huang, H.C. Optimization of separation and migration behavior of cephalosporins in capillary zone electrophoresis. *J. Chromatogr. A* **2000**, *879*, 197–210. [CrossRef]
64. Ribeiro, A.R.; Schmidt, T.C. Determination of acid dissociation constants (pKa) of cephalosporin antibiotics: Computational and experimental approaches. *Chemosphere* **2017**, *169*, 524–533. [CrossRef]
65. Legnoverde, M.S.; Simonetti, S.; Basaldella, E.I. Influence of pH on cephalixin adsorption onto SBA-15 mesoporous silica: Theoretical and experimental study. *Appl. Surf. Sci.* **2014**, *300*, 37–42. [CrossRef]
66. Peng, X.; Hu, F.; Lam, F.L.; Wang, Y.; Liu, Z.; Dai, H. Adsorption behavior and mechanisms of ciprofloxacin from aqueous solution by ordered mesoporous carbon and bamboo-based carbon. *J. Colloid Interface Sci.* **2015**, *460*, 349–360. [CrossRef] [PubMed]
67. Imanipoor, J.; Mohammadi, M. Porous Aluminum-Based Metal–Organic Framework–Aminoclay Nanocomposite: Sustainable Synthesis and Ultrahigh Sorption of Cephalosporin Antibiotics. *Langmuir* **2022**, *38*, 5323–5954. [CrossRef] [PubMed]
68. Cela-Dablanca, R.; Barreiro, A.; Rodríguez-López, L.; Santás-Miguel, V.; Arias-Estévez, M.; Fernández-Sanjurjo, M.J.; Álvarez-Rodríguez, E.; Núñez-Delgado, A. Amoxicillin Retention/Release in Agricultural Soils Amended with Different Bio-Adsorbent Materials. *Materials* **2022**, *15*, 3200. [CrossRef] [PubMed]
69. Proctor, A.; Toro-Vazquez, J.F. The Freundlich isotherm in studying adsorption in oil processing. *JAOCS* **1996**, *73*, 1627–1633. [CrossRef]
70. Tamer, A.; Elbana, H.; Selim, M.; Akrami, N.; Newman, A.; Shaheen, S.M.; Rinklebe, J. Freundlich sorption parameters for cadmium, copper, nickel, lead, and zinc for different soils: Influence of kinetics. *Geoderma* **2018**, *324*, 80–88. [CrossRef]
71. Foo, K.Y.; Hameed, B.H. Insights into the modeling of adsorption isotherm systems. *Chem. Eng. J.* **2010**, *156*, 2–10. [CrossRef]
72. Jafari, M.; Aghamiri, S.F.; Khaghanic, G. Batch Adsorption of Cephalosporins Antibiotics from Aqueous Solution by Means of Multi-Walled Carbon Nanotubes. *World Appl. Sci. J.* **2011**, *14*, 1642–1650.
73. Behnajady, M.A.; Bimeghdar, S. Synthesis of mesoporous NiO nanoparticles and their application in the adsorption of Cr (VI). *Chem. Eng. J.* **2014**, *239*, 105–113. [CrossRef]
74. Awwad, M.; Al-Rimawi, F.; Dajani, K.J.; Khamis, M.; Nir, S.; Karaman, R. Removal of amoxicillin and cefuroxime axetil by advanced membranes technology, activated carbon and micelle-clay complex. *Environ Technol.* **2015**, *36*, 2069. [CrossRef] [PubMed]
75. Ma, X.; Duan, D.; Chen, J.; Xie, B. Structure and Adsorption Performance of Cationic Entermorpha prolifera Polysaccharide-Based Hydrogel for Typical Pollutants: Methylene Blue, Cefuroxime, and Cr (VI). *Gels* **2022**, *8*, 546. [CrossRef] [PubMed]
76. Acelas, N.; Lopera, S.M.; Porras, J.; Torres-Palma, R.A. Evaluating the Removal of the Antibiotic Cephalixin from Aqueous Solutions Using an Adsorbent Obtained from Palm Oil Fiber. *Molecules* **2021**, *26*, 3340. [CrossRef]
77. Samarghandi, M.R.; Al-Musawi, T.J.; Mohseni-Bandpi, A.; Zarrabi, M. Adsorption of cephalixin from aqueous solution using natural zeolite and zeolite coated with manganese oxide nanoparticles. *J. Mol. Liq.* **2015**, *211*, 431–441. [CrossRef]

Disclaimer/Publisher’s Note: The statements, opinions and data contained in all publications are solely those of the individual author(s) and contributor(s) and not of MDPI and/or the editor(s). MDPI and/or the editor(s) disclaim responsibility for any injury to people or property resulting from any ideas, methods, instructions or products referred to in the content.

Article

Determination of 24 Trace Aromatic Substances in Rosemary Hydrosol by Dispersed Liquid–Liquid Microextraction–Gas Chromatography

Xiaoming Zeng, Hao He, Liejiang Yuan *, Haizhi Wu * and Cong Zhou

Hunan Provincial Institute of Product and Goods Quality Inspection, Changsha 410007, China; xiaomingzeng0731@163.com (X.Z.); 18673272562@163.com (H.H.); congzhou0731@163.com (C.Z.)

* Correspondence: yuanliejiang@163.com (L.Y.); whzh861028@126.com (H.W.)

Abstract: A combined dispersed liquid–liquid microextraction (DLLME) and chromatography (GC) method was developed for the determination of 24 aromatic substances in rosemary hydrosol in this work. The pretreatment method of DLLME was optimized by carefully selecting the appropriate extraction agents, dispersants, and their respective amounts. With carbon tetrachloride as the extractant and acetone as the dispersant, the enrichment factor of DLLME is 13.3, and the 24 target substances such as eucalyptol, camphor and verbenone can be separated within 31 min and quantified by an external standard method using gas chromatography (GC). The correlation coefficient r^2 of the linear regression equation is within the range of 0.9983 to 0.9991. The detection limit of the method was 0.02 mg/L, the recovery rate of the spiked solution was 76.4–118.4%, the relative standard deviation was 0.4–6.9% and the method was used to detect the semi-finished products of rosemary hydrosol and the finished rosemary hydrosol sold on the market. This method also provides a reference for the qualitative and quantitative determination of aromatic substances in other hydrosols.

Keywords: rosemary hydrosol; dispersed liquid–liquid microextraction; gas chromatography; external standard method; aromatic organics

Citation: Zeng, X.; He, H.; Yuan, L.; Wu, H.; Zhou, C. Determination of 24 Trace Aromatic Substances in Rosemary Hydrosol by Dispersed Liquid–Liquid Microextraction–Gas Chromatography. *Processes* **2024**, *12*, 498. <https://doi.org/10.3390/pr12030498>

Academic Editors: Avelino Núñez-Delgado, Elza Bontempi, Yaoyu Zhou, Esperanza Alvarez-Rodriguez, Maria Victoria Lopez-Ramon, Mario Coccia, Zhien Zhang, Vanesa Santas-Miguel and Marco Race

Received: 8 February 2024
Revised: 24 February 2024
Accepted: 25 February 2024
Published: 28 February 2024



Copyright: © 2024 by the authors. Licensee MDPI, Basel, Switzerland. This article is an open access article distributed under the terms and conditions of the Creative Commons Attribution (CC BY) license (<https://creativecommons.org/licenses/by/4.0/>).

1. Introduction

Rosemary, also known as *Rosmarinus officinalis*, is a perennial evergreen subshrub plant, belonging to the angiosperms, dicotyledonous plants and tubular flowering trees. Rosemary is native to Europe and North Africa along the Mediterranean coast and is now widely cultivated in many countries in Europe, North America and China [1–3]. Rosemary hydrosol has a natural rosemary fragrance, which can be used as a raw material for the production of cosmetics or facial masks [4]. It has antioxidant [5,6], antibacterial [7,8] and other effects. Tornuk et al. [9] used rosemary extract as a food disinfectant in their research. The composition of rosemary essential oils varies greatly due to different germplasm resources, growing regions, climates and environments [10,11]. Similar to rosemary essential oil, rosemary hydrosol can be divided into Tunisian, Moroccan and Spanish types according to their different germplasm resources. Among them, Tunisian and Moroccan rosemary hydrosol are habitually called “camphor rosemary hydrosol” because they are rich in camphor, and Spanish rosemary hydrosol is habitually called “verbenone rosemary hydrosol” because it is rich in verbenone [12,13].

In the field of rosemary hydrosol analysis, researchers have explored various methods to determine the composition and content of its components. Two commonly used techniques are direct injection and concentrated injection after ether extraction [5,14,15]. Direct injection involves directly injecting the rosemary hydrosol sample into the analytical instrument without any additional sample preparation steps. This method is simple and convenient but may not be sensitive enough to detect trace organic matter due to the low

organic content in rosemary hydrosol. Concentrated injection after ether extraction, on the other hand, involves extracting the components from the hydrosol using an ether solvent and then concentrating the extract before injection into the instrument. This method allows for better detection of trace organic compounds by increasing their concentration. However, it requires a significant amount of ether per sample and can lead to the loss of volatile components during the concentration process. In a study conducted by Kenichi Tomi et al., 1000 μL of hydrosol was transferred into a 1.5 mL sample tube, and then 100 μL of *n*-hexane and 50 mg of NaCl were added to extract aroma components into the organic fraction; finally, 0.5 μL of the resulting organic fraction was injected into the GC-MS system using a 5.0 μm micro syringe. However, the absolute content of analytes were not discussed in their work [15]. And in a study by Matteo Politi et al., the target analytes of rosemary samples were concentrated by solid phase microextraction (SPME) and analyzed by GC-MS. They also obtained the results of the relative content of rosemary samples [16]. To overcome these limitations, dispersive liquid–liquid microextraction (DLLME) has emerged as a promising technique for rosemary hydrosol analysis. DLLME involves dispersing a small volume of an extraction solvent (such as chloroform or dichloromethane) and a dispersant (typically a water-miscible organic solvent like acetone or ethanol) in the sample solution, creating a cloudy mixture [17–19]. Upon phase separation, the target analytes partition into the fine droplets of the extraction solvent, leading to improved enrichment efficiency and sensitivity. DLLME offers several advantages over traditional methods. It is relatively simple, rapid, cost-effective and requires only a small amount of extractants. Furthermore, DLLME reduces the consumption of organic solvents compared to other extraction techniques [20]. It can be easily coupled with various analytical instruments such as gas chromatography (GC) [21,22], liquid chromatography (LC) [23] or mass spectrometry (MS) [24] for the separation and detection of target compounds. However, there is currently a lack of literature reports utilizing DLLME as a pretreatment method for the determination of absolute content of aromatic compounds in rosemary by GC analysis. In this study, DLLME was selected as the extraction and concentration method for rosemary hydrosol analysis. The pretreatment method of DLLME was optimized by carefully selecting appropriate extraction agents, dispersants, and their respective amounts. By fine-tuning the extraction parameters, the method achieved a very low detection limit, enabling accurate determination of trace components in rosemary hydrosol when combined with gas chromatography. This advanced approach provides valuable insights into the antioxidant, antibacterial and odor-related properties of rosemary hydrosol, contributing to a deeper understanding of its chemical composition and potential benefits in various applications. It offers a novel and efficient way to analyze rosemary hydrosol and can serve as a foundation for further research in this field.

2. Materials and Methods

2.1. Materials and Reagents

The specified purities of the following standard substances were obtained from Shanghai Aladdin Biochemical Technology Co., Ltd. (Shanghai, China): α -Pinene ($\geq 98.0\%$), (\pm)-Camphene ($\geq 95.0\%$), β -Pinene ($\geq 98.0\%$), Myrcene ($\geq 90.0\%$), α -Terpinene ($\geq 90.0\%$), (R)-(+)-Limonene ($\geq 99.0\%$), Eucalyptol ($\geq 99.5\%$), trans-2-Hexen-1-a ($\geq 98.0\%$), γ -Terpinene ($\geq 95.0\%$), 4-Isopropyltoluene ($\geq 99.5\%$), Terpinolene ($\geq 90.0\%$), Methyl heptenone ($\geq 98.0\%$), cis-3-Hexen-1-ol ($\geq 98.0\%$), D(+)-Camphor ($\geq 96.0\%$), Linalool ($\geq 98.0\%$), Linalyl Acetate ($\geq 96.0\%$), Isobornyl Acetate ($\geq 94.0\%$), (-)-trans-Caryophyllene ($\geq 98.0\%$), 4-Carvomenthenol ($\geq 98.0\%$), Isoborneol ($\geq 90.0\%$), α -Terpineol ($\geq 98.0\%$), (-)-Verbenone ($\geq 95.0\%$), Neryl acetate ($\geq 95.0\%$) and Geraniol ($\geq 98.0\%$).

HPLC-grade carbon tetrachloride (MackLin, Shanghai, China) was used as the extractant, while pesticide residue-grade chloroform (Anpel, Shanghai, China) and dichloromethane (Anpel, Shanghai, China) were used as alternative extractants. Pesticide residue-grade acetone (Anpel, Shanghai, China) served as the dispersant and was also used for standard preparation. Additionally, HPLC-grade carbon disulfide (MackLin, Shanghai, China), pesticide

residue-grade methanol (Anpel, Shanghai, China), pesticide-residue grade acetonitrile (Anpel, Shanghai, China), and HPLC-grade ethanol (Anpel, Shanghai, China) were utilized as dispersants. Analytical reagent sodium chloride (Sinopharm Chemical Reagent, Shanghai, China) was employed as an electrolyte. Ultrapure water (PERSEE, resistance = 18.2 M Ω , Shenzhen, China) was utilized for the experiment. Samples included both semi-finished rosemary hydrosols from a plant extract enterprise in Changsha, China, and finished rosemary hydrosols sourced from Taobao in Hangzhou, China. To prepare the calibration curve, the 24 types of standards were dissolved and freshly diluted in acetone to concentrations of 5, 10, 20, 50, 100 and 200 $\mu\text{g}/\text{mL}$.

2.2. Instruments and Equipment

An Nexis GC-2030 GC with a flame ionization detector (Shimadzu, Kyoto, Japan) and fused silica capillary column DB-WAX (polyethylene glycol coating, 30 m \times 0.32 mm, 0.25 μm , Agilent, Santa Clara, CA, USA) were used for data acquisition. The detail parameters of the GC can be seen in Table 1. BSA224S electronic balance (accuracy 0.1 mg, Sedoris, Göttingen, Germany) was used for weighing reagents; S225D-1CN electronic balance (accuracy 0.01 mg, Sartorius, Göttingen, Germany) was used for weighing standard substances; 200 μL and 1 mL pipette guns (Eppendorf, Hamburg, Germany) were used to transfer standard solutions, extractants, and dispersants; EOFO-945617 single-hole vortex mixer (digital type, Talboys, Columbia, MD, USA) was used for extraction; H/T16MM centrifuge (Hexi, Tianjin, China) was used for centrifugal stratification; high-purity nitrogen (purity \geq 99.999%, Changsha Rizhen, Changsha, China) was used for carrier gas.

Table 1. Instrumental parameters of GC data acquisition.

Instrumental Parameters	Value
Injection port	
Injection volume (μL)	1.0
Injection port temperature ($^{\circ}\text{C}$)	250
Split ratio	20:1
Chromatographic column	
Column flow (mL/min)	1.00
Programmed temperature rise procedure	50 $^{\circ}\text{C}$ for 3 min, 4 $^{\circ}\text{C}/\text{min}$ to 160 $^{\circ}\text{C}$, 0 min, 20 $^{\circ}\text{C}/\text{min}$ to 240 $^{\circ}\text{C}$, 5.5 min
Detector	
Detector temperature ($^{\circ}\text{C}$)	300
Hydrogen flow (mL/min)	32.0
Air flow (mL/min)	200.0
Tail gas flow (mL/min)	24.0

2.3. Method

2.3.1. Preparation of Standard Solution and Establishing of Standard Curve

We accurately measured 100 mg of a standard substance and transferred it into a 50 mL beaker. Subsequently, 10–20 mL of acetone was added to the beaker, followed by dissolution through ultrasound. The resulting solution was then transferred to a 5 mL brown volumetric flask and further diluted with acetone. After thorough shaking, a 20 mg/mL single standard stock solution was prepared. To obtain single standard solutions for analysis in gas chromatography (GC), each single standard stock solution was sequentially diluted stepwise with acetone to achieve a concentration of 100 $\mu\text{g}/\text{mL}$. Retention time, determined by GC analysis, served as the qualitative basis for identifying each standard substance. For the preparation of a mixed standard stock solution, precisely 200 μL of each single standard stock solution was transferred into a 5 mL brown volumetric flask, followed by dilution with acetone and thorough shaking. This resulted in an 800 $\mu\text{g}/\text{mL}$ mixed standard stock solution. Dilutions of the mixed standard stock solution with acetone

were performed to obtain concentrations of 5, 10, 20, 50, 100, and 200 $\mu\text{g}/\text{mL}$ for each standard substance. The pH value of rosemary hydrosol was approximately 5.5.

The enrichment factor (EF) plays a crucial role in evaluating the performance of the dispersive liquid–liquid microextraction (DLLME) method. It represents the concentration of the target substance in the extractant after extraction divided by the concentration of the target substance in the aqueous phase before extraction. Under the assumption that all target substances are fully extracted into the extractant, and the volumes of the extractant and aqueous phase remain constant before and after extraction, the enrichment factor can be calculated as the ratio of the volume of the aqueous phase to the volume of the extractant.

However, in practical analytical procedures, the volume of the organic phase may not necessarily match the volume of the added extractant after liquid–liquid microextraction. Some of the dispersant may be carried into the organic phase by the extractant, resulting in a larger final volume of the organic phase compared to the added extractant. Simultaneously, a portion of the extractant may be carried into the aqueous phase by the dispersant, leading to a smaller final volume of the organic phase than the added extractant. To account for these discrepancies, it becomes necessary to introduce a correction factor, denoted as K , to adjust the test results accordingly.

The incorporation of the correction factor K allows for accurate determination of the actual enrichment factor, considering the potential alterations in the volumes of both the organic phase and the extractant caused by the dispersant during the liquid–liquid microextraction process. This correction factor ensures the reliability and validity of the obtained results.

2.3.2. Sample Collection, Preparation and Detection

Eight samples were included in this study; Sample 1, Sample 2, Sample 3 and Sample 5 were purchased through the Taobao network. Sample 7 was a hydrosol produced from imported rosemary leaves and was provided by a plant extract company. Additionally, samples of hydrosol produced from rosemary leaves in Hunan (Sample 8), Henan (Sample 9), and Yunnan (Sample 10) were also included.

For the sample preparation, we referred to a previous study [19] and conducted certain optimizations based on them, the detailed steps were as follows: a 10 mL hydrosol sample was taken and mixed with 1.5 mL of acetone, followed by the addition of 2 g of NaCl. Subsequently, 0.75 mL of carbon tetrachloride was added to the mixture. The resulting solution was manually shaken 100 times and then subjected to scrolling for 30 s. After allowing the solution to stand undisturbed for 3 min, centrifugation was performed at a speed of 6000 r/min for 5 min. The organic phase present at the bottom of the centrifuge tube was carefully collected and transferred to an injection vial for further determination. Figure 1 shows the flow chart of sample pretreatment for 24 trace aromatic substances in rosemary hydrosol.

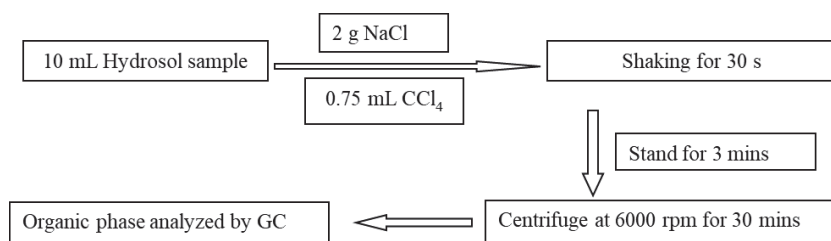


Figure 1. A flow chart of sample pretreatment for 24 trace aromatic substances in rosemary hydrosol.

3. Results and Discussion

3.1. Gas Chromatograms of Target Analytes in Samples

As can be seen from Figure 2a, the 24 aromatic organic compounds of the gas chromatogram were completely separated in 31 min. After conducting calculations, the resolu-

tion of the 24 compounds ranged from 2.03 to 39.76, exceeding the minimum requirement of 1.5. This indicates that our method satisfies the criteria for both chromatographic separation and quantitative analysis. Table 2 presents the identification of the 24 target compounds along with their corresponding retention times, as denoted by the serial numbers in Figure 2a–c. Figure 2b,c show the gas chromatograms of the rosemary hydrosol produced by the imported rosemary leaves and the rosemary hydrosol produced by the Chinese rosemary leaves, respectively. As can be seen from Figure 2a and Table 2, the main components of rosemary hydrosol produced from imported leaves were eucalyptol and camphor, while the main components of hydrosol produced from domestic leaves were eucalyptol and verbenone.

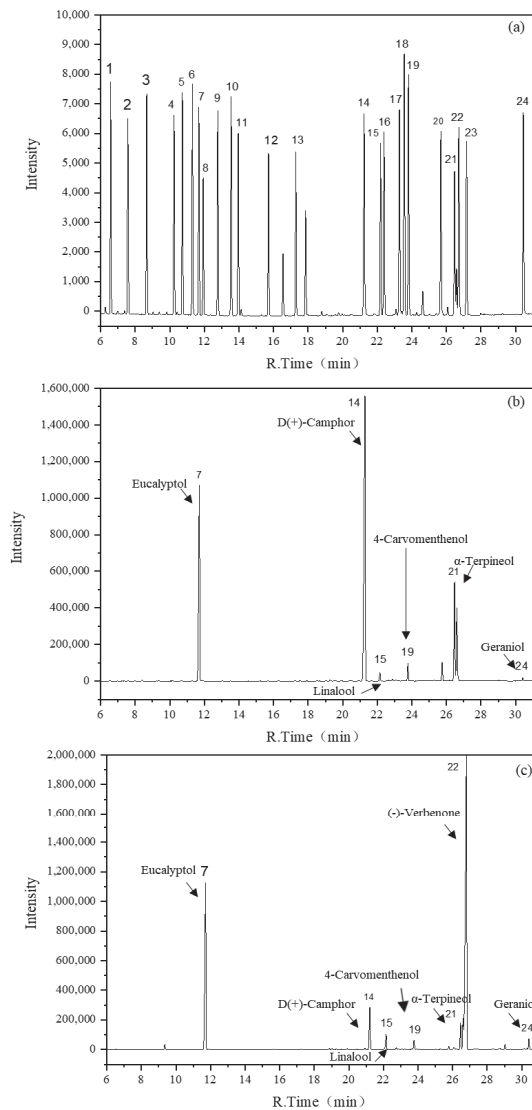


Figure 2. (a) Gas chromatogram of reference materials (concentration: 20 µg/mL) (a), natural rosemary hydrosol (imported rosemary leaves) (b) and natural rosemary hydrosol (rosemary leaves from China) (c).

Table 2. The retention time of 24 target analytes in rosemary hydrosol separated by GC.

No.	Target Analytes	Retention Time (min)	No.	Target Analytes	Retention Time (min)
1	α -Pinene	6.589	13	cis-3-Hexen-1-ol	17.298
2	(\pm)-Camphene	7.581	14	D(+)-Camphor	21.248
3	β -Pinene	8.674	15	Linalool	22.199
4	Myrcene	10.261	16	Linalyl Acetate	22.401
5	α -Terpinene	10.739	17	Isobornyl acetate	23.294
6	(R)-(+)-Limonene	11.318	18	(-)-trans-Caryophyllene	23.575
7	Eucalyptol	11.693	19	4-Carvomenthenol	23.817
8	trans-2-Hexen-1-al	11.945	20	Isoborneol	25.690
9	γ -Terpinene	12.788	21	α -Terpineol	26.479
10	4-Isopropyltoluene	13.559	22	(-)-Verbenone	26.730
11	Terpinolene	13.972	23	Neryl acetate	27.174
12	Methyl heptenone	15.720	24	Geraniol	30.458

3.2. Selection of Extractant

Selection of an appropriate extractant is crucial for the extraction process to ensure the complete dissolution of all standard substances. The solubility of the target substance in the chosen extractant should be significantly higher compared to water. Additionally, the density of the chosen extractant should be notably greater than that of water to facilitate efficient centrifugation and stratification post-extraction. In this study, trichloromethane, dichloromethane, carbon tetrachloride and carbon disulfide were chosen as the extractants. To evaluate the recovery rates of the 24 standard substances at different spiking levels, mixed standard solution spikes with concentrations of 1.5 μg , 15 μg and 150 μg were added to the blank matrix for each extractant tested. Comparisons were made between the recovery rates of the 24 standard substances across the various extractants and concentrations. The recovery rates of the 24 standard substances were presented in Figure 3a–c. Notably, when carbon disulfide was employed as the extractant, significant variations were observed among different analytes, which could be attributed to their varying solubilities in carbon disulfide. Consequently, carbon disulfide was excluded from consideration as an extractant in this study. Comparative analysis revealed that carbon tetrachloride exhibited significantly higher recoveries (around 100%) for the 24 analytes compared to dichloromethane and chloroform. Furthermore, the chromatographic peak of trichloromethane substantially overlapped with (\pm)-2-pinene, while dichloromethane demonstrated a propensity to emulsify with water when used as an extractant. Therefore, carbon tetrachloride was selected as the preferred extractant for this investigation.

3.3. Selection of Dispersant

In order to facilitate the transfer of target analytes between the aqueous and organic phases, it is crucial for the dispersant to possess favorable solubility in both water and the chosen extractant. Additionally, the dispersant should demonstrate excellent solubility in the 24 reference materials. For the purpose of this study, acetone, hexane and methanol were carefully chosen as the dispersants for comprehensive evaluation. To evaluate the recovery rates of the 24 analytes at different concentrations, a standard solution containing 15 μg was added to the blank matrix using each dispersant. The main objective was to compare the recovery rates of the 24 analytes across various concentrations and dispersants, with the ultimate goal of identifying the most suitable dispersant that could effectively facilitate the smooth transfer of the reference materials between the aqueous and organic phases while achieving optimal recovery rates. The recovery rates of the 24 standard substances are presented in Figure 4. When methanol was utilized as the dispersant, it led to a higher migration of cis-3-hexene-1-ol into the water phase, resulting in an insufficient recovery rate of the spiked compound. Conversely, when acetone was used as the dispersant, the recovery rate of the added standard exceeded that of acetonitrile. Additionally, it was

observed that acetonitrile had a propensity to cause losses in the gas chromatographic column. Consequently, acetone was chosen as the preferred dispersant for this study.

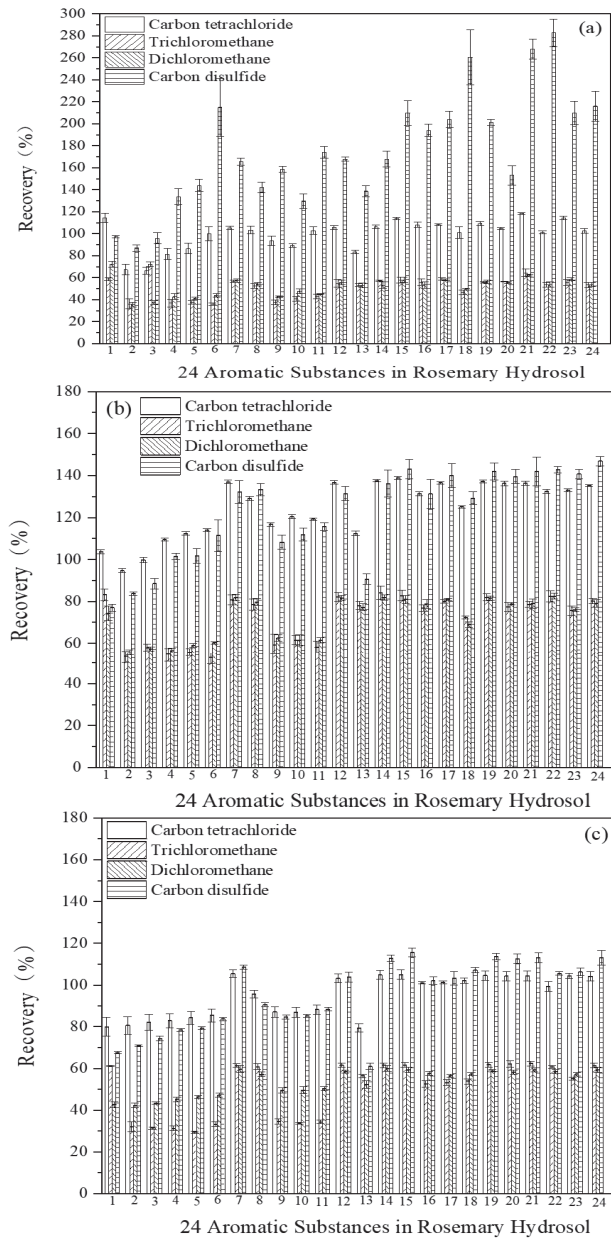


Figure 3. The recovery rate of 24 target substances using different extractants spiked with concentrations of 1.5 µg (a), 15 µg (b) and 150 µg (c) ($n = 3$).

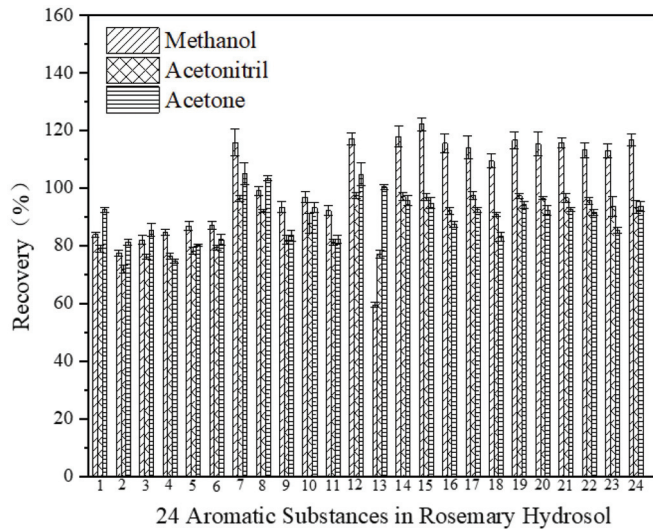


Figure 4. The recovery rate of 24 target substances when using different dispersants ($n = 3$).

3.4. Optimization of Extractant Volume

The volume of the extractant plays a crucial role in determining the extraction efficiency. Insufficient extractant volume may result in incomplete transfer of the target substance from the aqueous phase to the organic phase, while excessive extractant volume can lead to reduced enrichment factor and higher detection limits for the target substances, thereby negating the advantages of dispersed liquid–liquid microextraction. In this study, carbon tetrachloride was selected as the extractant, and volumes of 0.25 mL, 0.50 mL, 0.75 mL, and 1.00 mL were chosen for evaluation of the extraction of 24 aromatic organic compounds in samples. Each volume of extractant was added to the blank matrix containing 15 μg of the mixed standard solution. The objective of this investigation was to compare the recovery rates of the 24 standard substances under different dispersants at varying volumes of carbon tetrachloride extractant. And the recovery rate of 24 standard substances in samples is shown in Figure 5. The recovery rates of carbon tetrachloride extractant at 0.75 and 1.0 mL were significantly higher than that at 0.25 and 0.50 mL. When the volume of extractant was 0.75 mL and 1.0 mL, the recovery rate of spiking was similar. Considering the same sample volume, the larger the volume of the extractant was, the smaller the enrichment factor was. So, 0.75 mL was selected as the volume of carbon tetrachloride as the extractant in this study.

3.5. Optimization of Dispersant Volume

The volume of the dispersant plays a crucial role in determining the efficiency of extraction. Insufficient dispersant volume can hinder the rapid transfer of the target substance between the aqueous and organic phases, while excessive dispersant volume can result in a larger organic phase volume and reduced enrichment factor. Moreover, some dispersants may dissolve in the water phase after microextraction, leading to the loss of target substances and lower recovery rates. In this study, acetone was chosen as the dispersant. Each volume of dispersant was added to the blank matrix containing 15 μg of the mixed standard solution. The recovery rates of the 24 standard substances when varying the volume of acetone dispersant to 0.75, 1.0, 1.5 and 2.0 mL, respectively, are shown in Figure 6. It was observed that there was minimal variation in the recovery of the 24 reference materials as the volume of dispersant changed. Therefore, for this study, a volume of 1.5 mL was selected as the appropriate amount of acetone dispersant.

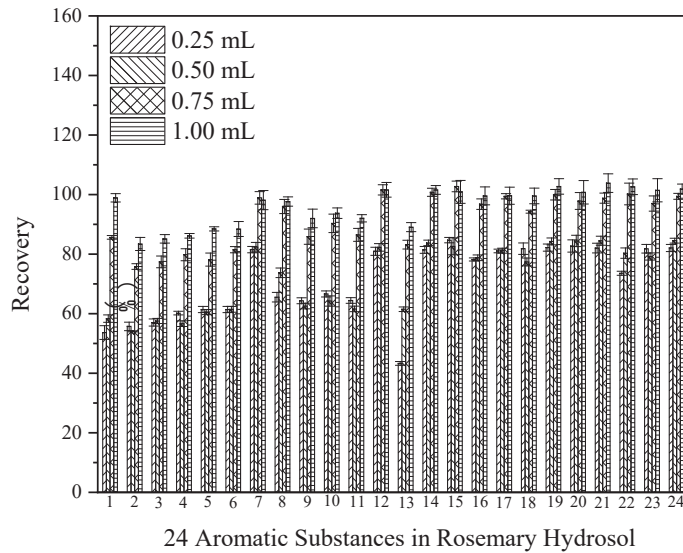


Figure 5. Recovery rate of 24 target substances with different extractant volumes ($n = 3$).

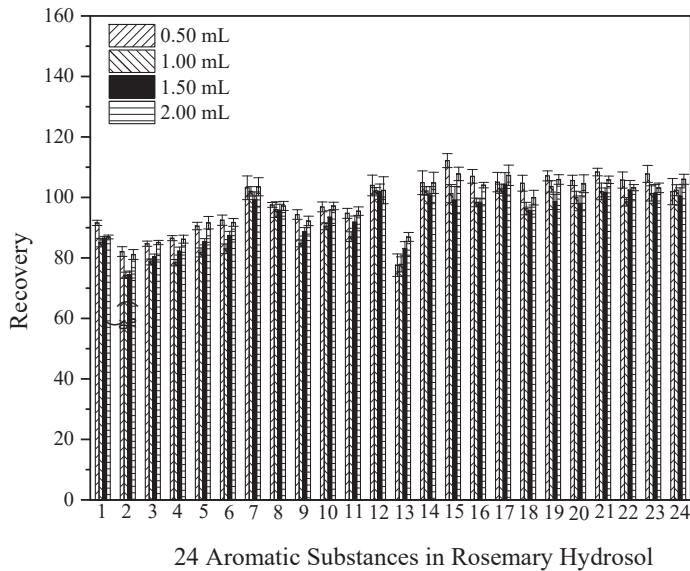


Figure 6. Recovery rate of 24 target substances with different dispersant volumes ($n = 3$).

3.6. Optimization of DLLME Parameters

The pretreatment parameters of DLLME, including extraction time, temperature and pH value, may affect the extraction recovery of the 24 target analytes in rosemary hydrosol samples. So, in this work, the parameters of extraction time (10, 20, 30, 60, 120 s), temperature (10, 15, 20, 25, 30 °C) and pH (4, 5, 6 and 7) were optimized. As shown in Figure 7a, extraction temperature had a minimal impact on the recovery rate of analytes, so the extraction experiments can be conducted at room temperature (10–30 °C). As for the extraction time (see Figure 7b), the extraction efficiency gradually increases when the extraction time is between 10 and 30 s, and it stabilizes when the extraction time is between

30 and 120 s. According to the principles of DLLME, the dispersant transfers multiple times between the sample and the extraction solvent during the extraction process. The target analytes are quickly extracted from the sample into the extraction solvent. This is one of the advantages of DLLME compared to other extraction methods. Thus, 30 s was chosen as the optimal extraction time. Moreover, as can be seen from Figure 7c, pH had a negligible effect on the recovery rate when the pH value was in the range of 4–6. Consequently, there was no requirement for pH adjustment during the analytical determination of the sample.

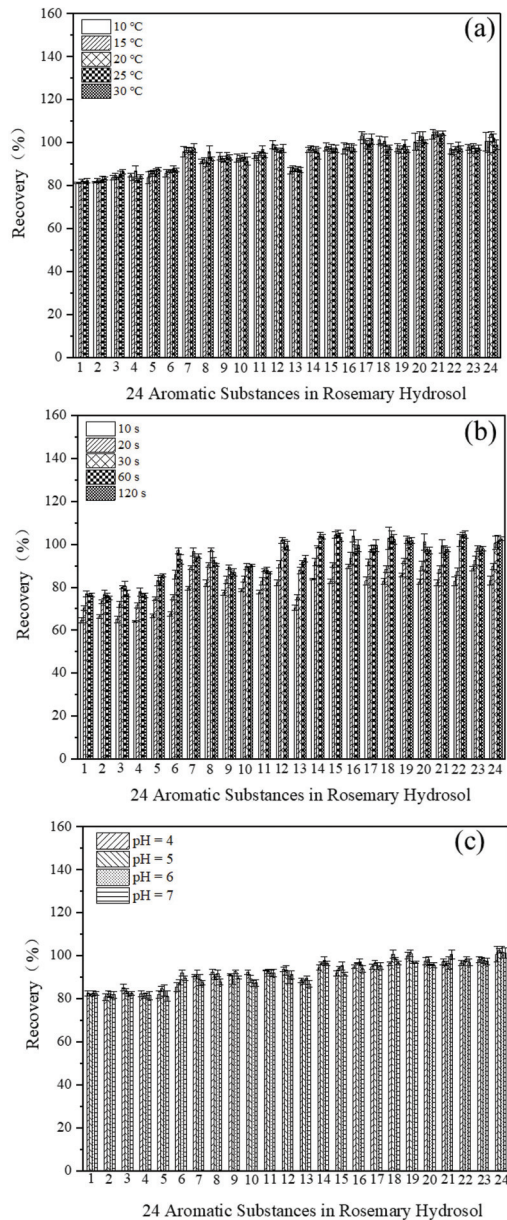


Figure 7. Optimization of DLLME parameters: (a) extraction temperature, (b) extraction time and (c) pH ($n = 3$).

3.7. Retention Time, Method Detection Limit, Linear Regression Equation and Correlation Coefficient

The peak time, method detection limit, linear regression equation and correlation coefficient r^2 of 24 standard substances are shown in Table 3. The linearity of 24 reference materials was good in the range of 5–200 $\mu\text{g/mL}$, and the detection limits of the method were 0.02 mg/L. The detection limits of the liquid–liquid microextraction method were significantly lower than those of the direct injection and liquid–liquid extraction method.

Table 3. Retention time, method detection limit, linear regression equation and correlation coefficient r of 24 target substances r ($n = 3$).

Serial No.	Target Analytes	Retention Time (min)	Method Detection Limit (mg/L)	Linear Regression Equation	Correlation Coefficient r
1	α -Pinene	6.581	0.02	$Y = 1166.1X - 659.2$	0.9991
2	(\pm)-Camphene	7.573	0.02	$Y = 1174.7X - 548.5$	0.9991
3	β -Pinene	8.665	0.02	$Y = 1237.2X - 723.1$	0.9990
4	Myrcene	10.245	0.02	$Y = 1143.4X - 695.7$	0.9990
5	α -Terpinene	10.728	0.02	$Y = 1276.8X - 793.4$	0.9989
6	(R)-(+)-Limonene	11.307	0.02	$Y = 1318.4X - 964.5$	0.9989
7	Eucalyptol	11.681	0.02	$Y = 1247.9X - 905.1$	0.9990
8	trans-2-Hexen-1-al	11.934	0.02	$Y = 758.4X - 598.9$	0.9989
9	γ -Terpinene	12.777	0.02	$Y = 1192.9X - 796.6$	0.9990
10	4-Isopropyltoluene	13.548	0.02	$Y = 1302.2X - 982.0$	0.9989
11	Terpinolene	13.961	0.02	$Y = 1090.2X - 680.4$	0.9990
12	Methyl heptenone	15.710	0.02	$Y = 975.7X - 868.1$	0.9988
13	cis-3-Hexen-1-ol	17.289	0.02	$Y = 925.4X - 804.8$	0.9989
14	D(+)-Camphor	21.238	0.02	$Y = 1398.6X - 1343.3$	0.9989
15	Linalool	22.191	0.02	$Y = 1041.4X - 1030.9$	0.9987
16	Linalyl Acetate	22.389	0.02	$Y = 1194.6X - 1132.6$	0.9988
17	Isobornyl acetate	23.282	0.02	$Y = 1416.6X - 1406.3$	0.9988
18	(-)-trans-Caryophyllene	23.561	0.02	$Y = 1850.6X - 1710.0$	0.9987
19	4-Carvomenthenol	23.807	0.02	$Y = 1542.2X - 1693.4$	0.9986
20	Isoborneol	25.678	0.02	$Y = 1207.1X - 1193.3$	0.9989
21	α -Terpineol	26.471	0.02	$Y = 897.5X - 718.5$	0.9988
22	(-)-Verbenone	26.718	0.02	$Y = 1321.7X - 1808.1$	0.9985
23	Neryl acetate	27.166	0.02	$Y = 1146.7X - 1024.0$	0.9987
24	Geraniol	30.450	0.02	$Y = 1300.5X - 1759.0$	0.9983

Table 4 shows the comparison of different pretreatment methods for the detection of aromatic compounds in rosemary hydrosol. The aromatic substances in rosemary hydrosol were directly injected and detected using GC-MS, obtaining the relative content of compounds through the reported studies [25–27]. And in the work conducted by Dganit Sadeh, 1 g sample was added into 0.01 L solvent, and then shaken for 24 h at room temperature, then 2 mL sample was injected into the GC-MS system after the cleaning steps, obtaining the relative content of analytes [10]. Through comparative analysis, the method of DLLME combined with GC for the detection of 24 aromatic compounds in rosemary hydrosol exhibits several advantages, including reduced pre-processing time and lower reagent consumption. Most significantly, our method allows for the absolute quantification of aromatic compounds in rosemary, a capability that distinguishes it from other approaches in the field.

Table 4. Comparison of different pretreatment methods.

References	Pretreatment Methods	Pretreatment Time	Detector	Organic Reagent Dosage	LOD (mg/L)	Quantitative Method
[25]	Direct injection	0 h	GC and GC-MS	0 mL	/	Area normalization method
[27]	Direct injection	0 h	GC-MS	0 mL	/	Area normalization method
[26]	Direct injection	0 h	GC-MS	0 mL	/	Area normalization method
[10]	Solvent extraction	24 h	GC-MS	10 mL	/	Area normalization method
This method	DLLME	10 min	GC	2.25 mL	0.02	External standard method

3.8. Recovery, Precision, Enrichment Factor and Correction Factor

All figures and tables show that, for the samples spiked with 1.5, 15 and 150 µg concentrations determined by GC, as can be seen from Table 4, the recovery rate was in the range of 76.4–138.8%, and the relative standard deviation of the 24 target substances was 0.4–6.9%. This indicated that most of the aromatic organic compounds in samples could be extracted using the DLLME method. High recoveries of target compounds in samples demonstrated that the proposed method could be efficient in determining the 24 target substances in realistic rosemary hydrosol.

In this study, the sampling volume was 10 mL, and the extraction volume was 0.75 mL, resulting in an enrichment factor of 13.3. In the actual testing process, the volume of the organic phase may not be consistent with the volume of the added extractant in liquid–liquid microextraction. This is due to the potential transfer of dispersants between phases, leading to variations in the final organic phase volume compared to the added extractant volume. To account for these effects, a correction factor (K) is introduced. The value of the correction factor (K) can be determined based on the recovery rates of the 24 target substances at different spiked concentrations.

From Table 5, it can be observed that when the mixed standard was added at a quantity of 1.5 µg, the recovery range was between 76.4% and 118.4%, indicating good recovery rates. Therefore, for sample contents equal to or less than 0.15 mg/L, the correction factor was considered as 1. Similarly, when the mixed standard was added at a quantity of 150 µg, the recovery range ranged from 81.3% to 105.4%, demonstrating satisfactory recovery rates. Hence, for sample contents greater than or equal to 15 mg/L, the correction factor was also determined as 1. Additionally, when the mixed standard plus scalar quantity amounted to 15 µg, the recovery rate fell within the range of 94.6% to 137.0%, indicating relatively high recovery rates. After multiplying the recovery rates of the 24 target substances by 0.85, the corrected recovery rates were found to range from 80.4% to 116.4%. Therefore, for sample contents ranging from 1.5 mg/L to 15 mg/L, the target substance content in the sample should be multiplied by the correction factor of 0.85.

3.9. Determination of Real Samples

Table 6 reveals significant differences in the content of main components among various samples. The semi-finished rosemary hydrosol products (Sample 7, Sample 8, Sample 9 and Sample 10) exhibited considerably higher content levels compared to commercially available rosemary products (Sample 1, Sample 2, Sample 3 and Sample 5). Additionally, the aroma of the semi-finished products was noticeably stronger than that of regular rosemary products. These findings suggest potential dilution or blending practices during the production of semi-finished rosemary hydrosol products. Moreover, the main component content varied significantly between semi-finished rosemary hydrosol products made from imported rosemary leaves and those produced using domestically grown leaves from

Hunan, Henan, and Yunnan Provinces in China. This indicates that the origin of the raw materials influences the composition of the semi-finished hydrosol products.

Table 5. The recoveries and relative standard deviation of 24 target substances at different spiked concentration levels ($n = 6$).

Serial No.	Scalar Target Substance	1.5 µg		15 µg		150 µg	
		Recovery %	RSD %	Recovery %	RSD %	Recovery %	RSD %
1	α-Pinene	107.6	2.0	103.6	1.0	82.5	5.0
2	(±)-Camphene	77.3	6.9	94.6	1.0	81.3	3.8
3	β-Pinene	76.4	4.9	99.8	1.3	82.2	4.6
4	Myrcene	81.6	5.9	109.4	0.7	82.9	4.1
5	α-Terpinene	86.4	5.5	112.4	0.8	84.3	3.7
6	(R)-(+)-Limonene	100.0	6.4	114.1	0.7	85.4	3.6
7	Eucalyptol	105.1	1.6	137.0	0.7	105.4	1.8
8	trans-2-Hexen-1-al	103.3	3.4	129.0	0.7	95.7	2.0
9	γ-Terpinene	93.3	4.5	116.8	0.7	87.0	3.0
10	4-Isopropyltoluene	89.3	2.0	120.4	0.7	86.8	2.7
11	Terpinolene	102.7	3.4	119.2	0.6	88.2	2.6
12	Methyl heptenone	105.6	1.6	136.7	0.6	103.2	2.0
13	cis-3-Hexen-1-ol	83.6	2.0	112.4	0.9	81.3	2.4
14	D(+)-Camphor	106.2	1.6	137.5	0.4	104.8	2.0
15	Linalool	113.8	0.9	138.8	0.5	105.0	2.1
16	Linalyl Acetate	108.0	2.2	131.3	0.7	101.1	0.6
17	Isobornyl acetate	108.2	0.7	136.6	0.4	101.2	0.7
18	(-)-trans-Caryophyllene	100.9	5.3	125.0	0.4	102.0	1.3
19	4-Carvomenthenol	109.3	1.6	137.3	0.5	104.5	2.2
20	Isoborneol	104.9	1.0	136.2	0.7	104.2	2.1
21	α-Terpineol	113.4	0.6	136.3	0.8	104.4	2.4
22	(-)-Verbenone	101.1	1.4	132.4	0.7	99.3	2.3
23	Neryl acetate	114.2	1.5	132.9	0.5	104.3	1.2
24	Geraniol	102.7	1.9	135.2	0.4	104.1	2.2

Table 6. Detection of target substances in 8 rosemary hydrosol samples (unit: mg/L) ($n = 3$).

No.	Target Substance	Sample 1	Sample 2	Sample 3	Sample 5	Sample 7	Sample 8	Sample 9	Sample 10
1	α-Pinene	36.8 ± 0.70	0.6 ± 0.06	0.6 ± 0.06	0.6 ± 0.10	0.7 ± 0.06	0.7 ± 0.06	0.7 ± 0.06	0.6 ± 0.06
2	(±)-Camphene	9.7 ± 0.21	ND ¹	ND	0.6 ± 0.06	0.4 ± 0.06	0.4 ± 0.06	ND	ND
3	β-Pinene	2.1 ± 0.06	ND	ND	ND	ND	ND	ND	ND
4	Myrcene	3 ± 0.10	ND	ND	ND	0.6 ± 0.06	0.7 ± 0.06	0.7 ± 0.06	ND
5	α-Terpinene	0.9 ± 0.06	ND	0.4 ± 0.06	ND	0.4 ± 0.06	ND	0.4 ± 0.12	ND
6	(R)-(+)-Limonene	4.6 ± 0.21	ND	ND	ND	0.5 ± 0.06	0.5 ± 0.10	0.5 ± 0.06	0.5 ± 0.06
7	Eucalyptol	154.6 ± 2.27	103.9 ± 1.65	36.3 ± 0.45	2.9 ± 1.2	217.6 ± 3.89	224.3 ± 3.27	237.7 ± 2.45	226.4 ± 6.95
8	trans-2-Hexen-1-al	ND	ND	ND	ND	1.2 ± 0.10	1.2 ± 0.10	1.3 ± 0.06	1.1 ± 0.06
9	γ-Terpinene	1 ± 0.06	ND	ND	ND	ND	ND	ND	ND
10	4-Isopropyltoluene	3.9 ± 0.10	ND	ND	ND	0.4 ± 0.12	ND	ND	ND
11	Terpinolene	0.8 ± 0.06	ND	ND	ND	ND	ND	ND	ND
12	Methyl heptenone	0.4 ± 0.06	0.6 ± 0.06	0.6 ± 0.06	ND	0.5 ± 0.12	0.9 ± 0.10	0.9 ± 0.06	0.8 ± 0.10
13	cis-3-Hexen-1-ol	0.4 ± 0.06	0.6 ± 0.06	0.6 ± 0.06	ND	1.1 ± 0.12	1.8 ± 0.15	1.5 ± 0.15	1.7 ± 0.21
14	D(+)-Camphor	32.3 ± 0.40	16 ± 0.46	11 ± 0.31	1 ± 0.12	354.1 ± 5.46	57.3 ± 0.71	77.3 ± 1.05	48.5 ± 0.85
15	Linalool	3.6 ± 0.06	18 ± 0.31	7.6 ± 0.21	0.7 ± 0.12	10.4 ± 0.30	19.2 ± 1.05	14.7 ± 0.72	21.7 ± 1.56
16	Linalyl Acetate	ND	ND	ND	ND	ND	ND	ND	ND
17	Isobornyl acetate	0.6 ± 0.06	0.6 ± 0.06	0.5 ± 0.06	ND	1 ± 0.15	1.2 ± 0.15	1.3 ± 0.12	1.2 ± 0.06
18	(-)-trans-Caryophyllene	3.4 ± 0.10	ND	ND	ND	0.7 ± 0.12	ND	1.5 ± 0.06	ND
19	4-Carvomenthenol	2.2 ± 0.10	4.6 ± 0.15	3.4 ± 0.10	0.6 ± 0.06	14.6 ± 0.53	9.8 ± 0.50	10.9 ± 0.42	9.6 ± 0.32
20	Isoborneol	1.6 ± 0.06	ND	ND	ND	ND	ND	ND	ND
21	α-Terpineol	7.5 ± 0.06	15.2 ± 0.26	17 ± 0.36	1.3 ± 0.06	152.2 ± 2.95	47.9 ± 1.57	52.3 ± 0.8	45.6 ± 1.12
22	(-)-Verbenone	ND	62.7 ± 1.61	130.4 ± 3.67	12.4 ± 0.29	ND	576.5 ± 4.31	545.2 ± 6.45	569.2 ± 14.50
23	Neryl acetate	0.4 ± 0.06	ND	ND	ND	ND	ND	ND	ND
24	Geraniol	0.6 ± 0.06	7.7 ± 0.15	3.2 ± 0.21	0.5 ± 0.06	4.4 ± 0.15	13 ± 6.76	10.7 ± 0.21	13.4 ± 0.55

¹ Note: ND means not detected.

4. Conclusions

A method for the determination of 24 target substances in rosemary hydrosol using external standard dispersion liquid–liquid microextraction and gas chromatography was established. The effects of different extractants, dispersant types and contents on the recovery rate of spiking were compared. Carbon tetrachloride and acetone were selected as extractants and dispersants, respectively. The volume of extractant was 0.75 mL and the volume of dispersant was 1.5 mL. The linearity was good, within the range of 5–200 µg/mL, the detection limit of the method was 0.02 mg/L and the recovery rate and precision were good. It is a good method to detect the absolute content of trace aromatic substances in rosemary hydrosol, and also provides a reference for the detection of trace aromatic substances in other hydrosols.

Author Contributions: Experimental design, X.Z.; Experimental operation and article writing, H.H.; Spectra analysis, L.Y.; Data processing and statistics, H.W.; Sample pretreatment, C.Z. All authors have read and agreed to the published version of the manuscript.

Funding: This work was financially supported by the National Natural Science Foundation of Hunan province (Grant no. 2023JJ60528 and 2023JJ60147), and Hunan Provincial Market Supervision Administration Science and Technology Plan Project (2023KJH21).

Data Availability Statement: The data presented in this study are available on request from the corresponding author.

Conflicts of Interest: The authors declare no conflicts of interest.

References

- Dai, P.; Liu, H. Research on the biological activity of rosemary extracts and its application in food. *E3S Web Conf. EDP Sci.* **2021**, *251*, 02034. [CrossRef]
- Touafek, O.; Nacer, A.; Kabouche, A.; Kabouche, Z.; Bruneau, C. Chemical composition of the essential oil of *Rosmarinus officinalis* cultivated in the Algerian Sahara. *Chem. Nat. Compd.* **2004**, *40*, 28–29. [CrossRef]
- Holmes, P. Rosemary oil The wisdom of the heart. *Int. J. Aromather.* **1998**, *9*, 62–66. [CrossRef]
- Damianova, S.; Tasheva, S.; Stoyanova, A.; Damianov, D. Investigation of extracts from rosemary (*Rosmarinus officinalis* L.) for application in cosmetics. *J. Essent. Oil Bear. Plants* **2010**, *13*, 1–11. [CrossRef]
- Jeon, D.H.; Moon, J.Y.; Hyun, H.B.; Cho, S.K. Composition analysis and antioxidant activities of the essential oil and the hydrosol extracted from *Rosmarinus officinalis* L. and *Lavandula angustifolia* Mill. produced in Jeju. *J. Appl. Biol. Chem.* **2013**, *56*, 141–146. [CrossRef]
- Aazza, S.; Lyoussi, B.; Miguel, M.G. Antioxidant activity of some Moroccan hydrosols. *J. Med. Plants Res.* **2011**, *5*, 6688–6696.
- Dheyab, A.S.; Kanaan, M.Q.; Hussein, N.A.; AlOmar, M.K.; Sabran, S.F.; Abu Bakar, M.F. Antimycobacterial Activity of *Rosmarinus officinalis* (Rosemary) Extracted by Deep Eutectic Solvents. *Separations* **2022**, *9*, 271. [CrossRef]
- Jiang, Y.; Wu, N.; Fu, Y.-J.; Wang, W.; Luo, M.; Zhao, C.-J.; Zu, Y.-G.; Liu, X.-L. Chemical composition and antimicrobial activity of the essential oil of Rosemary. *Environ. Toxicol. Pharmacol.* **2011**, *32*, 63–68. [CrossRef]
- Tornuk, F.; Cankurt, H.; Ozturk, I.; Sagdic, O.; Bayram, O.; Yetim, H. Efficacy of various plant hydrosols as natural food sanitizers in reducing *Escherichia coli* O157: H7 and *Salmonella* Typhimurium on fresh cut carrots and apples. *Int. J. Food Microbiol.* **2011**, *148*, 30–35. [CrossRef]
- Sadeh, D.; Nitzan, N.; Chaimovitch, D.; Shachter, A.; Ghanim, M.; Dudai, N. Interactive effects of genotype, seasonality and extraction method on chemical compositions and yield of essential oil from rosemary (*Rosmarinus officinalis* L.). *Ind. Crop. Prod.* **2019**, *138*, 111419. [CrossRef]
- Celiktas, O.Y.; Kocabas, E.E.H.; Bedir, E.; Sukan, F.V.; Ozek, T.; Baser, K.H.C. Antimicrobial activities of methanol extracts and essential oils of *Rosmarinus officinalis*, depending on location and seasonal variations. *Food Chem.* **2007**, *100*, 553–559. [CrossRef]
- Singh, M.; Guleria, N. Influence of harvesting stage and inorganic and organic fertilizers on yield and oil composition of rosemary (*Rosmarinus officinalis* L.) in a semi-arid tropical climate. *Ind. Crop. Prod.* **2013**, *42*, 37–40. [CrossRef]
- Issabeagloo, E.; Kermanizadeh, P.; Taghizadieh, M.; Forughi, R. Antimicrobial effects of rosemary (*Rosmarinus officinalis* L.) essential oils against *Staphylococcus* spp. *J. Microbiol. Res.* **2012**, *6*, 5039–5042.
- Boussalah, N.M. Chemical composition and biological activities of essential oil and hydrosol extract from aerial parts of *Cynoglossum cheirifolium* L. from Algeria. *J. Essent. Oil Bear. Plants* **2020**, *23*, 97–104. [CrossRef]
- Tomi, K.; Kitao, M.; Konishi, N.; Murakami, H.; Matsumura, Y.; Hayashi, T. Enantioselective GC–MS analysis of volatile components from rosemary (*Rosmarinus officinalis* L.) essential oils and hydrosols. *Biosci. Biotechnol. Biochem.* **2016**, *80*, 840–847. [CrossRef]

16. Politi, M.; Ferrante, C.; Menghini, L.; Angelini, P.; Flores, G.A.; Muscatello, B.; De Leo, M. Hydrosols from *Rosmarinus officinalis*, *Salvia officinalis*, and *Cupressus sempervirens*: Phytochemical analysis and bioactivity evaluation. *Plants* **2022**, *11*, 349. [CrossRef]
17. Ding, M.; Liu, W.; Peng, J.; Liu, X.; Tang, Y. Simultaneous determination of seven preservatives in food by dispersive liquid-liquid microextraction coupled with gas chromatography-mass spectrometry. *Food Chem.* **2018**, *269*, 187–192. [CrossRef] [PubMed]
18. Luo, M.; Liu, D.; Zhou, Z.; Wang, P. A new chiral residue analysis method for triazole fungicides in water using dispersive liquid-liquid microextraction (DLLME). *Chirality* **2013**, *25*, 567–574. [CrossRef] [PubMed]
19. Rezaee, M.; Assadi, Y.; Hosseini, M.-R.M.; Aghaee, E.; Ahmadi, F.; Berijani, S. Determination of organic compounds in water using dispersive liquid-liquid microextraction. *J. Chromatogr. A* **2006**, *1116*, 1–9. [CrossRef] [PubMed]
20. Dmitrienko, S.G.; Apyari, V.V.; Tolmacheva, V.V.; Gorbunova, M.V. Dispersive liquid-liquid microextraction of organic compounds: An overview of reviews. *J. Anal. Chem.* **2020**, *75*, 1237–1251. [CrossRef]
21. Rezk, M.R.; Abd El-Aleem, A.E.; Khalile, S.M.; El-Naggar, O.K. Determination of residues of diazinon and chlorpyrifos in lavender and rosemary leaves by gas chromatography. *J. AOAC Int.* **2018**, *101*, 587–592. [CrossRef] [PubMed]
22. Chandra, S.; Mahindrakar, A.N.; Shinde, L.P. Gas chromatography-mass spectrometry determination of pesticide residue in fruits. *Int. J. Chemtech. Res.* **2014**, *6*, 124–130.
23. Newair, E.F.; Garcia, F. Identification of adducts between oxidized rosmarinic acid and glutathione compounds by electrochemistry, liquid chromatography and mass spectrometry. *Anal. Methods* **2022**, *14*, 286–297. [CrossRef] [PubMed]
24. Herrero, M.; Plaza, M.; Cifuentes, A.; Ibáñez, E. Green processes for the extraction of bioactives from Rosemary: Chemical and functional characterization via ultra-performance liquid chromatography-tandem mass spectrometry and in-vitro assays. *J. Chromatogr. A* **2010**, *1217*, 2512–2520. [CrossRef]
25. Nanashima, N.; Kitajima, M.; Takamagi, S.; Fujioka, M.; Tomisawa, T. Comparison of chemical composition between Kuromoji (*Lindera umbellata*) essential oil and hydrosol and determination of the deodorizing effect. *Molecules* **2020**, *25*, 4195. [CrossRef]
26. Allal, A.; Bellifa, S.; Benmansour, N.; Selles, C.; Semaoui, M.; Hassaine, H.; Muselli, A. Essential oil and hydrosol extract chemical profile, antioxidant and antimicrobial potential of *Daphne gnidium* L. from Algeria. *J. Essent. Oil Bear. Plants* **2019**, *22*, 1277–1288. [CrossRef]
27. El Amine Dib, M.; Djabou, N.; Allali, H.; Paolini, J.; Tabti, B.; Costa, J.; Muselli, A. Chemical composition of essential oils and hydrosol extracts of *Daucus muricatus* and assessment of its antioxidant activity. *J. Herbs Spices Med. Plants* **2015**, *21*, 23–37. [CrossRef]

Disclaimer/Publisher’s Note: The statements, opinions and data contained in all publications are solely those of the individual author(s) and contributor(s) and not of MDPI and/or the editor(s). MDPI and/or the editor(s) disclaim responsibility for any injury to people or property resulting from any ideas, methods, instructions or products referred to in the content.

Article

A Study on Sensitivity of Soil-Based Building Mixtures to Biodeterioration by Fungi: Towards Sustainable Earth Structures

Amer Al-Jokhadar ^{1,*}, Yasmine Soudi ¹, Suzanne Abdelmalek ², Sarah R. Badran ¹ and Yasser Abuhashem ¹

¹ Department of Architecture, Faculty of Architecture and Design, University of Petra, Amman 11196, Jordan; ysoudi@uop.edu.jo (Y.S.); sarahbadran@gmail.com (S.R.B.); dr-abuhashem@gmx.de (Y.A.)

² Department of Pharmacology and Biomedical Sciences, Faculty of Pharmacy and Medical Sciences, University of Petra, Amman 11196, Jordan; sabdelmalek@uop.edu.jo

* Correspondence: amer.aljokhadar@uop.edu.jo

Abstract: Earth structures have a significant sustainable impact on regulating indoor environmental qualities. Yet, using soil materials can lead to fungal growth, impacting occupant health and structural stability. This study investigates the susceptibility of earth-based construction materials with cement, limestone, and acrylic-based additives to fungal growth. Laboratory tests were conducted on mixtures under conditions found in inhabited buildings in hot–arid regions. The proposed methodology was based on a 7-week artificial incubation of fungi obtained from moldy walls through regulating the room temperature to fall between 18 °C and 19 °C and a controlled humidity level of around 45%. These conditions were adopted according to the readings monitored in typical buildings in the study area. The results showed that fungal growth was evident on the surface of mixtures, including higher percentages of soil and lower percentages of additives. Mixtures comprising 50% soil, 15% acrylic-based additive, 15% quicklime, and 20% cement supported the least fungal growth, presenting the best choice as a sustainable, efficient replacement. Visual observation followed by microscopic examination ensured the results. Furthermore, results of an environmental post-occupancy evaluation of a constructed rammed earth building using the optimized mixture showed no signs of fungal proliferation on the inner walls afterward.

Keywords: fungal growth; mold; soil; humidity; rammed earth; green solution; sustainability

Citation: Al-Jokhadar, A.; Soudi, Y.; Abdelmalek, S.; Badran, S.R.; Abuhashem, Y. A Study on Sensitivity of Soil-Based Building Mixtures to Biodeterioration by Fungi: Towards Sustainable Earth Structures. *Sustainability* **2024**, *16*, 1294. <https://doi.org/10.3390/su16031294>

Academic Editors: Elza Bontempi, Marco Race, Maria Victoria Lopez-Ramon, Zhen Zhang, Avelino Núñez-Delgado, Yaoyu Zhou, Mario Coccia, Vanesa Santas-Miguel and Esperanza Alvarez-Rodriguez

Received: 25 December 2023

Revised: 29 January 2024

Accepted: 31 January 2024

Published: 3 February 2024



Copyright: © 2024 by the authors. Licensee MDPI, Basel, Switzerland. This article is an open access article distributed under the terms and conditions of the Creative Commons Attribution (CC BY) license (<https://creativecommons.org/licenses/by/4.0/>).

1. Introduction

The attention garnered by utilizing local resources in constructing sustainable structures, such as soil, stems from its significant environmental impact. This noteworthy method not only contributes to the enhancement of air quality but also aids in regulating temperature and humidity, ultimately ensuring a pleasant living environment for the inhabitants of the structures [1–4]. Furthermore, it diminishes the dependence on energy resources for heating and cooling [5–7].

However, such a building system can enhance fungal growth. Fungi are abundant in nature. They can grow on almost all natural and manmade materials. Depending on the original location, an ambient temperature between cold and moderate levels is the optimum requirement for most fungi [8]. Additionally, a correlation was established between the moisture content during the construction of earth walls and its possible influence on mold development [9,10]. Fungal growth potentially impacts the health of occupants and the structural stability of the buildings [11]. This is because of the capacity of earth materials to absorb water, and hence, the moisture content within materials and the humidity levels on their surface determine the rate at which fungi develop [12] and subsequently impact the structure’s durability [13–16]. Laborel-Préneron et al. (2018) studied earth-based materials enhanced with plant aggregates such as straw [17]. These enhancements improved insulation and helped prevent shrinkage cracks; however, they also observed fungal growth under specific humidity and temperature conditions after

four weeks. Mensah-Attipoe et al. (2015) focused their research on the proliferation of environmentally friendly construction materials, shedding light on how organic matter facilitates the growth of fungi [18].

To mitigate the effects of fungal growth on the durability of earth constructions, it is possible to modify a combination of mixtures, reduce moisture, and ensure the maintenance of the building [19]. Lime, fly ash, cement, polymers, and red clay binders with epoxy emulsion have been used as additives to improve the properties of soils against water erosion [20–25]. Moreover, reducing clay content in mixtures has proven effective [26,27]. Narloch and Woyciechowski (2020) conducted a study using the Standard NZS 4298 by incorporating a cement dosage of 6% into the mixture [28]. Their findings indicated that there were no signs of surface degradation. Yet, they emphasized that protective measures are necessary for long-term resilience. Moreover, it was found that adding cement to earth mixtures can improve resistance to water vapor, although it is still not as effective as concrete. Another method involves changing the mixture composition by incorporating admixtures, like silicone water additives, which help protect against the impact of weathering. Additionally, surface treatments can address moisture-related issues [29].

Since earthen building materials are one of the green solutions for contemporary constructions, and fungal growth can lead to health risks for occupants, questions are raised about the optimized soil mixture to be used in hot–arid regions that reduces fungal development. This study investigates susceptibility to fungal growth on the surface of earth constructions. Additionally, it aims to explore the impact of adding cement, limestone, and a fast acrylic-based bond to a mixture for moisture resistance. Laboratory tests were conducted on mixtures under conditions found in inhabited buildings in hot–arid regions, where fungal growth is expected. The study’s findings will highlight the optimized mixture of a stabilized earth material that prevents fungal growth and maintains acceptable indoor air quality. The selected mixture was used to construct a prototype rammed earth building in the study area to examine the efficiency of such material in preventing mold growth.

2. Materials and Methods

The experiment in this study was performed in Amman, Jordan, a city recognized for its hot and arid summer climate, juxtaposed with its cold and damp winter climate. In this regard, the mean percentage of outdoor relative humidity is 48% [30]. Moreover, the mean maximum outdoor air temperature for 30 years (1989 to 2018) ranged between 32.8 °C and 12.6 °C, with an average of 23.9 °C annually, while the mean minimum outdoor air temperature ranges between 20.8 °C and 3.6 °C, with an average of 12.7 °C, annually [31].

Regarding indoor environmental conditions, profile readings of previous studies implemented in the same study area show that the mean indoor air temperature monitored in typical buildings in Amman ranges between 17.2 °C and 19.4 °C in cold months (November to February), while relative humidity levels fall between 42% and 48% in the same months [32,33]. Research examining the indoor environmental quality (IEQ) of typical classrooms in Amman in winter (between December and January) showed that the relative humidity measured between 43.5% and 55.2%, with a mean of 47.6%. In the same surveyed rooms, the indoor air temperature varied between 17.3 °C and 21.4 °C, with a mean of 19.35 °C [32]. In another study aimed to assess the IEQ of schools in Amman, results showed that air temperature ranged between 16 °C and 18.3 °C in February, and between 21.1 °C and 22.9 °C in July [33]. Relative humidity measurements ranged between 42% and 47% in winter, while it was recorded between 40.5% and 47.9% in summer [33].

Different techniques and laboratory tests could be used to investigate fungal growth at the surface of building materials. The first step includes preparing mixture samples and then decontaminating them to remove mold by exposing materials to heat [34] or treating them with gamma rays, which is more expensive [35].

The second step is to collect fungi from moldy walls and inoculate them artificially at the surface of the mixture samples using a cotton swab [36]. This process is faster than natural inoculation and allows an easier quantitative comparison with the initial state [37].

The third step is to incubate samples in a closed chamber to maintain controlled temperature and relative humidity, similar to regular room conditions. The average time of the incubation process is six weeks [37].

Finally, periodic macroscopic and microscopic observations are used to monitor fungal growth. Depending on the inoculation method, different scales that classify fungal growth intensity could be used. One of these scales was established by Johansson et al. in 2012 [38]. It includes five values, starting from 0 to 4. The lowest value means no fungal growth, while the highest value indicates growth all over the surface. Health risks are associated with growth values of 2 and above.

The procedure, explained in the subsequent paragraphs, is focused on thoroughly examining the laboratory tests employed to observe fungal growth.

2.1. Preparation of Samples and Decontamination

A total of six types of mixtures, with three replicates of each type, were prepared, as shown in Table 1. The six mixtures are as follows: three types of different soil mixtures with additives, a control sample that includes soil without any additives, a concrete mixture without any treatment, and a concrete mixture that is painted with emulsion paint. Soil obtained from a depth of two meters was used to prepare mixtures to avoid silt and high concentrations of organic material. The reason for choosing these types of soil mixtures is to select the optimum combination that can be used for contemporary earth constructions and compare soil with ordinary Portland cement commonly used in the study area. It is essential to mention, though, that straws or plants, which were found to be a major cause of fungal growth, were not used in the mixtures [35,39,40].

Table 1. Description of types of samples.

Type Code	Composition of Samples
(1A)	Soil (70%) Acrylic-based additive (15%) Quicklime (15%)
(2B)	Soil (65%) Acrylic-based additive (15%) Ordinary Portland cement (20%)
(3C)	Soil (50%) Acrylic-based additive (15%) Quicklime (15%) Ordinary Portland cement (20%)
(4D) Control sample	Soil (100%) with no additions
(5E)	Concrete mixture (100%)
(6F)	Concrete mixture (100%), finished with emulsion paint

At an earlier phase of the current study, a laboratory structural investigation was performed to verify the strength of soil mixtures. The results showed that the soil mixture denoted as type (1A) accomplished a compressive strength of 2.06 MPa after 28 days while being subjected to a water content of 37%. The sample type 2B yielded a compressive strength valued at 4.18 MPa and a water content of 33%. Surprisingly, the sample labeled as type 3C manifested the highest compressive strength of 4.39 MPa while being exposed to a water content of 42% [41].

All samples underwent decontamination, exposing them to exceptionally elevated temperatures in an oven that reached up to a scorching 150 °C for 24 h. The fundamental

aim of this process was to successfully eliminate any probable existence of mold, thereby ensuring the integrity and purity of the samples under investigation.

2.2. Inoculation

Fungal specimens were obtained from mold-infested walls of residential dwellings in Jordan to simulate natural conditions (Figure 1). Wet sterile cotton swabs were used to swab moldy walls. These swabs were then cultured on Sabouraud Dextrose Agar (SDA). These cultures were used to inoculate the samples in question. The inoculation was carried out at room temperature, set at 24 °C, to be within the acceptable comfort range, between 19.4 °C and 27.7 °C, as defined in the ANSI/ASHRAE 55 (2017) guidelines [42].

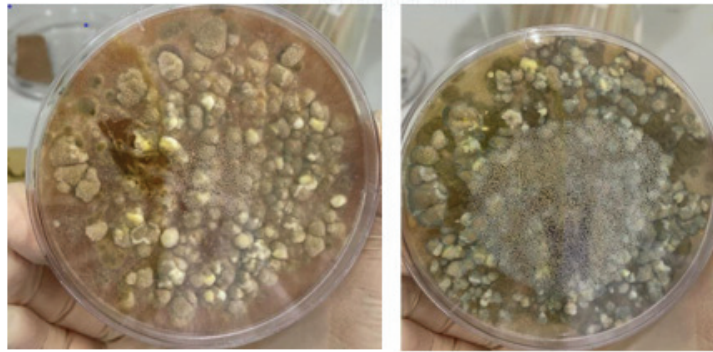


Figure 1. Fungal growth was obtained from mold-infested walls of residential dwellings in Jordan.

Sterile and immaculate Petri dishes were marked with the precise date and their unique material code, which can be observed in Figure 2:

- Label (1A): 80% soil, 5% acrylic-based additive, and 15% quicklime.
- Label (2B): 65% soil, 15% acrylic-based additive, and 15% cement.
- Label (3C): 50% soil, 15% acrylic-based additive, 15% quicklime, and 20% cement.
- Label (4D): 100% soil (control sample).
- Label (5E): 100% concrete mixture.
- Label (6F): 100% concrete mixture, painted with emulsion.

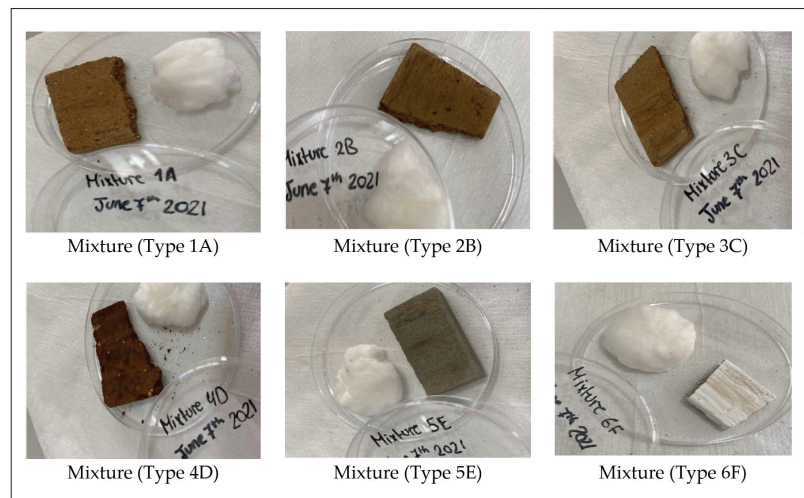


Figure 2. Mixtures of earth construction samples were used in the study.

To execute the procedure, it was necessary to implement a consistent and unvarying relative humidity factor, which was maintained at approximately 45%. This value was carefully chosen to ensure that it simulated the indoor environmental conditions of typical buildings in the study area.

Standardization of Humidity Level

The test commenced on the 10th of May, with the primary focus being observing petri dishes containing solely the material samples following inoculation with fungi. However, the humidity levels were significantly low, measuring approximately 25%. To reach the required level of humidity, which is 45%, a quantity of cotton wool was thoroughly saturated with (2 to 4) water sprays. Subsequently, this wet cotton wool was placed alongside a sample in a petri dish (Figure 3). A susceptible wireless transmitting sensor was incorporated within the same petri dish to measure relative humidity (RH) levels and indoor air temperature (Figure 4). Specifications of the used instrument are shown in Table 2. A 45% RH threshold was successfully achieved on the 7th of June. To maintain the desired humidity level of approximately 45%, the samples were kept under observation, and the cotton wool was consistently re-sprayed each time the samples were assessed.

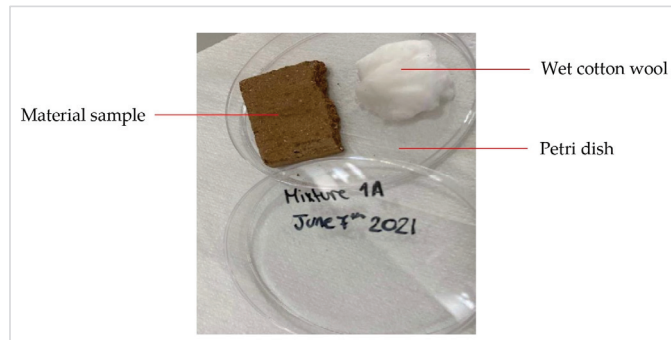


Figure 3. Incubation setup.

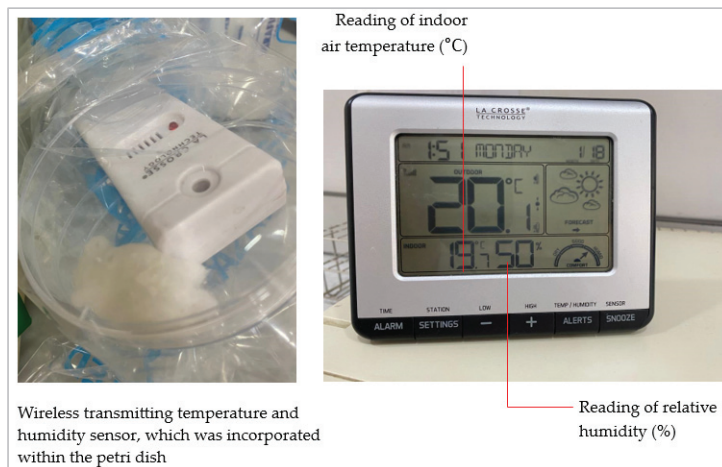


Figure 4. Humidity- and temperature-measuring devices were used in the experiments.

Table 2. Specifications of the instrument used to measure relative humidity and air temperature.

Investigated Variable	Specifications of the Measuring Tool
Indoor air temperature	Temperature sensor Indoor temperature range: 0 to 50 °C Accuracy: ± 0.6 °C Resolution: 0.1 °C Update interval: every 31 s
Relative humidity	RH sensor Indoor humidity range: 10% to 99% Accuracy: $\pm 3\%$ RH Resolution: 0.1% RH Update interval: every 31 s

2.3. Incubation

Samples were incubated for seven weeks, from the 7th of June to the 25th of July. Throughout this time, meticulous measures were implemented to maintain optimal conditions for the experiment, specifically by regulating the room temperature to fall within the range of 18 °C and 19 °C. Furthermore, humidity levels were carefully controlled to fluctuate between 45% and 50%. These specific parameters were selected due to their suitability in fostering the growth of fungi within the study area and to ensure the simulation of indoor environmental conditions of typical buildings in Jordan.

The temperature and humidity conditions of the incubation process during the experiment are presented in Table 3. The experiment, which spanned 49 days, was subject to an unwavering commitment to precision and accuracy, ensuring that the data obtained would be reliable and robust.

Table 3. Temperature and humidity conditions of the incubation process.

	Week #1	Week #2	Week #3	Week #4	Week #5	Week #6	Week #7
	From 7/6 to 13/6	From 14/6 to 20/6	From 21/6 to 27/6	From 28/6 to 4/7	From 5/7 to 11/7	From 12/7 to 18/7	From 19/7 to 25/7
Average Relative Humidity	45%	49%	46%	45%	43%	43%	40%
Average Room Temperature	18 °C	18.9 °C	19 °C	18.3 °C	18.7 °C	19.1 °C	18.4 °C

2.4. Macroscopic and Microscopic Examination

The samples were examined macroscopically during the 7th week for visual signs of mycelial growth or spores. After a long examination period, substantial results were recorded to facilitate comparison.

2.5. Microscopic Observation

Samples were swabbed properly from all sides of the specimen with a wet swab, and the swab was then mixed in a drop of the lacto phenol blue stain and placed on a clean and dry microscopic slide. The smear was then covered with a cover slip and observed under a bright field microscope at 400 \times magnification.

2.6. Environmental Post-Occupancy Evaluation for the Experimental Rammed Earth Building

An experimental rammed earth building was constructed in the study area using the optimized mixture with the least fungal growth. An environmental post-occupancy study was conducted during the winter season, between December 2022 and March 2023, to assess fungal growth. The indoor air temperature and relative humidity levels inside the building were measured using a susceptible instrument (Table 4). The tool was calibrated according to the manufacturer's instructions and ANSI/ASHRAE 55 specifications [42]

and was firmly positioned within the confines of the room to measure and document the readings accurately.

Table 4. Specifications of the instrument used to measure indoor environmental conditions.

Investigated Variable	Specifications of the Measuring Tool
Indoor air temperature	Temperature sensor Measuring range: $-10\text{--}60\text{ }^{\circ}\text{C}$ Accuracy: $\pm 0.6\text{ }^{\circ}\text{C}$ Resolution: $0.1\text{ }^{\circ}\text{C}$ Time interval: 5 s
Relative humidity	RH sensor Measuring range: $0.1\text{--}99.9\%$ Accuracy: $\pm 3\%$ RH (at $25\text{ }^{\circ}\text{C}$, $10\text{--}90\%$ RH) Resolution: 0.1% RH Time interval: 5 s

3. Results

The experiment mentioned above was conducted to ascertain if specific combinations of construction materials are susceptible to fungus development. After infecting the samples with fungi, the results obtained are as follows.

During the second and third weeks, specifically from the 16th to the 24th of June, morphological alterations were observed on the surface of the samples labeled (1A), (2B), and (4D), as shown in Figure 5. It should be noted that fungal growth was observed in the wet cotton wool in petri dishes on the 16th of June.

On the 24th of June, when the relative humidity stood at 45%, and the room temperature was recorded as $18.3\text{ }^{\circ}\text{C}$, fungal growth at the surface of samples was rated based on the scale established by Johansson et al. in 2012 [38]. The samples labeled (1A) and (4D) received a rating of 2 due to minimal growth. On the other hand, the sample (2B) received a rating of 1, signifying the commencement of growth. The remaining three samples, labeled (3C), (5E), and (6F), were rated 0, indicating the absence of any mold growth, as presented in Figure 6.

Careful observations were made on the 25th of July. It was noted that the growth of fungi exhibited an irregular distribution pattern when the relative humidity was 40% and the room temperature was $18.4\text{ }^{\circ}\text{C}$. Among the notable instances, one can point to the back side of the samples marked as (1A) and (4D), both of which were assigned a rating of 3 due to the significant extent of their fungal growth. Furthermore, it was observed that sample (2B) displayed limited growth, leading to its classification as a level-2 rating. Conversely, samples (3C), (5E), and (6F) had no fungal growth, resulting in their designation as a rating of 0, as demonstrated in Figures 7–9.

The microscopic examination of fungal growth of materials labeled (1A), (2B), and (4D) was carried out at the end of week 7 to gain detailed insights. It was noted that a substantial amount of fungal growth was observed on mixtures (1A) and (4D), compared to the mixture type (2B), which showed a minimal amount of such growth. This clear distinction was visually evident and was further substantiated by the data presented in Figure 10. These empirical findings corroborated the visual observations made on the same samples.

It is worth noting that the microscopic analysis did not reveal any evidence of fungal growth on the mixture type (3C). After the laboratory test, the optimized stabilized mixture type (3C), which includes 50% soil, 15% acrylic-based additive, 15% quicklime, and 20% Portland cement, was employed to construct an experimental rammed earth building within the designated study area. This mixture also yielded the highest compressive strength of 4.39 MPa according to laboratory structural examinations at an earlier phase of the current study [41]. The building consists of three rooms, each with a wall

width measuring 40 cm and a total height measuring 4 m. The building was completed in August 2022.

Date of Observation	Mid of Week 2 (16 th June)	End of Week 2 (20 th June)	Mid of Week 3 (24 th June)
Time	11:51 a.m.	10:56 a.m.	12:16 p.m.
Relative Humidity	50%	46%	45%
Room Temperature	18.7 °C	19 °C	18.3 °C


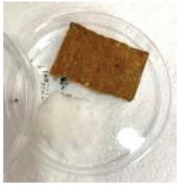




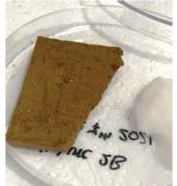



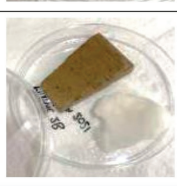
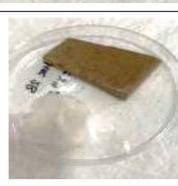






Mixture (Type 1A)	Front			
	Back			
Mixture (Type 2B)	Front			
	Back			
Mixture (Type 4D)	Front			
	Back			

Figure 5. Macroscopic changes on the surface of the samples (1A), (2B), and (4D) during weeks 2 and 3.

Date of Observation	Mid of Week 2 (16 th June)	End of Week 2 (20 th June)	Mid of Week 3 (24 th June)
Time	11:51 a.m.	10:56 a.m.	12:16 p.m.
Relative Humidity	50%	46%	45%
Room Temperature	18.7 °C	19 °C	18.3 °C

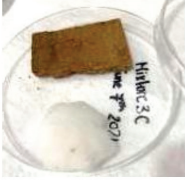


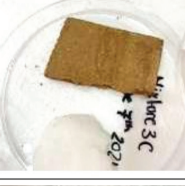


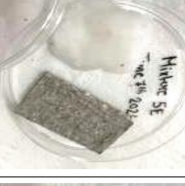


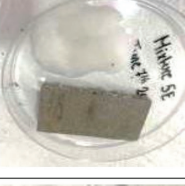




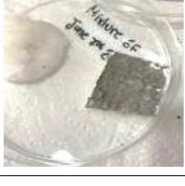
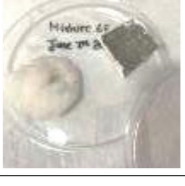

Mixture (Type 3C)	Front			
	Back			
Mixture (Type 5E)	Front			
	Back			
Mixture (Type 6F)	Front			
	Back			

Figure 6. Morphological changes on the surface of the samples (3C), (5E), and (6F) during weeks 2 and 3.

Date of Observation	Start of Week 1 (7 th June)	End of Week 7 (25 th July)
Time	12:30 p.m.	12:45 p.m.
Relative Humidity	45%	40%
Room Temperature	18 °C	18.4 °C

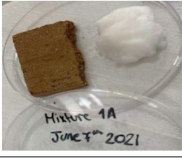

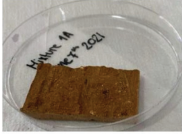


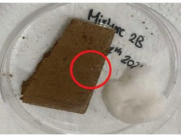
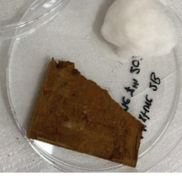
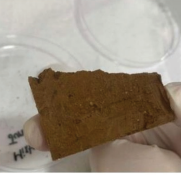
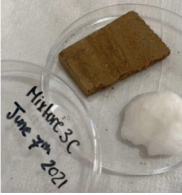

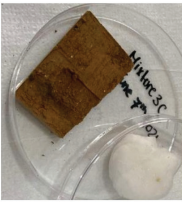
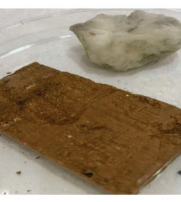
Mixture (Type 1A)	Front		
	Back		
Mixture (Type 2B)	Front		
	Back		
Mixture (Type 3C)	Front		
	Back		

Figure 7. Detailed fungal growth on materials (1A), (2B), and (3C) at the start and end dates of the laboratory test.

Date of Observation	Start of Week 1 (7 th June)	End of Week 7 (25 th July)
Time	12:30 p.m.	12:45 p.m.
Relative Humidity	45%	40%
Room Temperature	18 °C	18.4 °C

Mixture (Type 4D)	Front		
	Back		
Mixture (Type 5E)	Front		
	Back		
Mixture (Type 6F)	Front		
	Back		

Figure 8. Detailed fungal growth on materials (4D), (5E), and (6F) at the start and end dates of the laboratory test.

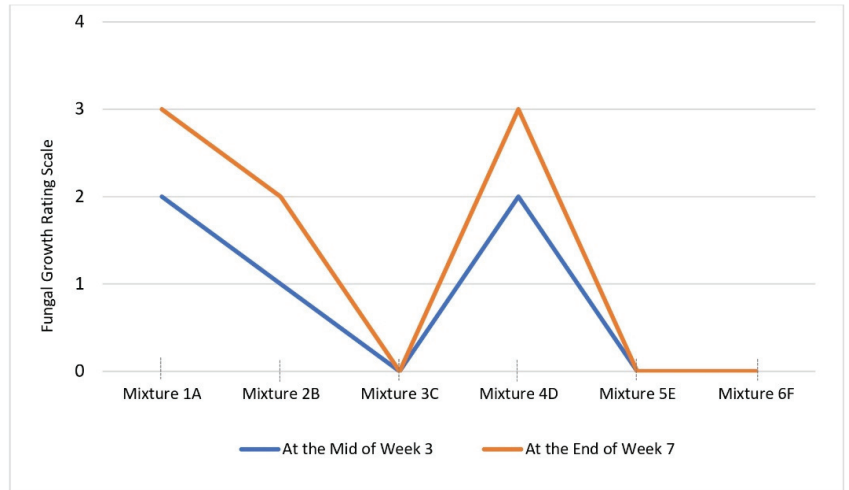


Figure 9. Rating scale of fungal growth on materials at the middle of week 3 and the end of week 7 of the laboratory test.

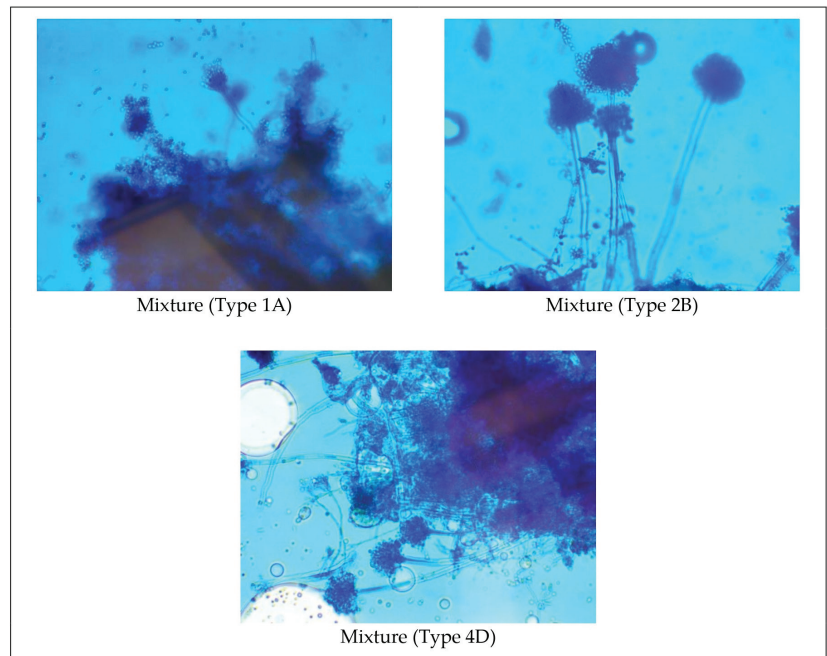


Figure 10. The microscopic observation of fungal growth in week 7.

During the winter season, between December 2022 and March 2023, an environmental post-occupancy study was conducted to assess fungal growth based on the achieved thermal conditions. Readings of the indoor air temperature and relative humidity levels inside the building are presented in Table 5.

Table 5. Air temperature and relative humidity conditions of the constructed building.

	December 2022		March 2023	
	Indoor Air Temperature	Indoor Relative Humidity	Indoor Air Temperature	Indoor Relative Humidity
Room 1	26.1 °C	38.4%	23.2 °C	38.7%
Room 2	26.7 °C	35.8%	23.5 °C	34.4%
Room 3	27.9 °C	34.7%	24.1 °C	35.2%

Based on the extensive examination conducted during that specific timeframe, findings indicated that the optimized combination employed did not exhibit any signs of fungal proliferation on the inner walls, as depicted in Figure 11.

**Figure 11.** External and internal views of the constructed rammed earth building.

4. Discussion

Although straws or plants were used historically in earth construction materials, this research did not utilize such additives, as they are significant causes of fungal growth due to the carbon and cracks which may increase moisture [35,39,40].

Laboratory tests were conducted on six mixtures under conditions found in inhabited buildings in hot–arid regions, where fungal growth is expected. The proposed methodology suggested an artificial incubation of fungi cultured from existing moldy walls. The procedure started with decontamination by exposing samples to high temperatures. Although previous studies suggested more effective methods to remove mold, such as gamma rays [36], the decontamination method was helpful in terms of time and cost.

After that, fungi were inoculated and added to the samples, then placed under a consistent relative humidity factor (45%) achieved using wet cotton wool. The incubation of samples lasted seven weeks by regulating the room temperature to fall between 18 °C and 19 °C and maintaining a controlled humidity level between 45% and 50%. These specific parameters were selected due to their suitability in fostering the growth of fungi within the study area and to ensure similar indoor environmental conditions in typical buildings in Jordan.

Although natural inoculation represents actual circumstances in buildings, artificial sourcing of fungal cultures from moldy walls is faster and is preferred by scholars [17,43].

This requires incubating cultured samples for a week at room temperature (24 °C) and a constant relative humidity of 45%. However, placing wet cotton wool near the samples and spraying it regularly can maintain the required humidity.

The incubation time of 7 weeks was enough to determine the fungal growth; although, several studies determined a range of 6 to 30 weeks to implement the test [17,36]. The results showed that fungi grew more efficiently on soil mixtures, including higher percentages of soil and lower percentages of additives. Mixture type (1A) consists of 80% soil, 5% acrylic-based additive, and 15% quicklime; mixture type (4D), was composed of 100% soil; and mixture type (2B), consists of 65% Soil, 15% acrylic-based additive, and 15% cement, and they all approved this claim. Mixtures (1A) and (4D) scored the highest rate of fungal growth; however, they had a lower intensity of fungal growth on the surface of mixture type (2B).

Mixtures that were stabilized with both quicklime and ordinary Portland cement revealed they were the best choice of soil mixtures. These additives could reduce the cracks and roughness of surfaces, so water accumulation would not be a source of mold growth [44]. These results agreed with previous studies that using Portland cement enhances materials' durability against water erosion and reduces surface degradation [26,28,45]. Furthermore, adding 15% of acrylic-based additives can protect the mixture against dampness [29].

Compared to the most used concrete mixtures in contemporary buildings, the study showed that the optimized mixture, type (3C), composed of 50% soil, 15% acrylic-based additive, 15% quicklime, and 20% Portland cement, can be used as a green, efficient replacement. No fungal growth was observed on the surface of the mixture. Moreover, the post-occupancy evaluation of the constructed building using mixture type (3C) proved that no fungal growth was spotted on the interior walls because of the environmental comfort conditions achieved by the utilized rammed earth materials. Although it is essential to perform the tests in high humidity conditions close to 90% [17], this setting is challenging to obtain and maintain in hot–arid regions. A future study in which proper funding is available would allow such an experiment. However, the humidity values studied cover the humidity range in residential buildings in the study area, based on the profile of environmental readings from previous studies.

5. Conclusions

This study investigated mold growth on the surface of earth constructions in the hot–arid region of Jordan. In addition, it explored the impact of adding cement, limestone, and a fast acrylic-based bond to the mixture on fungal growth resistance. Observations after seven weeks, under a regulated room temperature ranging between 18 °C and 19 °C, and a controlled humidity level between 45% and 50%, which covers the environmental conditions of residential buildings in the study area, showed that the growth of fungi was exhibited on mixtures that included higher percentages of soil and lower percentages of additives. Mixtures stabilized with quicklime, ordinary Portland cement, and acrylic-based additives were revealed as the best soil mixtures, which showed no fungal growth. The sample composed of 50% soil, 15% acrylic-based additive, 15% quicklime, and 20% Portland cement was put to the test in a rammed earth construction project and proved to be suitable for use as a green, sustainable, and efficient replacement after post-occupancy evaluation.

Author Contributions: Conceptualization, A.A.-J., Y.S., S.A. and Y.A.; methodology, S.A.; software, Y.S.; validation, A.A.-J., Y.S. and S.A.; formal analysis, A.A.-J., S.A. and Y.S.; investigation, S.A. and S.R.B.; resources, A.A.-J., Y.S. and S.A.; data curation, S.A. and S.R.B.; writing—original draft preparation, A.A.-J., Y.S. and S.A.; writing—review and editing, A.A.-J., Y.S. and S.A.; visualization, Y.S. and S.R.B.; supervision, A.A.-J., Y.S. and S.A.; project administration, A.A.-J., Y.S. and S.A.; funding acquisition, Y.A. All authors have read and agreed to the published version of the manuscript.

Funding: The study was fully supported and funded by the University of Petra, Amman, Jordan (Grant number 1/6/2020).

Institutional Review Board Statement: Not applicable.

Informed Consent Statement: Not applicable.

Data Availability Statement: The data presented in this study are available in the article (results).

Acknowledgments: The authors would like to thank Engineer Ahmad Masoud from the Civil Engineering Department at the University of Petra for his valuable support in preparing samples.

Conflicts of Interest: The authors declare no conflicts of interest.

References

- Hamard, E.; Cazacliu, B.; Razakamanantsoa, A.; Morel, J.-C. Cob, a vernacular earth construction process in the context of modern sustainable building. *Build. Environ.* **2016**, *106*, 103–119. [CrossRef]
- Gao, Q.; Wu, T.; Liu, L.; Yao, Y.; Jiang, B. Prediction of wall and indoor hygrothermal properties of rammed earth folk house in Northwest Sichuan. *Energies* **2022**, *15*, 1936. [CrossRef]
- Chen, Z.; Guo, Y.; Zhang, L.; Yan, J.; Fu, W.; Wan, J.; Tang, X. Research on rural community construction with modern rammed earth materials. *IOP Conf. Ser. Mater. Sci. Eng.* **2020**, *768*, 022023. [CrossRef]
- Hadjri, K.; Osmani, M.; Baiche, B.; Chifunda, C. Attitude towards earth building for Zambian housing provision. *Proc. ICE Inst. Civ. Eng. Eng. Sustain.* **2007**, *160*, 141–149. [CrossRef]
- Ivan, H.; Golub, K.; Arpad, C.; Nedo, D.; Danijel, K.; Danilo, V. Energy sustainability of rammed earth buildings. *Arch. Tech. Sci.* **2017**, *17*, 39–48. [CrossRef]
- Zami, M.S.; Lee, A. Stabilised or unstabilised earth construction for contemporary urban housing? In Proceedings of the 5th International Conference on Responsive Manufacturing—Green Manufacturing (ICRM 2010), University of Nottingham, Nottingham, UK, 11–13 January 2010.
- Ciancio, D.; Beckett, C. Rammed Earth: An Overview of a Sustainable Construction Material. In Proceedings of the Third International Conference on Sustainable Construction Materials and Technologies, Kyoto, Japan, 18–21 August 2013. Available online: <http://www.claisse.info/2013%20papers/data/e053.pdf> (accessed on 15 May 2023).
- Pietikainen, J.; Pettersson, M.; Baath, A. Comparison of temperature effects on soil respiration and bacterial and fungal growth rates. *FEMS Microbiol. Ecol.* **2005**, *52*, 49–58. [CrossRef] [PubMed]
- Canivell, J.; Martín-del-Río, J.J.; Falcón, R.M.; Rubio-Bellido, C. Rammed earth construction: A proposal for a statistical quality control in the execution process. *Sustainability* **2020**, *12*, 2830. [CrossRef]
- Bui, Q.B.; Morel, J.C.; Hans, S.; Walker, P. Effect of moisture content on the mechanical characteristics of rammed earth. *Constr. Build. Mater.* **2014**, *54*, 163–169. [CrossRef]
- Al Hallak, M.; Verdier, T.; Bertron, A.; Roques, C.; Bailly, J. Fungal contamination of building materials and the aerosolization of particles and toxins in indoor air and their associated risks to health: A review. *Toxins* **2023**, *15*, 75. [CrossRef]
- Kazemian, N.; Pakpour, S.; Milani, A.S.; Klironomos, J. Environmental factors influencing fungal growth on gypsum boards and their structural biodeterioration: A university campus case study. *PLoS ONE* **2019**, *14*, e0220556. [CrossRef]
- Carpino, C.; Loukou, E.; Chen Austin, M.; Andersen, B.; Mora, D.; Arcuri, N. Risk of fungal growth in nearly zero-energy buildings (nZEB). *Buildings* **2023**, *13*, 1600. [CrossRef]
- Simons, A.; Bertron, A.; Roux, C.; Laborel-Préneron, A.; Aubert, J.; Roques, C. Susceptibility of earth-based construction materials to fungal proliferation: Laboratory and in situ assessment. *RILEM Tech. Lett.* **2019**, *3*, 140–149. [CrossRef]
- Andersen, B.; Frisvad, J.C.; Sondergaard, I.; Rasmussen, I.S.; Larsen, J.S. Associations between fungal species and water-damaged building materials. *Appl. Environ. Microbiol.* **2011**, *77*, 4180–4188. [CrossRef]
- Al-Sakkaf, Y.K.; Abdullah, G.M. Soil properties for earthen building construction in Najran city, Saudi Arabia. *Comput. Mater. Contin.* **2021**, *67*, 127–140. [CrossRef]
- Laborel-Préneron, A.; Amed, K.; Ouedraogo, J.; Simons, A.; Labat, M.; Bertron, A.; Magniont, C.; Roques, C.; Roux, C.; Aubert, J. Laboratory test to assess sensitivity of bio-based earth materials to fungal growth. *Build. Environ.* **2018**, *142*, 11–21. [CrossRef]
- Mensah-Attipoe, J.; Reponen, T.; Salmela, A.; Veijalainen, A.-M.; Pasanen, P. Susceptibility of green and conventional building materials to microbial growth. *Indoor Air* **2015**, *25*, 273–284. [CrossRef] [PubMed]
- Vyncke, J.; Kupers, L.; Denies, N. Earth as building material—An overview of RILEM activities and recent innovations in geotechnics. *MATEC Web Conf.* **2018**, *149*, 02001. [CrossRef]
- Kumar, A.; Singh, V.; Singh, S.; Kumar, R.; Bano, S. Prediction of unconfined compressive strength of cement–lime stabilized soil using artificial neural network. *Asian J. Civ. Eng.* **2023**, *25*, 2229–2246. [CrossRef]
- Kocak, S.; Grant, A. Enhancing the mechanical properties of polymer-stabilized rammed earth construction. *Constr. Mater.* **2023**, *3*, 377–388. [CrossRef]
- Gharib, M.; Saba, H.; Barazesh, A. The Effect of Additives on Clay Soil Properties Using Cement and Lime. *Int. J. Basic Sci. Appl. Res.* **2012**, *1*, 66–78. Available online: https://web.archive.org/web/20180421003631id_/http://isicenter.org/fulltext/paper-15.pdf (accessed on 1 October 2023).
- Kim, J.; Choi, H.; Yoon, K.B.; Lee, D.E. Performance evaluation of red clay binder with epoxy emulsion for autonomous rammed earth construction. *Polymers* **2020**, *12*, 2050. [CrossRef]

24. Maraisa, P.; Littlewooda, J.; Karania, G. The use of polymer stabilised earth foundations for rammed earth construction. *Energy Procedia* **2015**, *83*, 464–473. [CrossRef]
25. Kariyawasam, K.; Jayasinghe, C. Cement stabilized rammed earth as a sustainable construction material. *Constr. Build. Mater.* **2016**, *105*, 519–527. [CrossRef]
26. Avila, F.; Puertas, E.; Gallego, R. Characterization of the mechanical and physical properties of stabilized rammed earth: A review. *Constr. Build. Mater.* **2022**, *325*, 126693. [CrossRef]
27. Niroumand, H.; Zain, M.; Jamil, M.; Niroumand, S. Earth architecture from ancient until today. *Procedia—Soc. Behav. Sci.* **2013**, *89*, 222–225. [CrossRef]
28. Narloch, P.; Woyciechowski, P. Assessing cement stabilized rammed earth durability in a humid continental climate. *Buildings* **2020**, *10*, 26. [CrossRef]
29. Kebao, R.; Kagi, D. Integral admixtures and surface treatments for modern earth buildings. In *Modern Earth Buildings*; Woodhead Publishing: Oxford, UK, 2012; pp. 256–281. [CrossRef]
30. Weather and Climate. Available online: <https://weather-and-climate.com/average-monthly-Humidity-perc,Amman,Jordan> (accessed on 5 October 2023).
31. Jordan Meteorological Department. Available online: <http://jometeo.gov.jo/> (accessed on 10 April 2021).
32. Al-Jokhadar, A.; Alnusairat, S.; Abuhashem, Y.; Soudi, Y. The impact of indoor environmental quality (IEQ) in design studios on the comfort and academic performance of architecture students. *Buildings* **2023**, *13*, 2883. [CrossRef]
33. Odeh, I.; Abu Dayyeh, A.; Safran, M.; Odeh, L.; Nazer, H.; Hussein, T. Infiltration Rate (Air Leakage) in Modern Urban Jordanian Buildings in Amman. *Int. J. Adv. Sci. Eng. Technol. (IJASEAT)* **2018**, *6*, 47–50. Available online: https://ijaseat.iraq.in/paper_detail.php?paper_id=14725 (accessed on 15 December 2023).
34. Simons, A.; Laborel-Préneron, A.; Bertron, J.E.; Aubert, C.; Magniont, C.; Roux, C.; Roques, C. Development of bio-based earth products for healthy and sustainable buildings: Characterization of microbiological, mechanical and hygrothermal properties. *Matériaux Tech.* **2015**, *103*, 206. [CrossRef]
35. Hoang, C.P.; Kinney, K.A.; Corsi, R.L.; Szaniszló, P.J. Resistance of green building materials to fungal growth. *Int. Biodeterior. Biodegrad.* **2010**, *64*, 104–113. [CrossRef]
36. Nielsen, K.F.; Holm, G.; Uttrup, L.P.; Nielsen, P.A. Mould growth on building materials under low water activities: Influence of humidity and temperature on fungal growth and secondary metabolism. *Int. Biodeterior. Biodegrad.* **2004**, *54*, 325–336. [CrossRef]
37. Palumbo, M. Contribution to the Development of New Bio-Based Thermal Insulation Materials Made from Vegetal Pith and Natural Binders. Ph.D. Thesis, Universitat Politècnica de Catalunya, Barcelona, Spain, 2015. Available online: <https://upcommons.upc.edu/handle/2117/95754> (accessed on 1 October 2023).
38. Johansson, P.; Ekstrand-Tobin, A.; Svensson, T.; Bok, G. Laboratory study to determine the critical moisture level for mould growth on building materials. *Int. Biodeterior. Biodegrad.* **2012**, *73*, 23–32. [CrossRef]
39. Lugauskas, A.; Levinskaitė, L.; Peciulyte, D. Micromycetes as deterioration agents of polymeric materials. *Int. Biodeterior. Biodegrad.* **2023**, *52*, 233–242. [CrossRef]
40. Van den Bulcke, J.; Van Acker, J.; Stevens, M. Laboratory testing and computer simulation of blue stain growth on and in wood coatings. *Int. Biodeterior. Biodegrad.* **2007**, *59*, 137–147. [CrossRef]
41. Al-Jokhadar, A.; Soudi, Y.; Abuhashem, Y.; Masoud, A. Moisture content and compressive strength of rammed earth construction mixtures in hot-arid regions: The case of Amman, Jordan. *J. Mater. Civ. Eng.* **2024**, *36*. [CrossRef]
42. ASHRAE. *ANSI/ASHRAE 55: Thermal Environmental Conditions for Human Occupancy*; American Society for Heating, Refrigerating and Air Conditioning Engineers, Inc.: Atlanta, GA, USA, 2017; p. 66.
43. Johansson, P.; Ekstrand-Tobin, A.; Bok, G. An innovative test method for evaluating the critical moisture level for mould growth on building materials. *Build. Environ.* **2014**, *81*, 404–409. [CrossRef]
44. Van den Bulcke, J.; De Windt, I.; Defoirdt, N.; De Smet, J.; Van Acker, J. Moisture dynamics and fungal susceptibility of plywood. *Int. Biodeterior. Biodegrad.* **2011**, *65*, 708–716. [CrossRef]
45. Khan, A.; Gupta, R.; Garg, M. Determining material characteristics of rammed earth using non-destructive test methods for structural design. *Structures* **2019**, *20*, 399–410. [CrossRef]

Disclaimer/Publisher’s Note: The statements, opinions and data contained in all publications are solely those of the individual author(s) and contributor(s) and not of MDPI and/or the editor(s). MDPI and/or the editor(s) disclaim responsibility for any injury to people or property resulting from any ideas, methods, instructions or products referred to in the content.

Article

Assessing Biodegradation Processes of Atrazine in Constructed Wetland Using Compound-Specific Stable Isotope Analysis

Songsong Chen ^{1,*}, Yuncai Wang ¹ and Limin Ma ^{2,*}

¹ College of Architecture and Urban Planning, Tongji University, 1239, Siping Road, Shanghai 200092, China; wyc1967@tongji.edu.cn

² College of Environmental Science and Engineering, Tongji University, 1239, Siping Road, Shanghai 200092, China

* Correspondence: chss@tongji.edu.cn (S.C.); lmma@tongji.edu.cn (L.M.); Tel.: +86-21-65980439 (L.M.)

Abstract: To bridge the gap between lab-scale microcosm research and field application in the compound-specific stable isotope analysis (CSIA) of atrazine, we studied the characteristics of carbon and nitrogen isotope fractionation in the atrazine degradation processes within a constructed wetland. In the wetland, we observed multiple element (C, N) isotope fractionation parameters, such as kinetic isotope effects and dual isotope slopes. These parameters are very consistent with those observed in the cultivation of AtzA- or TrzN-harboring strains, suggesting a similarity in the pathway and reaction mechanism of atrazine biodegradation between the two settings. However, we recorded variable carbon (ϵ_C : $-3.2 \pm 0.6\text{‰}$ to $-4.3 \pm 0.6\text{‰}$) and nitrogen isotope fractionation (ϵ_N : $1.0 \pm 0.3\text{‰}$ to $2.2 \pm 0.3\text{‰}$) across different phases. This variance could lead to an over- or underestimation of the biodegradation extent of atrazine when employing the large or small enrichment factor of the carbon isotope. Intriguingly, the estimation accuracy improved considerably when using the enrichment factor (-4.6‰) derived from the batch cultivation of the pore water. This study advances the application of CSIA in tracking atrazine biodegradation processes in ecosystems, and it also underlines the importance of the careful selection and application of the enrichment factor in quantifying the intrinsic biodegradation of atrazine in ecosystems.

Keywords: atrazine; carbon isotope; nitrogen isotope; compound-specific stable isotope analysis; constructed wetland; biodegradation; degradation pathway

Citation: Chen, S.; Wang, Y.; Ma, L. Assessing Biodegradation Processes of Atrazine in Constructed Wetland Using Compound-Specific Stable Isotope Analysis. *Processes* **2023**, *11*, 3252. <https://doi.org/10.3390/pr11113252>

Academic Editors: Avelino Núñez-Delgado, Elza Bontempi, Yaoyu Zhou, Esperanza Alvarez-Rodriguez, Maria Victoria Lopez-Ramon, Mario Coccia, Zhien Zhang, Vanesa Santas-Miguel and Marco Race

Received: 18 October 2023
Revised: 9 November 2023
Accepted: 15 November 2023
Published: 20 November 2023



Copyright: © 2023 by the authors. Licensee MDPI, Basel, Switzerland. This article is an open access article distributed under the terms and conditions of the Creative Commons Attribution (CC BY) license (<https://creativecommons.org/licenses/by/4.0/>).

1. Introduction

The emergence of organic micropollutants, particularly pesticides, in aquatic environments is a significant concern due to the potential risks they pose to ecosystems and human health [1,2]. Among the extensively discussed pesticides, the herbicide atrazine has garnered considerable attention [3,4]. Atrazine has been found to persist in the environment [5,6] and has shown diverse toxic effects on soil microorganisms, plant growth, aquatic organisms, and human health [3,7]. Assessing the degradation processes of pesticides in the environment, however, can be challenging due to complex factors such as dilution, sorption, desorption, and biotic and abiotic biodegradation [8]. Traditional methods relying on concentration monitoring often struggle to differentiate the reduction of concentration between destructive and nondestructive processes, making it difficult to assess the in-situ pesticide degradation.

Compound-specific stable isotope analysis (CSIA) has emerged as a monitoring approach that offers distinct advantages over traditional tools by enabling the differentiation of competing environmental sinks [9]. CSIA takes advantage of the kinetic isotope effect (KIE), which results in faster bond breakage for lighter isotopes (e.g., ^{12}C) compared to heavier isotopes (^{13}C) during degradation. As a result, the remaining fraction of contaminants becomes relatively enriched in the heavier isotope as the degradation progresses [10].

The average compound-specific isotope value (e.g., $\delta^{13}\text{C}$) of the remaining contaminant can be used to quantitatively assess the in situ degradation extent according to the Rayleigh distillation equation [11] when the isotope fractionation factors of the relevant reaction processes are available [12]. CSIA also allows for the differentiation between transformation pathways (e.g., the hydrolysis vs. oxidative transformation of atrazine) [13,14] and provides insights into the underlying biochemical reaction mechanisms [15,16]. Although most CSIA studies of micropollutants have been conducted on the lab-scale cultivation of monocultures [17,18], determining isotope effects for atrazine degradation using mixed cultures and applying CSIA to pesticides in ecosystems remains limited [19,20].

Accurately measuring isotope fractionation parameters, such as the isotope enrichment factor (ϵ) and kinetic isotope effects (KIEs), in field conditions remains a challenge. The common approach for applying CSIA involves obtaining these parameters through batch experiments in laboratory settings. Subsequently, these parameters are used to evaluate the degradation extent of contaminants by combining the isotope signatures (e.g., $\delta^{13}\text{C}$) obtained from field monitoring. However, significant variability in isotope enrichment factors has been reported in the biotransformation processes of organic contaminants, even in controlled laboratory settings. For instance, trichloroethylene exhibits ϵ_{C} values ranging from -2.5% to -19.6% depending on the microbial species involved [21–23]. Likewise, the degradation process of dichloromethane exhibits significant variability [24], as do the carbon isotope enrichment factors for the herbicide atrazine. Systematic CSIA studies have been conducted on the lab-scale cultivation of different atrazine-degrading microorganisms, such as *atzA*- and *trzN*-harboring bacterial strains [13,14,25,26]. The carbon isotope enrichment factors vary from -0.5% to -5.5% , even within the same hydrolysis pathway of atrazine [20]. The isotope fractionation was found to be sensitive to the bacterial species involved [27] as well as to the mass transfer and bioavailability limitation of atrazine [26,28–30]. This raises the challenge of selecting a representative isotope enrichment factor of atrazine for CSIA application in the field.

To bridge the gap between the lab-scale microcosm research and the field applications of CSIA, the current study investigates isotope fractionation characteristics in atrazine degradation processes within a two-stage vertical flow constructed wetland as a model system. This research aims to advance our understanding of the isotope effects in atrazine biodegradation processes in ecosystems and promote the application of CSIA in assessing pesticide degradation in real-world environmental scenarios.

2. Materials and Methods

2.1. Configuration of the Bench-Scale Two-Stage Vertical Flow Wetland System

The hybrid wetland system setup is detailed in our previous study [31]. In brief, the wetland comprises two polyvinyl chloride tanks, A (L-W-H, 0.6 m-0.6 m-1.0 m) and B (0.6 m \times 0.6 m \times 1.0 m) (Figure S1, Supporting Information). The tanks were filled with gravel, sand, and a surface layer of soil to facilitate microbial immobilization and growth. Additionally, *Phragmites australis* were planted in the tanks.

Four sampling ports were installed for pore water collection: in Tank A, ports were placed at heights of 15 cm (S1) and 50 cm (S2) from the bottom, while in Tank B, ports were located at 5 cm (S4) and 40 cm (S3) from the bottom. Atrazine-containing synthetic wastewater was stored in a 70L tank and pumped into the system. The hybrid wetland received wastewater in a vertical flow mode, allowing it to flow from the bottom to the top of Tank A and subsequently cascade from the top to the bottom of Tank B.

The onset of wastewater supply to the wetland was defined as day 0. On days 51 and 57, a mixed culture of atrazine-degrading microbes was introduced into the hybrid wetland. The experiment lasted 240 days and was divided into six phases based on varying operational conditions, including the inflow of atrazine concentration, wastewater retention time, and addition of atrazine-degrading mixed cultures (Table 1). The chemical reagents and the synthetic wastewater composition are provided in the Supporting Information file (SI).

Table 1. The operation conditions of the hybrid wetland system at different phases. * Indicates the start of microbial inoculation. The inflow concentration of atrazine was summed according to the monitoring results of each sampling event.

Phases	Dates	Duration (d)	HRT (d)	Inflow (L/d)	Inflow Atrazine Range (mg/L)	Inflow Atrazine Average (mg/L)
I	1st March to 20th April	51	6	64	4.1 to 9.3	6.3 ± 1.4
II *	21st April to 7th June	46	6	64	4.9 to 15.6	9.9 ± 3.9
III	8th June to 19th July	42	6	64	15.6 to 19.3	17.4 ± 1.2
IV	20th July to 20th August	32	6	64	28.4 to 31.9	30.4 ± 1.1
V	21st August to 29th September	40	4	96	29.1 to 32.0	30.6 ± 0.8
VI	30th September to 21st October	29	2	192	28.8 to 32.8	30.5 ± 1.2

2.2. Bioaugmentation of the Wetland System Using Atrazine-Degrading Mixed Cultures

The mixed cultures of atrazine-degrading bacterial strains were introduced into the wetland system to enhance the degradation capacity of atrazine in the hybrid wetland system. These monocultures included *Rhizobium* sp. CX-Z, *Rhizobium* sp. (strains CS-1, CS-2, CS-15, CS-X, and CS-Y), *Stenotrophomonas* sp., *Enterobacter cloacae*, *Hyphomicrobium* sp., and *Cohnella phaseoli*. These bacterial strains were isolated from the atrazine-contaminated soils of a pesticide plant in Changxing county, China. The mixed cultures were further detailed in Figure S2 of the Supporting Information (SI). The *Rhizobium* sp. CX-Z was particularly significant, as it harbored the key degradation genes (*atzA*) involved in the mineralization of atrazine. The gene sequences of these atrazine-degrading bacterial monocultures were deposited in the NCBI database with the accession numbers of MH819518 and MK092988-MK092996. To prepare the bacterial inoculum, the atrazine-degrading monocultures and mixed culture were cultured in mineral salt medium (MSM), then harvested and resuspended in phosphate-buffered saline (PBS, pH 7.2–7.4). The compositions of MSM and PBS were described in the Supporting Information (SI).

2.3. Cultivation of the Pore Water Taken from the Wetland System

To calculate the isotope fractionation factors of atrazine degradation in the mixed cultures of atrazine-degrading microbes within the wetland, pore water was collected from sampling port S1 on day 110. An amount of 2.0 L of the pore water was used and it was filtered using a 0.8 µm filter to eliminate suspended particles. The filtered water was then incubated at 30 °C with 300 rpm of shaking to stimulate bacterial growth. The bacterial growth was approximated by monitoring the optical density (OD600) in the cultivation process. The concentration of atrazine and the metabolites were examined using the high-performance liquid chromatography with diode-array detection (HPLC-DAD) system. Furthermore, changes in the carbon and nitrogen isotope signatures (δ -values) were tracked throughout the cultivation process. This measurement was done using the gas chromatograph-coupled combustion isotope ratio mass spectrometry (GC-C-IRMS) system.

2.4. Quantification of Atrazine and the Transformation Metabolites in Pore Water of the Wetland

Aquatic samples were collected from the inflow, outflow, and four sampling ports of the hybrid wetland system to quantitatively analyze atrazine and its main metabolites. The analytical procedure was performed using the HPLC-DAD system (LC-20 series system, Shimadzu), with conditions adapted from previous studies [29,32]. A C18-AR column (5 µm, 250 × 4.6 mm) was used for the separation of atrazine and its degradation products. The initial elution gradient consisted of a 30% acetonitrile and 70% KH₂PO₄ buffer (1 mM) with a flow rate of 0.8 mL/min. The acetonitrile percentage increased linearly to 55% within 8 min. The acetonitrile gradient then increased to 90% over the next 17 min (held for 3 min). The initial conditions were restored within 4 min, and the column was left to equilibrate for another 3 min. To quantify atrazine and its metabolites, an external standard working curve was employed. Atrazine and the metabolite 2-hydroxyatrazine were measured at

a wavelength of 220 nm, and while cyanuric acid, another metabolite, was measured at 213 nm.

2.5. Compound-Specific Carbon and Nitrogen Isotope Signature ($\delta^{13}\text{C}$, $\delta^{15}\text{N}$) Analysis of Atrazine

The preconcentration of the collected pore water was performed after filtering by the 0.22 μm filter. The filtered aquatic samples were then subjected to a solid-phase extraction (SPE) (CNW LC-C18 SPE tubes 500 mg) to achieve a final concentration of approximately 200 mg/L in ethyl acetate. The procedures for the SPE are detailed in the supplemental information (SI). Table S1 in the SI confirms that significant isotope effects did not occur during the SPE procedures. The analytical conditions of the carbon and nitrogen isotopes of atrazine were adapted from previous study [33], and were performed using the GC-C-IRMS system (Ultra gas chromatograph-coupled Finnigan MAT 253 isotope ratio mass spectrometer with Combustion III interface). The injection was conducted at 250 $^{\circ}\text{C}$ with a flow rate of 1.0 mL/min helium (Grade 5.0). The oven temperature program was initially at 40 $^{\circ}\text{C}$ (held for 1 min), followed by a rate of 50 $^{\circ}\text{C}/\text{min}$, then led to 100 $^{\circ}\text{C}$ (held for 5 min), and subsequently increased to 250 $^{\circ}\text{C}$ (held for 5 min) at a ramp of 5 $^{\circ}\text{C}/\text{min}$. Both the carbon and nitrogen isotope signatures were shown as δ -value in ‰ relative to the international reference standard Vienna Pee Dee Belemnite (VPDB) for carbon and the Air- N_2 for nitrogen according to Equation (1) [34], where R_s and R_{ref} represent isotope ratios of the samples (for carbon and nitrogen element (E)) and the international reference standards.

$$\delta_E(\text{‰}) = \frac{R_s - R_{ref}}{R_{ref}} \times 1000 \quad (1)$$

2.6. Calculation of Stable Isotope Fractionation

The carbon and nitrogen isotope enrichment factors (ϵ_C , ϵ_N) in atrazine degradation processes were calculated through linear fitting of the Rayleigh distillation equation (Equation (2)) [11]. The Rayleigh model directly relates the initial concentration of contaminants and the isotope signatures (δ -value) (e.g., c_0 , $\delta_0^{13}\text{C}$) at the beginning of the reaction to the values observed at reaction time t (c_t , $\delta_t^{13}\text{C}$):

$$\ln\left(\frac{\delta_t + 1000}{\delta_0 + 1000}\right) = \epsilon \times \ln\left(\frac{c_t}{c_0}\right) \quad (2)$$

Subsequently, the isotope enrichment factor in bulk can be converted to the apparent kinetic isotope effect (AKIE) according to the empirical formula (Equation (3)) [35]:

$$AKIE = \frac{1}{1 + z \cdot \frac{n}{x} \cdot \epsilon} \quad (3)$$

where n , x , and z are the number of atoms of each concern element, the atoms involved in the active site, and competitive atoms in the reactive site, respectively. The simultaneous application of the Rayleigh model to the carbon and nitrogen isotope can be shown as:

$$\ln\left(\frac{\delta_t^{13}\text{C} + 1000}{\delta_0^{13}\text{C} + 1000}\right) = \epsilon_C \cdot \ln\left(\frac{c_t}{c_0}\right) \quad (4)$$

$$\ln\left(\frac{\delta_t^{15}\text{N} + 1000}{\delta_0^{15}\text{N} + 1000}\right) = \epsilon_N \cdot \ln\left(\frac{c_t}{c_0}\right) \quad (5)$$

We can obtain the slope of the dual isotope plot ($\lambda_{N/C}$) since the remaining fractionation ($f = c_t/c_0$) of the contaminants for the carbon and nitrogen isotopes are the same:

$$\lambda_{N/C} = \frac{\varepsilon_N}{\varepsilon_C} = \frac{\ln\left(\frac{\delta_t^{15}N+1000}{\delta_0^{15}N+1000}\right)}{\ln\left(\frac{\delta_t^{13}C+1000}{\delta_0^{13}C+1000}\right)} \quad (6)$$

2.7. Quantitative Assessment of Biodegradation of Atrazine Based on CSIA

To assess the biodegradation extent of atrazine (BE) in the wetland system, the Rayleigh model does the calculation independently on the concentration evidence. The BE value was calculated using the originated carbon isotope signatures ($\delta_0^{13}C$) as monitored at sampling time t ($\delta_t^{13}C$), as well as the enrichment factors (ε_C) determined in the concern reaction pathway:

$$BE(\%) = \left[1 - \left(\frac{\delta_t + 1000}{\delta_0 + 1000}\right)^{\frac{1}{\varepsilon_C}}\right] \cdot 100 \quad (7)$$

The BE values can subsequently be used to predict the atrazine concentrations at each sampling event (c_t), taken with the inflow atrazine concentration of the synthetic wastewater as the initial value (c_0):

$$c_t = c_0 \cdot \left[1 - \frac{BE(\%)}{100}\right] \quad (8)$$

3. Results and Discussion

3.1. Atrazine Degradation and Carbon Isotope Signature Changes in the Wetland

The performance of the hybrid-constructed wetland systems in removing atrazine was examined by monitoring the concentrations of atrazine and its isotope signatures. Throughout the whole experiment period, the atrazine concentration in the inflow wastewater ranged from 4.1 to 32.8 mg/L. In phase I, an average of 6.3 ± 1.4 mg/L of atrazine entered the system, while the average outflow concentration was approximately 4.8 ± 1.0 mg/L during the initial 50-day experimental period (Figure 1). The data indicated a modest decrease in the atrazine concentration after the wastewater passed through the system, consistent with the low atrazine removal efficiency (RE) of 14.5% to 37.6% (excluding the initial week) in phase I. This low RE aligned with the results reported by Runes et al. [36], who observed an atrazine removal efficiency of 13% to 24% in constructed wetlands and wetland sediment, averaging around 20%. During the first week of the experiment, the atrazine concentration exhibited a substantial decrease, corresponding to a significantly higher removal efficiency of atrazine (>90%) (Figure 1). However, one week later, the RE values rapidly dropped to the 14% to 37% range. This swift decline can be primarily attributed to the adsorption effects of the wetland's sediment compartment, as adsorption processes merely reduce atrazine concentration after achieving equilibrium. The findings suggest a limited destructive attenuation of atrazine in the first stage, with non-destructive processes playing a more significant role in its removal. This was further evidenced by the outflow concentrations of the metabolites of hydroxyatrazine and cyanuric acid. Both of these metabolites had outflow concentrations around 0.3 ± 0.2 mg/L in the first stage, subtly hinting at a slight atrazine biodegradation. Additionally, the $\delta^{13}C$ values associated with the remaining atrazine in outflow fluctuated between -30.0% and -28.0% with a mean value of $-28.8 \pm 0.7\%$ in first phase (Figure 1). No considerable isotope fractionation occurred during the 50-day period of experiment, based on the advised 2‰ analytical uncertainty of the stable isotope analysis intended for this in situ study [37,38]. This minor alteration in isotopic signatures aligns well with the minimal removal efficiency of atrazine, confirming atrazine was primarily eliminated by abiotic procedures, such as adsorption to the environmental matrix within the wetland. This is because isotope fractionation com-

monly occurs during the degradation processes and, by contrast, exhibits limited isotope fractionation during physical processes [15].

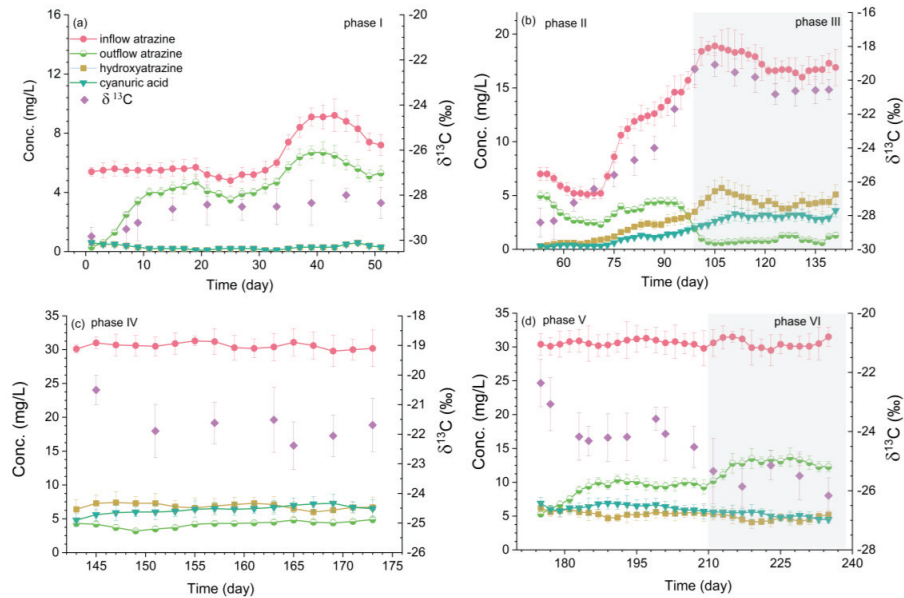


Figure 1. Changes of atrazine and its metabolites of hydroxyatrazine and cyanuric acid, as well as the compound-specific isotope signatures in different operational phases.

Surprisingly, a significant decrease in the atrazine concentration occurred after introducing atrazine-degrading bacterial strains into the wetland system. The mean outflow of atrazine concentration was quite low, ranging between 1.5 ± 0.4 and 4.2 ± 0.6 mg/L (Table 2), despite the average inflow concentration of atrazine increasing from 9.9 ± 3.9 to 30.4 ± 1.1 mg/L. The corresponding removal efficiency (RE) of atrazine significantly increased to a range between $60.9 \pm 8.7\%$ and $90.6 \pm 4.1\%$. This efficiency is comparable to that reported in studies of bioaugmented wetlands using two monocultures [39], with an atrazine removal of 70% to 90%. The removal efficiency exceeded prior studies on triazine herbicide removal within various constructed wetlands [40]. The high degree of atrazine degradation can be attributed to the use of mixed cultures, further emphasized by the accumulation of metabolites. For instance, the cyanuric acid and hydroxyatrazine in the outflow rose from less than 0.3 ± 0.2 mg/L to 0.9 ± 0.5 mg/L and 1.8 ± 0.9 mg/L, respectively, in the second phase. During operation phase IV, the average concentration of cyanuric acid gradually increased to 6.8 ± 0.5 mg/L, and subsequently, 6.3 ± 0.8 mg/L. This significant increase is associated with the atrazine degradation process. The rapid accumulation of metabolic by-products indicates an active microbial degradation process is occurring within the wetland [40].

During the biodegradation process of atrazine, notable changes in the isotope signature were detected following the induction of mixed cultures. In the second phase, the $\delta^{13}\text{C}$ values ranged from -27.6 to -20.0 ‰ with a mean value of -24.8 ± 2.6 ‰ (Figure 1b), with carbon isotope enrichment at approximately 5‰. Subsequently, the mean isotope signature escalated to -20.1 ± 1.1 ‰ within a range from -21.6 ‰ to -18.8 ‰ in the third phase, demonstrating a marked shift of around 10.0‰, and correspondingly, the RE values peaked in this phase. Progressively, a modest decline in the δ -value was noted, correlating with the reduction in RE throughout phases IV to VI. In phase IV, the δ -values fell within a range of between -22.7 ‰ and -19.5 ‰ (mean -21.5 ± 1.1 ‰), followed by a range between -25.0 ‰ and -22.0 ‰ in phase V (mean -23.8 ± 0.9 ‰), and finally in phase VI,

a range between -26.3‰ and -24.8‰ was observed (mean $-25.7 \pm 0.7\text{‰}$). The carbon isotope enrichments were about 8.5‰ , 6.0‰ , and 4.2‰ , respectively, relative to the inflow isotope signatures. The patterns of isotope signature variations coincide well with the changing trends in RE values, thus indicating their potential accuracy for quantifying the biodegradation of atrazine accurately within the wetland.

Table 2. The atrazine concentration changes of outflow (Atz-outflow) and stable carbon isotope signatures changes ($\delta^{13}\text{C}$) in different operational phases and the corresponding concentration-based removal efficiency (RE) and CSIA-based biodegradation extent of atrazine (BE).

Phase	Atz-Outflow Aver. (mg/L)	Atz-Outflow Range (mg/L)	RE Aver. (%)	RE Range (%)	$\delta^{13}\text{C}$ -Aver. (‰)	$\delta^{13}\text{C}$ -Range (‰)	BE-CSIA Aver. (%) ($\epsilon = -4.6\text{‰}$)	BE-CSIA Range (%)
I	4.8 ± 1.1	2.9–7.0	26.9 ± 6.9	14.5–37.6	-28.8 ± 0.7	-30.0 – -28.0	32.1 ± 10.5	11.6–43.8
II	3.5 ± 0.9	2.0–4.6	60.9 ± 8.7	45.2–75.5	-24.8 ± 2.6	-27.6 – -20.0	68.7 ± 15.1	44.5–90.6
III	1.5 ± 0.4	0.9–2.6	90.6 ± 4.1	76.9–95.4	-20.1 ± 1.1	-21.6 – -18.8	90.1 ± 2.6	86.5–92.8
IV	4.2 ± 0.6	2.8–4.9	86.7 ± 2.0	84.4–90.8	-21.5 ± 1.1	-22.7 – -19.5	86.5 ± 2.9	82.8–91.5
V	8.8 ± 1.9	4.9–11.3	72.0 ± 6.6	63.5–84.2	-23.8 ± 0.9	-25.0 – -22.0	77.5 ± 4.7	71.4–85.3
VI	13.0 ± 0.9	12.0–14.3	58.4 ± 5.5	50.4–70.6	-25.7 ± 0.7	-26.3 – -24.8	66.2 ± 5.0	61.7–72.2

3.2. Characteristics of Carbon and Nitrogen Isotope Fractionation in Different Operational Phases

To qualitatively assess the isotope fractionation in the biotransformation processes of atrazine within the wetland system, carbon and nitrogen isotope signatures were measured in phases II, III, and IV. This measurement was conducted by tracking the changes in isotope signatures within the inflow, outflow, and four sampling ports of the wetland. As depicted in Figure 2, the degradation process of atrazine led to an enrichment of the heavy isotope ^{13}C relative to the lighter ^{12}C atom in the remaining atrazine at the outflow, showing a normal carbon isotope effect. Specifically, the $\delta^{13}\text{C}$ value increased from -31.2‰ to -24.9‰ alongside the decrease of atrazine concentration from 12.6 mg/L to 3.0 mg/L during the sampling carried out in phase II (Figure 2a). Similar trends were noted in phases III and IV, the $\delta^{13}\text{C}$ values rose from -30.4‰ to -21.3‰ in phase III and from -29.9‰ to -23.8‰ in phase IV, respectively, commensurate with the decrease in atrazine concentration along the flow path (Figure 2b,c). Interestingly, however, the heavy nitrogen isotope ^{15}N showed depletion in the remaining atrazine in the outflow samples, suggesting an inverse nitrogen isotope effect in the atrazine degradation process. The $\delta^{15}\text{N}$ values decreased from -2.0‰ to -4.4‰ in phase II and from -1.9‰ to -7.0‰ in phase III, and subsequently decreased from -2.0‰ to -4.1‰ in phase IV, respectively, along the flow path (Figure 2a–c). The corresponding carbon enrichment factor (ϵ_{C}) varied from $-3.2 \pm 0.6\text{‰}$ to $-4.3 \pm 0.6\text{‰}$, whereas the nitrogen enrichment factors fluctuated between $1.0 \pm 0.3\text{‰}$ and $2.2 \pm 0.3\text{‰}$ throughout the three phases (Figure 2d–f).

The observed variability in isotope fractionation within the wetland ecosystem displayed divergences across different operation phases, suggesting differences in the biochemical processes. An interesting contrast was observed in the degree of the nitrogen isotope fractionation, which did not align with the fractionation of the carbon isotopes. The significant enrichment factor of the carbon isotopes predominantly emerged in phase II, while the nitrogen isotopes presented maximum enrichment during phase III. Clearly, isotope fractionation based on this in situ data, when subject to Rayleigh linear fitting, may potentially display bias. This can be attributed to the physical processes that result in concentration changes of atrazine within the wetland ecosystem without fundamentally altering the isotope composition. Moreover, the constraints on atrazine bioavailability due to the mass transfer limitations at the pore scale may reduce the observed isotope fractionation, in accordance with findings from previous studies [41]. For a more comprehensive investigation of the variation in isotope fractionation, pore water was extracted from the wetland on day 110 and subjected to laboratory cultivation. As shown in Figure 3, the atrazine experienced a rapid degradation during the cultivation processes, alongside considerable shifts in both carbon and nitrogen isotope fractionation. A consistent pattern of normal carbon and inverse nitrogen isotope fractionation was identified throughout the

cultivation processes. The enrichment factor was calculated as $\epsilon_C = -4.6 \pm 0.5\text{‰}$ for carbon and $\epsilon_N = 1.7 \pm 0.1\text{‰}$ for nitrogen in the degradation processes of atrazine, with a magnitude similar to the findings from phase II (Figure 2d). This suggests that the reduced carbon isotope fractionation observed in phases III and IV may be attributed to the mass transfer limitations of atrazine at the pore or cellular membrane scale. Nevertheless, the observed isotope fractionation of carbon within the wetland remained within the range of between -0.5‰ and -5.5‰ [20] that has been observed in laboratory cultivations. Likewise, the nitrogen isotope fractionation fell within the range of between 0.6‰ and 3.3‰ [26]. Such variations in single elemental isotope fractionation (ϵ_C , or ϵ_N) may introduce uncertainties in accurately quantifying the microbial degradation processes within the wetland.

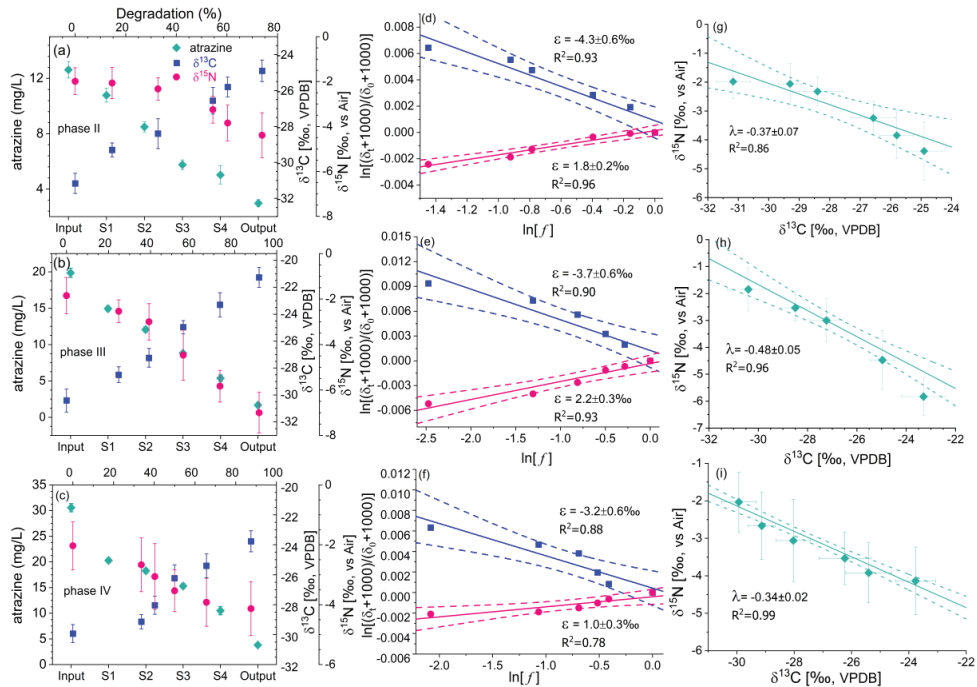


Figure 2. Stable carbon and nitrogen isotope fractionation in different operational phases. The left panel illustrates carbon and nitrogen isotope changes accompanying the atrazine decay, and the middle panel and right panel show the corresponding enrichment factors and dual-isotope plots.

Additionally, the stable carbon and nitrogen isotope fractionation patterns were consistent with that shown in the cultivation processes of atrazine by monocultures in laboratory settings [13,25,26], wherein normal carbon and inverse nitrogen isotope effects occurred during the biotic hydrolysis of the s-triazine Cl atom [42]. Normal carbon isotope effects typically indicate that the transition state is less constrained compared to the reactant. This phenomenon was observed in the alkaline hydrolysis of atrazine, where both normal carbon and nitrogen isotope effects supported the presence of a tightly bound nucleophilic aromatic substitution transition state. In this case, the attacking nucleophile and the leaving group are simultaneously bonded to the aromatic ring [43]. However, in contrast to these observations, an inverse nitrogen isotope effect suggests a more rigid and restricted bonding environment in the transition state compared to the reactant [44,45]. This indicates that the reaction follows a stepwise mechanism in the hydrolysis pathway, with bond formation and bond breaking occurring sequentially. The tighter transition state can be attributed to the additional bonding to the aromatic N atom. For instance, the protonation of the

aromatic N atom in the transition state can lead to a tighter transition state: the lone pair of electrons on the heterocyclic ring N atom can act as a hydrogen bond acceptor and be protonated by hydrogen bond donors, such as the hydrogen ion in an acidic solution, or the hydrogen on the amino acid residue of the reactive site in an enzyme [42,46]. Therefore, the normal carbon and nitrogen isotope fractionation patterns suggest that the microbial degradation of atrazine in wetlands follows the pathway reported in the cultivation of monocultures in laboratory settings. In this pathway, the protonation of the N atoms embedded in the π - π system activates the heterocyclic ring, facilitating the nucleophilic substitution of the Cl atom [42].

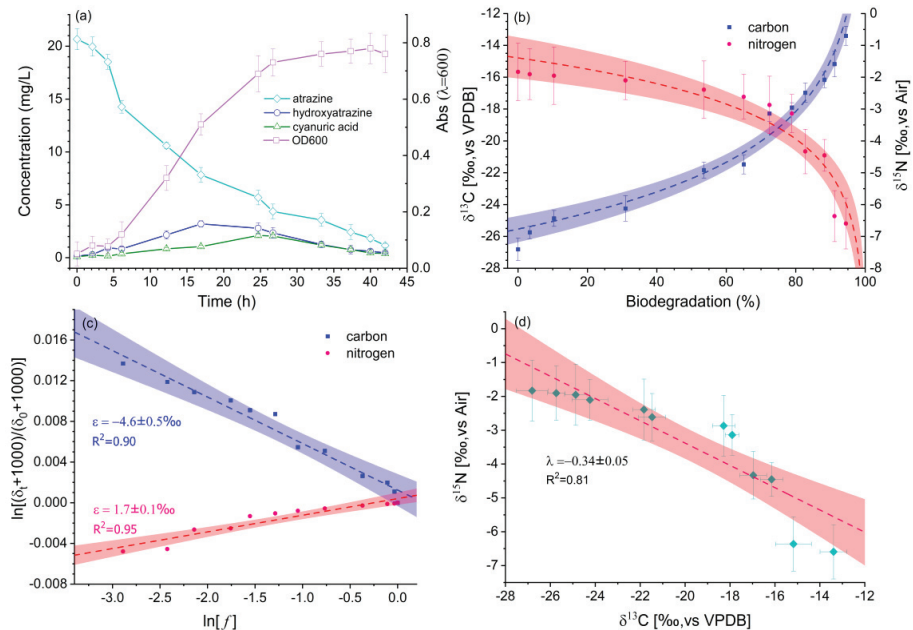


Figure 3. Stable carbon and nitrogen isotope fractionation in cultivation of pore water. (a) Concentration changes of atrazine and the metabolites. (b) Carbon and nitrogen isotope fractionation change along with atrazine decay. (c) Linear fitting of carbon and nitrogen isotope fractionation according to Rayleigh equation. (d) Linear fitting of C-N dual-isotope plot. Error bars represent the standard deviation of triple measurements for one sampling event, filling areas shown at the 95% confidence interval.

3.3. Reaction Pathway and Activation Mechanism of Atrazine Insight from Dual-Isotope Plots and Kinetic Isotope Effects

A comprehensive two-dimensional isotope fractionation examination was facilitated to astutely determine the microbial degradation process of atrazine. This investigation focused on both the carbon and the nitrogen isotope, achieved through the simultaneous measurement of carbon ($\delta^{13}\text{C}$) and nitrogen ($\delta^{15}\text{N}$) during different operational phases, as graphically depicted in Figure 2. The effects of the non-fractionating processes and the masking effects can be minimized in the dual-isotope plot, under the assumption that both carbon and nitrogen will be affected similarly, thus, maintaining a constant ratio between carbon and nitrogen isotope fractionation [9]. A dual-isotope plot was constructed to show the relationship between the $\delta^{13}\text{C}$ and $\delta^{15}\text{N}$ values of atrazine at varying concentrations. Through intensive analysis and the application of linear regression to the plot, the slope of the regression line (λ) proffers notable insights into the preliminary activation mechanism implicated in atrazine degradation. This method has been validated conclusively through

previous lab microcosm experiments and applications in real-world settings, such as with aromatic hydrocarbons, chloroalkane, and gasoline additives [47–50].

Regarding studies focusing on the herbicide atrazine, $\delta^{13}\text{C}$ and $\delta^{15}\text{N}$ measurements were performed on various pure cultures known to possess atrazine degradation capabilities [51]. These measurements uncovered distinct λ values, which were contingent upon the specific bacterial strains involved and the degradation pathways followed. For instance, in oxidative dealkylation processes facilitated by the bacterial strain *Rhodococcus* sp. NI86/21 or the cytochrome P450, a small positive λ value (0.36 ± 0.06) was observed during the reaction processes [14]. Remarkably, this λ value is akin to those (ranging from 0.06 to 0.88) reported for abiotic oxidative dealkylation processes using permanganate [52]. Conversely, negative dual-isotope slopes were commonly observed in biotic hydrolysis processes mediated by bacterial strains containing enzyme AtzA or TrzN, as well as in acidic-assisted abiotic hydrolysis processes, shown to have a wide range from -0.32 to -1.17 [51]. In this study, based on the dual-isotope signatures detected in three sampling campaigns (phase II, III, and IV), the slopes (λ) for the different phases were -0.37 ± 0.07 , -0.48 ± 0.05 , and -0.34 ± 0.02 , respectively (Figure 2g–i). These values fall within the reported range (-0.32 to -1.17) for the biotic hydrolysis of atrazine, and suggests the initial reaction pathway for atrazine in the wetland is similar to the biotic hydrolysis of the C–Cl bond as reported in monocultures of bacterial strains containing enzyme AtzA and TrzN [13]. Additionally, the observed dual-isotope slopes fall within a narrow range between -0.34 and -0.48 and align with those observed in *Rhizobium* sp. CX-Z and *Pseudomonas* sp. ADP, indicating that these bacterial strains may play a key role in atrazine degradation in this wetland. This finding is further supported by the increased abundance of *Rhizobium* sp. and *Pseudomonas* sp. following the addition of mixed cultures (Figures S3 and S4).

To gain insight into the activation mechanism of atrazine, apparent kinetic isotope effects (AKIEs) were calculated based on the empirical formula outlined in Equation (3). Table 3 shows the derived AKIE_C for various phases ranging from 1.026 to 1.038, with an average value of approximately 1.032. This closely aligned with an established kinetic isotope effect (KIE) value of around 1.028, typically observed during a dehalogenation process involving an aromatic carbon [53]. These findings are consistent with the reported KIE values ranging from 1.03 to 1.07, usually observed during a bimolecular nucleophilic substitution ($\text{S}_\text{N}2$ type) reaction involving a C–Cl bond [35]. A normal carbon KIE_C effectively indicates a weaker C–Cl bond within the transition states, representing the energy difference between the initial reactants and the transition states, coherently corresponding to the fundamental definition of the KIE [54]. Despite minor variations between the apparent kinetic isotope effects across different phases, the AKIE_C values support the theory that the initial transformation of atrazine involves an $\text{S}_\text{N}2$ -type aromatic C–Cl bond break. Further supportive evidence for the reaction mechanics is provided by the kinetic isotope effects associated with nitrogen. A secondary inverse nitrogen isotope effect was observed during different operational phases, with values ranging from 0.989 to 0.995 (average 0.992). Such an inverse isotope effect implies that the bonding environment of the nitrogen atom faces more constraints during transition states compared to the pre-reaction phase during enzymatic reactions [55]. The AKIE_N values observed in this study fall within the range of 0.984 to 0.997, as previously observed in the atrazine biodegradation by pure cultures [27]. Presumably, the inverse AKIE_N likely results from the protonation of one aromatic N atom of atrazine [42]. Therefore, these observed AKIEs of carbon and nitrogen suggest the initial activation mechanism in the biodegradation process for atrazine involves the protonation of an aromatic N atom in the molecule, then facilitates the $\text{S}_\text{N}2$ type C–Cl bond cleavage of atrazine.

Table 3. Enrichment factors (ϵ) and apparent kinetic isotope effects (AKIEs) of carbon and nitrogen isotopes, as well as the slopes of C-N dual-isotope plot monitored in different operational phases and batch incubation of pore water from the constructed wetland. Batch represents the data observed in the cultivation of pore water taken from the wetland.

Phases	ϵ (C)-‰	ϵ (N)-‰	AKIE-C	AKIE-N	$\lambda = \delta^{15}\text{N vs. } \delta^{13}\text{C}$
II	-4.3 ± 0.6	1.8 ± 0.2	1.036 ± 0.005	0.991 ± 0.001	-0.37 ± 0.07
III	-3.7 ± 0.6	2.2 ± 0.3	1.031 ± 0.005	0.989 ± 0.001	-0.48 ± 0.05
IV	-3.2 ± 0.6	1.0 ± 0.3	1.026 ± 0.005	0.995 ± 0.001	-0.34 ± 0.02
Batch	-4.6 ± 0.5	1.7 ± 0.1	1.038 ± 0.004	0.992 ± 0.000	-0.34 ± 0.05

3.4. Quantification of Atrazine Biodegradation in the Wetland using Carbon Isotope Signatures

The extent of the inherent biodegradation of atrazine [BE] within the hybrid wetland was meticulously evaluated using stable carbon isotope signatures obtained from each sampling event. This assessment followed the foundation laid out by the Rayleigh model (Equation (7)). Integrating various carbon enrichment factors from recognized transformation pathways coupled with current study data allowed us to make an informed evaluation of the biodegradation extent. (Figure 4). We estimated the biotic hydrolysis of atrazine using a range of values, with -0.5‰ being the lower limit and -5.5‰ being the upper limit. Additionally, the intermediate values of -3.7‰ (from Phase III) and -4.6‰ (from batch cultivation) were factored into the analysis. The predicted BE values based on these calculations then served as a significant indicator to forecast the outflow atrazine concentration, with the inflow atrazine concentration as the initial reference point (Equation (8)).

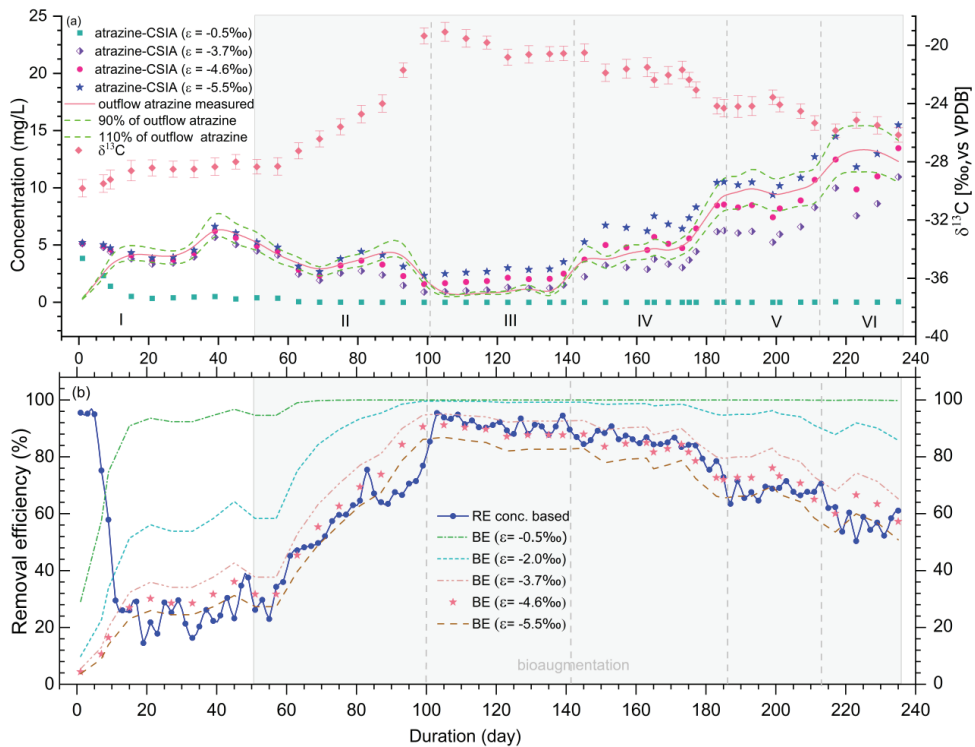


Figure 4. Carbon isotope signature change in the 240-days-long experimental period and the CSIA predicted outflow atrazine concentration (a), as well as the CSIA-based biodegradation extent (BE) changes throughout the whole experiment (b).

As shown in Figure 4b, the biodegradation extent (BE) at each sampling event was calculated using the selected carbon enrichment factor and the difference in $\delta^{13}\text{C}$ values between inflow and outflow samples. Utilizing smaller enrichment factors such as -0.5% and 2.0% resulted in BE values significantly exceeding the RE value for the entire experimental period. This implies a likely overestimation of the atrazine biodegradation within the wetland when using small enrichment factors. Meanwhile, applying the median enrichment factor of -3.7% produced a notable gap between the predicted BE and the concentration-based RE for the whole experiment. This suggests that even medium enrichment factors could overstate the inherent biodegradation potential of atrazine within the wetland. Interestingly, using the enrichment factor of -4.6% obtained from the batch cultivation of the pore water showed considerable improvements in the estimation. The yields of BE values corresponded well with the RE values from phases III and IV but differed from those observed in phases I, II, V, and VI. The most compelling agreement between the CSIA-based BE and the concentration-based RE was shown in phases III and IV, with BE scatter almost mirroring the RE line. Contrarily, in phases II, V, and VI, the BE scatter exceeded the RE line, while the differential between the average values of BE and RE was less than 10% for the majority of samples (Table 2). This suggests that assessing the inherent biodegradation extent of atrazine with a high accuracy is achievable when degradation exceeds 80%, using the enrichment factor derived from batch cultivation. Nevertheless, this method would overestimate the degradation extent of atrazine when degradation fell below 80%. Considering the largest enrichment factor, -5.5% , the BE values aligned well with the RE calculated from phases I and VI, while they were considerably smaller than the RE values in phases II to V. This indicates an underestimation of the inherent degradation of atrazine when a high percentage of atrazine is removed from the wetland. This further suggests the inapplicability of the largest enrichment factors for assessing atrazine degradation in wetland systems.

The concentrations of the outflow atrazine were then calculated from carbon isotope signatures as depicted in Figure 4a. With the use of lower and medium enrichment factors (-0.5% , -3.7%), the scatter points significantly differed from the measured atrazine concentration, with the majority of scatter points falling outside the 90–110% range of the measured concentration, barring the points in phase I and III. In contrast, using the larger enrichment factor (-5.5%) led to the majority of scatter points falling within the 90–110% range of the observed atrazine, specifically for phases I, II, V, and VI. Yet, in phases III and IV, where the removal efficiency plateaued, most of the scatter points fell outside the 90–110% range of the measured atrazine. This suggests that using the highest enrichment factor underestimates the atrazine degradation when substantial atrazine removal is taking place, but is accurate in estimating when there is lower-level atrazine degradation within the wetland. Regarding the enrichment factor (-4.6%) obtained from batch cultivation, the scatter points predominantly fell within a 90–110% range around the outflow atrazine, with phase III being an exception. It is crucial to note that the maximal enrichment factor is commonly utilized when quantifying the extent of biodegradation [56]. Nonetheless, solely depending on this method to evaluate the degradation of specific compounds, such as atrazine, in constructed wetlands could result in an underestimation. These findings illustrate that the enrichment factor determined from the batch cultivation of pore water offers a more representative model when estimating the in situ degradation of atrazine in an ecosystem.

4. Conclusions

This study investigated the characteristics of the carbon and nitrogen isotope fractionation of atrazine degradation within a constructed wetland. The dual-isotope (C, N) fractionation pattern was consistent with those reported in the cultivation of atrazine-degrading pure strains, confirming the validity of multiple element isotope analysis in identifying the transformation pathway and activation mechanism of atrazine within the wetland system. However, the variation in single element isotope fractionation underscores

the necessity for careful selection and application of isotope enrichment factors when quantitatively assessing atrazine degradation in ecosystems. This research bridges the gap between microcosm study and the field application of the compound-specific stable isotope analysis of atrazine, and enhances our understanding of stable isotope fractionation in the biodegradation processes of atrazine within the ecosystem. Future studies could explore the additional factors influencing single element isotope fractionation in ecosystems and further refine the quantification strategy based on stable isotope fractionation analysis.

Supplementary Materials: The supporting information can be downloaded at: <https://www.mdpi.com/article/10.3390/pr11113252/s1>.

Author Contributions: S.C.: conceptualization, methodology, data curation, writing—original draft preparation. L.M.: writing—review and editing, supervision, funding acquisition. Y.W.: writing—review and editing, supervision. All authors have read and agreed to the published version of the manuscript.

Funding: This research was funded by the National Key R&D Program of China, grant number: 2018YFC180310.

Data Availability Statement: All data generated during this study are included in this article.

Conflicts of Interest: The authors declare no conflict of interest.

References

- de Souza, R.M.; Seibert, D.; Quesada, H.B.; Bassetti, F.d.J.; Fagundes-Klen, M.R.; Bergamasco, R. Occurrence, impacts and general aspects of pesticides in surface water: A review. *Process Saf. Environ. Prot.* **2020**, *135*, 22–37. [CrossRef]
- Tang, F.H.M.; Lenzen, M.; McBratney, A.; Maggi, F. Risk of pesticide pollution at the global scale. *Nat. Geosci.* **2021**, *14*, 206–210. [CrossRef]
- Hu, Y.; Jiang, Z.; Hou, A.; Wang, X.; Zhou, Z.; Qin, B.; Cao, B.; Zhang, Y. Impact of atrazine on soil microbial properties: A meta-analysis. *Environ. Pollut.* **2023**, *323*, 121337. [CrossRef] [PubMed]
- Hennig, T.B.; Bandeira, F.O.; Puerari, R.C.; Fraceto, L.F.; Matias, W.G. A systematic review of the toxic effects of a nanopesticide on non-target organisms: Estimation of protective concentrations using a species sensitivity distribution (SSD) approach—The case of atrazine. *Sci. Total Environ.* **2023**, *871*, 162094. [CrossRef] [PubMed]
- Triassi, M.; Montuori, P.; Provisiero, D.P.; De Rosa, E.; Di Duca, F.; Sarnacchiaro, P.; Díez, S. Occurrence and spatial-temporal distribution of atrazine and its metabolites in the aquatic environment of the Volturno River estuary, southern Italy. *Sci. Total Environ.* **2022**, *803*, 149972. [CrossRef]
- Vonberg, D.; Vanderborght, J.; Cremer, N.; Puetz, T.; Herbst, M.; Vereecken, H. 20 years of long-term atrazine monitoring in a shallow aquifer in western Germany. *Water Res.* **2014**, *50*, 294–306. [CrossRef]
- Urseler, N.; Bachetti, R.; Biolo, F.; Morgante, V.; Morgante, C. Atrazine pollution in groundwater and raw bovine milk: Water quality, bioaccumulation and human risk assessment. *Sci. Total Environ.* **2022**, *852*, 158498. [CrossRef]
- Shukla, A.; Parde, D.; Gupta, V.; Vijay, R.; Kumar, R. A review on effective design processes of constructed wetlands. *Int. J. Environ. Sci. Technol.* **2022**, *19*, 12749–12774. [CrossRef]
- Palau, J.; Trueba-Santiso, A.; Yu, R.; Mortan, S.H.; Shouakar-Stash, O.; Freedman, D.L.; Wasmund, K.; Hunkeler, D.; Marco-Urrea, E.; Rosell, M. Dual C-Br Isotope Fractionation Indicates Distinct Reductive Dehalogenation Mechanisms of 1,2-Dibromoethane in Dehalococoides- and Dehalogenimonas-Containing Cultures. *Environ. Sci. Technol.* **2023**, *57*, 1949–1958. [CrossRef]
- Ojeda, A.S.; Phillips, E.; Lollar, B.S. Multi-element (C, H, Cl, Br) stable isotope fractionation as a tool to investigate transformation processes for halogenated hydrocarbons. *Environ. Ence Process. Impacts* **2020**, *22*, 567–582. [CrossRef]
- Scott, K.M.; Lu, X.; Cavanaugh, C.M.; Liu, J.S. Optimal methods for estimating kinetic isotope effects from different forms of the Rayleigh distillation equation. *Geochim. Et Cosmochim. Acta* **2004**, *68*, 433–442. [CrossRef]
- Breukelen, B.M.V.; Prommer, H. Beyond the Rayleigh Equation: Reactive Transport Modeling of Isotope Fractionation Effects to Improve Quantification of Biodegradation. *Environ. Sci. Technol.* **2008**, *42*, 2457–2463. [CrossRef] [PubMed]
- Meyer, A.H.; Penning, H.; Elsner, M. C and N Isotope Fractionation Suggests Similar Mechanisms of Microbial Atrazine Transformation Despite Involvement of Different Enzymes (AtzA and TrzN). *Environ. Sci. Technol.* **2009**, *43*, 8079–8085. [CrossRef] [PubMed]
- Meyer, A.H.; Elsner, M. C-13/C-12 and N-15/N-14 Isotope Analysis To Characterize Degradation of Atrazine: Evidence from Parent and Daughter Compound Values. *Environ. Sci. Technol.* **2013**, *47*, 6884–6891. [CrossRef] [PubMed]
- Li, J.; Liang, E.; Huang, T.; Zhao, X.; Wang, T. Insights into atrazine degradation by thermally activated persulfate: Evidence from dual C-H isotope analysis and DFT simulations. *Chem. Eng. J.* **2023**, *454*, 140207. [CrossRef]
- Liang, E.; Huang, T.; Li, J.; Wang, T. Degradation pathways of atrazine by electrochemical oxidation at different current densities: Identifications from compound-specific isotope analysis and DFT calculation. *Environ. Pollut.* **2023**, *332*, 121987. [CrossRef]

17. Elsner, M.; Imfeld, G. Compound-specific isotope analysis (CSIA) of micropollutants in the environment—Current developments and future challenges. *Curr. Opin. Biotechnol.* **2016**, *41*, 60–72. [CrossRef]
18. Ouyang, W.-Y.; Kümmel, S.; Adrian, L.; Zhu, Y.-G.; Richnow, H.H. Carbon and hydrogen stable isotope fractionation of sulfamethoxazole during anaerobic transformation catalyzed by *Desulfovibrio vulgaris* Hildenborough. *Chemosphere* **2023**, *311*, 136923. [CrossRef]
19. Alvarez-Zaldívar, P.; Payraudeau, S.; Meite, F.; Masbou, J.; Imfeld, G. Pesticide degradation and export losses at the catchment scale: Insights from compound-specific isotope analysis (CSIA). *Water Res.* **2018**, *139*, 198–207. [CrossRef]
20. Arar, M.; Bakkour, R.; Elsner, M.; Bernstein, A. Microbial hydrolysis of atrazine in contaminated groundwater. *Chemosphere* **2023**, *322*, 138226. [CrossRef]
21. Nijenhuis, I.; Andert, J.; Beck, K.; Kästner, M.; Diekert, G.; Richnow, H.H. Stable isotope fractionation of tetrachloroethene during reductive dechlorination by *Sulfurospirillum multivorans* and *Desulfotobacterium* sp. strain PCE-S and abiotic reactions with cyanocobalamin. *Appl. Environ. Microbiol.* **2005**, *71*, 3413–3419. [CrossRef]
22. Lee, P.K.H.; Conrad, M.E.; Alvarez-Cohen, L. Stable carbon isotope fractionation of chloroethenes by dehalorespiring isolates. *Environ. Sci. Technol.* **2007**, *41*, 4277–4285. [CrossRef]
23. Harding, K.C.; Lee, P.K.H.; Bill, M.; Buscheck, T.E.; Conrad, M.E.; Alvarez-Cohen, L. Effects of Varying Growth Conditions on Stable Carbon Isotope Fractionation of Trichloroethene (TCE) by *tceA*-containing *Dehalococcoides mccartyi* strains. *Environ. Sci. Technol.* **2013**, *47*, 12342–12350. [CrossRef] [PubMed]
24. Hermon, L.; Denonfoux, J.; Hellal, J.; Joulian, C.; Ferreira, S.; Vuilleumier, S.; Imfeld, G. Dichloromethane biodegradation in multi-contaminated groundwater: Insights from biomolecular and compound-specific isotope analyses. *Water Res.* **2018**, *142*, 217–226. [CrossRef] [PubMed]
25. Lihl, C.; Heckel, B.; Grzybkowska, A.; Dybala-Defratyka, A.; Ponsin, V.; Torrentó, C.; Hunkeler, D.; Elsner, M. Compound-specific chlorine isotope fractionation in biodegradation of atrazine. *Environ. Ence Process. Impacts* **2020**, *2*, 792–801. [CrossRef] [PubMed]
26. Ehrl, B.N.; Gharasoo, M.; Elsner, M. Isotope Fractionation Pinpoints Membrane Permeability as a Barrier to Atrazine Biodegradation in Gram-negative *Polaromonas* sp. Nea-C. *Environ. Sci. Technol.* **2018**, *52*, 4137–4144. [CrossRef]
27. Chen, S.; Yang, P.; Rohit kumar, J.; Liu, Y.; Ma, L. Inconsistent carbon and nitrogen isotope fractionation in the biotransformation of atrazine by *Ensifer* sp. CX-T and *Sinorhizobium* sp. K. *Int. Biodeterior. Biodegrad.* **2017**, *125*, 170–176. [CrossRef]
28. Chen, S.; Zhang, K.; Jha, R.K.; Ma, L. Impact of atrazine concentration on bioavailability and apparent isotope fractionation in Gram-negative *Rhizobium* sp. CX-Z. *Environ. Pollut.* **2020**, *257*, 113614. [CrossRef]
29. Chen, S.; Zhang, K.; Jha, R.K.; Chen, C.; Yu, H.; Liu, Y.; Ma, L. Isotope fractionation in atrazine degradation reveals rate-limiting, energy-dependent transport across the cell membrane of gram-negative rhizobium sp. CX-Z. *Environ. Pollut.* **2019**, *248*, 857–864. [CrossRef]
30. Kundu, K.; Marozava, S.; Ehrl, B.; Merl-Pham, J.; Griebler, C.; Elsner, M. Defining lower limits of biodegradation: Atrazine degradation regulated by mass transfer and maintenance demand in *Arthrobacter aurescens* TC1. *ISME J.* **2019**, *13*, 2236–2251. [CrossRef]
31. Chen, S.; Ma, L.; Yao, G.; Wang, Y. Efficient atrazine removal in bioaugmentation constructed wetland: Insight from stable isotope fractionation analysis. *Int. Biodeterior. Biodegrad.* **2023**, *185*, 105691. [CrossRef]
32. Cantu, R.; Evans, O.; Kawahara, F.K.; Shoemaker, J.A.; Dufour, A.P. An HPLC method with UV detection, pH control, and reductive ascorbic acid for cyanuric acid analysis in water. *Anal. Chem.* **2000**, *72*, 5820–5828. [CrossRef] [PubMed]
33. Meyer, A.H.; Penning, H.; Lowag, H.; Elsner, M. Precise and Accurate Compound Specific Carbon and Nitrogen Isotope Analysis of Atrazine: Critical Role of Combustion Oven Conditions. *Environ. Sci. Technol.* **2008**, *42*, 7757–7763. [CrossRef] [PubMed]
34. Coplen, T.B. Guidelines and recommended terms for expression of stable-isotope-ratio and gas-ratio measurement results. *Rapid Commun. Mass Spectrom.* **2011**, *25*, 2538–2560. [CrossRef] [PubMed]
35. Elsner, M.; Zwank, L.; Hunkeler, D.; Schwarzenbach, R.P. A new concept linking observable stable isotope fractionation to transformation pathways of organic pollutants. *Environ. Sci. Technol.* **2005**, *39*, 6896–6916. [CrossRef]
36. Runes, H.B.; Jenkins, J.J.; Moore, J.A.; Bottomley, P.J.; Wilson, B.D. Treatment of atrazine in nursery irrigation runoff by a constructed wetland. *Water Res.* **2003**, *37*, 539–550. [CrossRef]
37. Hunkeler, D.; Meckenstock, R.U.; Lollar, B.S.; Schmidt, T.C.; Wilson, J.T. *A Guide for Assessing Biodegradation and Source Identification of Organic Ground Water Contaminants Using Compound Specific Isotope Analysis (CSIA)*; U.S. Environmental Protection Agency: Washington, DC, USA, 2009; EPA/600/R-08/148.
38. Braeckvelt, M.; Fischer, A.; Kästner, M. Field applicability of Compound-Specific Isotope Analysis (CSIA) for characterization and quantification of in situ contaminant degradation in aquifers. *Appl. Microbiol. Biotechnol.* **2012**, *94*, 1401–1421. [CrossRef]
39. Zhao, X.; Bai, S.; Li, C.; Yang, J.; Ma, F. Bioaugmentation of atrazine removal in constructed wetland: Performance, microbial dynamics, and environmental impacts. *Bioresour. Technol.* **2019**, *289*, 121618. [CrossRef]
40. Vymazal, J.; Bfezinova, T. The use of constructed wetlands for removal of pesticides from agricultural runoff and drainage: A review. *Environ. Int.* **2015**, *75*, 11–20. [CrossRef]
41. Thullner, M.; Fischer, A.; Richnow, H.-H.; Wick, L.Y. Influence of mass transfer on stable isotope fractionation. *Appl. Microbiol. Biotechnol.* **2013**, *97*, 441–452. [CrossRef]

42. Schuerner, H.K.V.; Seffernick, J.L.; Grzybkowska, A.; Dybala-Defratyka, A.; Wackett, L.P.; Elsner, M. Characteristic Isotope Fractionation Patterns in s-Triazine Degradation Have Their Origin in Multiple Protonation Options in the s-Triazine Hydrolase TrzN. *Environ. Sci. Technol.* **2015**, *49*, 3490–3498. [CrossRef] [PubMed]
43. Grzybkowska, A.; Kaminski, R.; Dybala-Defratyka, A. Theoretical predictions of isotope effects versus their experimental values for an example of uncatalyzed hydrolysis of atrazine. *Phys. Chem. Chem. Phys.* **2014**, *16*, 15164–15172. [CrossRef] [PubMed]
44. Kobayashi, K.; Makabe, A.; Yano, M.; Oshiki, M.; Kindaichi, T.; Casciotti, K.L.; Okabe, S. Dual nitrogen and oxygen isotope fractionation during anaerobic ammonium oxidation by anammox bacteria. *Isme J.* **2019**, *13*, 2426–2436. [CrossRef] [PubMed]
45. Casciotti, K.L. Inverse kinetic isotope fractionation during bacterial nitrite oxidation. *Geochim. Et Cosmochim. Acta* **2009**, *73*, 2061–2076. [CrossRef]
46. Peat, T.S.; Newman, J.; Balotra, S.; Lucent, D.; Warden, A.C.; Scott, C. The structure of the hexameric atrazine chlorohydrolase AtzA. *Acta Crystallogr. Sect. D-Struct. Biol.* **2015**, *71*, 710–720. [CrossRef]
47. Melsbach, A.; Torrento, C.; Ponsin, V.; Bolotin, J.; Lachat, L.; Prasuhn, V.; Hofstetter, T.B.; Hunkeler, D.; Elsner, M. Dual-Element Isotope Analysis of Desphenylchloridazon to Investigate Its Environmental Fate in a Systematic Field Study: A Long-Term Lysimeter Experiment. *Environ. Sci. Technol.* **2020**, *54*, 3929–3939. [CrossRef]
48. Palau, J.; Yu, R.; Hatijah Mortan, S.; Shouakar-Stash, O.; Rosell, M.; Freedman, D.L.; Sbarbati, C.; Fiorenza, S.; Aravena, R.; Marco-Urrea, E.; et al. Distinct Dual C-Cl Isotope Fractionation Patterns during Anaerobic Biodegradation of 1,2-Dichloroethane: Potential To Characterize Microbial Degradation in the Field. *Env. Sci Technol* **2017**, *51*, 2685–2694. [CrossRef]
49. Fischer, A.; Gehre, M.; Breitfeld, J.; Richnow, H.H.; Vogt, C. Carbon and hydrogen isotope fractionation of benzene during biodegradation under sulfate-reducing conditions: A laboratory to field site approach. *Rapid Commun. Mass Spectrom.* **2009**, *23*, 2439–2447. [CrossRef]
50. Haderlein, S.B.; Schmidt, T.C.; Elsner, M.; Zwank, L.; Berg, M.; Schwarzenbach, R.P. New Evaluation Scheme for Two-Dimensional Isotope Analysis to Decipher Biodegradation Processes: Application to Groundwater Contamination by MTBE. *Environ. Ence Technol.* **2005**, *39*, 8543–8544. [CrossRef]
51. Chen, S.; Ma, L.; Wang, Y. Kinetic isotope effects of C and N indicate different transformation mechanisms between atzA- and trzN-harboring strains in dechlorination of atrazine. *Biodegradation* **2022**, *33*, 207–221. [CrossRef]
52. Meyer, A.H.; Dybala-Defratyka, A.; Alaimo, P.J.; Geronimo, I.; Sanchez, A.D.; Cramer, C.J.; Elsner, M. Cytochrome P450-catalyzed dealkylation of atrazine by *Rhodococcus* sp. strain N186/21 involves hydrogen atom transfer rather than single electron transfer. *Dalton Trans.* **2014**, *43*, 12175–12186. [CrossRef] [PubMed]
53. Dybala-Defratyka, A.; Szatkowski, L.; Kaminski, R.; Wujec, M.; Siwek, A.; Paneth, P. Kinetic Isotope Effects on Dehalogenations at an Aromatic Carbon. *Environ. Sci. Technol.* **2008**, *42*, 7744–7750. [CrossRef] [PubMed]
54. Manna, R.N.; Grzybkowska, A.; Gelman, F.; Dybala-Defratyka, A. Carbon-bromine bond cleavage—A perspective from bromine and carbon kinetic isotope effects on model debromination reactions. *Chemosphere* **2018**, *193*, 17–23. [CrossRef] [PubMed]
55. He, Y.; Li, L. Density functional theory calculations of nitrogen and oxygen equilibrium isotope fractionations in NO_3^- - NO_2^- - H_2O aqueous system reveal inverse kinetic isotope effects during nitrite oxidation. *Appl. Geochem.* **2022**, *139*, 105265. [CrossRef]
56. Hofstetter, T.B.; Berg, M. Assessing transformation processes of organic contaminants by compound-specific stable isotope analysis. *Trac-Trends Anal. Chem.* **2011**, *30*, 618–627. [CrossRef]

Disclaimer/Publisher’s Note: The statements, opinions and data contained in all publications are solely those of the individual author(s) and contributor(s) and not of MDPI and/or the editor(s). MDPI and/or the editor(s) disclaim responsibility for any injury to people or property resulting from any ideas, methods, instructions or products referred to in the content.

Article

Visualization Network Analysis of Studies on Agricultural Drainage Water Treatment

Chaoqun Wang ^{1,†}, Yongxiang Zhang ^{2,†}, Lirong Deng ², Mingtao Zhao ¹, Meiqi Liang ¹, Lien-Chieh Lee ³, Cristhian Chicaiza-Ortiz ^{4,5}, Long Yang ⁶ and Tonghui He ^{1,*}

¹ School of Ecology and Environment, Ningxia University, Yinchuan 750021, China; 2021130890@stu.nxu.edu.cn (C.W.); 12020130863@stu.nxu.edu.cn (M.Z.); 12022131065@stu.nxu.edu.cn (M.L.)

² College of Resources and Environment, Yangtze University, Wuhan 430100, China; 2022720593@yangtzeu.edu.cn (Y.Z.); LirongDeng@hotmail.com (L.D.)

³ School of Environmental Science and Engineering, Hubei Polytechnic University, Huangshi 435003, China; leelienchieh@hbpu.edu.cn

⁴ School of Environmental Science and Engineering, China-UK Low-Carbon College, Shanghai Jiao Tong University, Shanghai 200240, China; cristhianchicaiza@sjtu.edu.cn

⁵ Biomass to Resources Group, Faculty of Life Science, Universidad Regional Amazónica IKIAM, Tena 150150, Ecuador

⁶ School of Ecology and Environment, Institute of Disaster Prevention, Sanhe 065201, China; yanglong@cucd.com

* Correspondence: heth@nxu.edu.cn; Tel.: +86-1300-7998829

† These authors contributed equally to this work.

Citation: Wang, C.; Zhang, Y.; Deng, L.; Zhao, M.; Liang, M.; Lee, L.-C.; Chicaiza-Ortiz, C.; Yang, L.; He, T. Visualization Network Analysis of Studies on Agricultural Drainage Water Treatment. *Processes* **2023**, *11*, 2952. <https://doi.org/10.3390/pr11102952>

Academic Editors: Avelino Núñez-Delgado, Elza Bontempi, Yaoyu Zhou, Esperanza Alvarez-Rodriguez, Maria Victoria Lopez-Ramon, Mario Coccia, Zhien Zhang, Vanesa Santas-Miguel and Marco Race

Received: 15 August 2023

Revised: 29 September 2023

Accepted: 29 September 2023

Published: 11 October 2023



Copyright: © 2023 by the authors. Licensee MDPI, Basel, Switzerland. This article is an open access article distributed under the terms and conditions of the Creative Commons Attribution (CC BY) license (<https://creativecommons.org/licenses/by/4.0/>).

Abstract: Excessive chemical substances in agricultural drainage water have serious adverse effects on the ecological environment of the watershed into which they are discharged. Therefore, it has attracted widespread attention from scholars worldwide. In this paper, 282 scientific articles related to agricultural drainage water treatment are selected from the Web of Science Core Collection database, and CiteSpace was used to visualize and analyze the knowledge map of this field. The most productive authors, institutions, and countries in agricultural drainage water research are graphically presented in this paper. Developing countries are becoming the core force in this realm of inquiry. In addition, this paper explains the changes in research topics in this field over time and reveals current research hotspots, including “desalination”, “denitrification”, and “phosphorus removal”. Future research endeavors in using bioreactors and agricultural drainage water ditches for treating agricultural drainage water are implied to become a research focus in this field. This paper also emphasizes that future environmental protection research should increase case studies in developing countries and develop corresponding solutions based on the actual situation of agriculture in rural areas of developing countries.

Keywords: agricultural drainage water; visual analysis; CiteSpace

1. Introduction

Agricultural production inevitably results in the production of a certain amount of agricultural drainage water. The excessive use of fertilizers and pesticides in agricultural production has led to numerous water quality issues in watersheds affected by agricultural drainage water. For example, the excessive amounts of nitrogen (N) and phosphorus (P) in the water have exceeded their reasonable threshold ranges, directly leading to eutrophication of the water, excessive algal growth, and fish death [1–3]. Currently, the impact of agricultural drainage water quality represents a significant concern [4,5].

In response to this situation, scholars from around the world have proposed a series of physical, chemical, and biological techniques to treat agricultural drainage water [6,7]. For instance, fertilizer management, cover crops, perennial crops, groundwater management, constructed wetlands, buffer strips, drainage ditches, saturated buffer zones, and

bioreactors [8–14]. Among them, agricultural drainage water ditches and bioreactors have received widespread attention from scholars worldwide due to their unique advantages. Currently, research on agricultural drainage water treatment has evolved from a single discipline to a multidisciplinary one, which emphasizes the strong contribution of research developments in Engineering and Environmental Engineering to the study of agricultural drainage water treatment.

Agricultural drainage water ditches represent a direct link between farmland and natural water bodies, which play an important role in agricultural production [15–17]. In addition, agricultural drainage water ditches have been demonstrated to be suitable tools for mitigating agricultural pollution. Previous research has indicated that vegetated drainage ditches provide a suitable mechanism for the effective removal of nutrients, suspended solids, and organic matter from water bodies compared to unvegetated drainage ditches [18–23]. The cost of removing nitrates from agricultural drainage water using nitrification bioreactors is low, making it another proven technology that has been successfully applied in many places in addition to agricultural drainage water ditches [24]. In summary, although the environmental cost of agricultural drainage water is high, and the treatment methods are diverse, it is unquestionable that it can be used to help farmers achieve higher yields by controlling crop water status [25,26].

To date, few have investigated the entire knowledge domain of agricultural drainage water treatment, including how they change over time and the potential factors influencing such changes. To fill these research gaps, this paper downloaded all relevant English-language scientific publications from the Web of Science Core Collection (WOSCC) and visualized the research in the field of agricultural drainage water treatment using CiteSpace, a literature metric software based on computational and statistical methods (Chen, 2017). This paper visualizes knowledge graphs of countries, institutions, authors, disciplines, and terms, aiming to provide a clear overview of the overall research status of agricultural drainage water treatment, summarize and describe the current situation, predict possible research focuses in the future, and provide some references for future researchers and related policymakers.

2. Data Sources and Analytical Methods

2.1. Data Sources and Screening

Web of Science (WOS) is an accurate scientific and technical knowledge literature indexing tool that provides insights into the most important areas of scientific and technical research, and WOS is often considered one of the best sources of data collection for global bibliometric analysis [27,28]. In addition, Web of Science and search tools such as Scopus are of equal strength and have their own strengths, and the content of search tools such as Scopus also overlap with Web of Science. Therefore, we chose Web of Science as our literature search tool [29–31].

The data sources used for the recent study were the Science Citation Index Expanded (SCIE), the Emerging Science Citation Index (ESCI), the Social Science Citation Index (SSCI), the Citation Index to Conference Proceedings-Science (CPCI-S), the Citation Index to Conference Papers-Social Sciences and Humanities (CPCI-SSH), Current Chemical Reactions (CCR-Expanded), and the Index Chemist (IC) under the umbrella of WOS Core Collection (WOSCC) databases. The data were obtained on 1 March 2023.

The search keywords were as follows: (TS = (“agricultural drainage water” OR “agricultural drainage” OR “farmland drainage”)) AND TS = (“purification” OR “purify” OR “decontamination” OR “treatment” OR “remove” OR “dispose” OR “remediation”). We obtained 311 literature records, and from the data obtained above, we refined the data by removing “revised” literature and selecting the literature language as “English”. The data were downloaded as plain text to form a local database and imported into CiteSpace (6.1.R6.64-bit) <http://cluster.ischool.drexel.edu/~cchen/citespace/download/> (accessed on 25 January 2023) for automatic software de-duplication to obtain 282 documents and the pre-processed data as the basis of our study.

2.2. Analytical Methods

The emerging and innovative method for bibliometric investigations contains a visualization of scientific contributions based on social network analyses and colored graph theory. Among numerous tools/methods established for scientometric analyses, Java-based software (CiteSpace) was used to visualize and map the scientific knowledge domain. It is freely available software and was initially established at Drexel University in the United States by Dr. Chen Chaomei [32]. Given the large number of publications we identified, it would be difficult to manually extract their information, so it was necessary to use the software. At the same time, CiteSpace has visualization capabilities that can help us solve these problems [33]. Therefore, we chose the CiteSpace software (version 6.1.R6.64-bit) as the main tool, thus providing a comprehensive analysis of the selected literature.

CiteSpace was used to explore publications and collaborative networks, agricultural drainage water research development, and collaboration and distribution among countries, research institutions, and authors. It was carried out by setting the node types in the CiteSpace software to “country”, “institution”, “author”, “keyword”, etc., to achieve this goal. Since a remarkable correlation exists between country and institution nodes (an institution is a subset of a country), country and institution nodes were shown in the same graph. The node type was changed to “Category” and the specialized software was used to conduct a timeline analysis, which facilitated the visualization of the progression of the research themes within the field. Modifying the node type configuration made it possible to conduct a co-citation analysis. For this academic article, a co-citation was defined as the occurrence in which papers A and B cited paper C. This method enabled the identification of influential papers and the extraction of pertinent data from them. By “term” clustering and co-occurrence analysis, it was possible to identify pioneering research and areas of intense focus at various phases of the development of the field. The integration of these analyses allowed for the identification of overarching trends in the evolution of agricultural drainage water research and the forecasting of upcoming issues and advances requiring future attention. The flow of data processing, as well as analysis of the article, is shown in Figure 1.

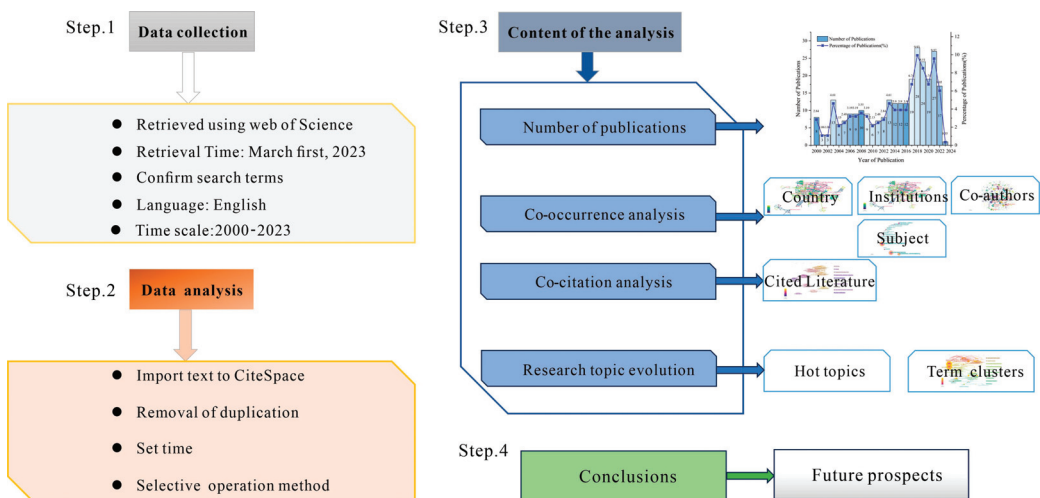


Figure 1. Data processing and analysis flow of this article.

3. Result and Discussion

3.1. Basic Situation Analysis

3.1.1. Publication of Papers at Different Stages

We analyzed 282 publications from 1 January 2000 to 1 March 2023 based on the available data (Figure 2). The number of publications was divided into two stages. During the 10 years, from 2003 to 2012, the number of publications accounted for only 39.4% of the total, and no more than 10 papers were published in any year during this stage except for 2003. Although this phase was not extensive in research, the acceptance of the agricultural drainage water treatment definition and research methods laid the theoretical foundation for subsequent studies. Consequently, the aforementioned 13-year duration can be categorized as the developmental phase of research pertaining to farmland drainage. Between 2013 and 2022, the number of published papers in the field of agricultural drainage water increased to 7.7 times the number in 2013, accounting for 64.9% of the publications during our study period. We call this the “high growth” agricultural drainage water research phase. During this stage, research in agricultural drainage water has become an active area of research for many scholars, with more than 10 papers published each year. During the 4 years from 2018 to 2021, about 20 articles were published each year, especially in 2018, a year in which the number of articles published reached a peak of 28 during the research period. During this stage, some scholars conducted case studies on agricultural drainage water [34,35]. Most scholars recognize that agricultural drainage water is the largest part of pesticide-contaminated water, and therefore, removing all pesticides from it is necessary. In the current study, the main focus is on the effects of different measures on the migration and transformation processes of pollutants in drainage ditches [36]. Meanwhile, some scholars have also focused on other related aspects, such as the effect of agricultural drainage water on the greenhouse effect of agricultural systems [19].

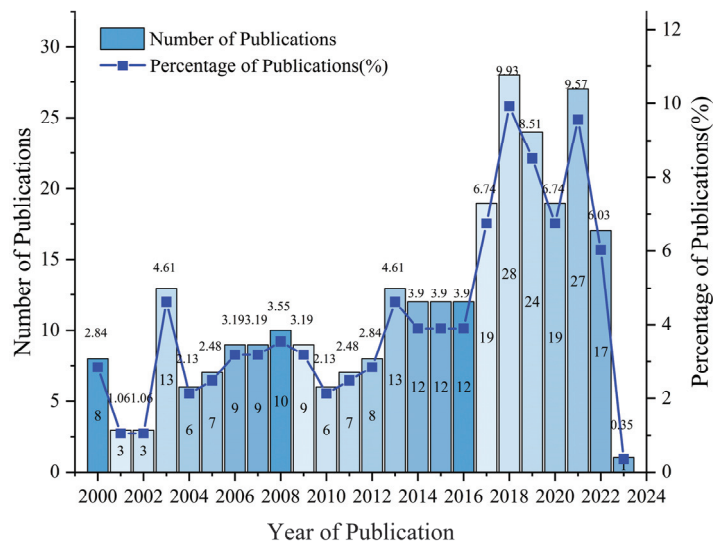


Figure 2. Number of publications in the field of agricultural drainage water treatment per year from 2000 to 2023. The data for 2023 are until 1 March 2023.

As for 2023, the data for this year are not representative, since we only collected the data until 1 March 2023.

3.1.2. Cooperation Networks

By analyzing the cooperation networks among countries and institutions, it was possible to identify key countries and research institutions with a large number of publications

and a strong influence in the field of agricultural drainage water and to identify the cooperative relationships among them. We found two hundred and ninety-four institutions from forty countries or regions involved in research on agricultural drainage water with five countries and eighteen institutions publishing a more significant number of papers (Figure 3).

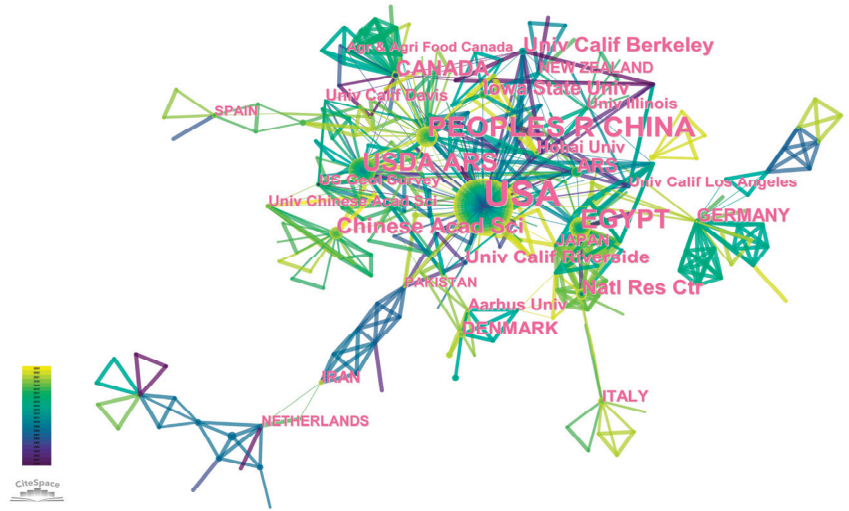


Figure 3. Visualization result of the productive institution and country with their collaborative links.

We list the top 20 leading countries for articles related to agricultural drainage water treatment in Table 1. Among them, the United States (Number of publications [Count] = 142) and China (Count = 49) are the dominant countries. Figure 4 shows in detail the top ten countries in terms of the number of articles issued in recent years.

Table 1. The top 20 active institutions for articles related to agricultural drainage water treatment.

Sr.No.	Count	Centrality	Year	Institution	City	Country
1	29	0.22	2002	USDA ARS	Washington	America
2	17	0.05	2017	Chinese Academy Science	Beijing	China
3	14	0.08	2000	University California Berkeley	Berkeley	America
4	14	0.04	2003	National Research Centre	Paris	French
5	12	0.16	2010	U.S Agricultural Research Service	Washington	America
6	12	0.05	2009	Iowa State University	Ames	America
7	11	0.00	2003	University California Riverside	Riverside	America
8	8	0.02	2015	Hohai University	Nanjing	China
9	8	0.02	2013	Aarhus University	Aarhus	Denmark
10	8	0.07	2000	University California Davis	Davis	America
11	7	0.02	2000	U.S. Geological Survey	Reston	America
12	7	0.00	2014	University Illinois	Urbana	America
13	6	0.02	2003	University California Los Angeles	Los Angeles	America
14	6	0.05	2017	University Chinese Academy Science	Beijing	China
15	5	0.10	2010	Alexandria University	Alexandria	Egypt
16	5	0.04	2006	Agriculture & Agri Food Canada	Guelph	Canada
17	5	0.04	2013	Tokyo Institute Technology	Tokyo	Japan
18	4	0.00	2000	University Waterloo	Waterloo	Canada
19	4	0.05	2004	Southern Illinois University	Carbondale	America
20	4	0.03	2000	California Department of Water Resources	Sacramento	America

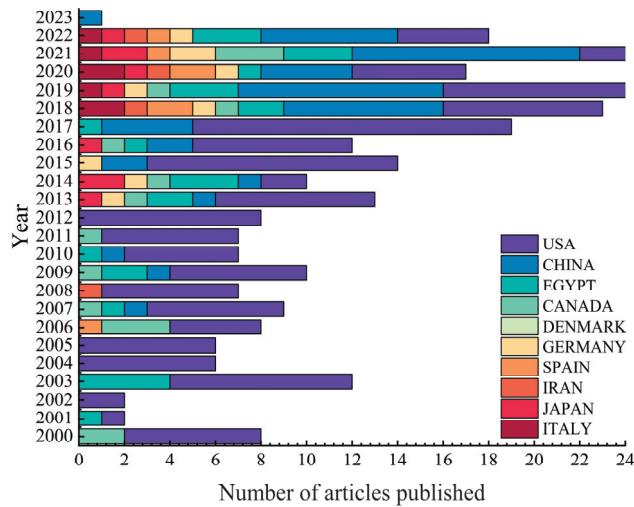


Figure 4. Top ten countries in the area of agricultural drainage water treatment in terms of the specific stack of publications in each year from 2000 to 2023. The data for 2023 are through 1 March 2023.

The top 20 active institutions for articles related to agricultural drainage water treatment are listed in Table 2. The U.S. has a more significant number of research institutions on agricultural drainage water, such as the USDA Agricultural Research Service, the National Laboratory for Agriculture and the Environment (USDA ARS, 29 papers), the University of California, Berkeley (14), the National Research Center (USA) (14), the U.S. Agricultural Research Service (12), Iowa State University (12), and the University of California, Riverside (11), etc. Each institution has published more than 10 papers in the above list of American institutions. Among them, the USDA ARS ranks first in the number of publications in this field in the U.S. and worldwide. In contrast, Chinese research results are concentrated in a few major research institutions, such as the Chinese Academy of Sciences (17), Hohai University (8), and the University of Chinese Academy of Sciences (6). The Chinese Academy of Sciences ranks first in terms of the number of publications in this field in China and second worldwide.

From the perspective of cooperative networks, intermediary centrality is important. Mediation centrality refers to the strength of the number of connections a node has with other nodes in the network; high Mediation centrality represents that the node has a strong influence within the network and is a critical node in the network relationships [33]. The United States has the highest degree of centrality (Degree of centrality [Centr] = 0.55), followed by China (Centr = 0.53). There is also a certain amount of cooperation between the two countries. Furthermore, these two countries have also established cooperative relationships with other countries, such as Egypt and Canada.

We analyzed the number of papers and collaborative networks among authors and discovered that 524 authors are actively engaged in researching agricultural drainage water (Figure 5). Among these authors, twenty-seven authors have published three or more articles. A more detailed list of the top 20 active authors of articles related to agricultural drainage water treatment is displayed in Table 3. Among these highly productive researchers, Norman Terry from the University of California, Berkeley, was one of the earliest to focus on this field. Z.H. Ye from the School of Life Sciences at Sun Yat-sen University in China was one of the earliest Chinese scholars to study this area. In addition, three Chinese Academy of Sciences authors have published two or more papers. The network of authors resembles a sky filled with stars, appearing more scattered.

Table 2. Top 20 dominant countries for articles related to agricultural drainage water treatment.

Sr.No.	Count	Centrality	Year	Countries
1	142	0.55	2000	USA
2	49	0.53	2009	China
3	30	0.36	2001	Egypt
4	16	0.00	2000	Canada
5	10	0.00	2013	Denmark
6	9	0.31	2013	Germany
7	7	0.01	2013	Japan
8	7	0.18	2006	Spain
9	7	0.00	2018	Italy
10	7	0.24	2008	Iran
11	6	0.00	2001	New Zealand
12	5	0.38	2003	Pakistan
13	5	0.17	2000	The Netherlands
14	4	0.00	2018	Czech Republic
15	4	0.00	2000	France
16	4	0.00	2005	Denmark
17	4	0.09	2007	Sweden
18	4	0.31	2002	Australia
19	3	0.00	2014	Korea
20	3	0.00	2009	England

Table 3. Top 20 active authors of articles related to agricultural drainage water treatment (note that the year here refers to the time when this author's first relevant article appeared during our search using Web of Science).

Sr.No.	Count	Institution	Authors	Year
1	6	University of California	Terry, N.	2000
2	5	USDA—Agricultural Research Service National Sedimentation Laboratory	Moore, M.T.	2008
3	5	University of California	Frankenberger, W.T.	2003
4	5	Alexandria University	Fleifle, A.	2013
5	4	National Ground Water Association USA	Allred, B.J.	2012
6	4	Southern Illinois University Edwardsville	Lin, Z.Q.	2000
7	4	University of California	Cohen, Y.	2006
8	4	Alexandria University	Elzeir, M.	2013
9	4	Egypt-Japan University of Science and Technology (E-JUST)	Tawfik, A.	2013
10	3	Aarhus University	Elsgaard, L.	2021
11	3	University of California	Rahardianto, A.	2006
12	3	University of Bologna	Blasioli, S.	2018
13	3	University of Bologna	Braschi, I.	2018
14	3	University of California	William, T.	2007
15	3	Iowa State University	Christianson, L.	2013
16	3	USDA—Agricultural Research Service National Sedimentation Laboratory	Cooper, C.M.	2008
17	3	Kansas State University	Bhandari, A.	2013
18	3	University of California	Mccool, B.C.	2010
19	3	University of California	Zhang, Y.Q.	2004
20	3	Southern Illinois University Edwardsville	Lin, Z.Q.	2006

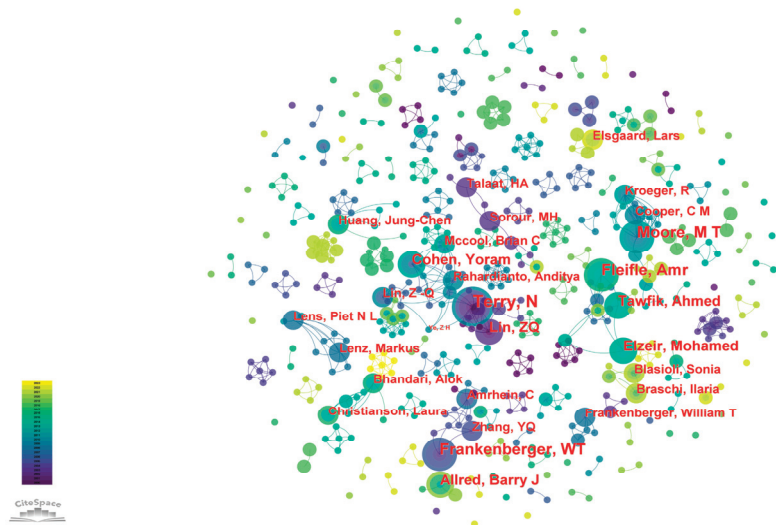


Figure 5. Visualization result of the productive authors with their collaborative links.

In contrast, the strong connections are shown by national and institutional collaborations. Some small-scale fixed cooperative relationships demonstrate the emergence of cooperative groups. Among them, the largest collaborative group is the University of California Berkeley research group, with Norman Terry and other scholars as the core. Z. H. Ye, a scholar from the School of Life Sciences at Sun Yat-sen University in China, collaborates with the U.C. Berkeley research group centered on Norman Terry and other scholars.

3.1.3. Subject Evolution

Through co-occurrence analysis of the subjects in the publications, we constructed a subject network for agricultural drainage water research, showcasing the evolution of mainstream and interdisciplinary disciplines in this field (Figure 6, Table 4). In general, the study of treating agricultural drainage water has evolved from being primarily focused on environmental sciences and water resources to encompassing a range of disciplines. In 2000, agricultural drainage water research appeared in environmental science (Count = 177, Centr = 0.39) and water resources (Count = 82, Centr = 0.35). At this time, it is well known that frequent human agricultural activities and the widespread use of pesticides have led to substantial agricultural water pollution and environmental pollution. In addition, with the maturity of modern environmental ecology theories and methods, the use of environmental ecology concepts and methods to solve the environmental problems caused by this situation have become the focus of scholars.

Currently, environmental science and water resources are still the main topics of agricultural drainage water research, accounting for 91.8% of the research papers in this field. Since 2000, with the development of social economy, science, and technology, agricultural drainage water treatment began to appear in engineering, environmental engineering, and chemistry. Among them, the connection between agricultural drainage water research and engineering is very close, so their intermediary centrality is high (Centr = 0.33).

Subsequently, agricultural drainage water treatment developed into a multidisciplinary approach. In 2004, research on agricultural drainage water treatment began to appear in agriculture. Since 2006, agricultural drainage water research has appeared in various natural or social disciplines, such as geography, energy, and economics. Soil science (Count = 11, Centr = 0.77) and green and sustainable science and technology (Count = 7, Centr = 0.08) also show a relatively high frequency and centrality. Certainly, the development of various disciplines has contributed to the research process to some extent.

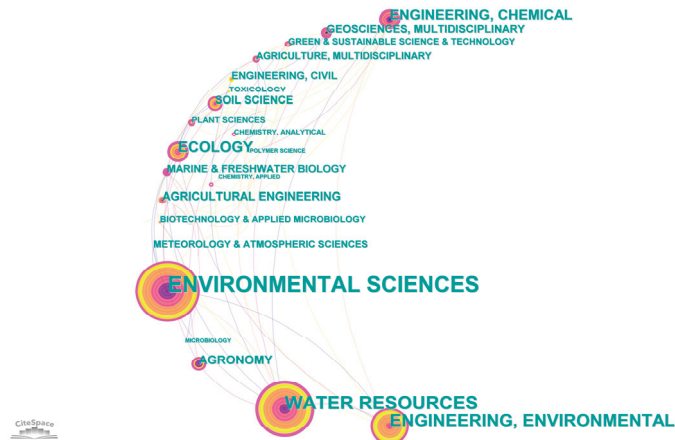


Figure 6. Visualization result of the productive subject with their collaborative links (produced by CiteSpace).

Table 4. The evolution of disciplines in the field of agricultural drainage water treatment (Top 20 by frequency).

Sr.No.	Count	Centrality	Year	Subject Category
1	177	0.39	2000	Environmental Sciences
2	82	0.35	2000	Water Resources
3	58	0.19	2001	Engineering, Environmental
4	31	0.12	2000	Ecology
5	25	0.33	2003	Engineering, Chemical
6	15	0.05	2006	Agronomy
7	13	0.01	2004	Agricultural Engineering
8	12	0.17	2000	Geosciences, Multidisciplinary
9	11	0.07	2000	Soil Science
10	9	0.01	2000	Engineering, Civil
11	9	0.11	2000	Marine and Freshwater Biology
12	8	0.00	2003	Meteorology and Atmospheric Sciences
13	8	0.14	2002	Agriculture, Multidisciplinary
14	7	0.08	2001	Biotechnology and Applied Microbiology
15	7	0.08	2006	Green and Sustainable Science and Technology
16	6	0.00	2003	Toxicology
17	6	0.00	2003	Plant Sciences
18	4	0.24	2014	Chemistry, Analytical
19	3	0.00	2001	Microbiology
20	3	0.00	2003	Chemistry, Applied

3.2. Knowledge Base Analysis

3.2.1. Co-Citation Clustering

Co-citation analysis can assist in identifying the papers that are commonly read and cited in agricultural drainage water treatment research. According to the statistical information extracted from our data by CiteSpace, the 282 publications we analyzed cited 710 papers. Publications cited more than once are shown in Supplementary Materials Table S1. By clustering the cited publications (based on their frequency) and selecting the top five clusters, we were able to identify the knowledge base of agricultural drainage water treatment research to some extent (Figure 7).

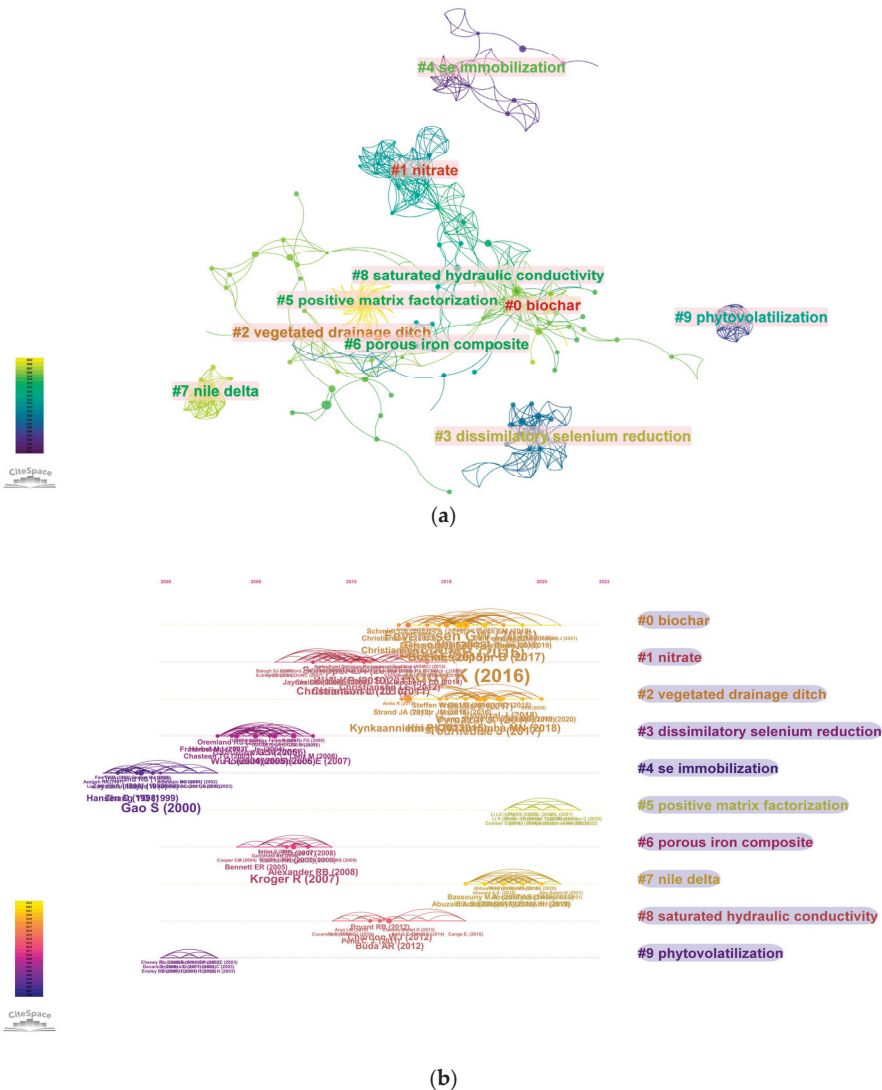


Figure 7. Clustering of frequently co-cited literature in the field of agricultural drainage water treatment. ((a) Clustering diagram of co-citations; (b) Timeline diagram of co-citation clusters, produced by CiteSpace).

The “selenium fixation” cluster began in 1997. This is due to the fact that selenium may be present in agricultural drainage, and selenium fixation through chemical and biological reduction processes can remove selenium from agricultural drainage water and address possible agricultural water pollution during the process [37]. Current research has shown that plant uptake of selenium may be an effective means of removing selenium from drainage sediments [38]. The cluster “dissimilatory selenium reduction” started in 2003 and lasted until 2008, ranking fourth among the clusters we analyzed. In addition, selenate was also a common pollutant in selenium-containing agricultural drainage, which could be converted into elemental selenium nanoparticles under the action of microorganisms [39]. To some extent, it further reflects the current attention paid to selenium in the field of agricultural drainage water treatment.

The largest cluster is “biochar”, which emerged from 2013 to 2021, lasting for 9 years. At the same time, it also indirectly reflects the application of biochar in agricultural drainage water treatment. To date, the utilization of biochar as a means of adsorbing pollutants in agricultural drainage water continues to be a significant aspect of the agricultural drainage water treatment process. Global scholars actively seek biochar types with higher adsorption efficiency and relatively low cost. In this cluster, “biochar” is closely related to agricultural drainage water treatment and has become a keyword in research papers. The “nitrate” cluster lasted the longest (2006–2015) and focused on case studies such as the use of denitrification bioreactors for reducing nitrate nitrogen in agricultural drainage [40].

The presence of vegetation in water bodies serves to purify pollutants, resulting in the formation of a cluster known as a “vegetated drainage ditch”, which has demonstrated a relatively prolonged lifespan. Agricultural drainage water is an important cause of eutrophication in rivers, lakes, reservoirs, and coastal areas. The vegetated drainage ditch is a promising technology for eliminating nutrients and suspended matter from agricultural drainage. The results of some studies have shown that a vegetated drainage ditch is comparable to an artificial wetland in terms of nutrients, and suspended and organic matter treatment efficiency [11,41].

Meanwhile, keywords such as “green agriculture”, “green development”, and “sustainability” provide ideas for the determination and implementation of agricultural drainage water treatment methods.

3.2.2. Frequently Cited Literature

We found twelve papers with more than five citations in the co-citation graph (Figure 8), which to some extent shows the development of the discipline to date, general patterns of research, interdisciplinary cooperation, research patterns, and methods. The 12 most frequently cited publications contribute to accumulating the knowledge base of agricultural drainage water.

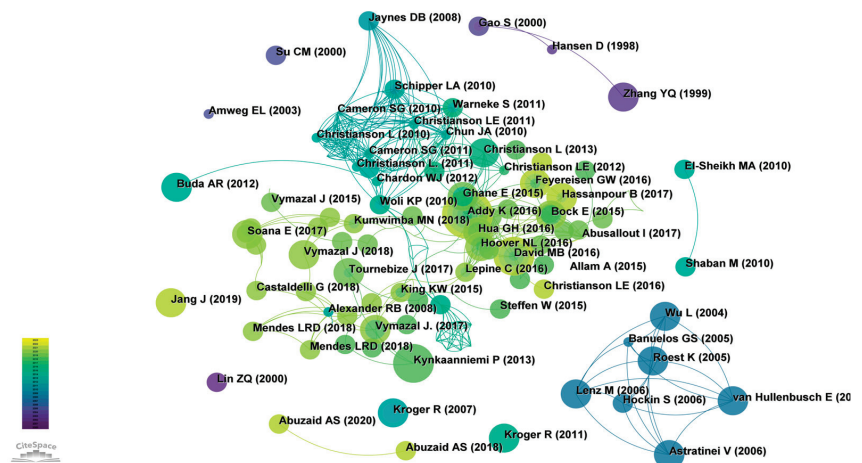


Figure 8. Map of frequently co-cited references in the field of agricultural drainage water treatment.

Among the 12 most frequently cited publications, 16.7% were journal articles that provided a perspective or viewpoint of the literature review. Tournebize, Addy, and other researchers mentioned solutions for nitrate removal in their articles, but they exhibited variations in their approaches and proposed remedies [42,43]. Tournebize et al. analyzed that specific substances and artificial wetlands effectively remove nitrate and pesticides from agricultural drainage water [42]. Addy et al. used meta-analysis to synthesize the first quantitative denitrifying wood chip bioreactor to assess nitrate removal under environmental and design conditions from 26 published studies. In his paper, he points out the

promise of denitrifying bioreactors as a strategy for degrading nitrate and reducing water quality degradation in the treatment of agricultural drainage water and other wastewater, while presenting his view on the orientation of future work in this field, thus becoming the most cited publication (18 citations) [43].

The case study accounted for 66.6% of the 12 most frequently cited publications, and these papers served as a reference for the methodology and content of the subsequent research. Some scholars have pointed out that denitrifying bioreactors utilizing woody material as a carbon substrate is highly effective in removing nitrate and ammonia nitrogen from agricultural drainage water [44,45]. Hoover et al. evaluated the performance of bioreactors under different controlled conditions, including woodchip age, hydraulic retention times (HRTs), and temperature, among others, and their findings provided information to help improve the design of woodchip denitrification bioreactors under specific climatic conditions and existing $\text{NO}_3\text{-N}$ loads [44]. Hassanpour and Bock, among others, added woody material and wood chip-biochar to the bioreactor during the experiment. They found that adding biochar improved the removal of both NO_3^- and P from denitrifying bioreactors (DNBRs) and reduced N_2O emissions [45,46]. This result suggests that variations in biochar materials may improve the removal efficiency of pollutants such as bacteria, pesticides, or drugs. This finding also opens up possibilities for future research on investigating internal fill materials in bioreactors.

These scholars are still actively exploring more efficient methods for removing excessive nitrate and ammonia nitrogen from agricultural drainage water [44–48]. The study conducted by Feyereisen et al. replaced wood chip media with agriculturally derived media to compare and test the nitrate removal rate (NRR) of denitrification bioreactors under warm and cold temperatures. Using the temperature of early spring drainage in the northern United States as the time point, some nitrate removal profiles could be expected under field conditions at the first drainage, with agricultural-derived media performing better than wood chips [44]. Kröger, Hoover, Hua, and others conducted case studies on agricultural drainage water in the Midwest region, the Mississippi River, New York State, and Iowa, respectively. Their research findings have provided references for subsequent research [44,48,49].

The proportion of papers focusing on models and methods is 16.7%, which is not high but still reflects the extent that scholars in this field are aware of the importance of exploring innovative modeling methods. Among them, Ghaneet al. conducted experiments on denitrification beds by modeling the treatment of agricultural drainage water in denitrification beds, and the results showed that the greenhouse gas emissions on the surface of denitrification beds were low. The model evaluation statistics showed a satisfactory prediction of bed outflow nitrate concentration during subsurface drainage flow of agricultural drainage water. The model provides a favorable value for designing efficient denitrification beds, thus improving agricultural drainage water quality [50]. Mark B. David et al. installed two temperature and substrate-controlled woodchip bioreactors for the treatment of agricultural drainage water in the Shibras River watershed in east-central Illinois, USA, which tested the performance of the nitrate load [51]. In addition, the development of biological and chemical disciplines has provided important support for agricultural drainage water research.

3.3. Research Topic Evolution

3.3.1. Hot Topics during Each Stage of the Discipline's Development

Term co-occurrence indicates a situation where two keywords simultaneously appear in multiple articles. The term co-occurrence analysis can reflect the frontiers and hot spots in the research and evolution of agricultural drainage water treatment in different research periods, thus revealing the hot changes in this research topic. We manually classified thirty-four research topics (Supplementary Materials Table S2) into five categories based on the terminology counted by the CiteSpace software (version 6.1.R6.64-bit), which appeared five or more times: research purpose, research topic, research content, research method, and

research factor. During the period spanning from 2000 to 2012, it was observed that while the quantity of papers published annually did not reach significant levels, the quantity of terms utilized was not insignificant. Between 2013 and 2023, along with the increase in the number of papers, there was also an increase in the number of new terms (it should be noted that the number of papers and terms in 2023 is low due to our data collection as of 1 March 2023). Between 2013 and 2023, 60.6% of articles of the total were published, and the number of new terms in this period represents 50.8%. Despite the increase in research papers, the number of new terms is particularly high due to some terms already having been defined before 2013.

Among the studies on the treatment of agricultural drainage water that appeared from 2000 to 2012, 68.6% were related to “content”, followed by “factors” (18.4%) and “methods” (7.65%). Themes and objectives received less attention, resulting in lower representation for both categories. Terms classified under “topic” have been available since 2000, while there are only 12 terms classified under “purpose”. From 2000 to 2012, the term “agricultural drainage” appeared multiple times (71 times) and exhibited high mediating centrality (Centr = 0.34), which serves as a significant node in terms of co-occurrence. Agricultural drainage water emerged as a crucial theme throughout this phase. During this period, the “removal of excessive selenite” from agricultural drainage [52] became a significant research purpose and appeared multiple times. “Pretreatment” became a more important methodological term in this phase, which reflects to some extent that researchers had already considered pretreatment as a means of improving water quality in agricultural drainage water treatment processes at an early stage.

From 2013 to 2023, the number of papers increased, as did the topic of agricultural drainage water treatment research, with 42.5% of new terms appearing in this period. “Research content” remains the most prominent topic of interest; it accounts for 74.5% of the total number of terms in this period, while “research factors” remain the second most popular (13.8%), but “research topic” and “research purpose” are still relatively small, accounting for only 2.8% and 2.1%, respectively, while “research method” accounts for 7.9%. Nitrate removal (15 times, Center = 0.07) is the most important new term under “research purpose” at this stage, indicating that researchers are very concerned about how to efficiently remove excessive nitrate from agricultural drainage water, which, of course, also indicates that “desalination” is still a focus of researchers, rather than only existing in the early stage of this field of research [53,54]. In addition, water quality [55] and removal efficiency [56] became two hot topics in this phase. Agricultural drainage water (63 times, Center = 0.42) [57] was the most frequent and mediated centrality term under the “research topic” category, reflecting the continuity and continued interest in the research topic. Agricultural chemicals emerged as an important “research factor”. In particular, the large-scale use of agricultural chemicals (pesticides) has become an important factor in the pollution of agricultural drainage water. At the same time, the proportion of “research purpose” is deficient, at only 2%, and the removal of pollutants such as nitrogen and phosphorus from agricultural drainage water and the achievement of good overall ecological benefits are the main purposes at this stage [41,58]. It also indicates that research scholars are paying more attention to its impact on the overall ecological environment. In terms of the “research method”, the chemical remediation method (e.g., activated carbon adsorption of pollutants in agricultural drainage) and bioremediation method (e.g., plant adsorption) [11] were used. Denitrification bioreactors [59], especially those based on wood chips as a substrate [60] have also become a method of treating excessive substances in agricultural drainage water.

3.3.2. Evolution of Term Clusters

By clustering the terms, we identified the top ten clusters (Figure 9). The timeline mapping generated by CiteSpace shows that the longest-lasting cluster is “macrophyte-based systems” (2000–2023), and it is also the largest cluster, which existed throughout the study period (Figure 9b). The early terminology of this cluster is mostly agricultural

in theme, such as agricultural land, agricultural run-off, and agricultural ditches. In the middle of the cluster’s development, terms such as agricultural drainage water were increasingly emphasized. Some scholars found differences in the nutrient mitigation capacity of agricultural ditches with and without vegetation, which may also have an impact on the sorption capacity of pesticide chemicals [61,62].

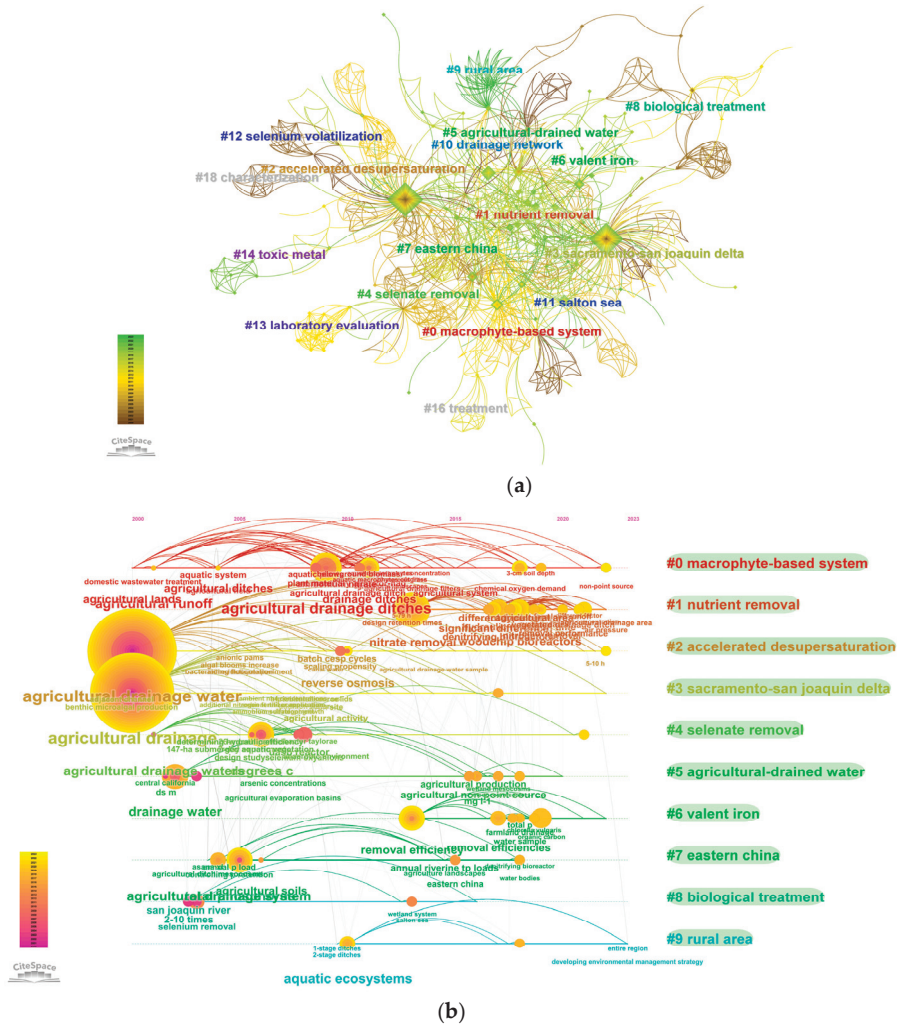


Figure 9. Clusters of agricultural drainage water treatment research based on the terms. ((a) clustering diagram for term analysis; (b) timeline diagram for term clustering).

“Nutrient removal”, “accelerated desupersaturation”, and “Sacramento-sanjoaquin delta” are three clusters that were more important during the research period and will remain important for a long time. The eutrophication of water in agricultural drainage water is a common problem, and “nutrient removal” [63] primarily addresses the issue of water eutrophication, such as removing excessive nitrates from agricultural drainage water. Through the analysis of the cluster “accelerated supersaturation”, it was found that accelerated supersaturation has a certain impact on water treatment in agricultural drainage. For example, Anditya Rahardianto et al. used a two-step chemically-enhanced seeded precipitation (CESP) process, which was demonstrated for the accelerated desupersatura-

tion of antiscalant-containing, gypsum-supersaturated model solutions, which mimicked reverse osmosis (R.O.) concentrate from the R.O. desalting of agricultural drainage water of high mineral scaling propensity. Experimental studies have demonstrated that accelerated desupersaturation can enhance the recovery rate of agricultural drainage water [64]. The cluster pertaining to the removal of selenate remains a significant area of investigation among scholars, as evidenced by our observations on co-occurrence. Later, two relatively small clusters emerged, “rural areas” (2010–2023) and “biological treatment” (2003–2016), which also appeared relatively late. It is inevitable for “rural areas” to form top-ten clusters, and agricultural drainage water primarily occurs in rural areas. Consequently, the water environmental issues arising from it also require urgent attention and treatment. “Biological treatment” has been favored by researchers as an important treatment method to deal with excess pollutants in agricultural drainage water. Within this cluster, the term “wetland system” has become a frequent term, and researchers have found that wetland systems may effectively remove pollutants from agricultural drainage water [65].

4. Conclusions and Future Prospects

In this study, we conducted a comprehensive and systematic visual analysis of agricultural drainage water treatment research by CiteSpace. We revealed the current status of the field, as well as the characteristics of literature citations and research topics. Agricultural drainage water treatment research has made some achievements in terms of theory, methodology, framework, and case studies. Developing countries have emerged as a new focus of research. The research has evolved from laying theoretical foundations to practical applications and from a single-discipline focus on water resources to a multidisciplinary approach.

The study of the current status and characteristics of agricultural drainage water treatment, along with a review of the current state of development and a summary of the primary methodologies and frameworks, provides researchers with a basis on which to focus and from which to draw conclusions. The removal of salts (nitrates, selenate), particularly through denitrification bioreactors, has become an important research hotspot in agricultural drainage water treatment. In the contemporary context of environmental protection, the topics of salt removal, nitrogen removal, and phosphorus removal will continue to be relevant for researchers and factors.

Based on our research findings, we propose the following directions for future research, aiming to provide new insights for researchers and government managers, with the confidence that they will be useful in decision-making:

(1) Currently, there is a higher prevalence of case studies in developed countries such as the United States, while case studies in developing countries are relatively limited. In the future, developing countries should conduct more case studies, drawing upon the experiences of developed countries. Simultaneously, researchers should expand the scope of case studies to include agricultural areas near urban regions, aiming to explore the variations in pollution types and removal effectiveness between these areas and rural agricultural development regions.

(2) Looking ahead, the overall goal of future research may shift from how to treat the excess pollutants present in agricultural drainage water bodies to how to achieve good overall ecological benefits through agricultural drainage water treatment.

(3) Achieving high-quality agricultural drainage water treatment in rural agricultural development areas poses challenges for developing countries, influenced by various factors such as treatment costs. Currently, most agricultural areas in developing countries adopt low-cost drainage ditches and natural ponds, while developed countries employ bioreactors, large artificial ecological ponds, various types of drainage ditches, etc. It is believed that measures and methods for agricultural drainage water treatment in developing countries will become more enriched with the development of the economy and technology.

Supplementary Materials: The following supporting information can be downloaded at: <https://www.mdpi.com/article/10.3390/pr11102952/s1>, Table S1: Publications cited more than once; Table S2: Research topics.

Author Contributions: Conceptualization, C.W., Y.Z., L.Y. and T.H.; methodology, C.W., Y.Z. and T.H.; software, C.W. and Y.Z.; validation, C.W., Y.Z. and T.H.; formal analysis, C.W., Y.Z. and T.H.; investigation, C.W., Y.Z., L.-C.L., C.C.-O. and T.H.; resources, C.W. and Y.Z.; data curation, C.W. and Y.Z.; writing—original draft preparation, C.W. and Y.Z.; writing—review and editing, L.D., M.Z., M.L., L.-C.L., C.C.-O., L.Y. and T.H.; visualization, T.H.; supervision, L.Y. and T.H.; project administration, T.H.; funding acquisition, T.H. T.H. leads this research project and is the corresponding author of the paper. C.W. is the first author of the paper and Y.Z. is co-first author of the paper. C.W. and Y.Z. contributed equally to this work. All authors have read and agreed to the published version of the manuscript.

Funding: The Ningxia Hui Autonomous Region key research and development project: No.2021BEG02011; the National Natural Science Foundation of China: No. 41761102.

Data Availability Statement: The original data in this paper comes from Web of Science, and the analysis results are obtained by CiteSpace.

Conflicts of Interest: The authors declare no conflict of interest.

References

- Sethna, L.R.; Royer, T.V.; Speir, S.L.; Trentman, M.T.; Mahl, U.H.; Hagemeyer, L.P.; Tank, J.L. Silicon concentrations and stoichiometry in two agricultural watersheds: Implications for management and downstream water quality. *Biogeochemistry* **2022**, *159*, 265–282. [CrossRef]
- Mng'ong'o, M.; Munishi, L.K.; Blake, E.; Comber, S.; Hutchinson, T.H.; Ndakidemi, P.A. Towards sustainability: Threat of water quality degradation and eutrophication in Usangu agro-ecosystem Tanzania. *Mar. Pollut. Bull.* **2022**, *181*, 113909. [CrossRef]
- Grenon, G.; Singh, B.; De Sena, A.; Madramootoo, C.A.; von Sperber, C.; Kumar Goyal, M.; Zhang, T. Phosphorus fate, transport and management on subsurface drained agricultural organic soils: A review. *Environ. Res. Lett.* **2021**, *16*, 013004. [CrossRef]
- Mitchell, M.E.; Newcomer-Johnson, T.; Christensen, J.; Crumpton, W.; Richmond, S.; Dyson, B.; Canfield, T.J.; Helmers, M.; Lemke, D.; Lechtenberg, M.; et al. Potential of water quality wetlands to mitigate habitat losses from agricultural drainage modernization. *Sci. Total Environ.* **2022**, *838*, 156358. [CrossRef]
- Hay, C.H.; Reinhart, B.D.; Frankenberger, J.R.; Helmers, M.J.; Jia, X.; Nelson, K.A.; Youssef, M.A. Frontier: Drainage water recycling in the humid regions of the US: Challenges and opportunities. *Trans. Asabe* **2021**, *64*, 1095–1102. [CrossRef]
- Hakeem, K.R.; Sabir, M.; Ozturk, M.; Akhtar, M.S.; Ibrahim, F.H. Nitrate and Nitrogen Oxides: Sources, Health Effects and Their Remediation. *Rev. Environ. Contam. Toxicol.* **2017**, *242*, 183–217. [CrossRef]
- Daba, A.W.; Qureshi, A.S. Review of Soil Salinity and Sodicty Challenges to Crop Production in the Lowland Irrigated Areas of Ethiopia and Its Management Strategies. *Land* **2021**, *10*, 1377. [CrossRef]
- King, K.W.; Williams, M.R.; LaBarge, G.A.; Smith, D.R.; Reutter, J.M.; Duncan, E.W.; Pease, L.A. Addressing agricultural phosphorus loss in artificially drained landscapes with 4R nutrient management practices. *J. Soil Water Conserv.* **2018**, *73*, 35–47. [CrossRef]
- Williams, M.R.; King, K.W.; Duncan, E.W.; Pease, L.A.; Penn, C.J. Fertilizer placement and tillage effects on phosphorus concentration in leachate from fine-textured soils. *Soil Tillage Res.* **2018**, *178*, 130–138. [CrossRef]
- Stefani, D.; Bojie, F.; Lixin, W.; Pierre-André, J.; Wenwu, Z. Quantitative synthesis on the ecosystem services of cover crops. *Earth-Sci. Rev.* **2018**, *185*, 357–373. [CrossRef]
- Vymazal, J.; Brezinova, T.D. Removal of nutrients, organics and suspended solids in vegetated agricultural drainage ditch. *Ecol. Eng.* **2018**, *118*, 97–103. [CrossRef]
- Maxwell, B.M.; Birgand, F.; Schipper, L.A.; Christianson, L.E.; Tian, S.; Helmers, M.J.; Williams, D.J.; Chescheir, G.M.; Youssef, M.A. Drying–Rewetting Cycles Affect Nitrate Removal Rates in Woodchip Bioreactors. *J. Environ. Qual.* **2018**, *48*, 93–101. [CrossRef] [PubMed]
- Jaynes, D.B.; Isenhardt, T.M. Performance of Saturated Riparian Buffers in Iowa, USA. *J. Environ. Qual.* **2019**, *48*, 289–296. [CrossRef]
- Mander, L.; Tournebise, J.; Espenberg, M.; Chaumont, C.; Soosaar, K. High denitrification potential but low nitrous oxide emission in a constructed wetland treating nitrate-polluted agricultural run-off. *Sci. Total Environ.* **2021**, *779*, 146614. [CrossRef] [PubMed]
- Avila-Diaz, J.A.; Gonzalez-Marquez, L.C.; Longoria-Espinoza, R.M.; Ahumada-Cervantes, R.; Leyva-Morales, J.B.; Rodriguez-Gallegos, H.B. Chlorpyrifos and Dimethoate in Water and Sediments of Agricultural Drainage Ditches in Northern Sinaloa, Mexico. *Bull. Environ. Contam. Toxicol.* **2021**, *106*, 839–843. [CrossRef]
- Wu, J.; Zhang, Q.; Guo, C.; Li, Q.; Hu, Y.; Jiang, X.; Zhao, Y.; Wang, J.; Zhao, Q. Effects of Aeration on Pollution Load and Greenhouse Gas Emissions from Agricultural Drainage Ditches. *Water* **2022**, *14*, 3783. [CrossRef]
- Allred, B.; Martinez, L.; Khanal, S.; Sawyer, A.H.; Rouse, G. Subsurface drainage outlet detection in ditches and streams with UAV thermal infrared imagery: Preliminary research. *Agric. Water Manag.* **2022**, *271*, 107737. [CrossRef]

18. Collins, S.D.; Shukla, S.; Shrestha, N.K. Drainage ditches have sufficient adsorption capacity but inadequate residence time for phosphorus retention in the Everglades. *Ecol. Eng.* **2016**, *92*, 218–228. [CrossRef]
19. Faust, D.R.; Kroger, R.; Miranda, L.E.; Rush, S.A. Nitrate Removal from Agricultural Drainage Ditch Sediments with Amendments of Organic Carbon: Potential for an Innovative Best Management Practice. *Water Air Soil Pollut.* **2016**, *227*, 378. [CrossRef]
20. Iseyemi, O.O.; Farris, J.L.; Moore, M.T.; Choi, S.E. Nutrient Mitigation Efficiency in Agricultural Drainage Ditches: An Influence of Landscape Management. *Bull. Environ. Contam. Toxicol.* **2016**, *96*, 750–756. [CrossRef] [PubMed]
21. Zhang, S.; Feng, L.; Xiao, R.; Yong, L.; Wu, J. Effects of vegetation on ammonium removal and nitrous oxide emissions from pilot-scale drainage ditches. *Aquat. Bot.* **2016**, *130*, 37–44. [CrossRef]
22. Moeder, M.; Carranza-Diaz, O.; Lopez-Angulo, G.; Vega-Avina, R.; Chavez-Duran, F.A.; Jomaa, S.; Winkler, U.; Schrader, S.; Reemtsma, T.; Delgado-Vargas, F. Potential of vegetated ditches to manage organic pollutants derived from agricultural runoff and domestic sewage: A case study in Sinaloa (Mexico). *Sci. Total Environ.* **2017**, *598*, 1106–1115. [CrossRef] [PubMed]
23. Nifong, R.L.; Taylor, J.M. Vegetation and Residence Time Interact to Influence Metabolism and Net Nutrient Uptake in Experimental Agricultural Drainage Systems. *Water* **2021**, *13*, 1416. [CrossRef]
24. Moloantoa, K.M.; Khetsha, Z.P.; Van Heerden, E.; Castillo, J.C.; Cason, E.D. Nitrate Water Contamination from Industrial Activities and Complete Denitrification as a Remediation Option. *Water* **2022**, *14*, 799. [CrossRef]
25. Huang, Y.; Tao, B.; Zhu, X.; Yang, Y.; Liang, L.; Wang, L.; Jacinthe, P.-A.; Tian, H.; Ren, W. Conservation tillage increases corn and soybean water productivity across the Ohio River Basin. *Agric. Water Manag.* **2021**, *254*, 106962. [CrossRef]
26. Awad, A.; Wan, L.; El-Rawy, M.; Eltarabily, M.G. Proper predictions of the water fate in agricultural lands: Indispensable condition for better crop water requirements estimates. *Ain Shams Eng. J.* **2021**, *12*, 2435–2442. [CrossRef]
27. Chen, X.; Liu, Y. Visualization analysis of high-speed railway research based on CiteSpace. *Transp. Policy* **2020**, *85*, 1–17. [CrossRef]
28. Azam, A.; Ahmed, A.; Kamran, M.S.; Hai, L.; Zhang, Z.; Ali, A. Knowledge structuring for enhancing mechanical energy harvesting (MEH): An in-depth review from 2000 to 2020 using CiteSpace. *Renew. Sustain. Energy Rev.* **2021**, *150*, 111460. [CrossRef]
29. De Granda-Orive, J.I.; Alonso-Arroyo, A.; Roig-Vázquez, F. Which Data Base Should We Use for our Literature Analysis? Web of Science versus SCOPUS. *Arch. Bronconeumol.* **2011**, *47*, 213. [CrossRef] [PubMed]
30. Lasda Bergman, E.M. Finding Citations to Social Work Literature: The Relative Benefits of Using Web of Science, Scopus, or Google Scholar. *J. Acad. Librariansh.* **2012**, *38*, 370–379. [CrossRef]
31. Wang, Q.; Waltman, L. Large-scale analysis of the accuracy of the journal classification systems of Web of Science and Scopus. *J. Informetr.* **2016**, *10*, 347–364. [CrossRef]
32. Liu, Z.; Yin, Y.; Liu, W.; Dunford, M. Visualizing the intellectual structure and evolution of innovation systems research: A bibliometric analysis. *Scientometrics* **2015**, *103*, 135–158. [CrossRef]
33. Wang, X.; Zhang, Y.; Zhang, J.; Chenling, F.U.; Zhang, X. Progress in urban metabolism research and hotspot analysis based on CiteSpace analysis—ScienceDirect. *J. Clean. Prod.* **2020**, *281*, 125224. [CrossRef]
34. Jame, S.A.; Frankenberger, J.R.; Reinhart, B.D.; Bowling, L. Mapping agricultural drainage extent in the us corn belt: The value of multiple methods. *Appl. Eng. Agric.* **2022**, *38*, 917–930. [CrossRef]
35. Zhang, F.; Hou, J.; Miao, L.; Chen, J.; Xu, Y.; You, G.; Liu, S.; Ma, J. Chlorpyrifos and 3,5,6-trichloro-2-pyridinol degradation in zero valent iron coupled anaerobic system: Performances and mechanisms. *Chem. Eng. J.* **2018**, *353*, 254–263. [CrossRef]
36. Abdelhameed, R.M.; Taha, M.; Abdel-Gawad, H.; Mahdy, F.; Hegazi, B. Zeolitic imidazolate frameworks: Experimental and Molecular Simulation studies for efficient capture of pesticides from wastewater. *J. Environ. Chem. Eng.* **2019**, *7*, 103499. [CrossRef]
37. Ostovar, M.; Saberi, N.; Ghiassi, R. Selenium contamination in water; analytical and removal methods: A comprehensive review. *Sep. Sci. Technol.* **2022**, *57*, 2500–2520. [CrossRef]
38. Banuelos, G.S.; Placido, D.F.; Zhu, H.; Centofanti, T.; Zambrano, M.C.; Heinitz, C.; Lone, T.A.; McMahan, C.M. Guayule as an alternative crop for natural rubber production grown in B- and Se-laden soil in Central California. *Ind. Crops Prod.* **2022**, *189*, 115799. [CrossRef]
39. Zhang, Z.M.; Xiong, Y.; Chen, H.; Tang, Y.N. Understanding the composition and spatial distribution of biological selenate reduction products for potential selenium recovery. *Environ. Sci. Water Res. Technol.* **2020**, *6*, 2153–2163. [CrossRef]
40. Christianson, L.E.; Cooke, R.A.; Hay, C.H.; Helmers, M.J.; Feyereisen, G.W.; Ranaivoson, A.Z.; McMaine, J.T.; McDaniel, R.; Rosen, T.R.; Pfluer, W.T.; et al. Effectiveness of denitrifying bioreactors on water pollutant reduction from agricultural areas. *Trans. Asabe* **2021**, *64*, 641–658. [CrossRef]
41. Dal Ferro, N.; Ibrahim, H.M.S.; Borin, M. Newly-established free water-surface constructed wetland to treat agricultural waters in the low-lying Venetian plain: Performance on nitrogen and phosphorus removal. *Sci. Total Environ.* **2018**, *639*, 852–859. [CrossRef] [PubMed]
42. Tournebise, J.; Chaumont, C.; Mander, L. Implications for constructed wetlands to mitigate nitrate and pesticide pollution in agricultural drained watersheds. *Ecol. Eng.* **2016**, *103*, 415–425. [CrossRef]
43. Addy, K.; Gold, A.J.; Christianson, L.E.; David, M.B.; Schipper, L.A.; Ratigan, N.A. Denitrifying Bioreactors for Nitrate Removal: A Meta-Analysis. *J. Environ. Qual.* **2016**, *45*, 873–881. [CrossRef] [PubMed]
44. Hoover, N.L.; Bhandari, A.; Soupir, M.L.; Moorman, T.B. Woodchip Denitrification Bioreactors: Impact of Temperature and Hydraulic Retention Time on Nitrate Removal. *J. Environ. Qual.* **2016**, *45*, 803–812. [CrossRef]

45. Hassanpour, B.; Giri, S.; Puer, W.T.; Steenhuis, T.S.; Geohring, L.D. Seasonal performance of denitrifying bioreactors in the Northeastern United States: Field trials. *J. Environ. Manag.* **2017**, *202*, 242–253. [CrossRef] [PubMed]
46. Bock, E.; Smith, N.; Rogers, M.; Coleman, B.; Easton, Z.M. Enhanced Nitrate and Phosphate Removal in a Denitrifying Bioreactor with Biochar. *J. Environ. Qual.* **2014**, *44*, 605–613. [CrossRef] [PubMed]
47. Feyereisen, G.W.; Moorman, T.B.; Christianson, L.E.; Venterea, R.T.; Coulter, J.A.; Tschirner, U.W. Performance of Agricultural Residue Media in Laboratory Denitrifying Bioreactors at Low Temperatures. *J. Environ. Qual.* **2016**, *45*, 779–787. [CrossRef]
48. Hua, G.; Salo, M.W.; Schmit, C.G.; Hay, C.H. Nitrate and phosphate removal from agricultural subsurface drainage using laboratory woodchip bioreactors and recycled steel byproduct filters. *Water Res.* **2016**, *102*, 180–189. [CrossRef] [PubMed]
49. Kröger, R.; Holland, M.M.; Moore, M.T.; Cooper, C.M. Hydrological Variability and Agricultural Drainage Ditch Inorganic Nitrogen Reduction Capacity. *J. Environ. Qual.* **2007**, *36*, 1646–1652. [CrossRef] [PubMed]
50. Ghane, E.; Fausey, N.R.; Brown, L.C. Modeling nitrate removal in a denitrification bed. *Water Res.* **2015**, *71*, 294–305. [CrossRef] [PubMed]
51. David, M.B.; Gentry, L.E.; Cooke, R.A.; Herbstritt, S.M. Temperature and Substrate Control Woodchip Bioreactor Performance in Reducing Tile Nitrate Loads in East-Central Illinois. *J. Environ. Qual.* **2016**, *45*, 822–829. [CrossRef] [PubMed]
52. Lashani, E.; Moghimi, H.; Turner, R.J.; Amoozegar, M.A. Selenite bio-reduction by a consortium of halophilic/halotolerant bacteria and/or yeasts in saline media. *Environ. Pollut.* **2023**, *331*, 121948. [CrossRef]
53. Dos Santos, G.M.; Navarro-Pedreno, J.; Pastor, I.M.; Lucas, I.G.; Candel, M.B.A.; Zorpas, A.A. Agricultural drainage water characterization to determine the desalination possibilities for irrigation in a semi-arid environment. *Desalination Water Treat.* **2021**, *227*, 34–41. [CrossRef]
54. El Sayed, M.M.; Abulnour, A.M.G.; Tewfik, S.R.; Sorour, M.H.; Hani, H.A.; Shaalan, H.F. Reverse Osmosis Membrane Zero Liquid Discharge for Agriculture Drainage Water Desalination: Technical, Economic, and Environmental Assessment. *Membranes* **2022**, *12*, 923. [CrossRef] [PubMed]
55. Halaburka, B.J.; LeFevre, G.H.; Luthy, R.G. Quantifying the temperature dependence of nitrate reduction in woodchip bioreactors: Experimental and modeled results with applied case-study. *Environ. Sci. Water Res. Technol.* **2019**, *5*, 782–797. [CrossRef]
56. Wang, T.; Zhu, B.; Zhou, M. Ecological ditch system for nutrient removal of rural domestic sewage in the hilly area of the central Sichuan Basin, China. *J. Hydrol.* **2019**, *570*, 839–849. [CrossRef]
57. Vymazal, J.; Dvorakova Brezinova, T. Treatment of a small stream impacted by agricultural drainage in a semi-constructed wetland. *Sci. Total Environ.* **2018**, *643*, 52–62. [CrossRef]
58. Wang, C.; Xu, Y.; Hou, J.; Wang, P.; Zhang, F.; Zhou, Q.; You, G. Zero valent iron supported biological denitrification for farmland drainage treatments with low organic carbon: Performance and potential mechanisms. *Sci. Total Environ.* **2019**, *689*, 1044–1053. [CrossRef] [PubMed]
59. Faramarzmanesh, S.; Mashal, M.; Ebrahim Hashemi Garmdareh, S. Effect of saline drainage water on performance of denitrification bioreactors. *Water Supply* **2021**, *21*, 98–107. [CrossRef]
60. Law, J.Y.; Soupir, M.L.; Raman, D.R.; Moorman, T.B.; Ong, S.K. Electrical stimulation for enhanced denitrification in woodchip bioreactors: Opportunities and challenges. *Ecol. Eng.* **2018**, *110*, 38–47. [CrossRef]
61. Martin, E.R.; Godwin, I.A.; Cooper, R.I.; Aryal, N.; Reba, M.L.; Bouldin, J.L. Assessing the impact of vegetative cover within Northeast Arkansas agricultural ditches on sediment and nutrient loads. *Agric. Ecosyst. Environ.* **2021**, *320*, 107613. [CrossRef]
62. Liu, L.H.; Ouyang, W.; Liu, H.B.; Zhu, J.Q.; Fan, X.P.; Zhang, F.L.; Ma, Y.H.; Chen, J.R.; Hao, F.H.; Lian, Z.M. Drainage optimization of paddy field watershed for diffuse phosphorus pollution control and sustainable agricultural development. *Agric. Ecosyst. Environ.* **2021**, *308*, 107238. [CrossRef]
63. García, J.; Ortiz, A.; Álvarez, E.; Belohlav, V.; García-Galán, M.J.; Díez-Montero, R.; Álvarez, J.A.; Uggetti, E. Nutrient removal from agricultural run-off in demonstrative full scale tubular photobioreactors for microalgae growth. *Ecol. Eng.* **2018**, *120*, 513–521. [CrossRef]
64. Rahardianto, A.; Mccool, B.C.; Cohen, Y. Accelerated desupersaturation of reverse osmosis concentrate by chemically-enhanced seeded precipitation. *Desalination* **2010**, *264*, 256–267. [CrossRef]
65. Li, S.; Wu, M.; Jia, Z.H.; Luo, W.; Fei, L.J.; Li, J.S. Influence of different controlled drainage strategies on the water and salt environment of ditch wetland: A model-based study. *Soil Tillage Res.* **2021**, *208*, 104894. [CrossRef]

Disclaimer/Publisher’s Note: The statements, opinions and data contained in all publications are solely those of the individual author(s) and contributor(s) and not of MDPI and/or the editor(s). MDPI and/or the editor(s) disclaim responsibility for any injury to people or property resulting from any ideas, methods, instructions or products referred to in the content.

Article

Effects of Chlortetracycline on the Growth of Eggplant and Associated Rhizosphere Bacterial Communities

Lingling Li, Yuanyuan Xue, Hengsheng Wang and Yansong Chen *

School of Biology and Food Engineering, Hefei Normal University, Hefei 230601, China; lingiae@163.com (L.L.); m15556918072@163.com (Y.X.); wang_h_s@126.com (H.W.)

* Correspondence: otffss7531_cn@126.com

Abstract: The widespread use of tetracycline antibiotics in the poultry and cattle sectors endangers both human health and the terrestrial ecosystem. Chlortetracyclines (CTCs), in particular, have been proven to affect soil microorganisms in addition to plants in the terrestrial ecosystem. In order to assess the effects of CTC on soil properties, eggplant growth, and soil microorganisms, a potted experiment was carried out in this study. CTC significantly reduced the levels of ammonium nitrogen (NH_4^+-N) and nitrite nitrogen (NO_2^--N) in soil. Meanwhile, the eggplant's growth was clearly hampered. CTC dramatically and dose-dependently lowered the fluorescence parameters except the quantum yield of non-regulated energy dissipation (Φ_{NO}). *Rhodoplanes* and *Cupriavidus*, which were involved in N cycle, were enriched by 10 mg/kg CTC, according to results about different microorganisms at the genus level. *Flavisolibacter* was reduced by 10 and 50 mg/kg CTC, while *Methylosinus* and *Actinocorallia* were enriched by 250 mg/kg CTC. Redundancy analysis highlighted the profound impact of CTC on the soil microbial community, where strong correlations were observed with soil potential of hydrogen (pH), nitrate nitrogen (NO_3^--N), and NO_2^--N . These findings demonstrated the interdependence between the microbial community and soil characteristics, with CTC primarily affecting the microbes responsible for nitrogen cycling. Consequently, chlortetracycline poses potential hazards to both eggplant plants and the soil microbes in eggplant cultivation soil.

Keywords: chlortetracycline; plant growth; fluorescence parameters; microorganisms; nitrogen cycling

Citation: Li, L.; Xue, Y.; Wang, H.; Chen, Y. Effects of Chlortetracycline on the Growth of Eggplant and Associated Rhizosphere Bacterial Communities. *Sustainability* **2023**, *15*, 14593. <https://doi.org/10.3390/su151914593>

Academic Editors: Avelino Núñez-Delgado, Elza Bontempi, Yaoyu Zhou, Esperanza Alvarez-Rodriguez, Maria Victoria Lopez-Ramon, Marco Race, Zhien Zhang, Vanesa Santas-Miguel and Mario Coccia

Received: 31 August 2023

Revised: 25 September 2023

Accepted: 7 October 2023

Published: 8 October 2023



Copyright: © 2023 by the authors. Licensee MDPI, Basel, Switzerland. This article is an open access article distributed under the terms and conditions of the Creative Commons Attribution (CC BY) license (<https://creativecommons.org/licenses/by/4.0/>).

1. Introduction

Tetracycline (TC) antibiotics, one of the primary antibiotics groups, have been used extensively in human and animal medicine to treat and prevent disease as well as to increase growth rates in livestock and poultry industries [1]. The repeated and widespread use of TCs has led to their accumulation in aquatic and terrestrial environments, subsequently triggering detrimental secondary toxic effects on the non-target organisms [2]. Notably, extensive soil sampling across several provinces in China has revealed alarmingly high concentrations of TCs, with average levels ranging from 102 to 1687 $\mu\text{g}/\text{kg}$ [3]. One of the most prevalent TCs and frequently found in agricultural soils is chlortetracycline (CTC), which has a higher adsorption coefficient value (K_d) [4,5]. It has been reported that CTC concentrations ranged from 2.94 to 1590 $\mu\text{g}/\text{kg}$ in agriculture soil of China [3,6,7]. In 2001, 4.6–7.3 $\mu\text{g}/\text{kg}$ CTC were found in Northern Germany [8]. According to Lee et al., the predicted environmental concentrations of CTC in soil in the world were in a range of 3.42–67.59 $\mu\text{g}/\text{kg}$ soil, for a 90% confidence level [9]. Thus, China, in which the CTC concentration is higher, faces more severe CTC pollution.

In terrestrial environments, the accumulation of TCs can produce toxic effects on various components such as soil flora, fauna, and microorganisms [2,10,11]. Ma et al. [12] found soil nitrification potential and dehydrogenase activity was greatly stimulated after 28 days exposure of 30 mg/kg OTC. The soil microbial community serves as the foundation of soil ecological function and plays a vital role in soil nutrient cycling (such as carbon

and nitrogen), soil fertility enhancement, and promotion of plant diversity [13,14]. The introduction of TCs can create a selective pressure on bacteria, inducing antibiotic resistance and subsequently altering the soil microbial community structure and function [15,16]. Zheng et al. [17] found tetracycline has a concentration-dependent impact on the structure of soil bacterial community. OTC, one of TCs, also can significantly reduce the abundances of certain genera which is related to plant growth-promoting in soil, such as *Arthrobacter*, *Gemmatimonas*, and *Sphingomonas* [2]. The study by Han et al. [18] which focused on the effects of CTC on soil microbial community discovered that microbial functional diversity followed a suppression-recovery-stimulation pattern in CTC-treated manured soil.

In addition to destroying the microbial community in the soil environment, TCs pollution would also be absorbed and accumulated by edible plants and even affect the growth of vegetables, posing a threat to global food security and soil ecosystem function, which has attracted growing concerns [19,20]. It has been reported that TCs can prevent the growth of crops and vegetables, such as wheat, ginger, and *Ipomoea aquatica* Forsk [2,19,21]. The influence of TCs on edible plants is closely related to the frequent use of livestock and poultry manure. In vegetable planting regions, livestock and poultry manure are frequently utilized as fertilizer to increase productivity, promote green and low-carbon agriculture sustainable development, improve the rural ecological environment, and achieve the double carbon objective [22]. However, antibiotics are typical pollutants in livestock and poultry manure, and long-term manure application will inevitably introduce a considerable number of exogenous antibiotics into the soil, particularly vegetable-based soil [6,22,23]. TCs which were detected in high concentrations in vegetable-based soil can affect the growth of vegetables, and even be absorbed and accumulated by vegetables, posing a serious threat to vegetable security and soil ecological security [24–27]. Studies about the effects of CTC on vegetables and crops growth have demonstrated the above results. Cheong et al. [28] found that CTC diminished chlorophyll content in leaves and photosynthetic efficiency, and downregulated the genes involved in the primary root growth of *Brassica campestris* seedlings. Guo et al. [2] found that antibiotics' bactericidal capabilities significantly decreased the abundances of certain rhizobacteria, which had a negative influence on biomass and height of wheat seedling. Plant growth, development, and biomass accumulation are all influenced by soil microbes, particularly rhizosphere microorganisms [29–31]. Thus, to understand the impact of antibiotics on plant growth, it is critical to investigate the microbial community structure in soil.

Eggplant (*Solanum melongena*), a vegetable crop distributed worldwide, has considerable nutritional benefits due to its high concentration of vitamins, phenolics, and antioxidants [32]. The top producer and consumer of eggplant worldwide is China. However, little information regarding the responses of eggplant and rhizobacteria to CTC exposure is currently available. This study aimed to investigate the impacts of CTC on eggplant growth, relative chlorophyll content, fluorescence metrics, soil characteristics, and the soil microbial population by conducting a potted experiment with varying concentrations of CTC. This study can provide data support for the risk assessment of antibiotic residues in agriculture, so as to ensure the safety of crops and promote the sustainable development of agriculture.

2. Materials and Methods

2.1. Materials Collection

The eggplant seed (*Solanum melongena*) was purchased from seed market in Hefei, Anhui Province, China. The clean soil (0–15) cm was obtained from Hefei Normal University, nutritional soil was purchased from gardening market. Chlortetracycline (CTC, $\geq 97\%$) was purchased from Sigma-Adrich (St. Louis, MO, USA). Other chemicals were bought from Hefei Meifeng Chemical Co., Ltd. in Hefei, Anhui province, China.

2.2. Potted Experiment

The clean soil was air-dried, sieved to a diameter of 4 mm, and mixed with nutritional soil with 1:1 (*v/v*). Each pot was filled with 4 kg soils, and the moisture content of the soils was carefully regulated to reach 55% of their maximum water-holding capacity (WHC) with distilled water. CTC was dissolved in distilled water and then poured evenly into each pot to obtain the concentrations of 10.0 (L), 50.0 (M), and 250.0 (H) mg/kg CTC. There were three replicates for each treatment. The same amount of distilled water was added to the pot in 0 (CK) mg/kg CTC treatment.

Hydrogen peroxide (3%, *v/v*) was used to disinfect the seeds, and they were then thoroughly rinsed with sterile deionized water. In a climate chamber with a temperature of 25 °C and a humidity of 60%, the sterilized seeds were then placed in a tray, covered with gauze, and allowed to germinate. After germination, 12 uniform healthy eggplant seedlings were transplanted to the corresponding pots and planted for 70 days at a temperature of 25 °C with a cycle of 12 h of light and 10 h of darkness. Twice every week, distilled water was used to make up for water loss. After being in culture for 70 days, the eggplant and related rhizosphere soil were harvested. To gauge the growth traits, eggplants were gently removed from the pots. Each plant's rhizosphere soil was collected using the shake-off method [33,34]. The soil that was weakly holding on was gently shaken off and thrown away. The soil that was firmly clung to the eggplant roots (0–1 mm) was brushed off and recorded as rhizosphere soil. All samples were divided into two parts: one part was immediately stored at −80 °C for soil DNA extraction; the other part was used to measure soil properties as follows.

2.3. Measurement of Soil Properties

The soil was air dried, crushed, and screened through a 2 mm sifter to measure its properties after the visible organic remains had been eliminated. Soil pH (1:2.5 soil/water suspension) was determined using pH-25 (precision of 0.05, Leici., Shanghai, China) with the People's Republic of China's agricultural industry standard NY/T 1377-2007 as a guide [35]. The People's Republic of China's agricultural industry standard NY/T 1121.6-2006 was used to measure the content of soil organic matter (OM) by using standard solution titration of ferrous sulfate [36]. Following the National Environmental protection standards of the People's Republic of China HJ 634-2012, potassium chloride solution extraction-spectrophotometry was used to measure the ammonium nitrogen (NH_4^+-N), nitrite nitrogen (NO_2^--N), and nitrate nitrogen (NO_3^--N) in soil [37]. The levels of microbial biomass N in soil were measured by fumigation [38].

2.4. Measurement of Growth and Physiological Indexes

The Soil Plant Analysis Development (SPAD)-502 Plus (Konica Minolta, Tokyo, Japan) chlorophyll meter was used to determine the relative chlorophyll amount of leaf (represented as SPAD value). The measuring point was the center of the first fully unfolded leaf at the top of the plant, avoiding the apparent vein. The three readings' average values were calculated.

Junior—PAM (Walz, Effeltrich, Germany) based modulation fluorometer was used for the determination of chlorophyll fluorescence parameters. First, after exposing the measuring object to darkness for 30 min, the maximal photochemical efficiency of PS II (F_v/F_m) was determined. The kinetic parameters of chlorophyll fluorescence induction were then automatically measured under 190 $\mu\text{mol}/\text{m}^2/\text{s}$ of light intensity for 15 times using an artificial light source. The main components were electron transfer efficiency (ETR), photochemical quenching coefficient (qP), non-photochemical quenching coefficient (NPQ), quantum efficiency of Photosynthetic system II (Φ_{PSII}), quantum yield of regulated energy dissipation (Φ_{NPQ}), and quantum yield of non-regulated energy dissipation (Φ_{NO}).

After the above experiment, all plants were carefully dug up and labeled. First, the root soil was cleaned with distilled water, and then the root soil was cleaned with double

distilled water three times. The root parts were used to measure the fresh weight, and a steel ruler was used to measure the root's height from the base.

2.5. Soil Microbial Community Analysis

Total DNA extraction of soil samples from the three replicates in each treatment was carried out as follows: Total DNA were extracted using FastDNA Soil Kit (MP Biomedicals). The concentration and purity of the final soil DNA were measured by Nano-Drop 2000, a UV-vis spectrophotometer from NanoDrop Technologies, Wilmington, DE, USA. And the DNA quality was determined by 1% agarose gel electrophoresis. The 16S rRNA gene of bacteria was amplified using primers 515F (5'-GTGYCAGCMGCCGCGGTAA-3') and 806R (5'-GGACTACNVGGGTWTCTAAT-3') [39]. Before sequencing on an Illumina Miseq (Illumina, San Diego, CA, USA), the individual samples of the amplicons were first barcoded and then pooled to create the sequencing library. Mothur software (Version 1.35.1) was used to remove low-quality and chimeric reads from the raw sequencing data generated from Illumina Miseq. After quality filtration, all datasets were rarefied to 21,213 sequences to achieve same sequencing depth. High-quality readings were grouped into OTUs at a 97% identity level using the Quantitative Insights into Microbial Ecology (QIIME, version 1.9.1). The parallel_pick_open_reference_otus workflow script and the Greengenes 13.8 Database were both used to conduct OTU searches. The α -diversity indexes (Chao, ACE, Simpson, and Shannon) and Good's coverage were calculated by QIIME. To determine the β -diversity of the soil microbiota, principal component analysis (PCA) and unweighted pair group method with arithmetic mean (UPGMA) clustering were carried out. The Ribosomal Database Project (RDP) Classifier (<http://rdp.cme.msu.edu/>, accessed on 30 September 2016) was used to classify representative sequences from each OUT using an 80% confidence level.

2.6. Statistical Analysis

All data in this study are expressed as the mean \pm SD. Differences between the treatment groups and the control group with respect to growth indexes, physiological indexes, soil properties and α -diversity indexes were detected by ANOVA test followed by LSD multiple comparison using SPSS 21.0 software (SPSS Inc., Chicago, IL, USA). One-way PERMANOVA test by PAST was used to analyze the difference of bacterial community structure. Different microorganisms at genus compared with the control were detected by a *t*-test.

3. Results

3.1. Changes in Soil Properties

The physicochemical properties of eggplant cultivated soil were shown in Table 1. The ammonium nitrogen (NH_4^+ -N) and nitrite nitrogen (NO_2^- -N) were significantly decreased by CTC (Table 1). The content of NH_4^+ -N and NO_2^- -N in 250 mg/kg group were 48.33% and 67.27% lower than that in the control group, respectively. All CTC groups in this study showed lower nitrate nitrogen (NO_3^- -N) levels. In this study, microbial biomass nitrogen was increased by CTC with a dose-effect relationship.

Table 1. Physicochemical properties of soil samples treated with different CTC concentrations (n = 3).

CTC Content (mg/kg)	0	10	50	250
NH_4^+ -N (mg/kg)	5.09 \pm 0.41 a	3.44 \pm 0.21 b	2.36 \pm 0.27 c	2.63 \pm 0.45 c
NO_2^- -N (mg/kg)	9.32 \pm 3.53 a	9.47 \pm 4.25 a	5.53 \pm 1.35 ab	3.05 \pm 0.45 b
NO_3^- -N (mg/kg)	5.27 \pm 1.64 a	3.80 \pm 0.59 a	3.81 \pm 0.23 a	4.01 \pm 1.10 a
Microbial biomass N (mg/kg)	7.88 \pm 1.29 a	8.71 \pm 2.85 a	9.11 \pm 3.11 a	9.53 \pm 1.99 a
Organic matter (g/kg)	120.00 \pm 15.00 a	114.33 \pm 11.59 a	119.33 \pm 21.94 a	110.67 \pm 7.02 a
pH	6.18 \pm 0.08 a	6.27 \pm 0.05 a	6.16 \pm 0.05 a	6.26 \pm 0.13 a

Data are expressed as mean \pm SD (n = 3). Figures with different letters in the same line means significantly different at $p < 0.05$. CTC is chlortetracycline, NH_4^+ -N is ammonium nitrogen, NO_2^- -N is nitrite nitrogen, NO_3^- -N is nitrate nitrogen, and pH is the potential of hydrogen.

3.2. Effects of CTC on Eggplant Growth and Fluorescence Parameters

In this study, the growth of eggplant was inhibited by CTC-contaminated soil. As illustrated in Figure 1, the root fresh weight, root length and SPAD value in the CTC treatment groups demonstrated a concentration-dependent decrease with an increase in CTC dosage. Root fresh weight, root length, and SPAD value were all significantly ($p < 0.05$) decreased with the highest CTC treatment (250 mg/kg), by 38.58%, 63.49%, and 16.35%, respectively.

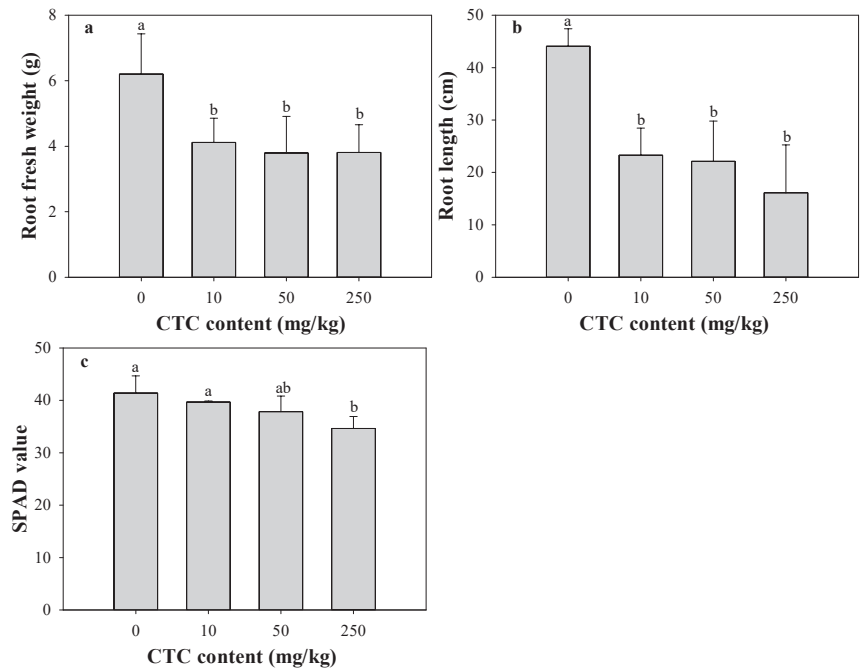


Figure 1. Effects of CTC on plant root fresh weight biomass (a), root length (b) and SPAD value (c) of eggplant. Data are expressed as mean \pm SD ($n = 3$). Data with different letters means significant difference at $p < 0.05$.

Table 2 showed that CTC posed a substantial impact on fluorescence parameters of eggplant. F_v/F_m value was decreased by 0.99 to 1.73% in the CTC groups, in which only 50 mg/kg group significantly decreased the F_v/F_m . The qP value was significantly decreased by CTC and decreased by 31.58% in the presence of 250 mg/kg CTC, indicating diminished electron transfer activity at PS II by CTC. The NPQ values rapidly declined with increasing CTC content and fell by 34.71% in the 250 mg/kg group, indicating heat dissipation performance of eggplant decreased. ETR and $\Phi_{PS II}$ were dramatically reduced by CTC treatments with a dose–effect relationship. The most important indexes of light protection and light damage are Φ_{NPQ} and Φ_{NO} , respectively. And in this study, the change in Φ_{NPQ} is small without significant difference. Φ_{NO} values increased significantly in the presence of CTC and increased by 42.86% in 250 mg/kg group.

Table 2. Chlorophyll fluorescence parameters of eggplants exposed to different CTC concentrations (n = 3).

CTC Content (mg/kg)	0	10	50	250
Fv/Fm	0.807 ± 0.002 a	0.796 ± 0.005 ab	0.793 ± 0.010 b	0.799 ± 0.006 ab
ETR	62.66 ± 3.92 a	54.49 ± 1.13 b	54.14 ± 4.22 b	45.66 ± 2.64 c
qP	0.57 ± 0.01 a	0.49 ± 0.02 b	0.48 ± 0.03 b	0.39 ± 0.02 c
NPQ	1.21 ± 0.17 a	1.01 ± 0.08 ab	0.88 ± 0.09 bc	0.79 ± 0.07 c
Φ _{PSII}	0.36 ± 0.02 a	0.31 ± 0.01 b	0.31 ± 0.02 b	0.26 ± 0.02 c
Φ _{NPQ}	0.37 ± 0.04 a	0.35 ± 0.02 a	0.34 ± 0.02 a	0.34 ± 0.02 a
Φ _{NO}	0.28 ± 0.02 c	0.34 ± 0.02 b	0.35 ± 0.01 b	0.40 ± 0.02 a

Data are expressed as mean ± SD (n = 3). Figures with different letters in the same line means significantly different at $p < 0.05$. CTC is chlortetracycline, Fv/Fm means the maximal photochemical efficiency of PS II, ETR means electron transfer efficiency, qP means photochemical quenching coefficient, NPQ means non-photochemical quenching coefficient, Φ_{PSII} means quantum efficiency of Photosynthetic system II, Φ_{NPQ} means quantum yield of regulated energy dissipation, and Φ_{NO} means quantum yield of non-regulated energy dissipation.

3.3. Effects of CTC on Soil Microorganism Communities

3.3.1. CTC Effects on Soil Microbial Diversity

High-throughput sequencing of the 16S rRNA gene amplicons convincingly demonstrated the alterations in the soil microbiota in response to the chronic CTC exposure. A total of 254,556 sequences were obtained from all samples. The sequences' rarefaction curves (Figure 2) revealed that enough sampling coverage was achieved for the soil samples.

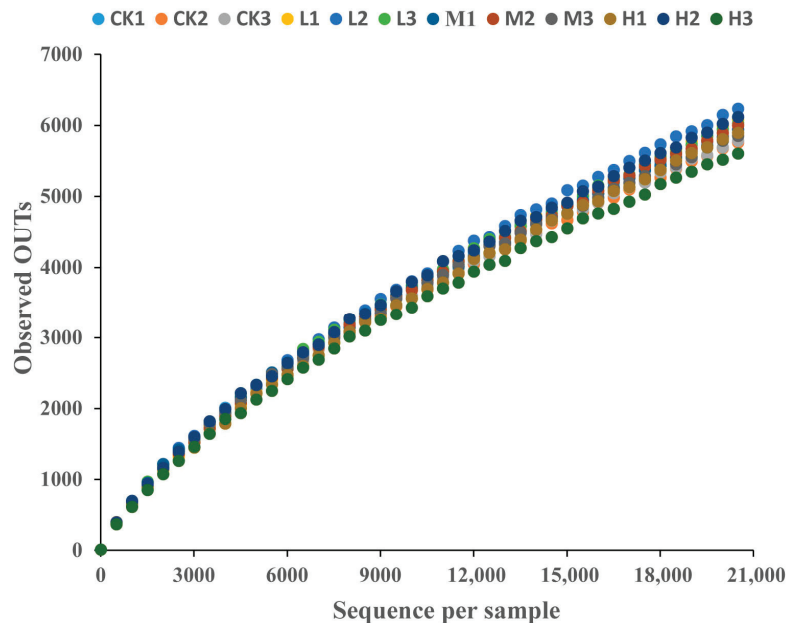


Figure 2. Rarefaction curve of soil microbial DNA samples under different concentrations of CTC. CK 1, 2 and 3 are the 3 replicated of 0 mg/kg CTC. L1, 2 and 3 are the 3 replicated of 10 mg/kg. M1, 2 and 3 are the 3 replicated of 50 mg/kg CTC. H1, 2 and 3 are the 3 replicated of 250 mg/kg CTC.

As shown in Table 3, the Good's coverage of each sample was greater than 80%. The observed OTUs in CTC groups were higher than those in control group. The community richness indexes Chao and ACE of soil microbiota were higher in CTC groups than those in the control group. Near parity existed in the community diversity indexes Simpson between the CTC groups and the control group. Table 3 indicated that CTC slightly

increased the community richness, but without significant differences and had no effect on the community diversity.

Table 3. Microbial α -diversities of soil samples treated with different CTC concentrations (n = 3).

CTC Content (mg/kg)	0	10	50	250
Chao	15,493.03 \pm 823.22 a	16,934.68 \pm 730.13 a	16,057.85 \pm 521.00 a	17,146.30 \pm 1462.67 a
Ace	15,826.9 \pm 502.09 a	17,650.74 \pm 987.84 a	16,577.00 \pm 503.5 a	17,576.4 \pm 921.40 a
Simpson	0.997 \pm 0.000 a	0.997 \pm 0.001 a	0.997 \pm 0.002 a	0.996 \pm 0.001 a
Observed_OTUs	5966.67 \pm 136.39 a	6253.33 \pm 112.83 a	6060.67 \pm 75.57 a	6007.67 \pm 253.25 a
Goods_coverage (%)	81.89 \pm 0.55 a	80.43 \pm 0.66 b	81.39 \pm 0.59 ab	80.95 \pm 0.90 ab

Data are expressed as mean \pm SD (n = 3). Data followed by different letters in the same line are significantly different at $p < 0.05$. CTC is chlortetracycline.

Figure 3 demonstrated that principal component (PC) 1 and 2 explained 68% of the total variance, with PC1 contributing 48.9%, showing that the first principal component was primarily responsible for the variations in microbes between control and CTC-treated soil. The PCA plot revealed that whereas soil samples from the CTC-treated groups displayed a more dispersed distribution, indicating some degree of variance, samples from the control group tended to be closely clustered, indicating a generally similar community makeup. The PCA plot in Figure 3 demonstrated that soil samples from several groups had a large difference in distribution distance, indicating that each group's microbial community composition varied greatly.

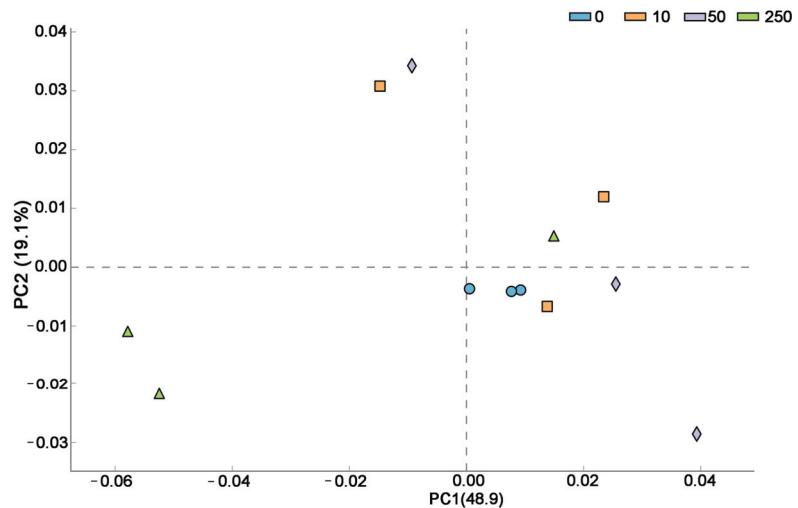


Figure 3. The soil microorganism community patterns (β -diversity) in the control and CTC-treated soils by PCA.

3.3.2. CTC Effects on Soil Microbial Composition

In all soil samples, the microbial composition revealed high variety. The microorganisms in all soil samples belonged to 48 phyla. *Proteobacteria* (39.9–47.6%) and *Actinobacteria* (18.6–21.8%) made up more than half of all bacterial phyla, making them the dominant phyla (Figure 4). Although the abundance of the detected phyla between the control and CTC-treated groups did not differ significantly according to the ANOVA test, microbes had a distinct pattern of change. Results demonstrated that all CTC treatments increased the relative abundance of *Proteobacteria*, but reduced the abundance of *Gemmatimonadetes* and *Cyanobacteria* with a dose-dependent relationship. In 250 mg/kg group, the relative abundance of *Bacteroidetes* was increased.

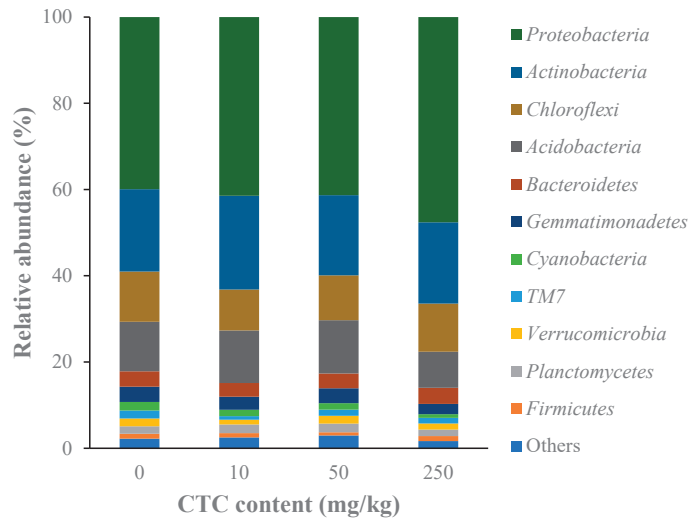


Figure 4. The relative abundances of microorganisms at the phylum level at different CTC treatments.

The chronic CTC exposure significantly ($p < 0.05$) altered the relative abundance of 11 genera (Figure 5). *Rhodoplanes* and *Cupriavidus* were enriched in 10 mg/kg CTC group indicating they may prefer low-dose CTC. *Methylosinus*, *Actinocorallia*, and *Sedimentibacter* were enriched in 250 mg/kg CTC group, indicating that high-dose CTC stimulated the growth of these genera. Compared with the control, the relative abundances of *Flavisolibacter* and *Ammoniphilus* were significantly reduced by 10 mg/kg CTC. The relative abundances of *Flavisolibacter*, *Segetibacter*, *Adhaeribacter*, and *Flavobacterium* were significantly reduced by 50 mg/kg CTC. A total of 250 mg/kg CTC significantly inhibited the growth of *Phycoccus*.

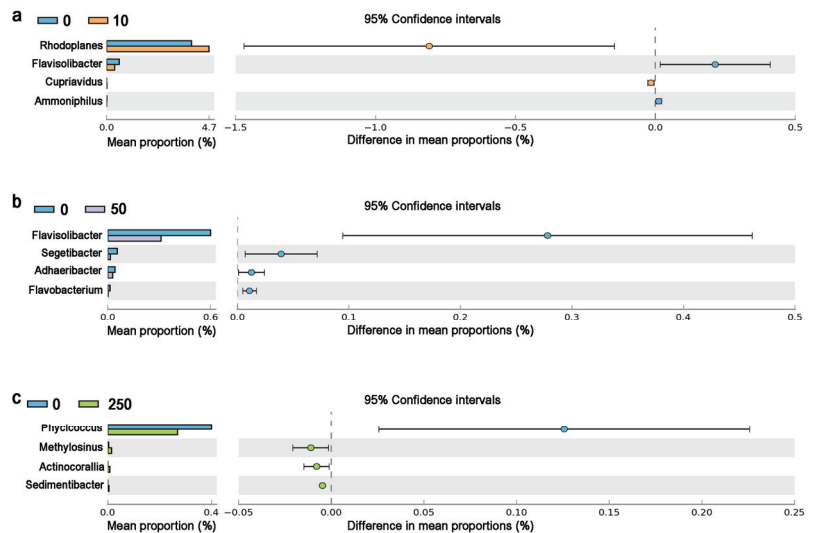


Figure 5. Relative abundance of significantly changed soil microbes at genus in CTC groups compared with the control. Notes: (a) represented the different genus between 10 mg/kg CTC and the control, (b) represented the different genus between 50 mg/kg CTC and the control, and (c) represented the different genus between 250 mg/kg CTC and the control.

3.4. Correlation between Each Indexes

Figure 6 shows the results of redundancy analysis (RDA) between the microbial communities and soil environment factors for the groups. Soil environmental factors had an overall explanation of 81.8% for the microorganism's community's differences. RDA1 and RDA2 had an overall explanation of 24.6%, with RDA 1 and RDA2 contributing 12.8% and 11.8%, respectively. As shown in Figure 6, CTC significantly influenced soil microbial community. Soil pH, NO_3^- -N and NO_2^- -N had strong correlation with the soil microbial community.

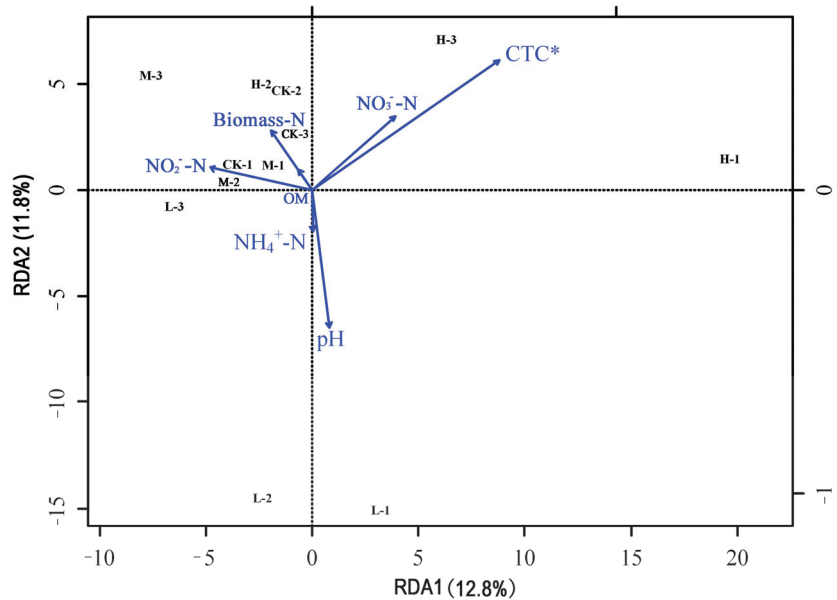


Figure 6. Redundancy analysis of soil microbial community and soil environmental factors. * represented CTC significantly influenced soil microbial community ($p < 0.05$).

To examine the interrelationships among different indexes, the correlation analysis (Pearson) was carried out in this study (Figure 7). The red and blue circles represented the positive and negative correlation between the two related indexes, respectively. And the size of the circles represented the absolute value of the correlation coefficient. As shown in Figure 7, there was some degree of correlation between CTC, soil characteristics, plant growth, fluorescence parameters, and soil bacteria, demonstrating that these variables were closely correlated. Root length had significant negative correlation with Φ_{NO} , positive correlation with ETR, qP, NPQ, Φ_{PSII} and NH_4^+ -N. In this study, *Rhodoplanes* demonstrated a positive correlation with *Methylosinus* and *Adhaeribacter*. *Actinocorallia* and *Sedimentibacter* exhibited a positive correlation. *Flavobacterium* exhibited a positive correlation with *Flavisolibacter* and *Segetibacter*.

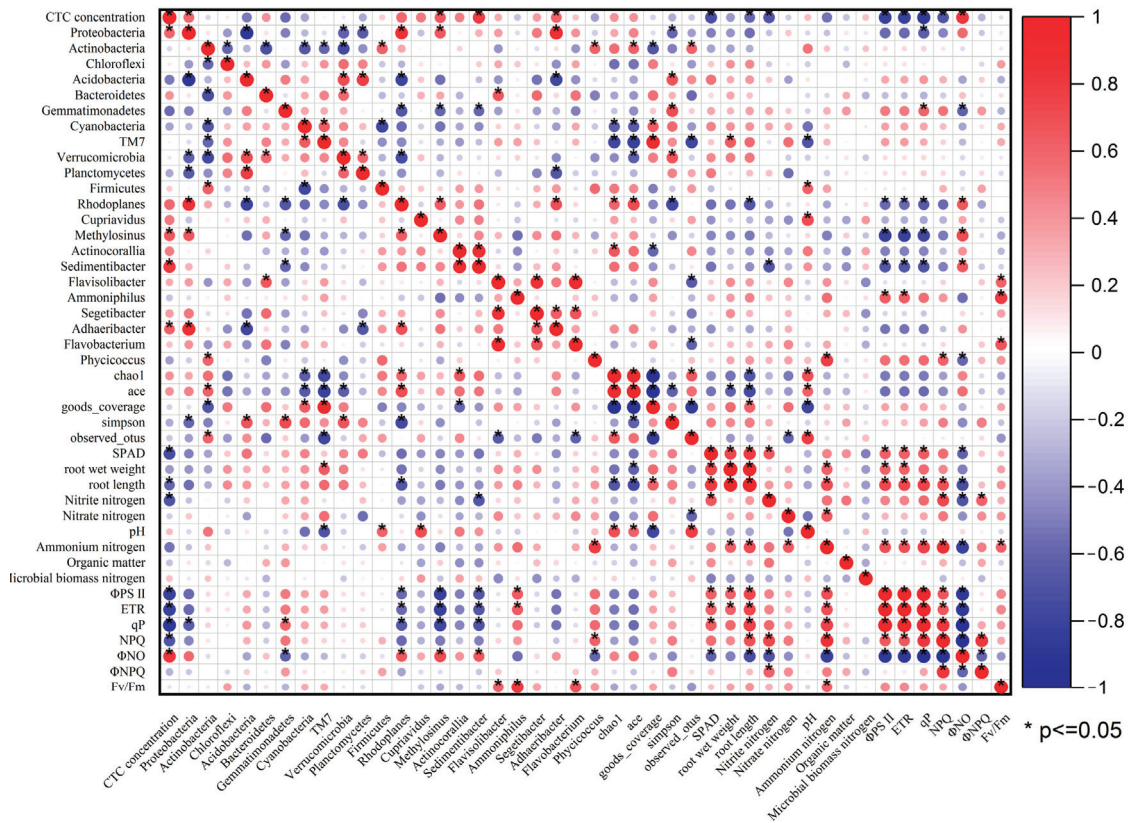


Figure 7. Heat map of Pearson correlation between all indexes in this experiment.

4. Discussion

Previous studies have demonstrated that $\text{NH}_4^+\text{-N}$ and $\text{NO}_3^-\text{-N}$ were the main forms of nitrogen absorbed and utilized by plants, and their content can influence plant growth and effectively indicate the nitrogen supply in soil [40]. In this study, the significant reduction in $\text{NH}_4^+\text{-N}$ and $\text{NO}_2^-\text{-N}$ by CTC may be related to the decline of azotification and nitrite bacteria activity. As a measure of soil nitrification capability, $\text{NO}_3^-\text{-N}$ concentration is much more sensitive to the presence of pharmaceuticals [41]. And due to high sensitivity of $\text{NO}_3^-\text{-N}$, all CTC groups showed lower nitrate nitrogen $\text{NO}_3^-\text{-N}$ levels. The inhibitory effects of CTC on soil nitrification capacity, which may be brought on by the inhibitory effects on nitrobacteria, are similar to previous studies on effects of pharmaceutical antibiotics on nitrification capacity [42–44].

Leaf SPAD observations which show the index of chlorophyll a and chlorophyll b in thylakoid membrane in the leaf mesophyll chloroplasts are collinearly correlated with leaf chlorophyll content for many crops [45]. CTC may be involved in the breakdown of chlorophyll by interacting with Mg^{2+} in the chlorophyll molecule and thus reduced chlorophyll content [46–48]. In this study, the root fresh weight, root length, and SPAD value in the CTC treatment groups all demonstrated a concentration-dependent decrease. This phenomenon of growth inhibition was supported by previous research on the impacts of CTC on the growth of maize and *Brassica campestris* [49,50]. According to the results in Table 1 and Figure 1, the inhibition of eggplant growth at CTC groups was thought to be related to the disturbance of chlorophyll fluorescence parameters, $\text{NH}_4^+\text{-N}$ and $\text{NO}_3^-\text{-N}$.

The maximal photochemical efficiency of PS II (Fv/Fm) was used to measure the efficiency of the primary conversion of light energy at the PS II reaction center [19,51,52]. In this study, the decrease in Fv/Fm in all CTC groups indicated that the eggplant suffered from severe stress of CTC. The photochemical quenching coefficient (qP) reflects the proportion of the light energy absorbed by the PS II antenna chlorophyll that is used in photochemical electron transfer, which can reflect the openness of PS II, and represents the electron transfer activity of PS II [19,53]. The qP value was significantly decreased by CTC, indicating diminished electron transfer activity at PS II by CTC. NPQ reflects the utilization of excitation energy in leaves and represents heat dissipation that defends against the destruction of photo inhibition, and is an important mechanism for plant protection of PS II [54]. The NPQ values rapidly declined with increasing CTC content, indicating heat dissipation performance of eggplant decreased. Both ETR and Φ_{PSII} serve as relative indicators of the electron transfer rate of plant leaves during photosynthesis and can reflect the actual photochemical reaction efficiency of plants in PS II [55]. In this study, ETR and Φ_{PSII} were dramatically reduced by CTC treatments with a dose–effect relationship, indicating that CTC exposure inhibited electron transport during photosynthesis. Φ_{NPQ} and Φ_{NO} are indexes of light protection and light damage, respectively. The values of Φ_{NPQ} were decreased but without significant difference, while the Φ_{NO} values increased significantly. The increase in Φ_{NO} indicated that there was a tendency of excess excitation energy to cause potential damage in CTC groups, and the photochemical energy conversion and protective regulated energy dissipation are not enough to coordinate the light energy absorption of photosynthetic apparatus [56,57]. The aforementioned findings demonstrated that with prolonged exposure to CTC, the photosynthetic system suffered serious damage, heat dissipation performance deteriorated, and reaction centers entered the closed state.

The community richness in this study was somewhat boosted by CTC, but there were no appreciable differences, and CTC had no impact on the community diversity. This phenomenon was also discovered in previous studies, which demonstrated that TCs had no significant effect or promotion effect on soil bacterial diversity, but had significant effect on different species at phyla and genera level [12,58]. In this study, all CTC groups increased the relative abundance of *Proteobacteria*, but reduced the abundance of *Gemmatimonadetes* and *Cyanobacteria*, and the highest CTC group increased the relative abundance of *Bacteroidetes*. The multiplication of *Proteobacteria* and *Bacteroidetes* suggested that they can tolerate the high dose of CTC. Similarly, Zhao et al. [59] indicated that the relative abundance of *Bacteroidetes* increased with the concentrations of antibiotic residues increased in typical greenhouse vegetable soils. Guo et al. [2] also revealed the reduction in *Gemmatimonadetes* after 150 mg/kg oxytetracycline treatment. *Cyanobacteria*, a sizable group of photosynthetic prokaryotes, play a significant role in the global CO₂ and N₂ fixation process [60]. Based on the results of previous studies, the reduction in *Cyanobacteria* would result in the reduction of nitrogen fixation and then the reduction in ammonium nitrogen content in this study.

According to a *t*-test examination of the microorganism differences between the control and CTC groups, *Rhodoplanes* and *Cupriavidus* were enriched in low-dose CTC group, and *Methylosinus* was enriched in the highest CTC group. *Rhodoplanes*, one of denitrifiers in soil, was affiliated with N cycling and involved in denitrification process [61,62]. *Cupriavidus* is highly resistant to heavy metals and can degrade toxic organic pollutants in soil to be benefit for plant growth [63,64]. Previous studies have found that *Cupriavidus* has the ability of heterotrophic nitrification and aerobic denitrification to remove ammonium, and nitrite [61]. These findings can explain the results that NH₄⁺-N and NO₃⁻-N were reduced at 10 mg/kg CTC group in this study. *Methylosinus* is a type II methane-oxidizing bacteria that reduces methane emissions, and participates in nitrogen oxide metabolism, and benefits the balance between nitrogen and methane cycling [65,66]. *Flavisolibacter* is one of plant growth promoting rhizobacteria, and its relative abundance was found to be negatively correlated with some stress, such as disease incidence [67]. The relative abundances of *Flavisolibacter* in this study were significantly reduced by 50 mg/kg CTC, explaining the

growth inhibition in this group. *Flavobacterium* is not only a kind of pathogenic bacteria, but also an important aerobic denitrifying bacteria, and has been proved to be related to NO_2^- -N and NO_3^- -N [68,69]. In this study, high-dose CTC reduced the *Flavobacterium* indicated that CTC could significantly inhibit the growth of this bacteria.

RDA analysis showed soil pH, NO_3^- -N, and NO_2^- -N had strong correlation with the soil microbial community. Soil pH and nutrients are closely related to the functional diversity of microbial community, since a large number of previous studies have proved that soil pH, organic carbon, and other nutrients have different degrees of influence on soil microorganisms [70,71]. Conversely, the change in soil microorganisms leads to the change in soil physical and chemical properties. Due to the complexity of the microbial community structure, it is unavoidable and reasonable for microbes to form a mutually facilitative or inhibitory relationship which is typically involves competition for resources and energy to help to determine the presence and relative abundance of species to some extent [72]. In this study, *Rhodoplanes* demonstrated a positive correlation with *Methylosinus* and *Adhaeribacter*. *Actinocorallia* and *Sedimentibacter* exhibited a positive correlation. *Flavobacterium* exhibited a positive correlation with *Flavisolibacter* and *Segetibacter*. These microbes play important roles in soil nutrient cycling and plant growth, and their positive correlation may be beneficial to improve the adaptability of plants under exogenous stress [62,66–69]. A heat map of the Pearson correlation demonstrated that soil pollutants, soil microorganisms, soil properties, and plant interact with and affect each other. However, due to the limited number of samples in our study, any correlation between these environmental factors and bacterial biodiversity requires further examination.

5. Conclusions

In this study, CTC treatment changed the soil properties and inhibited the growth of eggplant. The primary explanation may be the disruption of chlorophyll fluorescence parameters by CTC, particularly the light damage it causes. Additionally, varying doses of CTC disrupted the bacterial communities in the soil, particularly the rhizobacteria that promote plant growth and the bacterial communities that aid in denitrification. The mechanisms of CTC toxicity to eggplant should focus more on the metabolism of soil microbes and plant secretions. RDA showed CTC significantly influenced soil microbial community, and soil properties are closely related to the soil microbial community. Pearson correlation analysis demonstrated that CTC, soil microbes, soil nutrients, and the plant can interact with and affect each other. These results highlight the need for a thorough assessment of the dangers associated with tetracycline antibiotics and help us understand how they affect terrestrial ecosystems, to promote sustainable agricultural development. However, this study did not focus on the effects of CTC on the expression of plant-related resistance genes, and low-dose CTC exposure risk should be investigated in the future.

Author Contributions: Conceptualization, Y.C. and L.L.; methodology, Y.C., L.L. and Y.X.; software, H.W.; validation, Y.C. and L.L.; formal analysis, L.L.; investigation, Y.C.; resources, Y.X.; data curation, Y.C. and L.L.; writing—original draft preparation, L.L.; writing—review and editing, Y.C. and L.L.; visualization, L.L. and H.W.; supervision, Y.C.; project administration, Y.C. and L.L.; funding acquisition, Y.C. and L.L. All authors have read and agreed to the published version of the manuscript.

Funding: This research was funded by Anhui University Outstanding Top-of-the-line Talent Cultivation Project, grant number [NO. gxbjZD2021073], the Natural Science Foundation of Anhui Province, China, grant number [NO. 2008085QC103] and Hefei Normal University High-level Talents Research Start-up Fund, grant number [NO. 2020rcj49].

Institutional Review Board Statement: The study did not require ethical approval.

Informed Consent Statement: Not applicable.

Data Availability Statement: Not applicable.

Acknowledgments: Thanks to the suggestion of “State Key Laboratory of Pollution Control and Resource Reuse, School of the Environment, Nanjing University” during the whole experiment and

manuscript design. Thanks to the sequencing analysis of JiangSu ZhongYiJinDa Analytical & Testing Co., Ltd.

Conflicts of Interest: The authors declare no conflict of interest.

References

- Daghrir, R.; Drogui, P. Tetracycline antibiotics in the environment: A review. *Environ. Chem. Lett.* **2013**, *11*, 209–227. [CrossRef]
- Guo, A.; Pan, C.; Su, X.; Zhou, X.; Bao, Y. Combined effects of oxytetracycline and microplastic on wheat seedling growth and associated rhizosphere bacterial communities and soil metabolite profiles. *Environ. Pollut.* **2022**, *302*, 119046. [CrossRef] [PubMed]
- Lyu, J.; Yang, L.; Zhang, L.; Ye, B.; Wang, L. Antibiotics in soil and water in China—a systematic review and source analysis. *Environ. Pollut.* **2020**, *266*, 115147. [CrossRef] [PubMed]
- Patyra, E.; Kowalczyk, E.; Grelik, A.; Przeniosło-Siwczyńska, M.; Kwiatek, K. Screening method for the determination of tetracyclines and fluoroquinolones in animal drinking water by liquid chromatography with diode array detector. *Pol. J. Vet. Sci.* **2015**, *18*, 283–289. [CrossRef] [PubMed]
- Zhao, F.; Chen, L.; Yang, L.; Li, S.; Sun, L.; Yu, X. Distribution, dynamics and determinants of antibiotics in soils in a peri-urban area of Yangtze River Delta, Eastern China. *Chemosphere* **2018**, *211*, 261–270. [CrossRef] [PubMed]
- Wei, R.; He, T.; Zhang, S.; Zhu, L.; Shang, B.; Li, Z.; Wang, R. Occurrence of seventeen veterinary antibiotics and resistant bacteria in manure-fertilized vegetable farm soil in four provinces of China. *Chemosphere* **2019**, *215*, 234–240. [CrossRef]
- Pan, Z.; Yang, S.; Zhao, L.; Li, X.; Weng, L.; Sun, Y.; Li, Y. Temporal and spatial variability of antibiotics in agricultural soils from Huang-Huai-Hai Plain, northern China. *Chemosphere* **2021**, *272*, 129803. [CrossRef]
- Hamscher, G.; Sczesny, S.; Höper, H.; Nau, H. Determination of persistent tetracycline residues in soil fertilized with liquid manure by high-performance liquid chromatography with electrospray ionization tandem mass spectrometry. *Anal. Chem.* **2002**, *74*, 1509–1518. [CrossRef]
- Lee, C.; An, J.; Lee, Y.S.; Choi, K.; Kim, J.Y. Uncertainty-based concentration estimation of chlortetracycline antibiotics in swine farms and risk probability assessment for agricultural application of manure. *J. Hazard. Mater.* **2021**, *402*, 123763. [CrossRef]
- Jechalke, S.; Heuer, H.; Siemens, J.; Amelung, W.; Smalla, K. Fate and effects of veterinary antibiotics in soil. *Trends Microbiol.* **2014**, *22*, 536–545. [CrossRef]
- Ma, J.; Zhu, D.; Sheng, G.D.; O'Connor, P.; Zhu, Y.G. Soil oxytetracycline exposure alters the microbial community and enhances the abundance of antibiotic resistance genes in the gut of *Enchytraeus crypticus*. *Sci. Total Environ.* **2019**, *673*, 357–366. [CrossRef] [PubMed]
- Ma, T.T.; Pan, X.; Chen, L.K.; Liu, W.X.; Christie, P.; Luo, Y.M.; Wu, L.H. Effects of different concentrations and application frequencies of oxytetracycline on soil enzyme activities and microbial community diversity. *Eur. J. Soil Biol.* **2016**, *76*, 53–60. [CrossRef]
- Delgado-Baquerizo, M.; Grinyer, J.; Reich, P.B.; Singh, B.K. Relative importance of soil properties and microbial community for soil functionality: Insights from a microbial swap experiment. *Funct. Ecol.* **2016**, *30*, 1862–1873. [CrossRef]
- Delgado-Baquerizo, M.; Maestre, F.T.; Reich, P.B.; Jeffries, T.C.; Gaitan, J.J.; Encinar, D.; Berdugo, M.; Campbell, C.D.; Singh, B.K. Microbial diversity drives multifunctionality in terrestrial ecosystems. *Nat. Commun.* **2016**, *7*, 10541. [CrossRef]
- Chessa, L.; Pusino, A.; Garau, G.; Mangia, N.P.; Pinna, M.V. Soil microbial response to tetracycline in two different soils amended with cow manure. *Environ. Sci. Pollut. Res. Int.* **2016**, *23*, 5807–5817. [CrossRef] [PubMed]
- Xu, L.; Wang, W.; Xu, W. Effects of tetracycline antibiotics in chicken manure on soil microbes and antibiotic resistance genes (ARGs). *Environ. Geochem. Health* **2022**, *44*, 273–284. [CrossRef]
- Zheng, J.; Zhang, J.; Gao, L.; Kong, F.; Shen, G.; Wang, R.; Gao, J.; Zhang, J. The Effects of Tetracycline Residues on the Microbial Community Structure of Tobacco Soil in Pot Experiment. *Sci. Rep.* **2020**, *10*, 8804. [CrossRef]
- Han, L.; Zhang, H.; Long, Z.; Ge, Q.; Mei, J.; Yu, Y.; Fang, H. Exploring microbial community structure and biological function in manured soil during ten repeated treatments with chlortetracycline and ciprofloxacin. *Chemosphere* **2019**, *228*, 469–477. [CrossRef] [PubMed]
- Liu, X.; Lv, Y.; Xu, K.; Xiao, X.; Xi, B.; Lu, S. Response of ginger growth to a tetracycline-contaminated environment and residues of antibiotic and antibiotic resistance genes. *Chemosphere* **2018**, *201*, 137–143. [CrossRef] [PubMed]
- Geng, J.; Liu, X.; Wang, J.; Li, S. Accumulation and risk assessment of antibiotics in edible plants grown in contaminated farmlands: A review. *Sci. Total Environ.* **2022**, *853*, 158616. [CrossRef] [PubMed]
- Ma, T.; Chen, L.; Wu, L.; Christie, P.; Luo, Y. Toxicity of OTC to *Ipomoea aquatica* Forsk. and to microorganisms in a long-term sewage-irrigated farmland soil. *Environ. Sci. Pollut. Res. Int.* **2016**, *23*, 15101–15110. [CrossRef]
- Ding, D.; Huang, X.Y.; Gu, J.Y.; Chen, C.Y.; Long, X.X.; Zeng, Q.Y. Distribution Characteristics and Risk Assessment of Tetracycline Antibiotics (TCs) in Soil-Vegetable System with Soil Fertilized with Animal Manure. *Environ. Sci.* **2023**, *44*, 4440–4447. (In Chinese)
- Xiang, L.; Wu, X.L.; Jiang, Y.N.; Yan, Q.Y.; Li, Y.W.; Huang, X.P.; Cai, Q.Y.; Mo, C.H. Occurrence and risk assessment of tetracycline antibiotics in soil from organic vegetable farms in a subtropical city, south China. *Environ. Sci. Pollut. Res. Int.* **2016**, *23*, 13984–13995. [CrossRef] [PubMed]
- Pan, M.; Chu, L.M. Phytotoxicity of veterinary antibiotics to seed germination and root elongation of crops. *Ecotoxicol. Environ. Saf.* **2016**, *126*, 228–237. [CrossRef] [PubMed]

25. Zhou, X.; Wang, J.; Lu, C.; Liao, Q.; Gudda, F.O.; Ling, W. Antibiotics in animal manure and manure-based fertilizers: Occurrence and ecological risk assessment. *Chemosphere* **2020**, *255*, 127006. [CrossRef] [PubMed]
26. Sun, Y.; Guo, Y.; Shi, M.; Qiu, T.; Gao, M.; Tian, S.; Wang, X. Effect of antibiotic type and vegetable species on antibiotic accumulation in soil-vegetable system, soil microbiota, and resistance genes. *Chemosphere* **2021**, *263*, 128099. [CrossRef]
27. Wang, W.Z.; Chi, S.L.; Xu, W.H. Biological Effect of Tetracycline Antibiotics on a Soil-Lettuce System and Its Migration Degradation Characteristics. *Environ. Sci.* **2021**, *42*, 1545–1558. (In Chinese)
28. Cheong, M.S.; Choe, H.; Jeong, M.S.; Yoon, Y.E.; Jung, H.S.; Lee, Y.B. Different Inhibitory Effects of Erythromycin and Chlortetracycline on Early Growth of *Brassica campestris* Seedlings. *Antibiotics* **2021**, *10*, 1273. [CrossRef]
29. Grayston, S.J.; Wang, S.Q.; Campbell, C.D.; Anthony, C.E. Selective influence of plant species on microbial diversity in the rhizosphere. *Soil Biol. Biochem.* **1998**, *30*, 369–378. [CrossRef]
30. Lugtenberg, B.; Kamilova, F. Plant-growth-promoting rhizobacteria. *Annu. Rev. Microbiol.* **2009**, *63*, 541–556. [CrossRef]
31. Oleńska, E.; Małek, W.; Wójcik, M.; Swiecicka, I.; Thijs, S.; Vangronsveld, J. Beneficial features of plant growth-promoting rhizobacteria for improving plant growth and health in challenging conditions: A methodical review. *Sci. Total Environ.* **2020**, *743*, 140682. [CrossRef] [PubMed]
32. Gürbüz, N.; Uluişik, S.; Frary, A.; Doğanlar, S. Health benefits and bioactive compounds of eggplant. *Food Chem.* **2018**, *268*, 602–610. [CrossRef] [PubMed]
33. Riley, D.; Barber, S.A. Effect of ammonium and nitrate fertilization on phosphorus uptake as related to root-Induced pH changes at the root-soil interface. *Soil Sci. Soc. Amer. Proc.* **1971**, *35*, 301–306. [CrossRef]
34. Liu, F.; Mo, X.; Kong, W.; Song, Y. Soil bacterial diversity, structure, and function of *Suaeda salsa* in rhizosphere and non-rhizosphere soils in various habitats in the Yellow River Delta, China. *Sci. Total Environ.* **2020**, *740*, 140144. [CrossRef]
35. NY/T 1377-2007; Determination of pH in Soil. Ministry of Agriculture of the People's Republic of China. Standards Press of China: Beijing, China, 2007.
36. NY/T 1121.6-2006; Soil Testing Part 6: Method for Determination of Soil Organic Matter. Ministry of Agriculture of the People's Republic of China. Standards Press of China: Beijing, China, 2006.
37. HJ 634-2012; Soil-Determination of Ammonium, Nitrite and Nitrate by Extraction with Potassium Chloride Solution-Spectrophotometric Methods. Ministry of Environmental Protection of the People's Republic of China. China Environmental Press: Beijing, China, 2012.
38. Wu, J.S.; Lin, Q.M.; Huang, Q.Y.; Xiao, H.A. *Method for Calculating Soil Microbial Biomass and Its Application*; China Meteorological Press: Beijing, China, 2006; pp. 54–71.
39. Xue, Y.G.; Liu, F.; Zhou, L.L.; Jin, S.; Jiang, Y.; Wang, Y.C.; Jiang, X.D.; Wang, Q.; Shi, X.L.; Xue, K. Comparison study of bacterial community structure between groundwater and soil in industrial park based on high throughput sequencing. *Asian J. Ecotoxicol.* **2017**, *12*, 107–115. (In Chinese)
40. Mao, B.; Zeng, Y.; Lai, C.T.; Yang, Y.; Zhou, C.H.; Li, Z.T. Effects of nitrogen reduction fertilization on sugarcane biomass, soil nitrate nitrogen and ammonium nitrogen. *Chin. J. Ecol.* **2023**. Available online: <https://kns.cnki.net/kcms/detail/21.1148.q.20230303.1019.006.html> (accessed on 6 March 2023). (In Chinese)
41. Pashaei, R.; Zahedipour-Sheshglani, P.; Dzingelevičienė, R.; Abbasi, S.; Rees, R.M. Effects of pharmaceuticals on the nitrogen cycle in water and soil: A review. *Environ. Monit. Assess.* **2022**, *194*, 105. [CrossRef] [PubMed]
42. Chopra, I.; Roberts, M. Tetracycline antibiotics: Mode of action, applications, molecular biology, and epidemiology of bacterial resistance. *Microbiol. Mol. Biol. Rev.* **2001**, *65*, 232–260. [CrossRef] [PubMed]
43. Kotzerke, A.; Sharma, S.; Schauss, K.; Heuer, H.; Thiele-Bruhn, S.; Smalla, K.; Wilke, B.M.; Schloter, M. Alterations in soil microbial activity and N-transformation processes due to sulfadiazine loads in pig-manure. *Environ. Pollut.* **2008**, *153*, 315–322. [CrossRef]
44. Toth, J.D.; Feng, Y.C.; Dou, Z.X. Veterinary antibiotics at environmentally relevant concentrations inhibit soil iron reduction and nitrification. *Soil Biol. Biochem.* **2011**, *43*, 2470–2472. [CrossRef]
45. Yadava, U.L. A rapid and nondestructive method to determine chlorophyll in intact leaves. *Hortscience* **1986**, *21*, 1449–1500. [CrossRef]
46. Park, S.Y.; Yu, J.W.; Park, J.S.; Li, J.; Yoo, S.C.; Lee, N.Y.; Lee, S.K.; Jeong, S.W.; Seo, H.S.; Koh, H.J.; et al. The senescence-induced staygreen protein regulates chlorophyll degradation. *Plant Cell* **2007**, *19*, 1649–1664. [CrossRef]
47. Shimoda, Y.; Ito, H.; Tanaka, A. Arabidopsis STAY-GREEN, Mendel's Green Cotyledon Gene, Encodes Magnesium-Dechelataase. *Plant Cell* **2016**, *28*, 2147–2160. [CrossRef] [PubMed]
48. Rydzynski, D.; Piotrowicz-Cieślak, A.I.; Grajek, H.; Wasilewski, J. Investigation of chlorophyll degradation by tetracycline. *Chemosphere* **2019**, *229*, 409–417. [CrossRef] [PubMed]
49. Wen, B.; Liu, Y.; Wang, P.; Wu, T.; Zhang, S.; Shan, X.; Lu, J. Toxic effects of chlortetracycline on maize growth, reactive oxygen species generation and the antioxidant response. *J. Environ. Sci.* **2012**, *24*, 1099–1105. (In Chinese) [CrossRef] [PubMed]
50. Cheong, M.S.; Yoon, Y.E.; Kim, J.W.; Hong, Y.K.; Kim, S.C.; Lee, Y.B. Chlortetracycline inhibits seed germination and seedling growth in *Brassica campestris* by disrupting H₂O₂ signaling. *Appl. Biol. Chem.* **2020**, *63*, 1. [CrossRef]
51. Genty, B.; Briantais, J.M.; Baker, N.R. The relationship between the quantum yield of photosynthetic electron transport and quenching of chlorophyll fluorescence. *BBA-Gen. Subj.* **1989**, *990*, 87–92. [CrossRef]
52. Jägerbrand, A.K.; Kudo, G. Short-Term Responses in Maximum Quantum Yield of PSII (Fv/Fm) to ex situ Temperature Treatment of Populations of Bryophytes Originating from Different Sites in Hokkaido, Northern Japan. *Plants* **2016**, *5*, 22. [CrossRef]

53. Zhang, S.R. A discussion on Chlorophyll Fluorescence kinetics parameters and their significance. *Chin. Bull. Bot.* **1999**, *17*, 444–448.
54. Demmig-Adams, B.; Adams, W.W.I. Photoprotection and other responses of plants to high light stress. *Annu. Rev. Plant Physiol. Plant Mol. Biol.* **1992**, *43*, 599–626. [CrossRef]
55. Du, P.Z.; Liao, S.B.; Sun, B.; Chen, Y.; Luo, S.X.; Chen, L.; Huang, Y.F. Photosynthetic pigments and chlorophyll fluorescent characteristics of 17 provenances of *Banksia* seedlings. *J. Central South Univ. Forest. Technol.* **2014**, *34*, 49–54. (In Chinese)
56. Costa, E.S.; Bressan-Smith, R.; Oliveira, J.G.; Campostrini, E. Chlorophyll a fluorescence analysis in response to excitation irradiance in bean plants (*Phaseolus vulgaris* L. and *unguiculata* L. Walp) submitted to high temperature stress. *Photosynthetica* **2003**, *41*, 77–82. [CrossRef]
57. Shi, S.B.; Zhou, D.W.; Li, T.C.; De, K.J.; Gao, X.Z.; Ma, J.L.; Sun, T.; Wang, F.L. Responses of photosynthetic function of *Kobresia pygmaea* to simulated nocturnal low temperature on the Qingzang Plateau. *Chin. J. Plant Ecol.* **2023**, *47*, 361–373. (In Chinese) [CrossRef]
58. Liu, M.; Cao, J.; Wang, C. Bioremediation by earthworms on soil microbial diversity and partial nitrification processes in oxytetracycline-contaminated soil. *Ecotoxicol. Environ. Saf.* **2020**, *189*, 109996. [CrossRef]
59. Zhao, L.; Pan, Z.; Sun, B.; Sun, Y.; Weng, L.; Li, X.; Ye, H.; Ye, J.; Pan, X.; Zhou, B.; et al. Responses of soil microbial communities to concentration gradients of antibiotic residues in typical greenhouse vegetable soils. *Sci. Total Environ.* **2023**, *855*, 158587. [CrossRef]
60. Adams, D.G.; Duggan, P.S. Cyanobacteria-bryophyte symbioses. *J. Exp. Bot.* **2008**, *59*, 1047–1058. [CrossRef] [PubMed]
61. Sun, H.; Liu, F.; Xu, S.; Wu, S.; Zhuang, G.; Deng, Y.; Wu, J.; Zhuang, X. *Myriophyllum aquaticum* Constructed Wetland Effectively Removes Nitrogen in Swine Wastewater. *Front. Microbiol.* **2017**, *8*, 1932. [CrossRef] [PubMed]
62. Zhang, Z.; Chang, L.; Liu, X.; Wang, J.; Ge, X.; Cheng, J.; Xie, J.; Lin, Y.; Fu, Y.; Jiang, D.; et al. Rapeseed Domestication Affects the Diversity of Rhizosphere Microbiota. *Microorganisms* **2023**, *11*, 724. [CrossRef] [PubMed]
63. Espinoza, T.A.; Daghighi, M.; González, M.; Papacchini, M.; Franzetti, A.; Seeger, M. Toluene degradation by *Cupriavidus metallidurans* CH34 in nitrate-reducing conditions and in Bioelectrochemical Systems. *FEMS Microbiol. Lett.* **2018**, *365*, 4996784.
64. Bravo, G.; Vega-Celedón, P.; Gentina, J.C.; Seeger, M. Bioremediation by *Cupriavidus metallidurans* Strain MSR33 of Mercury-Polluted Agricultural Soil in a Rotary Drum Bioreactor and Its Effects on Nitrogen Cycle Microorganisms. *Microorganisms* **2020**, *8*, 1952. [CrossRef] [PubMed]
65. Stein, L.Y.; Klotz, M.G. Nitrifying and denitrifying pathways of methanotrophic bacteria. *Biochem. Soc. Trans.* **2011**, *39*, 1826–1831. [CrossRef]
66. Shinjo, R.; Oe, F.; Nakagawa, K.; Murase, J.; Asakawa, S.; Watanabe, T. Type-specific quantification of particulate methane monooxygenase gene of methane-oxidizing bacteria at the oxic-anoxic interface of a surface paddy soil by digital PCR. *Environ. Microbiol. Rep.* **2023**, *15*, 392–403. [CrossRef] [PubMed]
67. Tian, C.; Qiu, T.; Zhu, F.Y.; Xiao, J.L.; Wei, L.; Liang, Z.H. Calcium oxide regulation of fusarium wilt and rhizosphere bacterial community. *J. Hunan Agric. Univ. (Nat. Sci.)* **2018**, *44*, 620–624. (In Chinese)
68. Zhang, T.; Shao, M.F.; Ye, L. 454 pyrosequencing reveals bacterial diversity of activated sludge from 14 sewage treatment plants. *ISME J.* **2012**, *6*, 1137–1147. [CrossRef]
69. Zhu, J.S.; Qin, H.L.; Sun, Q.Y.; Wang, B.Z.; Gao, R.X.; Guo, R.L.; Li, W.B. Microbial Diversity and Influencing Factors in a Small Watershed in winter. *Environ. Sci.* **2020**, *41*, 5016–5026. (In Chinese)
70. Li, H.Y.; Yao, T.; Zhang, J.G.; Gao, Y.M.; Ma, Y.C.; Lu, Y.W.; Zhang, H.R.; Yang, X.L. Relationship between soil bacterial community and environmental factors in the degraded alpine grassland of eastern Qilian Mountains, China. *Chin. J. Appl. Ecol.* **2018**, *29*, 3793–3801. (In Chinese)
71. Guo, H.; Tang, W.P. Enzyme activity and microbial community diversity in rhizosphere and non-rhizosphere of *Larix principis-rupprechtii*. *Ecol. Environ. Sci.* **2020**, *29*, 2163–2170. (In Chinese)
72. Gilbert, J.A.; Steele, J.A.; Caporaso, J.G.; Steinbrück, L.; Reeder, J.; Temperton, B.; Huse, S.; McHardy, A.C.; Knight, R.; Joint, I.; et al. Defining seasonal marine microbial community dynamics. *ISME J.* **2012**, *6*, 298–308. [CrossRef]

Disclaimer/Publisher’s Note: The statements, opinions and data contained in all publications are solely those of the individual author(s) and contributor(s) and not of MDPI and/or the editor(s). MDPI and/or the editor(s) disclaim responsibility for any injury to people or property resulting from any ideas, methods, instructions or products referred to in the content.

Article

Examining the Relationship between Pro-Environmental Attitudes, Self-Determination, and Sustained Intention in Eco-Friendly Sports Participation: A Study on Plogging Participants

Jongho Kim ¹, Sujin Kim ² and Jinwook Chung ^{2,*}

¹ Department of Physical Education, Seoul National University, Seoul 08826, Republic of Korea; kikara77@snu.ac.kr

² Department of Sport Culture, Dongguk University, Seoul 04620, Republic of Korea; 03sujin27@gmail.com

* Correspondence: cjw826@dongguk.edu

Abstract: In response to rising environmental concerns and the increase in eco-friendly sports activities, this study investigated the determinants of sustained intention to participate in plogging, a combination of jogging and litter collection. A total of 288 randomly assigned plogging participants were surveyed to discern the effects of autonomy, competence, and relatedness experiences on sustained plogging intentions as suggested by self-determination theory. The study also examined the moderating role of eco-friendly attitudes. The analysis, executed using multi-group structural equation modeling, revealed that while autonomy and competence did not significantly influence extrinsic motivation, relatedness emerged as the most influential factor. This suggests that plogging primarily serves as a prosocial behavior, enhancing relationships, rather than a means to increase physical competence. The values derived from plogging and the intention to continue varied based on the participants' eco-friendly attitudes. The authors conclude that voluntary participation and socialization are the core values of plogging and understanding these can promote healthier and more sustainable behaviors.

Keywords: plogging; exercise participation; self-determination theory

Citation: Kim, J.; Kim, S.; Chung, J. Examining the Relationship between Pro-Environmental Attitudes, Self-Determination, and Sustained Intention in Eco-Friendly Sports Participation: A Study on Plogging Participants. *Sustainability* **2023**, *15*, 11806. <https://doi.org/10.3390/su151511806>

Academic Editors: Elza Bontempi, Marco Race, Maria Victoria Lopez-Ramon, Zhien Zhang, Avelino Núñez-Delgado, Yaoyu Zhou, Mario Coccia, Vanesa Santas-Miguel and Esperanza Alvarez-Rodriguez

Received: 23 June 2023

Revised: 20 July 2023

Accepted: 20 July 2023

Published: 1 August 2023



Copyright: © 2023 by the authors. Licensee MDPI, Basel, Switzerland. This article is an open access article distributed under the terms and conditions of the Creative Commons Attribution (CC BY) license (<https://creativecommons.org/licenses/by/4.0/>).

1. Introduction

Global environmental issues such as global warming, food and water scarcity, and energy depletion have been highlighted as critical challenges that need to be addressed [1]. In this context, the growing awareness among many members of society regarding the impact of their actions on the planet has resulted in the emergence of significant societal agendas, exemplified by terms such as 'environment', 'eco-friendly', 'sustainability', and 'green' [2]. For instance, the United Nations announced the 'Sustainable Development Goals', urging environmentally friendly actions (United Nations, 2015). Many large corporations appeal to consumers through green marketing strategies using environmental, social, and governance (ESG) management [3,4]. From this perspective, mature consumers are demonstrating a tendency towards 'pro-environmental behavior', considering both environmental protection and consumption behavior [5]. This phenomenon is spreading across various fields, adjusting human lifestyles in diverse ways.

The tendency towards eco-friendly sports is also evident in sports consumption and participation behaviors [6]. Notable examples include the organization of eco-friendly sports events, the promotion of eco-friendly ideologies through sports, and the development and expansion of eco-friendly sports initiatives [6]. One such eco-friendly sport is plogging, which originated in Sweden and involves combining jogging with the act of picking up discarded litter. Plogging serves as a volunteer activity for environmental protection while also promoting individual health and well-being [7–9]. The engagement of individuals in these activities demonstrates their active participation in environmental

preservation [7–9]. Moreover, these eco-friendly sports contribute to personal life satisfaction, the formation of self-identity, and overall happiness, as they simultaneously prioritize individual health and well-being along with environmental protection campaigns [10]. Previous research has highlighted the positive impact of participating in eco-friendly sports on personal life satisfaction, competence development, and physical fitness [7–9,11].

However, encouraging the intention for sustained participation in eco-friendly sports behavior, which is a serious leisure activity, is challenging as it cannot easily be carried out through regulatory measures or economic incentives [12]. For the positive social spread of eco-friendly sports and the personal life satisfaction and well-being of its participants to operate smoothly, it is necessary to understand how to induce intention for sustained participation [13–15]. In general, previous studies analyzing various socio-psychological factors that influence the intention for sustained participation in sports or physical activities primarily suggest that it occurs through the satisfaction of basic psychological needs and the formation of motivation, as suggested by the ‘Self-Determination Theory’ [16–19]. However, eco-friendly sports are both physical activities for promoting physical health and volunteer activities for conserving nature, so it is necessary to understand eco-friendly behavior in addition to the theory related to sports participation. In particular, studies related to the intention for the sustained participation of volunteers commonly suggest the importance of voluntary participation motivation using the public service motivation theory and report that the formation of eco-friendly attitudes has a significant influence on the formation of voluntary participation motivation [12,20]. Therefore, to encourage and promote participation in eco-friendly sports, it is necessary to theoretically approach it from a convergent perspective by considering the variables suggested in the research analyzing the psychological motivation of sports participation and the variables explaining the motivation of eco-friendly behavior participation.

Therefore, the study objective is to explore and analyze strategies for enhancing the sustained participation intention of eco-friendly sports participants. This will be achieved by concurrently examining the variables associated with sports participation and eco-friendly behavior. Specifically, for this purpose, we analyzed how the factors and motivations involved in the intention for sustained participation, suggested by the self-determination theory, and eco-friendly attitudes that affect eco-friendly behavior, influence the continuous participation intention by targeting the participants of plogging, a representative eco-friendly sport. Through this, we aim to provide useful information for writing effective participation promotion strategies by understanding the fundamental psychological processes of eco-friendly sports participants, which can help in both aspects of personal well-being and environmental protection. This eco-friendly sports study is meaningful in that it applies existing theories to new research subjects, thereby broadening the base of related disciplines, and attempts a multidisciplinary theoretical exploration in that it considers the concepts of sports and volunteering simultaneously.

2. Theoretical Background and Research Hypotheses

2.1. Eco-Friendly Sports: Plogging

Eco-friendly sports encompass different forms of sports consumption, events, and participatory activities that prioritize environmental protection and sustainability [21–24]. Eco-friendly sports, which aim to respect and protect the natural environment, conserve resources, and promote environmental education and eco-friendly awareness, are currently being implemented in various ways. Examples include incorporating environmental values into existing sports events and combining eco-friendly activities with sports. Efforts were made at the 2020 Tokyo Olympics to build temporary facilities using recyclable materials and to form an eco-friendly power supply network by installing solar power generation systems and renewable energy power plants. A pre-event called ‘spogomi’, a competition to pick up as much trash as possible in a limited time, was also held, and encouraged participation by demonstrating the positive social impact of eco-friendly sports [7]. Previous studies on eco-friendly sports have mainly focused on the production

of sports goods [23,25], the importance of hosting eco-friendly sports events [22], and the importance of the ESG management concept in sports [26,27].

Meanwhile, as interest in participatory eco-friendly sports has increased, studies related to the meaning and uniqueness of participation experience and motivation in eco-friendly sports have also been actively conducted. Participatory eco-friendly sports are highlighted as important activities that not only increase physical activity and maintain healthy lifestyle habits, but also play a positive role in stress relief and enhancing life satisfaction at the personal level [9,28]. Participation in eco-friendly sports provides mental rest through communion with nature, and it is reported that positive emotions such as ‘Helper’s High’ can be felt through altruistic volunteer activities [8,11]. Previous studies commonly reported that there was also an effect of strengthening bonds with others through the sharing of positive behaviors, and at the social level, it contributed to the improvement of the natural environment in the local community and the formation of social networks through the sharing of sports activities.

These eco-friendly sports are showing a trend of spreading mainly among the younger generation. A representative example is plogging, where many people around the world participate in picking up trash while jogging [7,11]. Previous studies conducted on plogging, where the attributes of an environmental protection campaign and exercise activities are combined, reported participation experiences and participation motivations in the special context of eco-friendly sports [8,29,30]. Raghavan, Panicker and Emmatty [11] suggested that plogging had a significant impact on aerobic exercise effects through jogging, as well as anaerobic lower body strength enhancement through squatting movements while picking up trash. Chae and Kim [9] reported that the participation efficacy of ploggers was influenced by the altruistic motivation of environmental protection, the motivation for self-development through sports activities, and the external motivation to enhance relationships with others, and that participating in a special form of eco-friendly sport that benefits others through their efforts played a positive role in personal values such as self-satisfaction. In addition, Yoon et al. [7] conducted in-depth interviews and reported that people who participated in plogging were aware of the seriousness of environmental pollution and had the will to execute environmental protection behaviors in their daily lives. Furthermore, they increased their intention for sustained participation through self-satisfaction and the fulfillment of the need for recognition through interaction with others. In conclusion, when synthesizing the results of these previous studies, it can be confirmed that plogging, which is a representative activity where the attributes of sports and volunteer activities are combined, acts as a producer of a sports culture that solves environmental problems through the act of sports itself, and participants acquire physical health and self-respect through the plogging experience. Many studies suggested the need for verification of social psychological variables to encourage special participation motivation and continuous participation in eco-friendly sports.

2.2. Factors Influencing the Intention of Sustained Participation in Environmental Sports: Application of Self-Determination Theory

As previously discussed, plogging, as a fitness activity and an environmental action, offers various benefits to individuals and society. Therefore, it is not only necessary for a large number of people to recognize and participate in the benefits of environmental sports, but it is also important to enhance the sustained participation intention of those who have experienced participation. This study aims to investigate the social and psychological factors necessary to promote and encourage sustained sports participation. For this purpose, we set up hypotheses about the factors influencing sustained participation intention and their relationships, focusing on the ‘Self-Determination Theory’ which has often been used in previous studies related to the intention of sustained sports or exercise participation.

Self-determination theory is a psychological theory proposed by Ryan and Deci [17,31] that explains human behavior motivation, and is often used to deeply analyze and explain the sustained participation motivation of exercise participants [32,33]. According to Ryan and

Deci [17], humans have a fundamental tendency to pursue psychological need satisfaction, and intrapersonal motivation which supports this need satisfaction influences sustained participation intention, performance, pleasure, etc. Specifically, the self-determination theory presents a human's basic psychological needs as autonomy, competence, and relatedness. Furthermore, Vallerand [34] conveyed through an integrated model that the satisfaction or expectation of the three basic psychological needs stimulates the voluntary behavior will of intrinsic and extrinsic motivation that occurs according to rewards or punishments. In addition, this intrinsic and extrinsic motivation plays a positive role in sustained behavior intention. According to the results of past research mainly conducted in sports psychology, an individual's intrinsic motivation makes them recognize exercise behavior itself as a purpose, which influences sustained exercise performance behavior [35,36]. Furthermore, the results show that life sports participants increase their intrinsic and extrinsic motivation through the satisfaction of self-determination factors, thereby increasing their participation and sustained intention [37,38]. Given the context, this study considers eco-friendly sports as a form of exercise and physical activity. We then formulated our research hypotheses by applying the self-determination theory's framework, which suggests a relationship between the three fundamental psychological needs, intrinsic and extrinsic motivation, and the intention for sustained participation, to the behavioral intentions of eco-friendly sports participants.

Firstly, the need for autonomy refers to the basic human psychological desire to feel that the control of their actions lies within themselves, to consider themselves as the regulators of their own lives, and to act as they wish [17]. Participants in sports or physical activities feel autonomy when they choose to participate because they like it, forming a sense of responsibility for their own choices. This sense of responsibility acts as intrinsic motivation in itself, while also functioning as extrinsic motivation by forming a psychological reward and punishment system. Numerous studies have been modeling the role of motivation that mediates the relationship between the satisfaction of basic psychological needs and the intention to continue exercising and have been verifying it in various environments [19,32,33]. In particular, plogging is very important as a voluntary action because it is both healthy exercise and an altruistic environmental action. Therefore, the degree of satisfaction with the need for autonomy, as perceived through plogging participation, is predicted to have a positive impact on the intrinsic and extrinsic motivation of plogging participation, thereby influencing continuous exercise participation.

Hypothesis 1. *The degree of autonomy experienced through plogging participation has a positive (+) impact on intrinsic/extrinsic motivation.*

Hypothesis 2. *The degree of autonomy experienced through plogging participation has a positive (+) impact on the intention to continue plogging participation.*

Hypothesis 3. *Intrinsic/extrinsic motivation mediates the relationship between the experience of autonomy through plogging participation and the intention to continue participation.*

Secondly, competence is a psychological need that is satisfied when an individual's abilities, skills, and talents are appropriately exercised in a specific environment [17]. The desire for competence creates the optimal conditions for demonstrating abilities, and plays a positive role in efforts to maintain and develop skills and abilities through specific activities [17]. In the context of sports, it has been reported that it plays an important role in stimulating intrinsic and extrinsic motivation for continuous training participation for health promotion or sports skill development [39–41]. These research results suggest that a sense of competence positively influences an individual's intrinsic motivation to feel confidence and efficiency, along with extrinsic rewards for acquiring sports skills and exercise abilities. Other previous research has shown that if the desire for competence is not satisfied due to failure to promote self-regulation or achieve goals in the context of sports participation, it can have a negative impact on intrinsic motivation.

Hypothesis 4. *The degree of competence experienced through plogging participation has a positive (+) impact on intrinsic/extrinsic motivation.*

Hypothesis 5. *The degree of autonomy experienced through plogging participation has a positive (+) effect on the sustainability of participation.*

Hypothesis 6. *Intrinsic/extrinsic motivation mediates the relationship between the experience of autonomy through plogging participation and the sustainability of participation.*

Thirdly, the need for relatedness refers to the desire to feel a sense of belonging and connection with others and to give and receive attention [17]. Relatedness is a fundamental psychological need that is associated with human attachment, which plays a crucial role in maintaining motivation and is particularly important in participating in activities [17,41]. The need for relatedness strengthens intrinsic and extrinsic motivation through stable relationships with meaningful others. From this perspective, numerous studies report that the establishment of stable relationships through interaction with others in exercise or sports activity participation situations has a positive impact on the intention to continue participating in exercise [39–41]. In Korea, plogging activities often take the form of a group of people jogging while picking up trash. Also, SNS posts about plogging activities play a positive role in exposing a positive self-image to others, which is a positive activity in satisfying the need for relatedness.

Hypothesis 7. *The degree of relatedness experienced through plogging participation has a positive (+) effect on intrinsic/extrinsic motivation.*

Hypothesis 8. *The degree of relatedness experienced through plogging participation has a positive (+) effect on the sustainability of participation.*

Hypothesis 9. *Intrinsic/extrinsic motivation mediates the relationship between the experience of relatedness through plogging participation and the sustainability of participation.*

2.3. An Eco-Friendly Environmental Attitude and Plogging Participation

As environmental issues have been set as a significant social agenda, the fact that individuals' daily behaviors collectively cause environmental pollution has become widely known, so consumers' socially responsible behaviors and pro-environmental (eco-friendly) consumption habits have begun to take root [42]. Karp [43] defined such socially responsible consumption behavior as self-transcendent behavior that contributes to the welfare of society as a whole rather than individual benefits, and many scholars have conceptualized eco-friendly environmental attitudes and primarily applied them to consumer behavior analysis research [44,45].

Specifically, environmental attitudes refer to an individual's beliefs or values about the environment and the importance of environmental protection [46,47], and many studies related to the execution of eco-friendly behavior commonly suggested that people with high eco-friendly attitudes were more likely to promote decision-making behavior when choosing products or services with environmentally friendly elements compared to people with low eco-friendly environmental attitudes [44,45]. Seo Mun-sik, Eom Sung-won, Son Eun-ji [48] reported that self-determination for pro-environmental consumption was important for consumers of general products to engage in continuous eco-friendly environmental consumption behavior, and that self-determination was regulated according to pro-environmental attitudes.

Plogging participants can be considered a type of consumer who has chosen and participated in plogging, an environmentally friendly sport, among various sports and exercise types. In other words, if plogging is considered a kind of environmentally friendly sports product, then the participants have made various considerations and invested

time and effort to execute participatory consumption. In addition, the satisfaction of basic psychological needs that are obtained in this process, together with the stimulation of motivation, affect the intention to participate continuously. In this case, participants with high pro-environmental attitudes are expected to have high self-determination for pro-environmental consumption, and accordingly, the entire decision-making process is strengthened, and the intention to participate continuously is higher. For example, individuals with high pro-environmental attitudes are likely to believe that the degree to which they feel connected to the environment and the community is strong, and that the stable relationship formation with others through plogging participation can be further strengthened through environmental protection activities. In other words, people with high pro-environmental attitudes can be expected to have a stronger intention to continue plogging participation, through the satisfaction of the need for relatedness conveyed by participation experience, than those with low attitudes.

3. Research Method

3.1. Data Collection

The study aimed to analyze the relationship between the sustained participation intention of plogging participants and the motivational factors mediating self-determination, and to further examine whether this model varies according to the level of formation of eco-friendly attitudes.

For this purpose, we surveyed plogging participants residing nationwide in South Korea using a purposive sampling method, one of the non-probability sampling methods. To collect plogging participants, we selected plogging-related clubs, related organizations, and universities, and conducted online/offline surveys targeting participants who expressed their willingness to participate in the research.

3.2. Survey Tools: Measurement Variables

Respondents completed the survey using a self-administration method. To measure the sustained participation intention of participants with plogging activity experience and the factors influencing it, we adapted measurement tools presented in previous studies to suit this study. All independent variables, including three sub-variables of individual psychological needs factors presented in the self-determination theory (autonomy, competence, and relatedness), and eco-friendly attitudes, were measured using Likert's 7-point scale (1: strongly disagree, 7: strongly agree).

To measure sustained participation intention in plogging activities, we adapted the intention to exercise scale presented by Vlachopoulos and Michailidou [49]. We adapted the scales for autonomy, competence, relatedness, intrinsic motivation, and extrinsic motivation developed by Niven and Markland [50] for analyzing self-determination and intrinsic and extrinsic motivation factors influencing continuous walking activity participation. Previous studies such as those by Fenton, Duda, and Barrett and Fletcher [51] also verified and presented that autonomy, competence, and relatedness presented in the self-determination theory had a deep relationship with continuous exercise participation, similar to Niven and Markland [50]. For eco-friendly attitudes, we used the eco-friendly attitude intensity measurement questions presented by Hodgkinson and Innes [52], which have been used in numerous studies measuring eco-friendly consumption intention or eco-friendly activity participation intention. Hodgkinson and Innes [52] restructured the eco-friendly attitude questions after quoting the environmental attitude scale (used in various fields) presented by Dunlap and Van [53] and Forgas and Jolliffe [54], and conducted statistical validity verification. Detailed information about the questions is presented in Table 1.

Table 1. Measurement items by variable.

Item	Frequency	Source
Sustained participation intention	1. I will continue to participate in plogging in the future;	Vlachopoulos, and Michailidou (2006) [49]
	2. Plogging is important in my life and it will continue to be;	
	3. I will continue to participate in plogging in any circumstance;	
	4. In the long term, I believe it is important for me to participate in plogging regularly.	
Autonomy	1. I believe I can participate in plogging anytime I want;	Niven, Markland, (2016)/ Fenton, Duda and Barrett (2016) [50,51]
	2. I was able to decide on participating in plogging by myself;	
	3. I was able to participate in plogging without any significant constraints;	
	4. I was the one who decided to participate in plogging;	
	5. I freely chose to participate in plogging of my own volition.	
Competence	1. I am confident in facing somewhat difficult challenges in plogging;	Niven, Markland, (2016)/ Fenton, Duda and Barrett (2016) [50,51]
	2. I was confident in my physical ability necessary for performing plogging;	
	3. I believe I was able to complete somewhat difficult plogging activities;	
	4. I believe my physical ability has improved through plogging;	
	5. I feel good thinking that I have the ability to complete plogging.	
Relatedness	1. I felt an attachment to my colleagues who participate in plogging together;	Niven, Markland, (2016)/ Fenton, Duda and Barrett (2016) [50,51]
	2. I feel like I am forming a common bond with people who participate in plogging together;	
	3. I felt camaraderie with people who participate in plogging together;	
	4. I felt a sense of intimacy with colleagues who have experienced difficulties by plogging together;	
	5. I felt connected with colleagues during the time of plogging together.	
Motivation	1. I think plogging is emotionally fun;	Niven, Markland, (2016)/ Fenton, Duda and Barrett (2016) [50,51]
	2. I participate in plogging to enjoy the time;	
	3. I think plogging is a fun activity;	
	4. I feel joy and satisfaction while plogging.	
	1. I have the motivation to participate in plogging because it brings me financial or other benefits;	
	2. I was motivated to participate in plogging to receive recognition from friends, family, or colleagues;	
	3. I have motivation to participate through my plogging, I think I feel the joy of others;	
	4. I was motivated to participate in plogging due to persuasion from friends, family, or colleagues.	

Table 1. Cont.

Item	Frequency	Source
Eco-Attitude	1. I think environmental issues should be prioritized among various social problems;	Hodgkinson and Innes (2001) [52]
	2. Seeing grey clouds over the city makes me feel depressed;	
	3. It annoys me to see people doing nothing for the environment;	
	4. I want to volunteer to help people working to prevent environmental pollution.	

3.3. Data Processing and Analysis

To verify the research hypotheses presented earlier, IBM's AMOS version 28 was utilized to conduct: (1) descriptive statistical analysis, (2) validation of the measurement model, (3) structural equation modeling, and (4) multi-group structural equation analysis.

The appropriateness of the data used in the descriptive statistical analysis was confirmed through the mean and standard deviation, skewness, kurtosis, correlation between independent variables, and item reliability analysis of the measurement variables. Subsequently, in the validation of the measurement model, a confirmatory factor analysis was conducted to determine whether the observed variables adequately explained the latent variables. Specifically, the convergent validity was confirmed through composite reliability (CR), and the discriminant validity was confirmed through the average variance extracted (AVE). This was because the average value of the sub-item measurements was used to measure a single independent variable in this study.

For hypothesis testing, a structural equation model was constructed based on the hypotheses of the preceding theories, and model verification was conducted. Specifically, in this study, a structural equation model including two mediating variables was verified. In this process, the appropriateness of the research model was evaluated, and upon confirmation that the research model was at an appropriate level, the validity, size, and direction of the path coefficients were interpreted. Additionally, a procedure was conducted to decompose the effects of the structural model and analyze the effectiveness of the mediating variables [55].

Finally, the moderating effect of eco-friendly attitudes was verified by analyzing the differences between groups with high eco-friendly attitudes and those without, using multi-group structural equation model analysis. Ultimately, the significance of the difference in path coefficients derived from the two models was verified, and the factors influencing the intention to sustain participation intention were interpreted based on the information obtained.

4. Results

4.1. Data: Research Subjects

This study surveyed 309 plogging participants residing nationwide in South Korea using a purposive sampling method, one of the non-probability sampling methods. To collect plogging participants, we selected plogging-related clubs, related organizations, and universities, and conducted online/offline surveys targeting participants who expressed their willingness to participate in the research. Out of a total of 309 people, data from 288 were used in the research, excluding 11 people whose response data or content was deemed unsuitable for analysis due to insincerity. All study subjects had participated in plogging activities at least three times, and it was confirmed that the number of plogging participations by the subjects was normally distributed. Detailed information on the research subjects is presented in Table 2.

Table 2. General characteristics of the study subjects.

Item		Frequency	Percentage (%)
Gender	Male	165	57.3
	Female	123	42.7
Age (years)	~19	60	20.8
	20~29	71	24.7
	30~39	57	19.8
	40~49	41	14.2
	50~59	40	13.9
	60~	19	6.6
Plogging experience (years)	~5	105	36.5
	5~7	70	24.3
	7~	113	39.2
Participation type	Regular	230	78.4
	Irregular	58	21.6
Region	Metropolitan	142	49.3
	Non-metropolitan	146	50.7
Income (Monthly)	~USD 1800	156	54.2
	USD 1800~3700	62	21.5

4.2. Descriptive Statistics, Correlation Analysis by Factor, and Reliability Analysis

Table 3 presents the descriptive statistics of the main variables measured in this study. All measured variables are continuous, and their mean, standard deviation, minimum value, maximum value, skewness, and kurtosis were examined. The mean values of the constructs indicate that the intention to sustain plogging was 4.56 (sd = 1.83), autonomy was 4.98 (sd = 1.75), competence was 4.92 (sd = 1.54), relatedness was 4.88 (sd = 1.64), intrinsic motivation was 4.62 (sd = 1.60), extrinsic motivation was 4.50 (sd = 1.56), and eco-friendly attitude was 5.11 (sd = 2.04). To verify the normality of the main variables, the skewness and kurtosis values were checked. Skewness showed values from -0.48 to -0.068 , and kurtosis showed values from -0.48 to 0.12 , confirming that they satisfy normality (West, Finch and Curran, 1995 [55]).

Table 3. Descriptive statistics of variables.

Variable	M	SD	Min	Max	Skewness	Kurtosis
SPI	4.56	1.83	1	7	-0.313	-0.228
AUT	4.98	1.75	1	7	-0.450	0.125
COM	4.92	1.54	1	7	-0.410	-0.298
REL	4.88	1.64	1	7	-0.482	0.250
MI	4.62	1.60	1	7	-0.068	-0.097
EI	4.50	1.56	1	7	-0.322	-0.358
EA	5.11	2.04	1	7	-0.377	-0.489

Table 4 presents the results of the correlation analysis for the main variables of this study. If the correlation coefficient between the constructs used in multiple regression analysis exceeds 0.7, multi-collinearity can occur, leading to statistical errors. However, the correlation coefficients among the main variables of this study were all at a level lower than 0.7, confirming that there were no issues with statistical errors due to multi-collinearity.

Table 4. Correlation analysis between independent variables.

	1	2	3	4	5	6	7
1. SPI	-						
2. AUT	0.673						
3. COM	0.679	0.652					
4. REL	0.691	0.623	0.692				
5. MI	0.697	0.622	0.639	0.683			
6. EI	0.419	0.336	0.324	0.584	0.442		
7. EA	0.504	0.416	0.392	0.489	0.462	0.378	

4.3. Assessment of Measurement Model: Reliability and Validity Analysis

In this study, Cronbach's α test and confirmatory factor analysis (CFA) were conducted to verify the reliability and validity of the measurement tools used. Particularly, as the reliability and validity of the measurement tool can vary depending on the subject, this study not only considered the entire group but also divided the group into those with high and low eco-friendly attitudes to verify whether the measured tools for each group were at a satisfactory level. For eco-friendly attitudes, the average value was 5.11, and the group was divided (mean split) based on this average.

Confirmatory factor analysis was conducted to analyze the fit of the measurement model. The results showed that the entire group ($\chi^2 = 198.822$ [df = 105, $p < 0.01$], $\chi^2/\text{df} = 1.893$, TLI = 0.927, CFI = 0.944, RMSEA = 0.058, SRMR = 0.062), the group with high eco-friendly attitudes ($\chi^2 = 211.454$ [df = 105 < 0.01], $\chi^2/\text{df} = 2.013$, TLI = 0.897, CFI = 0.881, RMSEA = 0.062, SRMR = 0.069), and the group with low eco-friendly attitudes ($\chi^2 = 231.778$ [df = 105 < 0.01], $\chi^2/\text{df} = 2.207$, TLI = 0.847, CFI = 0.834, RMSEA = 0.064, SRMR = 0.067) all exhibited satisfactory levels.

Upon conducting the reliability analysis in Table 5, the reliability α values of each sub-domain for the entire group were between 0.856 and 0.917, for the group with high eco-friendly attitudes they were between 0.856 and 0.911, and for the group with low eco-friendly attitudes, they were between 0.877 and 0.914. Since a reliability level of 0.6 or above is considered satisfactory, it was confirmed that the internal reliability of the items used in this study were all at a trustworthy level.

Table 5. Reliability analysis of measurement items (CFA).

Variable	b	SE	t	α			CR			AVE		
				Total	EA(H)	EA(L)	Total	EA(H)	EA(L)	Total	EA(H)	EA(L)
AUT 1	1.000	-	-	0.917	0.911	0.924	0.950	0.898	0.778	0.863	0.747	0.540
AUT 2	0.981	0.031	21.06									
AUT 4	0.905	0.033	19.55									
COM 2	1.000	-	-	0.909	0.900	0.886	0.875	0.793	0.812	0.701	0.561	0.591
COM 3	0.895	0.066	30.01									
COM 5	0.756	0.051	17.91									
REL 1	1.000	-	-	0.903	0.873	0.910	0.835	0.831	0.807	0.629	0.623	0.584
REL 2	0.815	0.037	18.66									
REL 3	0.701	0.020	18.89									
MI 1	1.000	-	-	0.911	0.856	0.896	0.866	0.845	0.799	0.683	0.647	0.572
MI 2	0.853	0.030	20.35									
MI 3	0.768	0.067	17.53									
EI 1	1.000	-	-	0.856	0.889	0.877	0.752	0.812	0.784	0.504	0.591	0.548
EI 2	0.749	0.056	15.64									
EI 3	0.657	0.075	16.35									

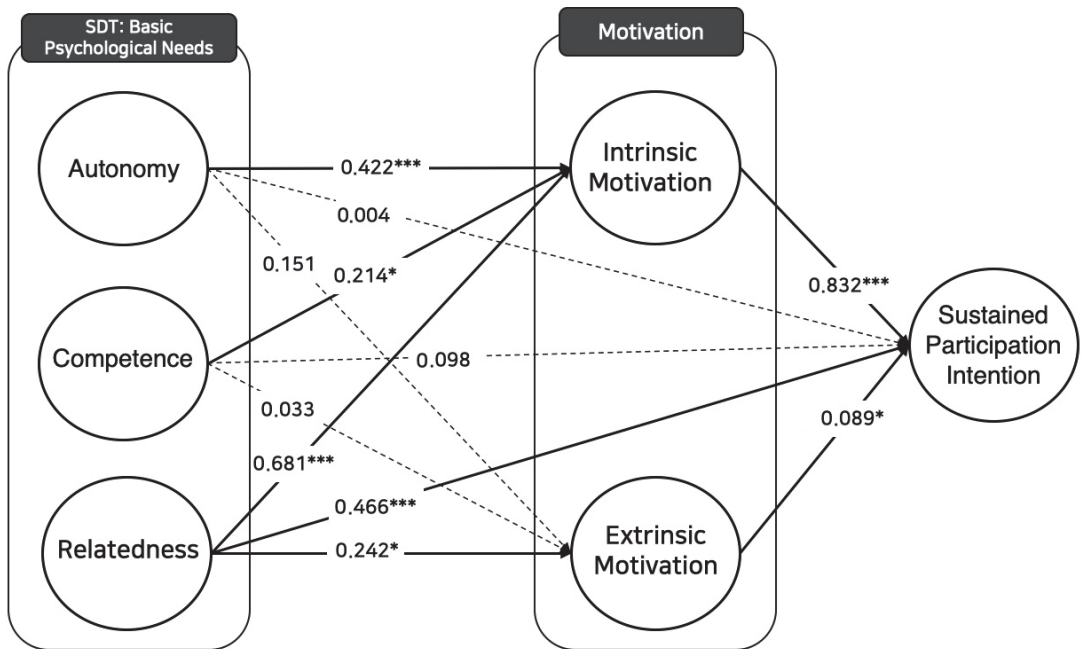
Note 1. Total model fit: $\chi^2 = 198.822$ (df = 105, $p < 0.01$), $\chi^2/\text{df} = 1.893$, TLI = 0.927, CFI = 0.944, RMSEA = 0.058, SRMR = 0.062. Note 2. EA high group: $\chi^2 = 211.454$ (df = 105 < 0.01), $\chi^2/\text{df} = 2.013$, TLI = 0.897, CFI = 0.881, RMSEA = 0.062, SRMR = 0.069. Note 3. EA low group: $\chi^2 = 231.778$ (df = 105 < 0.01), $\chi^2/\text{df} = 2.207$, TLI = 0.847, CFI = 0.834, RMSEA = 0.064, SRMR = 0.067.

The CR value for verifying the convergent validity of the measurement tool was 0.752–0.950 for the entire group, 0.793–0.898 for the group with high eco-friendly attitudes, and 0.778–0.812 for the group with low eco-friendly attitudes. Considering that the commonly accepted figure is 0.5, it was confirmed that the measurement tool of this study was at an appropriate level [56]. The AVE value, which was confirmed to verify the discriminant validity of the measurement tool, was 0.504–0.863 for the entire group, 0.561–747 for the group with high eco-friendly attitudes, and 0.540–591 for the group with low eco-friendly attitudes. Considering that the commonly accepted figure is between 0.5 and 0.95, it was confirmed that the measurement tool of this study would secure discriminant validity [57].

4.4. The Role of Motivation in Mediating the Relationship between Self-Determination Factors and Sustained Participation Intention: Structural Equation Analysis (Study 1)

This study conducted a structural equation modeling analysis to examine the relationship between the degree of self-determination factors experienced by plogging participants, their intrinsic and extrinsic motivation, and their intention to continue participating. Based on the hypotheses of research question 1 (Hypotheses 1–9), we constructed and analyzed the research model. First, the fit of the research model was analyzed and the results showed that $\chi^2(df) = 479.08(219)$, $TLI = 0.915$, $CFI = 0.903$, and $RMSEA = 0.056$. This indicated that the structural equation model was at an acceptable level for interpretation [58].

Looking at the path process of the structural model presented in [Figure 1] in detail, the basic psychological needs factors of autonomy ($b = 0.422, p < 0.001$), competence ($b = 0.214, p < 0.05$), and relatedness ($b = 0.681, p < 0.001$), proposed in the self-determination theory, were found to have a positive (+) impact on intrinsic motivation. This suggests that the stronger the experience of autonomy and competence in past plogging participation and the better the relatedness with the people who participated together, the stronger the intrinsic motivation for plogging participation. Among these, the experience of relatedness had the greatest impact on intrinsic motivation, and the experience of competence was analyzed as the lowest. Conversely, extrinsic motivation showed a somewhat different trend, where the intensity of the experience of autonomy ($b = 0.151, p > 0.05$) and competence ($b = 0.021, p > 0.05$) did not have a significant impact, and the experience of relatedness with the people who participated together ($b = 0.245, p < 0.01$) had a significantly positive (+) impact. This suggests that the relationship between the formation of plogging exercise participation motivation, according to the type and degree of basic human needs satisfaction proposed in the self-determination theory, is mainly related to intrinsic motivation, and for extrinsic motivation, only relatedness has an impact.



Note 1. *: $P < 0.05$, **: $P < 0.01$, ***: $P < 0.001$
 Note 2. —> Sig Path, - - - -> Non-Sig Path

Figure 1. Verification of the structural equation model.

In contrast, when analyzing the direct effect of the basic psychological needs satisfaction factors proposed in the self-determination theory on the relationship with the intention to continue plogging participation, the experience of autonomy ($b = 0.004, p > 0.05$) and competence ($b = 0.098, p > 0.05$) did not have a significant impact, whereas the experience of relatedness with the people who participated together ($b = 0.466, p < 0.001$) had a direct positive (+) effect. In addition, the intrinsic motivation ($b = 0.832, p < 0.001$) and extrinsic motivation ($b = 0.089, p < 0.05$) set as mediators both had a statistically significant positive (+) impact on the intention to continue participating, with intrinsic motivation having the greater impact.

In addition, an effect decomposition analysis was conducted to analyze the effect of intrinsic and extrinsic motivation mediating the relationship between the basic psychological needs satisfaction experience through plogging activities and the intention to continue plogging participation. The analysis results are presented in Table 6.

Table 6. Decomposition of effects in the structural model.

Path	Direct Effect	Indirect Effect	Total Effect	Bias Corrected, 95% (BC)
REL → MI → SPI	0.466	0.566	1.032	0.178~0.397 ***
REL → ME → SPI	0.466	0.021	0.487	0.012~0.201 *

Note 1. The mediating effect of intrinsic/extrinsic motivation between autonomy and intention to continue participating does not hold. Note 2. The mediating effect of intrinsic/extrinsic motivation between competence and intention to continue participating does not hold. Note2. *: $p < 0.05$, ***: $p < 0.001$.

In the case of autonomy, the direct effect on the intention to continue plogging participation and extrinsic motivation was not significant, and only a direct effect on intrinsic motivation was observed. Furthermore, since intrinsic motivation had a direct impact on the intention to continue participating, the mediation model of intrinsic and extrinsic motivation mediating the impact of autonomy on the intention to continue participating did not hold because the direct effect of autonomy on the intention to continue participating was not significant ($b = 0.004, p > 0.05$). Similarly, in the case of competence, the direct effect on the intention to continue participating was not significant, so the mediation model did not hold ($b = 0.098, p > 0.05$). In contrast, in the case of relatedness, the direct effect on the intention to continue participating was significant ($b = 0.466, p < 0.001$), and the effects of relatedness on both intrinsic motivation ($b = 0.681, p < 0.001$) and extrinsic motivation ($b = 0.242, p < 0.05$) were significant. Since both intrinsic motivation ($b = 0.832, p < 0.001$) and extrinsic motivation ($b = 0.089, p < 0.05$) had significant effects on the intention to continue participating, the mediation model held. Specifically, the indirect effect of intrinsic motivation mediating the relationship between relatedness and the intention to continue participating was 0.566 (B.C: 0.178~0.397, $p < 0.001$), and the indirect effect of extrinsic motivation was 0.021 (B.C: 0.012~0.201, $p < 0.001$). The indirect effect of intrinsic motivation was greater than the direct effect of relatedness on the intention to continue participating, and the indirect effect of extrinsic motivation was smaller. The sum of the indirect effects of intrinsic and extrinsic motivation (0.587) was greater than the direct effect of relatedness on the intention to continue participating (0.466), indicating that intrinsic and extrinsic motivation fully mediate the relationship between relatedness and the intention to continue participating. However, the fact that the indirect effect of extrinsic motivation (0.021) was significantly smaller than that of intrinsic motivation (0.566) confirms the important role of intrinsic motivation.

4.5. Verification of Group Differences According to Eco-Friendly Attitudes: Multi-Group Structural Equation Analysis (Study 2)

This study performed a multi-group structural equation analysis, to verify the differences in motivation, which mediates the relationship between the degree of perceived basic psychological needs satisfaction and the intention to continue participation through plogging participation analyzed earlier, according to eco-friendly attitudes. The average

value of eco-friendly attitudes was 5.11, and the group with a lower average was named the low eco-friendly attitude group (146 people), and the group with a higher average was named the high eco-friendly attitude group (142 people).

To compare the path coefficients between the two groups, we analyzed the similarity between the two models by comparing the form similarity and structure similarity. The results showed that the unconstrained model and the form similarity model exhibited a good fit with $\chi^2 = 524.375$ ($df = 187$), CFI = 0.915, and RMSEA = 0.051. In the measurement similarity model, when the path between the latent variable and the measurement variable was constrained to be the same, $\chi^2 = 589.758$ ($df = 200$), CFI = 0.913, and RMSEA = 0.048, the model and data showed a relatively good fit and there was no statistically significant difference from the form similarity model. Through this, it was confirmed that the observed variables measuring each construct were perceived equal between groups. In addition, in the structural similarity model, when the variance and covariance of the latent variables were constrained, it was analyzed as $\chi^2 = 605.217$ ($df = 218$), CFI = 0.910, and RMSEA = 0.044, and the model and data showed a relatively good fit. Furthermore, there was a statistically significant difference in the χ^2 difference comparison between the form similarity and measurement similarity models. Based on these results, it was confirmed that the two groups, divided according to eco-friendly attitudes, had an effect as control variables, and a path coefficient comparison analysis was performed for the high and low groups of eco-friendly attitudes. The analysis results are shown in Table 7.

Table 7. Estimated path coefficients and comparison by group.

Path	$\Delta\chi^2$	EA (Low)		EA (High)	
		b	SE	b	SE
AUT → MI	0.94	0.402 ***	0.102	0.500 ***	0.088
AUT → ME	3.09 **	0.243 *	0.143	0.113	0.160
AUT → SPI	0.55	0.073	0.097	0.085	0.084
COM → MI	4.01 **	0.194 **	0.118	0.054	0.114
COM → ME	3.09 **	0.001	0.167	0.056	0.211
COM → SPI	0.08	0.027	0.099	0.140	0.087
REL → MI	0.98	0.586 ***	0.125	0.633 ***	0.110
REL → ME	2.79 *	0.172 *	0.174	0.328 *	0.199
REL → SPI	0.43	0.563 ***	0.124	0.412 ***	0.102
MI → SPI	0.98	0.386 ***	0.100	0.447 ***	0.089
EI → SPI	0.99	0.104 *	0.063	0.028	0.045

Note 1. Indirect effect between AUT → MI → SPI (BC 95%): 0.047~0.191 **. Note 2. Indirect effect between COM → MI → SPI (BC 95%): 0.051~0.301 **. Note 3. Indirect effect between REL → MI/ME → SPI (BC 95%): 0.009~0.071 ***. Note 3. *: $p < 0.05$, **: $p < 0.01$ ***: $p < 0.001$.

First, in the case of the influence of autonomy on intrinsic motivation, both the low eco-friendly attitude group ($b = 0.402$, $p < 0.001$) and the high group ($b = 0.500$, $p < 0.001$) had a significant positive influence, and no difference was found in the two path coefficients ($\Delta\chi^2 = 0.94$, $p > 0.05$). In the case of the influence of autonomy on extrinsic motivation, while the low eco-friendly attitude group had a significant influence ($b = 0.243$, $p < 0.05$), the high eco-friendly attitude group did not have a statistically significant influence ($b = 0.113$, $p > 0.05$). The analysis of the difference in path coefficients was statistically significant ($\Delta\chi^2 = 3.09$, $p < 0.01$). In the case of the influence of autonomy on the intention to continue participation, neither the high eco-friendly attitude group ($b = 0.073$, $p > 0.05$) nor the low group ($b = 0.085$, $p > 0.05$) had a significant influence, and the difference in the two path coefficients was also not significant ($\Delta\chi^2 = 0.55$, $p > 0.05$). In the case of the influence of competence on intrinsic motivation, while the low eco-friendly attitude group ($b = 0.194$, $p < 0.01$) was significant, the high eco-friendly attitude group ($b = 0.054$, $p > 0.05$) was not significant, and the difference in the two path coefficients was also significant ($\Delta\chi^2 = 4.01$). In the case of the influence of competence on extrinsic motivation, neither the low eco-friendly attitude group ($b = 0.001$, $p > 0.05$) nor the high group ($b = 0.056$, $p > 0.05$) had a significant influence, and no difference

was found between the two path coefficients ($\Delta\chi^2 = 0.080, p > 0.05$). In the case of relatedness, both the low eco-friendly attitude group ($b = 0.586, p < 0.001$) and the high eco-friendly group ($b = 0.633, p < 0.001$) had a significant influence on intrinsic motivation. Both the low eco-friendly attitude group ($b = 0.563, p < 0.001$) and the high eco-friendly attitude group ($b = 0.412, p < 0.001$) had a significant influence on the intention to continue participation. However, only the high eco-friendly attitude group ($b = 0.328, p < 0.05$) had a significant influence on extrinsic motivation. The path coefficient difference verification results showed no significant differences between the two groups for the influence on intrinsic motivation ($\Delta\chi^2 = 0.98, p > 0.05$) and the influence on the intention to continue participation ($\Delta\chi^2 = 0.43, p > 0.05$), but a significant difference was confirmed between the two groups in the case of extrinsic motivation ($\Delta\chi^2 = 2.79, p < 0.01$).

To understand the different patterns of mediating effects that can occur depending on eco-friendly attitudes, we compared the mediating effect analysis for each model of the low and high eco-friendly attitude groups (Table 8). First, in the case of the low eco-friendly attitude group, the direct effect of autonomy on the intention to continue participation was not significant ($b = 0.55, p > 0.05$), so the mediating effects of intrinsic motivation and extrinsic motivation mediating autonomy and the intention to continue participation were not established. The same was true for competence, where the direct effect on the intention to continue participation ($b = 0.027, p > 0.05$) was not significant, so the mediating effects of intrinsic motivation and extrinsic motivation were not established. It was confirmed that there were significant correlations between relatedness and intrinsic motivation ($b = 0.633, p < 0.001$), relatedness and extrinsic motivation ($b = 0.172, p < 0.05$), intrinsic motivation and the intention to continue participation ($b = 0.447, p < 0.001$), and extrinsic motivation and the intention to continue participation ($b = 0.104, p < 0.05$). Also, the relationship between relatedness and the intention to continue participation ($b = 0.412, p < 0.001$) was significant. Through this, it was confirmed that the model in which intrinsic and extrinsic motivation mediated relatedness and the intention to continue participation was established, and the significance of the mediating effect was also confirmed through the Sobel test (B.C: 0.012~0.131, $p < 0.001$). Specifically, it was confirmed that only intrinsic motivation partially mediated the relationship between relatedness and the intention to continue participation, considering that the influence of relatedness on extrinsic motivation was not significant and that the direct effect ($b = 0.563$) of relatedness on the intention to continue participation was greater than the indirect effect ($b = 0.244$) that influenced through intrinsic motivation.

Table 8. Decomposition of effects in the structural model by generational groups.

Group	Path	Direct Effect	Indirect Effect	Total Effect	Bias Corrected, 95% (BC)
EA (Low)	REL → SPI	0.563	0.244	0.789	0.012~0.131 ***
EA (High)	REL → SPI	0.412	0.292	0.704	0.049~0.205 **

** $p < 0.01$, *** $p < 0.001$.

In both the high and low eco-friendly attitude groups, the mediating effects of intrinsic and extrinsic motivation were not established because there was no significant correlation between the intention to continue participation and autonomy and competence. However, a somewhat different pattern of mediating effects was found in relatedness. It was confirmed that there were significant correlations between relatedness and intrinsic motivation ($b = 0.633, p < 0.001$), and between intrinsic motivation and the intention to continue participation ($b = 0.447, p < 0.001$). In addition, the relationship between relatedness and the intention to continue participation ($b = 0.412, p < 0.001$) was significant. However, the relationship between extrinsic motivation and the intention to continue participation ($b = 0.028, p > 0.05$) was not significant. Through this, it was confirmed that the model in which intrinsic motivation mediated relatedness and the intention to continue participation was established, and the significance of the mediating effect was also confirmed through the Sobel test (B.C: 0.049~0.205,

$p < 0.001$). Specifically, it was confirmed that only intrinsic motivation partially mediated the relationship between relatedness and intention.

5. Discussion and Conclusions

Eco-friendly sports emphasize the interaction between humans and nature, allowing us to reconsider our lifestyles and responsibilities towards the environment. They also play a positive role in individual health and social life as healthy exercise [59]. This study analyzed the relationship between the three basic psychological needs of a human: autonomy, competence, and relatedness, intrinsic and extrinsic motivation, and the intention to continue participating in plogging, an eco-friendly sport. The study also analyzed the moderating effect of eco-friendly attitudes on the previously established model to understand the uniqueness of plogging activities as eco-friendly behaviors. Based on the theoretical background of self-determination theory and previous studies related to eco-friendly attitudes, a total of 10 hypotheses were set and verified.

First, Hypotheses 1–3, which analyzed the relationship between the fulfillment of autonomy and the intention to continue participating and intrinsic/extrinsic motivation, were partially supported for Hypothesis 1, but Hypotheses 2 and 3 were rejected. In the case of Hypothesis 1, the promotion of intrinsic motivation for plogging according to the degree of autonomy experienced through plogging participation was found, but extrinsic motivation was not found, so it was partially supported. In the case of Hypothesis 2, the influence of autonomy experienced through the intention to continue plogging was not significant, so it was rejected. Therefore, the mediating effect of intrinsic/extrinsic motivation mediating the relationship between autonomy and the intention to continue participating was not established, so Hypothesis 3 was also rejected. Although this supports the results of previous studies [60,61], in that the fulfillment of autonomy affects intrinsic motivation, the results differed in that it does not affect extrinsic motivation or have a direct impact on the intention to continue participating. This may be because plogging is related to volunteer activities as an eco-friendly sport, not a simple concept of healthy exercise. Volunteer activities are altruistic behaviors that are unrelated to extrinsic rewards. Therefore, it can be interpreted that the impact on extrinsic motivation was minimal. The fact that no difference in participation intention was found according to the degree of autonomy experience may be due to the small variance; specifically, most plogging participants did not feel a compulsion in the participation experience as volunteers, and, accordingly, no difference in the intention to continue participating was found.

Next, Hypotheses 4–6, which verified the relationship between competence and the intention to continue participating and intrinsic/extrinsic motivation, were partially supported for 4 but rejected for 5 and 6. Generally, the experience of competence is the factor that most influences the intention to continue participating in healthy exercise or sports activities [39–41]. Exercise participants feel a sense of competence in the process and experience of achieving goals such as skeletal muscle enhancement and weight loss through exercise participation [62]. Furthermore, sports activity participants feel a sense of competence through experiences of victory in competition or record reduction. This sense of competence has a strong influence on intrinsic motivation, such as pleasure and satisfaction, and also affects extrinsic motivation by acting as a reward. However, in the results of this study, competence did not directly influence the intention to continue exercising and extrinsic motivation, but only influenced intrinsic motivation, partially supporting the results of previous studies. A possible reason is that the participation motivation and experience of eco-friendly sports participants are different from general exercise for health activities. The results of this study coincide with numerous studies explaining eco-friendly consumer behavior, which argue that the intrinsic reward system does not operate in altruistic behavior, and that self-efficacy and the satisfaction obtained through environmental protection activities act as important motivations [44,45,48].

Third, Hypotheses 7–9, which verified the relationship between relatedness and intrinsic/extrinsic motivation and the intention to continue participating, were all supported, unlike

the previous results. As discussed earlier, relatedness is a basic psychological need defined by the desire to feel a sense of belonging by connecting with others and society and plays an important role in maintaining motivation [41]. While autonomy and competence only influenced intrinsic motivation and did not influence the intention to continue participating, relatedness influenced both intrinsic and extrinsic motivation, as well as the intention to continue participating. This result is consistent with the results of previous studies which showed that group participation was important in plogging, an eco-friendly sport, and played an important role in positive self-image exposure using social networks [7,9]. In this study, the partially mediating effects of intrinsic and extrinsic motivation were confirmed, but from the decomposition of the total effect, the effect of extrinsic motivation converged close to 0, confirming the importance of the role of intrinsic motivation.

Lastly, Hypothesis 10, which verified the moderating effect of eco-friendly attitudes, was also supported because some path differences in the structural model were found between the group with high eco-friendly attitudes and the group with low eco-friendly attitudes. In particular, there were differences in the path coefficients for the influence of autonomy on extrinsic motivation, the influence of competence on intrinsic and extrinsic motivation, and the influence of relatedness on extrinsic motivation. In the group with high eco-friendly attitudes, there was an effect of increasing extrinsic motivation according to the experience of autonomy, but no significant correlation was found in the group with low eco-friendly attitudes. In addition, competence did not influence either intrinsic or extrinsic motivation in the group with high eco-friendly attitudes. In other words, people with high eco-friendly attitudes understand that the intention to continue participating in plogging increases according to intrinsic motivation, regardless of the experience of autonomy or competence. The study results imply that the unique exercise effect of plogging, as suggested by Raghavan, Panicker and Emmatty [11], does not influence continuous participation, and the strategy to increase the intention to continue participating through the promotion of exercise effects may not be effective.

In summary, the study results support those of previous studies that have researched the relationship between the fulfillment of basic human needs such as autonomy, competence, and relatedness, as suggested by self-determination theory, and the intention to participate in sports activities, but also derive some different results. In particular, the results are different from previous studies in that while the experiences of autonomy, competence, and relatedness influence intrinsic motivation and affect the intention to continue participating, autonomy and competence do not affect extrinsic motivation, and relatedness operates as the most influential explanatory variable. These results confirm that plogging activities have a strong concept of volunteer activities, and the role of plogging activities is more related to pro-social behavior for enhancing relationships with others than to the physical competence gained from participation. It also confirms that autonomy plays an important role through it being a volunteer activity. Through this, it may be tentatively concluded that voluntary participation and socializing activities are the core values conveyed by plogging activities. In addition, the study results confirm that plogging is a volunteer activity that provides a sporting experience and an eco-friendly behavior, and the value felt by the participants and the effect of the various influencing factors on the intention to continue participating are different depending on the formation level of their eco-friendly attitudes.

The results of this study have the following academic and policy implications. First, from an academic perspective, this study contributes to understanding the role of self-determination factors for continuing participation in physical activities such as plogging from a theoretical perspective. Reconfirming the importance of the experience of autonomy, competence, and relatedness obtained through plogging participation and understanding how these experiences influence the intention to continue plogging through intrinsic/extrinsic motivation, as well as attempting an interdisciplinary approach to promote environmentally friendly behavior in the sports sector, also has academic significance in that it contributes to reducing the theoretical gap in the relationship between eco-friendly sports participation behavior, attitudes, and motivation. Many previous studies point out the situation that even if there

is consideration for or valuing of the environment, it is not often directly connected to eco-friendly behavior or eco-friendly consumption, and mention the need for research to reduce the gap between consideration for or valuing of the environment and eco-friendly behavior [63,64]. In this regard, this study contributes to reducing the theoretical gap in the relationship between eco-friendly sports participation behavior, attitudes, and motivation, which is also of academic significance.

Furthermore, from a policy perspective, the study results have significance in that they can be used as the basis for developing policies to develop and support eco-friendly sports to promote physical activity and environmental protection. From a sociological perspective, participation in eco-friendly sports contributes to raising the environmental awareness of society members, and these activities promote community participation and social responsibility for the environment [65]. Therefore, the study results provide the information necessary for policymakers to encourage and maintain plogging participation, which is meaningful. That is, through informed policy-making, plogging can play a role in creating a healthier and more sustainable society and environment while improving the physical and mental health of society members.

Author Contributions: Writing—original draft, J.K.; Writing—review & editing, S.K.; Supervision, J.C.; Project administration, J.K. All authors have read and agreed to the published version of the manuscript.

Funding: This research received no external funding.

Institutional Review Board Statement: The study was conducted in accordance with the Declaration of Helsinki, and approved by the Institutional Review Board of Bioethics Review Committee of Dongguk University.

Informed Consent Statement: Informed consent was obtained from all subjects involved in the study.

Data Availability Statement: This study does not contain personally identifiable information. However, data availability may be limited due to the absence of individual consent for public sharing.

Conflicts of Interest: The authors declare no conflict of interest.

References

1. United Nations. Transforming Our World: The 2030 Agenda for Sustainable Development. Available online: <https://sdgs.un.org/goals> (accessed on 15 March 2015).
2. Larranaga, A.; Valor, C. Consumers' Categorization of Eco-Friendly Consumer Goods: An Integrative Review and Research Agenda. *Sustain. Prod. Consum.* **2022**, *34*, 518–527.
3. Oprean-Stan, C.; Oncioiu, I.; Iuga, I.C.; Stan, S. Impact of Sustainability Reporting and Inadequate Management of ESG Factors on Corporate Performance and Sustainable Growth. *Sustainability* **2020**, *12*, 8536.
4. Li, T.-T.; Wang, K.; Sueyoshi, T.; Wang, D.D. ESG: Research Progress and Future Prospects. *Sustainability* **2021**, *13*, 11663.
5. Carrington, M.J.; Neville, B.A.; Whitwell, G.J. Lost in Translation: Exploring the Ethical Consumer Intention–Behavior Gap. *J. Bus. Res.* **2014**, *67*, 2759–2767.
6. Babiak, K.; Trendafilova, S. CSR and Environmental Responsibility: Motives and Pressures to Adopt Green Management Practices. *Corp. Soc. Responsib. Environ. Manag.* **2011**, *18*, 11–24.
7. Yun, J.H.; LEE, K.M.; Lim, S.M. Eco-Friendly Exercise Plogging: Meaning of the Motivation and Experience of Green Generation Plogging Participants. *Korean J. Phys. Educ.* **2022**, *61*, 343–354. [CrossRef]
8. Lee, W.; Choi, Y. Examining Plogging in South Korea as a New Social Movement: From the Perspective of Claus Offe's New Social Movement Theory. *Int. J. Environ. Res. Public Health* **2023**, *20*, 4469.
9. Chae, S.W.; Kim, J.K. The Effects of Motivation of Plogging Participants on Participation Efficacy, Self-Esteem and Life Satisfaction. *Korean J. Sport. Sci.* **2022**, *31*, 417–431. [CrossRef]
10. Mallen, C.; Stevens, J.; Adams, L.; McRoberts, S. The Assessment of the Environmental Performance of an International Multi-Sport Event. *Eur. Sport Manag. Q.* **2010**, *10*, 97–122.
11. Raghavan, R.; Panicker, V.V.; Emmatty, F.J. Posture Based Assessment of Plogging Activity. In Proceedings of the 2020 International Conference on System, Computation, Automation and Networking (ICSCAN), Pondicherry, India, 3–4 July 2020; IEEE: Piscataway, NJ, USA, 2020; pp. 1–5.
12. Kim, H.; Lee, M. An Analysis on the Influencing Factors on the Will of Persistent Volunteering: From the Perspective of PSM Theory. *Korean J. Local Gov. Stud.* **2012**, *16*, 249–272.
13. Kwon, S. Conceptualizing Sport-for-All for Enhancing Social Quality. *Korean Soc. Sociol. Sport* **2010**, *23*, 13–28.

14. Beak, H.; Shim, S. Analysis of Causal Model on the Leisure Experience, Leisure Function, Flow Experience and Sport Continuance Intention of Leisure Sports Participants'. *Korean J. Phys. Educ.* **2011**, *50*, 337–352.
15. Netz, Y.; Wu, M.-J.; Becker, B.J.; Tenenbaum, G. Physical Activity and Psychological Well-Being in Advanced Age: A Meta-Analysis of Intervention Studies. *Psychol. Aging* **2005**, *20*, 272–284.
16. Chatzisarantis, N.L.D.; Hagger, M.S. Effects of an Intervention Based on Self-Determination Theory on Self-Reported Leisure-Time Physical Activity Participation. *Psychol. Health* **2009**, *24*, 29–48. [CrossRef] [PubMed]
17. Ryan, R.M.; Deci, E.L. Intrinsic and Extrinsic Motivations: Classic Definitions and New Directions. *Contemp. Educ. Psychol.* **2000**, *25*, 54–67. [CrossRef] [PubMed]
18. Teixeira, P.J.; Carraça, E.V.; Markland, D.; Silva, M.N.; Ryan, R.M. Exercise, Physical Activity, and Self-Determination Theory: A Systematic Review. *Int. J. Behav. Nutr. Phys. Act.* **2012**, *9*, 78. [PubMed]
19. Vallerand, R.J. Intrinsic and Extrinsic Motivation in Sport and Physical Activity: A Review and a Look at the Future. In *Handbook of Sport Psychology*; Wiley Online Library: Hoboken, NJ, USA, 2007. [CrossRef]
20. Allen, N.J.; Rushton, J.P. Personality Characteristics of Community Mental Health Volunteers: A Review. *J. Volunt. Action Res.* **1983**, *12*, 36–49.
21. Kim, M.; Kwon, W. The Effects of Perceived Environmental Consciousness on the Image of an Eco-Friendly Sports Apparel Brand and Purchase Attitude. *J. Korean Soc. Wellness* **2017**, *12*, 63–74. [CrossRef]
22. Dolles, H.; Söderman, S. Addressing Ecology and Sustainability in Mega-Sporting Events: The 2006 Football World Cup in Germany. *J. Manag. Organ.* **2010**, *16*, 587–600. [CrossRef]
23. Kim, S.J.; Lee, S.I. The Effects of Green Consumers' Characteristics on Company Image and Purchase Intention of Green Marketing Sport Products Companies. *Korean Soc. Sport. Sci.* **2016**, *25*, 739–759.
24. Hwang, E.; Seo, S. Sports Facility Plans for Creating an Optimal Environment for Green Sports. *J. Sport. Entertain. Law* **2010**, *13*, 175–187. [CrossRef]
25. Heo, C.M. Effect of Sport Goods Company's Eco-Friendly Management Activity on Brand Image, Perceived Quality and Purchase Intention. *Korean Soc. Sport. Sci.* **2016**, *25*, 845–860.
26. Valeri, M.; Valeri, M. CSR Reporting of Sports Organizations. In *Corporate Social Responsibility and Reporting in Sports Organizations*; Springer: Cham, Switzerland, 2019; pp. 209–246.
27. Nguyen, S. Sustainability Marketing: How to Effectively Speak Greening in the Sport Industry. In *Sport Management and The Natural Environment*; Routledge: Abingdon, UK, 2015; pp. 115–130.
28. Choi, S.-B.; Jung, W.J. The Models to Predict Pro-Environment Behavior Based on the Theory of Planned Behavior of Leisure Recreation Participants. *Korean J. Sport* **2011**, *9*, 153–165.
29. Colio, B.B.; Aranda, L.M.M.; Hooli, E.; González-Fernández, F.T.; Ruiz-Montero, P.J. Approach to Service-Learning Methodology through the Physical Practice of Plogging and EFL Teaching. *J. Phys. Educ. Sport* **2023**, *23*, 579–588.
30. Hashim, N.I. Plogging: An environmentally friendly fitness trend, a sustainable initiative. *Ep. Nat. (EON)* **2023**, *7*.
31. Deci, E.L.; Ryan, R.M. The General Causality Orientations Scale: Self-Determination in Personality. *J. Res. Personal.* **1985**, *19*, 109–134. [CrossRef]
32. Frederick-Recascino, C.M. Self-determination theory and participation motivation research in the sport and exercise domain. In *Handbook of Self-Determination Research*; University of Rochester Press: New York, NY, USA, 2002; p. 277.
33. Kang, S.; Lee, K.; Kwon, S. Basic Psychological Needs, Exercise Intention and Sport Commitment as Predictors of Recreational Sport Participants' Exercise Adherence. *Psychol. Health* **2020**, *35*, 916–932. [CrossRef]
34. Vallerand, R.J. Deci and Ryan's self-determination theory: A view from the hierarchical model of intrinsic and extrinsic motivation. *Psychol. Inq.* **2000**, *11*, 312–318.
35. Jeon, H.; Lee, B. A Study on the Relationship among Participation Motivation, Exercise Commitment, and Exercise Continuation Intention of Adult Taekwondo Participants. *Korean J. Phys. Educ.* **2016**, *55*, 273–284.
36. Chung, C.H.; Kim, Y.; Seong, C.H. The Relationship Between Autonomy, Competence, Sport Motivation Level, and Effort in High School Football Players. *Korean Soc. Sport Psychol.* **2006**, *17*, 61–73.
37. Lee, J.; Cho, O. An Investigation of Sports Participation Motivation Applying Self-Determination Theory. *J. Sport Leis. Stud.* **2014**, *55*, 375–394. [CrossRef]
38. Ahn, J.; Kim, Y. The Relationship of Sensation Seek, Self-Determined Motivation and Exercise Participation Level in Extreme Sports Participants. *Korean Soc. Sport Psychol.* **2019**, *30*, 17–30. [CrossRef]
39. Park, D.; Kim, S.M. The Relationship among Basic Psychological Need, Emotional, and Intention of Exercise Adherence of College Student Athletes. *Korean Assoc. Sport Pedagog.* **2011**, *16*, 197–209.
40. Cho, H.S. Relationships between the Physical Education Teachers' Autonomy Support and the Students' Basic Psychological Needs and Help-Seeking Behavior. *Korean Assoc. Sport Pedagog.* **2011**, *18*, 17–32.
41. Standage, M.; Duda, J.L.; Ntoumanis, N. A Test of Self-Determination Theory in School Physical Education. *Br. J. Educ. Psychol.* **2005**, *75*, 411–433. [CrossRef]
42. McIntyre, A.; Milfont, T.L. Who Cares? In *Measuring Environmental Attitudes*; Wiley Online Library: Hoboken, NJ, USA, 2016. [CrossRef]
43. Karp, D.G. Values and Their Effect on Pro-Environmental Behavior. *Environ. Behav.* **1996**, *28*, 111–133. [CrossRef]

44. Rustam, A.; Wang, Y.; Zameer, H. Environmental awareness, firm sustainability exposure and green consumption behaviors. *J. Clean. Prod.* **2020**, *268*, 122016. [CrossRef]
45. Milfont, T.L.; Duckitt, J. The Environmental Attitudes Inventory: A Valid and Reliable Measure to Assess the Structure of Environmental Attitudes. *J. Environ. Psychol.* **2010**, *30*, 80–94. [CrossRef]
46. Maloney, M.P.; Ward, M.P. Ecology: Let’s Hear from the People: An Objective Scale for the Measurement of Ecological Attitudes and Knowledge. *Am. Psychol.* **1973**, *28*, 583–586. [CrossRef]
47. Ostman, R.E.; Parker, J.L. A Public’s Environmental Information Sources and Evaluations of Mass Media. *J. Environ. Educ.* **1987**, *18*, 9–17. [CrossRef]
48. Suh, M.; Won, E.S.; Son, E. A Study on Promotion of Sustainable Environment-Friendly Consumption Behavior of Consumers. *J. Consum. Stud.* **2017**, *28*, 65–93. [CrossRef]
49. Vlachopoulos, S.P.; Michailidou, S. Development and Initial Validation of a Measure of Autonomy, Competence, and Relatedness in Exercise: The Basic Psychological Needs in Exercise Scale. *Meas. Phys. Educ. Exerc. Sci.* **2006**, *10*, 179–201. [CrossRef]
50. Niven, A.G.; Markland, D. Using Self-Determination Theory to Understand Motivation for Walking: Instrument Development and Model Testing Using Bayesian Structural Equation Modelling. *Psychol. Sport Exerc.* **2016**, *23*, 90–100. [CrossRef]
51. Fenton, S.A.M.; Duda, J.L.; Barrett, T. Optimising Physical Activity Engagement during Youth Sport: A Self-Determination Theory Approach. *J. Sport. Sci.* **2016**, *34*, 1874–1884. [CrossRef] [PubMed]
52. Hodgkinson, S.P.; Innes, J.M. The Attitudinal Influence of Career Orientation in 1st-Year University Students: Environmental Attitudes as a Function of Degree Choice. *J. Environ. Educ.* **2001**, *32*, 37–40. [CrossRef]
53. Dunlap, R.E.; Van Liere, K.D. The “New Environmental Paradigm”. *J. Environ. Educ.* **1978**, *9*, 10–19. [CrossRef]
54. Forgas, J.P.; Jolliffe, C.D. How Conservative Are Greenies? Environmental Attitudes, Conservatism, and Traditional Morality among University Students. *Aust. J. Psychol.* **1994**, *46*, 123–130. [CrossRef]
55. West, S.G.; Finch, J.F.; Curran, P.J. Structural equation models with nonnormal variables: Problems and remedies. In *Structural Equation Modeling: Concepts, Issues, and Applications*; Hoyle, R.H., Ed.; Sage Publications, Inc.: New York, NY, USA, 1995; pp. 56–75.
56. Fornell, C.; Larcker, D.F. Structural Equation Models with Unobservable Variables and Measurement Error: Algebra and Statistics. *J. Mark. Res.* **1981**, *18*, 382–388. [CrossRef]
57. Bagozzi, R.P.; Yi, Y.; Nassen, K.D. Representation of Measurement Error in Marketing Variables: Review of Approaches and Extension to Three-Facet Designs. *J. Econom.* **1998**, *89*, 393–421. [CrossRef]
58. Browne, M.W.; Cudeck, R. Alternative Ways of Assessing Model Fit. *Sociol. Methods Res.* **1992**, *21*, 230–258. [CrossRef]
59. Kontogianni, E.; Kouthouris, C.; Zafeiroudi, A. Environmentally Friendly Behavior in Greek Leisure Centers and Different Participants’ Characteristics. *J. Manag. Res.* **2014**, *6*, 155–175.
60. Jung, Y.G. The Relationships between Basic Psychological Need Satisfaction, Sport Participation Motivation and Persistence Intention among Participants in Leisure Sport. *J. Sport Leis. Stud.* **2008**, *34*, 1591–1604. [CrossRef]
61. Hagger, M.; Chatzisarantis, N. Self-Determination Theory and the Psychology of Exercise. *Int. Rev. Sport Exerc. Psychol.* **2008**, *1*, 79–103. [CrossRef]
62. Sebire, S.J.; Standage, M.; Vansteenkiste, M. Predicting Objectively Assessed Physical Activity from the Content and Regulation of Exercise Goals: Evidence for a Mediation Model. *J. Sport Exerc. Psychol.* **2011**, *33*, 175–197. [CrossRef] [PubMed]
63. Davies, J.; Foxall, G.R.; Pallister, J. Beyond the Intention–Behaviour Mythology. *Mark. Theory* **2002**, *2*, 29–113. [CrossRef]
64. Kalafatis, S.P.; Pollard, M.; East, R.; Tsogas, M.H. Green Marketing and Ajzen’s Theory of Planned Behaviour: A Cross-market Examination. *J. Consum. Mark.* **1999**, *16*, 441–460. [CrossRef]
65. Sharma-Brymer, V.; Brymer, E.; Gray, T.; Davids, K. Affordances Guiding Forest School Practice: The Application of the Ecological Dynamics Approach. *J. Outdoor Environ. Educ.* **2018**, *21*, 103–115. [CrossRef]

Disclaimer/Publisher’s Note: The statements, opinions and data contained in all publications are solely those of the individual author(s) and contributor(s) and not of MDPI and/or the editor(s). MDPI and/or the editor(s) disclaim responsibility for any injury to people or property resulting from any ideas, methods, instructions or products referred to in the content.

Article

Efficient Degradation of Chlortetracycline by Graphene Supported Cobalt Oxide Activated Peroxydisulfate: Performances and Mechanisms

Wei Li ¹, Bin Yao ^{2,*}, Yuguo Zheng ¹, Guiqiang Zhang ¹, Dan Zhi ² and Yaoyu Zhou ^{1,2,*}

¹ Key Laboratory of Chemical Synthesis and Environmental Pollution Control-Remediation Technology of Guizhou Province, School of Biology and Chemistry, Minzu Normal University of Xingyi, Xingyi 562400, China; liweiwuxi@126.com (W.L.); yuguo Zheng@126.com (Y.Z.); guiqiangzhang@126.com (G.Z.)

² College of the Environment and Ecology, Hunan Agricultural University, Changsha 410128, China; zhidanvivien@163.com

* Correspondence: binyao121@163.com (B.Y.); zhoyuy@hunau.edu.cn (Y.Z.)

Abstract: Cobalt oxide has good catalytic activity for peroxydisulfate (PDS) activation but poor stability and is vulnerable to inactivation because of agglomeration. In this work, the chlortetracycline (CTC) degradation by peroxydisulfate (PDS) catalysis using the reduced graphene oxide support cobalt oxide (Co₃O₄/rGO) composite catalyst was investigated. It was found that 86.3% of CTC was degraded within 120 min in the Co₃O₄/rGO-800/PDS system. The influences of catalyst dosage, PDS concentration, solution pH, and reaction temperature were systematically explored. The excellent removal performance of CTC could be attributed to the synergistic effect between adsorption and catalytic degradation. $\equiv\text{Co}^{2+}$ and surface functional groups played as active sites to catalyze PDS, and the circulation of $\equiv\text{Co}^{2+}/\equiv\text{Co}^{3+}$ was achieved. Moreover, Co₃O₄/rGO-800 showed satisfactory reusability after three cycles. This research can provide useful information for the development of efficient PDS catalysts and facilitate insights into CTC degradation mechanism.

Keywords: antibiotic; advanced oxidation processes (AOPs); reduced graphene oxide; cobalt oxide; wastewater

Citation: Li, W.; Yao, B.; Zheng, Y.; Zhang, G.; Zhi, D.; Zhou, Y. Efficient Degradation of Chlortetracycline by Graphene Supported Cobalt Oxide Activated Peroxydisulfate: Performances and Mechanisms. *Processes* **2023**, *11*, 1381. <https://doi.org/10.3390/pr11051381>

Academic Editor: José A. Peres

Received: 7 February 2023

Revised: 2 April 2023

Accepted: 11 April 2023

Published: 3 May 2023



Copyright: © 2023 by the authors. Licensee MDPI, Basel, Switzerland. This article is an open access article distributed under the terms and conditions of the Creative Commons Attribution (CC BY) license (<https://creativecommons.org/licenses/by/4.0/>).

1. Introduction

Chlortetracycline (CTC) are tetracycline antibiotics that are widely prescribed and often applied as pharmaceutical ingredients and feed additives [1]. Owing to widespread utilization, CTC were detected as common species causing water contamination worldwide [2–4]. When CTC spreads among bacteria and natural microbial populations, it may trigger the imbalance of the ecosystem and threaten human health through the food chain [5]. At the same time, changes in bacterial adaptation caused by the misuse of antibiotics were investigated and evaluated, and the environmental risks posed by the development of drug-resistant bacteria in various countries cannot be underestimated [6,7].

To ensure food safety, control water contamination and the proliferation of drug-resistant bacteria, various approaches were proposed to eliminate CTC [8,9]. Advanced oxidation processes (AOPs) use the powerful oxidative free radicals (such as $\bullet\text{OH}$) to oxidize and even mineralize pollutants, it is considered as an efficient and insightful remediation technique [10]. Recently, sulfate radicals-based AOPs caused rising interests owing to the advantages of high performance and wide operation pH range [11]. Sulfate radicals ($\text{SO}_4^{\bullet-}$) could be generated through activating peroxymonosulfate (PMS) and peroxydisulfate (PDS) using different activation strategies, such as UV irradiation, heat, ultrasound, alkaline, and transition metals [12]. Transition metals activation is widely deemed as a promising approach since it is simple, low cost, and high performance [13]. Cobalt (Co) is the most efficient PDS catalyst compared with other transition metals,

and cobalt ion (Co^{2+}) was frequently reported as an effective PDS activator for organic pollutants degradation [14]. However, the application of homogeneous Co^{2+} would lead to the discharge of Co^{2+} . Co^{2+} is highly toxic and carcinogenic, and the remaining Co^{2+} in the aquatic solution are likely to have negative effects on human health [15].

Heterogeneous cobalt containing materials are considered promising alternative approaches. Recently, Co_3O_4 nanoparticles were widely used as PDS catalysts. For instance, Zhang et al. reported that orange G was completely degraded in the Co_3O_4 /PDS system in 180 min [16]. Yang et al. investigated the effective degradation of orange G with Co_3O_4 as persulfate catalyst. They found that orange G (30 mg/L) could be almost completely removed after 10 min reaction at 0.5 g/L Co_3O_4 catalyst and 8.0 mM persulfate [17]. However, a serious agglomeration problem was observed when using Co_3O_4 nanoparticles because of the high surface energy [13]. Loading cobalt oxide onto appropriate support materials is a feasible solution to solve this problem [18]. Graphene is a two-dimensional monolayer of sp^2 -hybridized carbon material [19]. It is considered as a potential carrier because of large surface area and excellent electrical conductivity [20]. It was reported that the combined transition metals with graphene could improve the stability as well as enhance its catalytic activity [15]. However, graphene will undergo considerable restacking through π - π and hydrophobic-hydrophobic interactions when used directly [21].

Recently, reduced graphene oxide (rGO) exhibited excellent persulfate activation activity for the generation of powerful reactive species [22]. It was reported that the defective structure and ketonic groups existed on rGO might play as active sites for persulfate activation [23]. For example, Olmez-Hanci et al. reported that rGO was an efficient persulfate activator for Bisphenol A degradation. They found that Bisphenol A can be completely removed by rGO/persulfate system within 10 min [23]. Cruz-Alcalde et al. developed the rGO membranes to activate persulfate for phenol and venlafaxine degradation. The results indicated that 90% and 94% of phenol and venlafaxine could be removed after treatment, respectively [24]. Therefore, the integration of rGO with Co_3O_4 nanoparticles can not only improve the dispersive forces within nanomaterial, but the catalyzing activity towards PDS could also be significantly enhanced [25]. For instance, Yan et al. developed reduced graphene oxide supported magnetite nanoparticle composite (nFe_3O_4 /rGO) and used it as PDS catalyst for the degradation of trichloroethylene (TCE). The degradation rate of TCE was 98.6% within 5 min at 6.94 g/L of nFe_3O_4 /rGO and 3 mM PDS [26]. Ahmad et al. developed reduced graphene oxide-iron nanocomposite (nZVI-rGO) to activate persulfate for trichloroethylene degradation. The results indicated that the nZVI-rGO/persulfate process could remove approximately 99% of trichloroethylene within 2 min [27]. However, there are no researches on the application of rGO-supported cobalt oxide composite as a PDS activator for CTC degradation.

In this work, the CTC degradation by PDS catalysis using the reduced graphene oxide support cobalt oxide (Co_3O_4 /rGO) composite catalyst was studied. Co_3O_4 /rGO was synthesized with a simple strategy. The crucial influencing factors, including catalyst dosage, PDS concentration, pH, and temperature on CTC degradation, were experimentally explored. CTC degradation mechanisms were investigated according to the experimental results and characterization analysis. The catalyst's reusability was examined using cyclic experiments. The main objectives of this research are to: (1) prepare and systematically characterize the Co_3O_4 /rGO-800 catalyst, (2) evaluate the activity of different catalysts that are synthesized under different conditions, (3) investigate the impacts of crucial environmental factors on CTC degradation, (4) elucidate CTC degradation mechanisms in the Co_3O_4 /rGO-800/PDS system. This research can provide useful information for the development of efficient PDS catalysts and facilitate insight into CTC degradation mechanism.

2. Materials and Methods

2.1. Chemicals

Urea, $\text{CoCl}_2 \cdot 6\text{H}_2\text{O}$, sodium peroxydisulfate, chlortetracycline hydrochloride (CTC), and NaOH were purchased from Shanghai Macklin Biochemical Co., Ltd., Shanghai, China.

Graphene oxide (GO) was obtained from JCNANO Tech Co., Ltd., Nanjing, China. Ethanol and sulfuric acid was obtained from Sinopharm Chemical Reagent Co., Ltd., Shanghai, China. Deionized (DI) water was used in the experiments.

2.2. Catalysts Synthesis

A total of 50 mg of dried GO was accurately weighed and transferred into a 100 mL beaker. An amount of 20 mL of DI water was added to the beaker, and it was sonicated and dispersed for 30 min to form a GO homogenate. Then, different amounts of $\text{CoCl}_2 \cdot 6\text{H}_2\text{O}$ were added to the homogenate (0.5–2 mM), and 2 g of urea was added to improve the loading success of metal atom. After stirring with an electromagnetic stirrer for 4 h, the homogenate was filtered and thoroughly washed, and dried at 60 °C. The solid was ground into powder form to obtain precursors of the material for subsequent experiments.

The above precursor materials were heated in a tube furnace under N_2 atmosphere at the heating rate of 5 °C min^{-1} . The temperature was set up to reach 700 °C, 800 °C, and 900 °C. Additionally, these temperatures were maintained for 2 h. The black powders were designated $\text{Co}_3\text{O}_4/\text{rGO-700}$, $\text{Co}_3\text{O}_4/\text{rGO-800}$, and $\text{Co}_3\text{O}_4/\text{rGO-900}$.

2.3. Experimental Procedures

CTC degradation was carried out in a 200 mL glass flask containing 100 mL of CTC (20 mg L^{-1}) with a constant stirring at 25 °C. Influences of crucial factors (catalyst dosage, PDS concentration, pH, temperature) were studied using single-factor experiments. A non-homogeneous system was formed by adding 50 mg of catalyst, stirring uniformly and then left to settle for 30 min under light-proof conditions. Then, solution pH was adjusted by using NaOH (1 M) and HCl (1 M). Thereafter, degradation was initiated through adding PDS to the stirred system. At the specified time interval, 1 mL of the sample solution was extracted and filtered through an aqueous microporous membrane (0.45 μm) before the measurement of concentration. The reusability of the catalyst was examined using cycling experiments.

3. Result and Discussion

3.1. Characterization

Scanning electron microscope (SEM) coupling energy dispersive spectrometer (EDS) (ZEISS Sigma 300) was applied for the analysis of surface morphology of catalyst. According to the SEM images (Figure 1a–d), the $\text{Co}_3\text{O}_4/\text{rGO-800}$ presented an irregular and curled flake structure, which was consistent with the results in other researches [28,29], indicating the reduction in GO was successful. Additionally, the rough and wrinkled surface of graphene flakes increased the effective contact area of the material and exposed more surface active sites, which was significant for the adsorption properties of the $\text{Co}_3\text{O}_4/\text{rGO-800}$ [23]. In addition, the loading of cobalt was also observed on the surface of the material, and the more uniform spherical or ellipsoidal particles were distributed on the surface of the graphene sheets. According to EDS images (Figure 1e–h), C, N, O, and Co elements were uniformly distributed on the catalyst surface, indicating that reduced graphene oxide-supported cobalt was successfully prepared, which was consistent with the SEM results.

X-ray diffraction (XRD, Panalytical Empyrean) was used to determine the composition of the catalyst. One sharp peak at $2\theta = 10.4^\circ$ attributed to the (001) crystal plane was observed at the XRD pattern of GO (Figure 2) [30]. For $\text{Co}_3\text{O}_4/\text{rGO-800}$, the peak at $2\theta = 10.4^\circ$ disappeared, and there were three peaks at $2\theta = 25.1^\circ$, 39.5° , and 49.8° , corresponding to the (002) facet of stacked graphene sheets [28], the (222) and (331) crystal faces of the cobalt oxide (Co_3O_4) nanoparticles, respectively (JCPDS No. 76-1802) [31]. These results were in accordance with the SEM results and elemental mapping results. In conclusion, the characterization analysis results demonstrated that cobalt oxide was successfully loaded onto rGO.

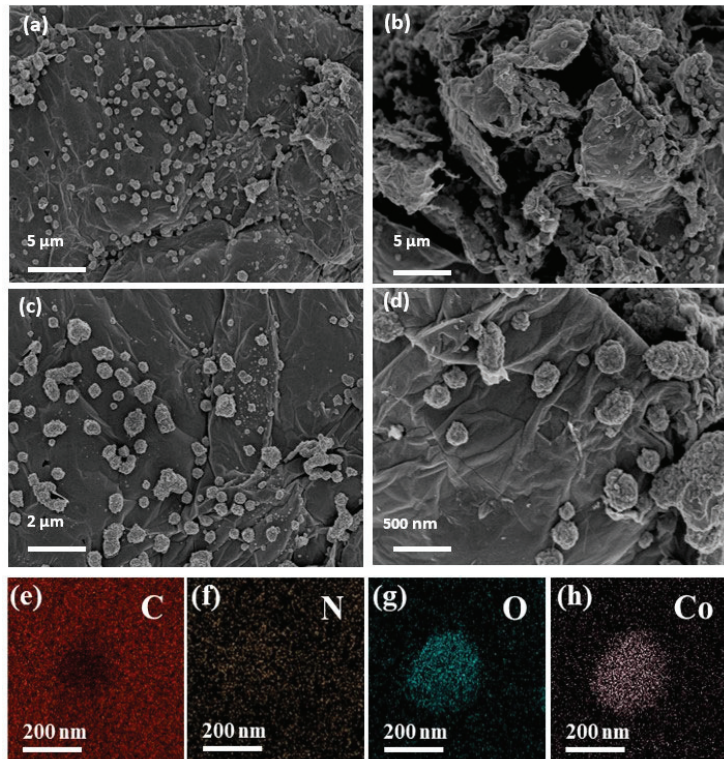


Figure 1. (a–d) SEM images of $\text{Co}_3\text{O}_4/\text{rGO}-800$; (e–h) the corresponding EDS mapping of $\text{Co}_3\text{O}_4/\text{rGO}-800$.

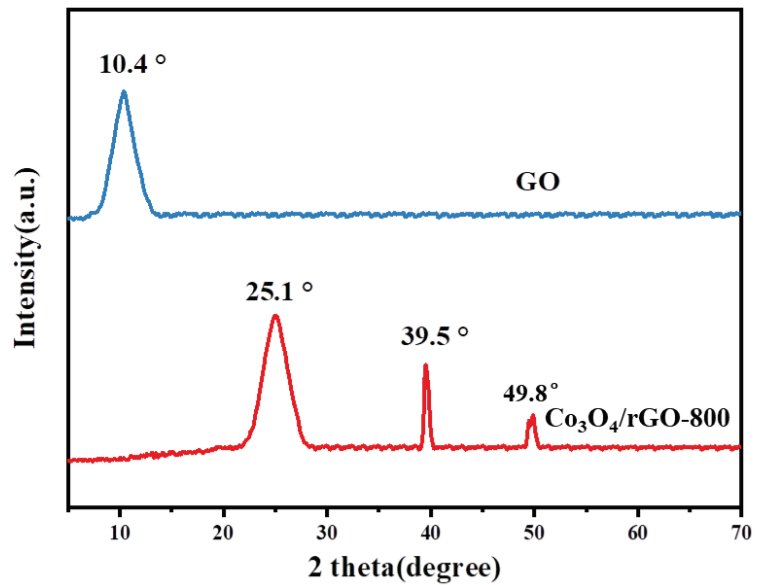


Figure 2. XRD patterns of GO and $\text{Co}_3\text{O}_4/\text{rGO}-800$.

3.2. Evaluation of Catalytic Performance

The catalytic activity of $\text{Co}_3\text{O}_4/\text{rGO-800}$ was evaluated (Figure 3). Clearly, CTC could not be efficiently removed with PDS alone and $\text{Co}_3\text{O}_4/\text{rGO-800}$ alone. Without $\text{Co}_3\text{O}_4/\text{rGO-800}$, only 6.8% of CTC was removed after 120 min, suggesting that CTC could not be efficiently degraded with unactivated PDS, and a catalyst was needed to catalytic reaction [28]. Additionally, the addition of $\text{Co}_3\text{O}_4/\text{rGO-800}$ only removed 23.6% CTC within 120 min. This demonstrated that adsorption was involved in CTC removal process but it was not the predominant mechanism [32]. Meanwhile, CTC degradation efficiency reached 86.3% within 120 min in the $\text{Co}_3\text{O}_4/\text{rGO-800}/\text{PDS}$ system. These results clearly demonstrated that CTC removal was mainly driven by the catalytic degradation, and $\text{Co}_3\text{O}_4/\text{rGO-800}$ was a promising PDS catalyst. The enhanced CTC degradation in the $\text{Co}_3\text{O}_4/\text{rGO-800}/\text{PDS}$ system might be attributed to the improved physiochemical characteristics after Co loading [33]. In addition, Co species could also play as active sites for PDS activation to generate powerful reactive oxygen species (ROS) [34].

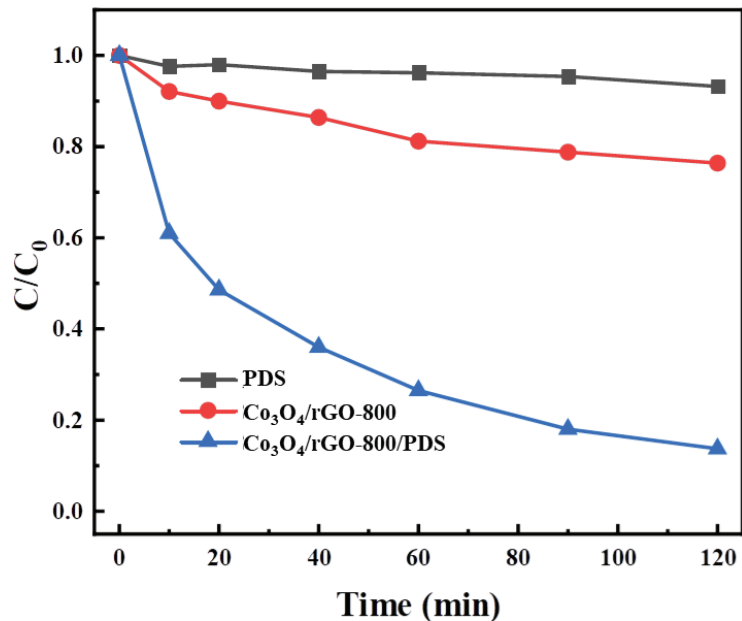


Figure 3. Different reaction systems on the degradation of CTC. (Reaction condition: CTC = 20 mg/L, PDS = 1 g/L, catalyst = 0.5 g/L, T = 25 °C and pH = 5.0).

The experimental result obtained in this research is in accordance with the previous reports. For example, Liu et al. developed carbon-coated Mn_3O_4 nanocube ($\text{Mn}_3\text{O}_4/\text{C}$) as a persulfate activator for the degradation of 2,4-dichlorophenol (2,4-D). They found that the adsorption removal of 2,4-D by $\text{Mn}_3\text{O}_4/\text{C}$ was about 37%, the direct degradation of 2,4-D by persulfate alone was approximately 26%, and the degradation rate of 2,4-D by $\text{Mn}_3\text{O}_4/\text{C}/\text{PS}$ system was 95% [35]. Ren et al. synthesized fishbone-derived biochar (FBBC) as an efficient persulfate catalyst for phenol degradation. They reported that 10.7% of phenol was removed by FBBC adsorption, persulfate could hardly degrade phenol, and the combination of FBBC and persulfate significantly improved phenol removal performances, phenol was completely removed within 60 min in the FBBC/persulfate system [36].

The adsorption of organic pollutants by carbon-based catalyst in persulfate catalyze degradation are very common [37]. The synergistic effect between adsorption and catalyze degradation in sulfate radicals-based AOPs were widely reported previously [38]. In most cases, the adsorption of organic contaminants onto a catalyst's surface is a prerequisite for

persulfate catalysis degradation. In brief, the organic contaminants existing in the reaction matrixes are enriched onto the surface of catalyst. Subsequently, the active sites on the catalyst can catalyze persulfate to generate surface-bound reactive oxygen species ($\bullet\text{OH}$ and $\text{SO}_4^{\bullet-}$). Then, the adsorbed organic pollutants are rapidly degraded by the attached reactive oxygen species [39]. Therefore, there is no doubt that both adsorption and catalyzed degradation contributed to CTC removal, and this conclusion was not only supported by the experimental results, but it could also be justified by the related scientific references.

The effect of calcination temperatures on the activation activity of $\text{Co}_3\text{O}_4/\text{rGO}$ catalyst was investigated (Figure 4a). When pyrolysis temperature increased from 700 °C to 800 °C, CTC degradation efficiency increased from 76.03% to 86.3%. This might be attributed to the formation of higher sp^2 carbon contents under high pyrolysis temperature [40]. However, as the calcination temperature further increased from 800 °C to 900 °C, CTC degradation rate declined from 86.3% to 78.97%. The collapse of carbon structure could be caused at excessively high pyrolysis temperature, and then, limit the catalytic activity [41]. Additionally, PDS activation and CTC degradation reactions occurred at the surface of catalyst, the adsorption of PDS and CTC onto the surface of catalyst is the prerequisite for CTC degradation [32]. The collapse of carbon skeleton would decrease the pore sizes and surface areas of catalysts, and the adsorption performances would be negatively affected [41]. Based on this, a catalyst calcined at 800 °C was selected for the subsequent experiments.

The effect of Co on the catalytic performance was systematically explored with catalyst synthesized using different amounts of Co for CTC degradation (Figure 4b). It could be found that CTC degradation efficiency enhanced with Co content increasing, and the degradation rate enhanced from 67.91% to 87.2% when the amount of Co increased from 0.5 mmol to 2 mmol. This suggested that the catalytic ability of $\text{Co}_3\text{O}_4/\text{rGO}$ could be improved through the addition of an appropriate amount of Co; therefore, the CTC degradation efficiency was enhanced [42]. In addition, CTC degradation performance increased slightly from 86.3% to 87.2% when the Co content increased from 1 mmol to 2 mmol. This might be because of the aggregation of nanomaterial [43]. Thus, 1 mmol was adopted for the subsequent experiments.

3.3. Influence of Reaction Parameters

3.3.1. Dosage of Catalyst

Figure 4c illustrated the influence of catalyst dosage on CTC degradation. Clearly, CTC degradation improved with the increase in catalyst dosage. When the $\text{Co}_3\text{O}_4/\text{rGO}-800$ dosage was 0.2 g/L, CTC degradation ratio was 57.9% within 120 min. As the dosage increased from 0.2 g/L to 0.5 g/L, CTC degradation significantly enhanced from 57.9% to 86.3%. This implied that the increase in catalyst dosage resulted in more active sites to catalyze PDS for CTC degradation [43]. However, it was reported that the degradation rate would not enhance significantly when the catalyst dosage further increased to a certain amount, which might be explained by the fact that the active sites were enough for PDS catalysis [44]. Consequently, the optimal dosage for $\text{Co}_3\text{O}_4/\text{rGO}-800$ was 0.5 g/L.

3.3.2. PDS Concentration

In Fenton-like reaction systems, apart from the amount of catalyst, the amount of oxidant was equally important. The influence of PDS concentration on CTC degradation was explored. As seen in Figure 4d, as the concentration of PDS gradually increased from 0.5 g/L to 2 g/L, the degradation rate markedly improved from 59.1% to 88.0%. It can be seen that the greater the dosage of PDS in a certain range, the more obvious the effect. At the same time, it can also be observed that there was no significant difference in the degradation ratio when PDS concentration increased from 1 g/L to 2 g/L, which might be explained that the excessive PDS would result in the self-quenching effect (Equations (1) and (2)) [45]. In addition, the excessive PDS would compete with CTC for the adsorption active sites on the surface of $\text{Co}_3\text{O}_4/\text{rGO}-800$ catalyst [32]. So, 1.0 g/L PDS was selected as the optimal concentration.

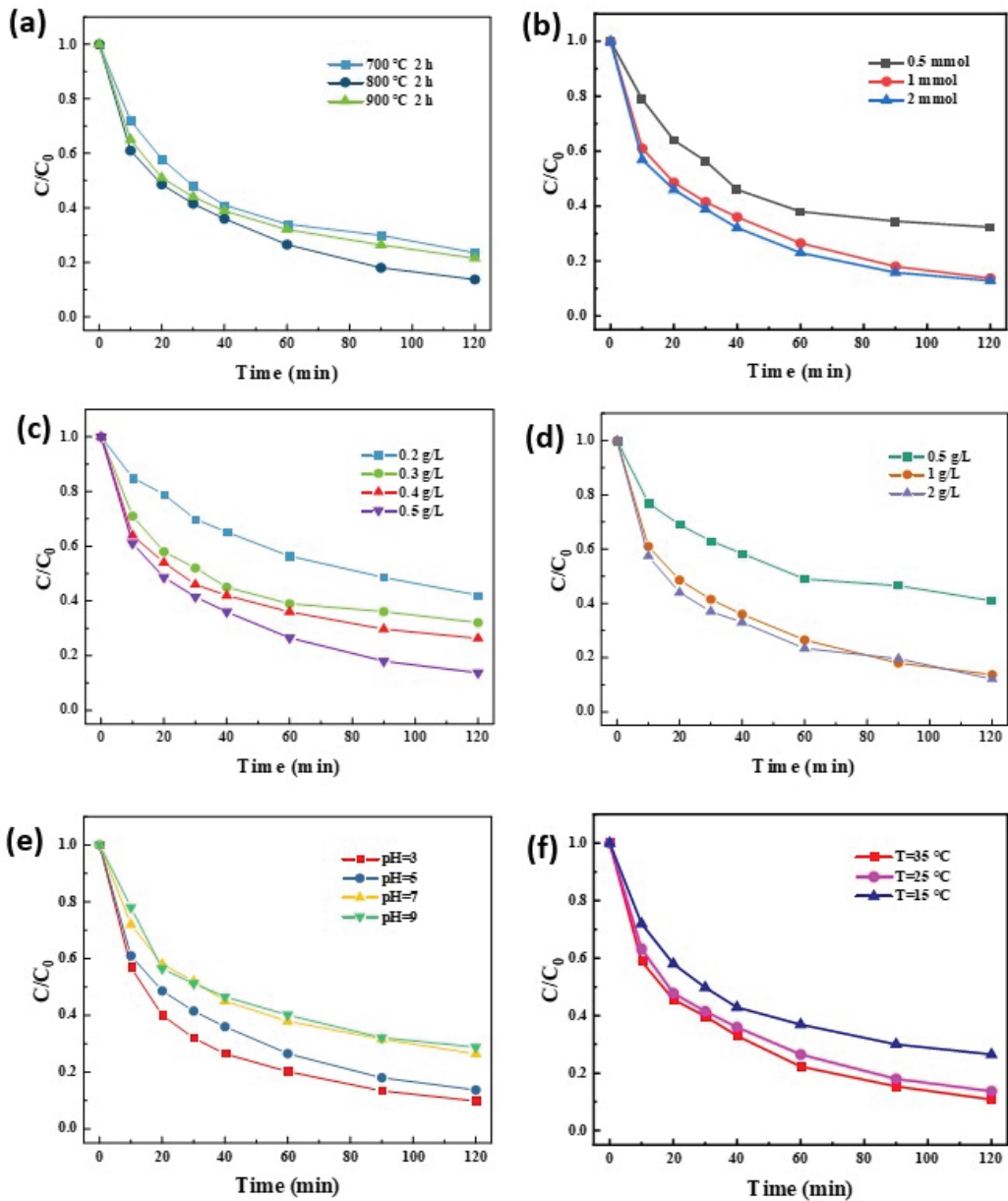
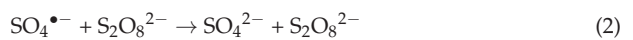
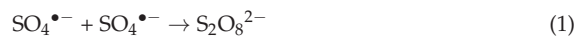
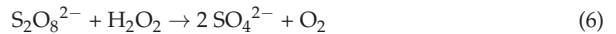
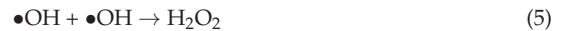


Figure 4. Influences of (a) calcination temperature, (b) Co loading amounts, (c) dosage of $\text{Co}_3\text{O}_4/\text{rGO}-800$, (d) concentration of PDS, (e) initial pH, (f) reaction temperature on the degradation of CTC. (Reaction condition: CTC = 20 mg/L, PDS = 0.5–2.0 g/L, catalyst = 0.2–0.5 g/L, T = 15–35 °C, and pH = 3–9).



3.3.3. Solution pH

Solution pH could significantly affect the surface charge of catalyst [46,47], leach of metal ions [32], ionization of CTC [48], and PDS activation [12]; thus, the impact of solution pH on CTC degradation was explored. As depicted in Figure 4e, CTC degradation rate reached the highest at pH 3 (90.2%), and it gradually declined to 71.2% when pH increased from 3 to 9. The results were in line with the previous reports [45,49]. The ineffective consumption of $\text{SO}_4^{\bullet-}$ and $\bullet\text{OH}$ under high pH conditions might be a major reason responsible for the decreased CTC degradation efficiency (Equations (3)–(6)) [49]. In addition, CTC is an amphiphilic molecule, the pK_a values for CTC were $\text{pK}_{a1} = 3.3$, $\text{pK}_{a2} = 7.44$, $\text{pK}_{a3} = 9.5$. CTC was negatively charged (CTC^- and CTC^{2-}) at high pH conditions, and positively charged (CTC^+) under acidic condition [50]. The surface of $\text{Co}_3\text{O}_4/\text{rGO}$ -800 was positively charged at acidic condition like other carbon materials [51,52]; therefore, it was expected that the strong electrostatic repulsion could occur between CTC and $\text{Co}_3\text{O}_4/\text{rGO}$ -800. The excellent CTC degradation performances might be because the leached Co^{2+} promoted PDS activation through homogenous catalysis [32]. However, 71.2% of CTC was degraded at pH 9 in the $\text{Co}_3\text{O}_4/\text{rGO}$ -800/PDS system, demonstrating that the $\text{Co}_3\text{O}_4/\text{rGO}$ -800/PDS system could remain high stability at a wide range of pH.



3.3.4. Reaction Temperature

Temperature was also considered as an important factor. The effect of solution temperature ($T = 15\text{ }^\circ\text{C}$, $25\text{ }^\circ\text{C}$ and $35\text{ }^\circ\text{C}$) on CTC degradation was studied. As revealed in Figure 4f, the optimal degradation effect was achieved when the solution temperature was $35\text{ }^\circ\text{C}$, reaching 89.2% in 120 min. With the solution temperature gradually decreased from $35\text{ }^\circ\text{C}$ to $15\text{ }^\circ\text{C}$, the degradation rate also decreased from 89.2% to 73.5%, which demonstrated that the system had a good degradation effect on CTC under a wide range of temperatures. The temperature accelerated the movement of molecules and the contact between the catalyst and PDS was more frequent, which promoted the faster generation of free radicals and the corresponding increase in the degradation rate of CTC [53].

3.4. Reusability of Catalyst

The durability and reusability of the $\text{Co}_3\text{O}_4/\text{rGO}$ -800 catalyst were significant indicators to be considered in practical applications. Recyclable materials will considerably reduce disposal costs and lower costs [54]. As displayed in Figure 5, the degradation rates of CTC reached 86.3%, 71.1%, and 63.7% in the first, second, and third cycle tests, respectively. The decrease in degradation rate in the second and third cycles was presumed because the active sites of the material were worn out or consumed during the previous experiments and part of the structure was destroyed, which led to the decrease in catalytic effect [32]. However, the removal rate in the third cycle was still higher than the related previous paper. For example, Su et al. developed graphene oxide-carbon nanotubes anchored $\alpha\text{-FeOOH}$ hybrid catalyst ($\alpha\text{-FeOOH@GCA}$) as a persulfate activator for the degradation of Orange II. The degradation rate obtained in the first run in the $\alpha\text{-FeOOH@GCA}$ /persulfate system was 99.1%, and the rate then decreased to 38.4% in the third cycle [55]. Pedrosa et al. prepared metal-free graphene-based catalytic membrane for persulfate activation to degrade phenol, they found that the degradation rate decreased from 94% to 27% after three cyclic experiments [30]. Olmez-Hanci et al. reported the degradation of Bisphenol A by reduced graphene oxide (rGO)/persulfate system. In the first run, Bisphenol A can be completely removed within 10 min. Additionally, the degradation rate gradually decreased to 68%,

33%, and 35% in the second, third, and fourth cycles after 30 min reaction, respectively [23]. Jiang et al. developed graphene-like carbon sheet supported nanoscale zero-valent iron (nZVI@CS) as a persulfate catalyst for the degradation of atrazine. The removal ratio of atrazine in the nZVI@CS/persulfate system was 84.27% in the first run, and then, it decreased to 82.0%, 63.1%, and 14.2% in the second, third, and fourth cycles, respectively [38]. Therefore, the as-synthesized Co₃O₄/rGO-800 catalyst was superior or comparable to the previous related papers. Additionally, it exhibited good stability and reusability in cyclic experiments. In fact, the decline in the catalytic reactivity of the carbon-based catalyst in sulfate radicals-based AOPs is very common, and it was extensively reported. Leaching of metal species, consumption of active sites, and the destruction of structure might all contribute to the decreased catalytic reactivity [56]. To further increase the stability of the catalyst, great efforts should be dedicated in future research.

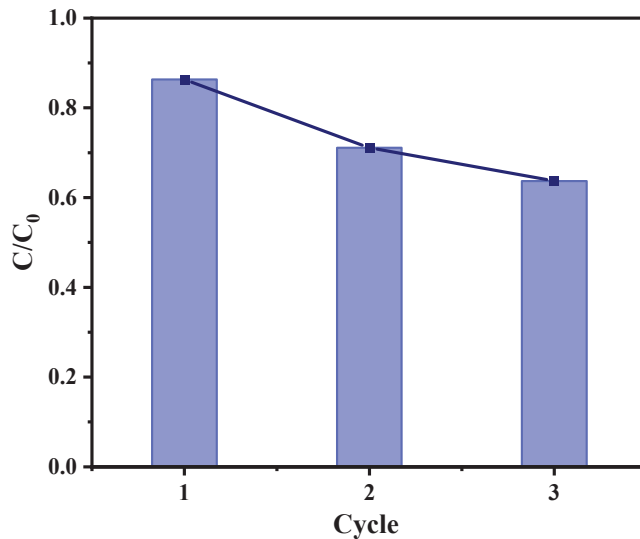
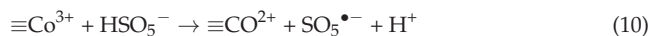
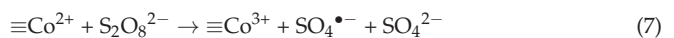


Figure 5. Cyclic degradation of CTC by the recycled Co₃O₄/rGO-800 (reaction condition: CTC = 20 mg/L, PDS = 1 g/L, catalyst = 0.5 g/L, T = 25 °C, and pH = 5.0). 3.5. Proposed degradation mechanisms.

According to the aforementioned results, CTC degradation mechanisms in the Co₃O₄/rGO-800/PDS system were concluded (Figure 6). Generally, CTC removal in the Co₃O₄/rGO-800/PDS system could be attributed to the synergistic effect between adsorption and catalytic oxidation. The predominant mechanism that was responsible for CTC removal was the catalyzed oxidation. Firstly, PDS and CTC were adsorbed onto the surface of Co₃O₄/rGO-800 catalyst. Thereafter, PDS was activated by the active sites existing on Co₃O₄/rGO-800 material to generate powerful radicals including •OH and SO₄•⁻. ≡Co²⁺ and surface functional groups played as active sites for PDS catalysis (Equations (7) and (8)) [11,57]. Meanwhile, ≡Co²⁺ could be regenerated during the reaction, and the circulation of ≡Co²⁺/≡Co³⁺ was achieved (Equations (9) and (10)) [58]. CTC was finally decomposed by powerful oxidative radicals to form small molecule compounds with less toxicity.



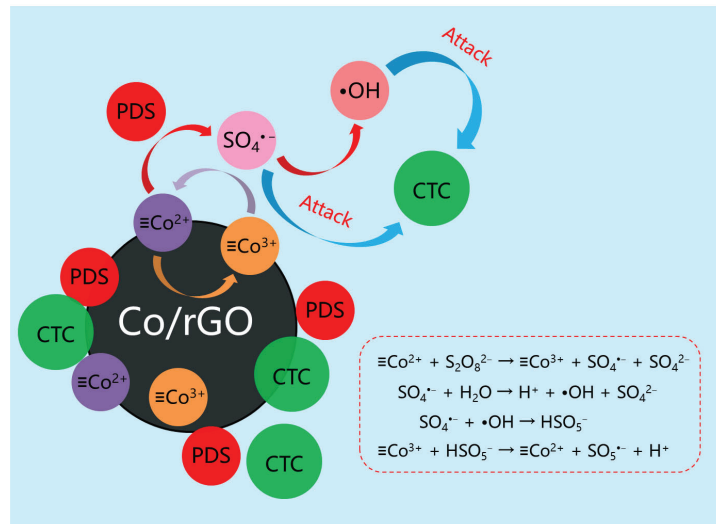


Figure 6. Proposed mechanism for CTC degradation in the Co/rGO/PS system.

4. Conclusions

In the present research, reduced graphene supported cobalt oxide ($\text{Co}_3\text{O}_4/\text{rGO}$) catalyst was successfully synthesized using a simple strategy to catalyze persulfate (PDS) for the degradation of chlortetracycline (CTC). The $\text{Co}_3\text{O}_4/\text{rGO}$ -800 presented an irregular and curled flake structure, large surface area, and abundant functional groups, which provided an excellent degradation performance for CTC (86.3% in 120 min). The excellent catalytic ability of Co/rGO material could be attributed to the synergistic effect between graphene and cobalt oxide. The study showed that both adsorption and catalyzed oxidation were involved in the removal process, and catalyzed oxidation was the predominant mechanism. PDS was activated by the active sites (cobalt oxide and oxygen-containing functional groups) on the surface of $\text{Co}_3\text{O}_4/\text{rGO}$ -800 catalyst, and the generated powerful radicals ($\text{SO}_4^{\bullet-}$ and $\bullet\text{OH}$) could attack CTC into byproducts with less toxic. $\text{Co}_3\text{O}_4/\text{rGO}$ -800 showed good stability in the cyclic experiments (63.7% removal of CTC after 3 cycles of reuse). This research demonstrated the practical application potential of $\text{Co}_3\text{O}_4/\text{rGO}$ as a PDS catalyst material with the advantages of simple production process and high catalytic performance. This work could provide a scientific basis for the future development and research of environmentally functional materials applied in wastewater treatment.

Author Contributions: Conceptualization, Y.Z. (Yaoyu Zhou); methodology, Y.Z. (Yuguo Zheng); software, G.Z.; validation, W.L.; formal analysis, W.L.; investigation, Y.Z. (Yuguo Zheng), G.Z., and W.L.; resources, Y.Z. (Yaoyu Zhou); data curation, W.L., Y.Z. (Yuguo Zheng), and G.Z.; writing—original draft preparation, W.L.; writing—review and editing, W.L., B.Y., D.Z., and Y.Z. (Yaoyu Zhou); visualization, W.L. and B.Y.; supervision, W.L. and Y.Z. (Yaoyu Zhou); project administration, W.L. and Y.Z. (Yaoyu Zhou); funding acquisition, W.L. and Y.Z. (Yaoyu Zhou). All authors have read and agreed to the published version of the manuscript.

Funding: The study was funded by the Youth Science and Technology Talents Development Project of Guizhou Education Department ([2020]220), The Doctoral Research Project (2020) of Minzu Normal University of Xingyi (20XYBS18), Science and Technology Innovation Leading Plan of High Tech Industry in Hunan Province (Grant No. 2021GK4055).

Informed Consent Statement: Not applicable.

Data Availability Statement: Data used in this work are available on reasonable request.

Conflicts of Interest: The authors declare no competing interests.

References

- Chen, Y.-P.; Zheng, C.-H.; Huang, Y.-Y.; Chen, Y.-R. Removal of chlortetracycline from water using spent tea leaves-based biochar as adsorption-enhanced persulfate activator. *Chemosphere* **2022**, *286*, 131770. [CrossRef] [PubMed]
- Leng, Y.; Xiao, H.; Li, Z.; Wang, J. Tetracyclines, sulfonamides and quinolones and their corresponding resistance genes in coastal areas of Beibu Gulf, China. *Sci. Total Environ.* **2020**, *714*, 136899. [CrossRef] [PubMed]
- Liu, L.; Liu, Y.-H.; Wang, Z.; Liu, C.-X.; Huang, X.; Zhu, G.-F. Behavior of tetracycline and sulfamethazine with corresponding resistance genes from swine wastewater in pilot-scale constructed wetlands. *J. Hazard. Mater.* **2014**, *278*, 304–310. [CrossRef] [PubMed]
- Yan, M.; Xu, C.; Huang, Y.; Nie, H.; Wang, J. Tetracyclines, sulfonamides and quinolones and their corresponding resistance genes in the Three Gorges Reservoir, China. *Sci. Total Environ.* **2018**, *631–632*, 840–848. [CrossRef]
- Martinez, J.L. Environmental pollution by antibiotics and by antibiotic resistance determinants. *Environ. Pollut.* **2009**, *157*, 2893–2902. [CrossRef]
- Gao, R.; Sui, M. Antibiotic resistance fate in the full-scale drinking water and municipal wastewater treatment processes: A review. *Environ. Eng. Res.* **2021**, *26*, 200324. [CrossRef]
- Sabri, N.A.; Schmitt, H.; Van der Zaan, B.; Gerritsen, H.W.; Zuidema, T.; Rijnaarts, H.H.M.; Langenhoff, A.A.M. Prevalence of antibiotics and antibiotic resistance genes in a wastewater effluent-receiving river in the Netherlands. *J. Environ. Chem. Eng.* **2020**, *8*, 102245. [CrossRef]
- Wang, J.; Wang, S. Removal of pharmaceuticals and personal care products (PPCPs) from wastewater: A review. *J. Environ. Manag.* **2016**, *182*, 620–640. [CrossRef]
- Yao, B.; Luo, Z.; Yang, J.; Zhi, D.; Zhou, Y. FeII/FeIII layered double hydroxide modified carbon felt cathode for removal of ciprofloxacin in electro-Fenton process. *Environ. Res.* **2021**, *197*, 111144. [CrossRef]
- Wang, J.; Zhuan, R. Degradation of antibiotics by advanced oxidation processes: An overview. *Sci. Total Environ.* **2020**, *701*, 135023. [CrossRef]
- Guan, R.; Yuan, X.; Wu, Z.; Jiang, L.; Zhang, J.; Li, Y.; Zeng, G.; Mo, D. Efficient degradation of tetracycline by heterogeneous cobalt oxide/cerium oxide composites mediated with persulfate. *Sep. Purif. Technol.* **2019**, *212*, 223–232. [CrossRef]
- Wang, J.; Wang, S. Activation of persulfate (PS) and peroxymonosulfate (PMS) and application for the degradation of emerging contaminants. *Chem. Eng. J.* **2018**, *334*, 1502–1517. [CrossRef]
- Jiang, Z.; Zhao, J.; Li, C.; Liao, Q.; Xiao, R.; Yang, W. Strong synergistic effect of Co₃O₄ encapsulated in nitrogen-doped carbon nanotubes on the nonradical-dominated persulfate activation. *Carbon* **2020**, *158*, 172–183. [CrossRef]
- Hu, P.; Long, M. Cobalt-catalyzed sulfate radical-based advanced oxidation: A review on heterogeneous catalysts and applications. *Appl. Catal. B Environ.* **2016**, *181*, 103–117. [CrossRef]
- Li, B.; Wang, Y.-F.; Zhang, L.; Xu, H.-Y. Enhancement strategies for efficient activation of persulfate by heterogeneous cobalt-containing catalysts: A review. *Chemosphere* **2022**, *291*, 132954. [CrossRef]
- Zhang, J.; Chen, M.; Zhu, L. Activation of persulfate by Co₃O₄ nanoparticles for orange G degradation. *RSC Adv.* **2016**, *6*, 758–768. [CrossRef]
- Yang, W.; Li, X.; Jiang, Z.; Li, C.; Zhao, J.; Wang, H.; Liao, Q. Structure-dependent catalysis of Co₃O₄ crystals in persulfate activation via nonradical pathway. *Appl. Surf. Sci.* **2020**, *525*, 146482. [CrossRef]
- Wu, S.; Yang, D.; Zhou, Y.; Zhou, H.; Ai, S.; Yang, Y.; Wan, Z.; Luo, L.; Tang, L.; Tsang, D.C.W. Simultaneous degradation of p-arsanilic acid and inorganic arsenic removal using M-rGO/PS Fenton-like system under neutral conditions. *J. Hazard. Mater.* **2020**, *399*, 123032. [CrossRef]
- Xu, L.; Wang, J. The application of graphene-based materials for the removal of heavy metals and radionuclides from water and wastewater. *Crit. Rev. Environ. Sci. Technol.* **2017**, *47*, 1042–1105. [CrossRef]
- Bekris, L.; Frontistis, Z.; Trakakis, G.; Sygellou, L.; Galiotis, C.; Mantzavinos, D. Graphene: A new activator of sodium persulfate for the advanced oxidation of parabens in water. *Water Res.* **2017**, *126*, 111–121. [CrossRef]
- Agarwal, V.; Zetterlund, P.B. Strategies for reduction of graphene oxide—A comprehensive review. *Chem. Eng. J.* **2021**, *405*, 127018. [CrossRef]
- Wang, Q.; Li, L.; Luo, L.; Yang, Y.; Yang, Z.; Li, H.; Zhou, Y. Activation of persulfate with dual-doped reduced graphene oxide for degradation of alkylphenols. *Chem. Eng. J.* **2019**, *376*, 120891. [CrossRef]
- Olmez-Hanci, T.; Arslan-Alaton, I.; Gurmen, S.; Gafarli, I.; Khoei, S.; Safaltin, S.; Ozcelik, D.Y. Oxidative degradation of Bisphenol A by carbocatalytic activation of persulfate and peroxymonosulfate with reduced graphene oxide. *J. Hazard. Mater.* **2018**, *360*, 141–149. [CrossRef] [PubMed]
- Cruz-Alcalde, A.; López-Vinent, N.; Ribeiro, R.S.; Giménez, J.; Sans, C.; Silva, A.M.T. Persulfate activation by reduced graphene oxide membranes: Practical and mechanistic insights concerning organic pollutants abatement. *Chem. Eng. J.* **2022**, *427*, 130994. [CrossRef]
- Chen, Y.; Bai, X.; Ji, Y.; Shen, T. Reduced graphene oxide-supported hollow Co₃O₄@N-doped porous carbon as peroxymonosulfate activator for sulfamethoxazole degradation. *Chem. Eng. J.* **2022**, *430*, 132951. [CrossRef]
- Yan, J.; Gao, W.; Dong, M.; Han, L.; Qian, L.; Nathanail, C.P.; Chen, M. Degradation of trichloroethylene by activated persulfate using a reduced graphene oxide supported magnetite nanoparticle. *Chem. Eng. J.* **2016**, *295*, 309–316. [CrossRef]

27. Ahmad, A.; Gu, X.; Li, L.; Lv, S.; Xu, Y.; Guo, X. Efficient degradation of trichloroethylene in water using persulfate activated by reduced graphene oxide-iron nanocomposite. *Environ. Sci. Pollut. Res.* **2015**, *22*, 17876–17885. [CrossRef]
28. Fan, M.; Zhang, P.; Wang, C.; Tang, J.; Sun, H. Tailored design of three-dimensional rGOA-nZVI catalyst as an activator of persulfate for degradation of organophosphorus pesticides. *J. Hazard. Mater.* **2022**, *428*, 128254. [CrossRef]
29. Zuo, S.; Jin, X.; Wang, X.; Lu, Y.; Zhu, Q.; Wang, J.; Liu, W.; Du, Y.; Wang, J. Sandwich structure stabilized atomic Fe catalyst for highly efficient Fenton-like reaction at all pH values. *Appl. Catal. B Environ.* **2021**, *282*, 119551. [CrossRef]
30. Pedrosa, M.; Drazic, G.; Tavares, P.B.; Figueiredo, J.L.; Silva, A.M.T. Metal-free graphene-based catalytic membrane for degradation of organic contaminants by persulfate activation. *Chem. Eng. J.* **2019**, *369*, 223–232. [CrossRef]
31. Anuma, S.; Mishra, P.; Bhat, B.R. Polypyrrole functionalized Cobalt oxide Graphene (COPYGO) nanocomposite for the efficient removal of dyes and heavy metal pollutants from aqueous effluents. *J. Hazard. Mater.* **2021**, *416*, 125929. [CrossRef]
32. Yao, B.; Luo, Z.; Du, S.; Yang, J.; Zhi, D.; Zhou, Y. Magnetic $MgFe_2O_4$ /biochar derived from pomelo peel as a persulfate activator for levofloxacin degradation: Effects and mechanistic consideration. *Bioresour. Technol.* **2022**, *346*, 126547. [CrossRef]
33. Yao, B.; Chen, X.; Zhou, K.; Luo, Z.; Li, P.; Yang, Z.; Zhou, Y. p-Arsanilic acid decontamination over a wide pH range using biochar-supported manganese ferrite material as an effective persulfate catalyst: Performances and mechanisms. *Biochar* **2022**, *4*, 31. [CrossRef]
34. Liang, X.; Wang, D.; Zhao, Z.; Li, T.; Chen, Z.; Gao, Y.; Hu, C. Engineering the low-coordinated single cobalt atom to boost persulfate activation for enhanced organic pollutant oxidation. *Appl. Catal. B Environ.* **2022**, *303*, 120877. [CrossRef]
35. Liu, Y.; Luo, J.; Tang, L.; Feng, C.; Wang, J.; Deng, Y.; Liu, H.; Yu, J.; Feng, H.; Wang, J. Origin of the Enhanced Reusability and Electron Transfer of the Carbon-Coated Mn_3O_4 Nanocube for Persulfate Activation. *ACS Catal.* **2020**, *10*, 14857–14870. [CrossRef]
36. Ren, X.; Wang, J.; Yu, J.; Song, B.; Feng, H.; Shen, M.; Zhang, H.; Zou, J.; Zeng, G.; Tang, L.; et al. Waste valorization: Transforming the fishbone biowaste into biochar as an efficient persulfate catalyst for degradation of organic pollutant. *J. Clean. Prod.* **2021**, *291*, 125225. [CrossRef]
37. Chen, X.; Oh, W.-D.; Lim, T.-T. Graphene- and CNTs-based carbocatalysts in persulfates activation: Material design and catalytic mechanisms. *Chem. Eng. J.* **2018**, *354*, 941–976. [CrossRef]
38. Jiang, Q.; Zhang, Y.; Jiang, S.; Wang, Y.; Li, H.; Han, W.; Qu, J.; Wang, L.; Hu, Y. Graphene-like carbon sheet-supported nZVI for efficient atrazine oxidation degradation by persulfate activation. *Chem. Eng. J.* **2021**, *403*, 126309. [CrossRef]
39. Wang, X.; Qin, Y.; Zhu, L.; Tang, H. Nitrogen-Doped Reduced Graphene Oxide as a Bifunctional Material for Removing Bisphenols: Synergistic Effect between Adsorption and Catalysis. *Environ. Sci. Technol.* **2015**, *49*, 6855–6864. [CrossRef]
40. Shang, Y.; Chen, C.; Zhang, P.; Yue, Q.; Li, Y.; Gao, B.; Xu, X. Removal of sulfamethoxazole from water via activation of persulfate by $Fe_3C@NCNTs$ including mechanism of radical and nonradical process. *Chem. Eng. J.* **2019**, *375*, 122004. [CrossRef]
41. Li, X.; Liao, F.; Ye, L.; Yeh, L. Controlled pyrolysis of MIL-88A to prepare iron/carbon composites for synergistic persulfate oxidation of phenol: Catalytic performance and mechanism. *J. Hazard. Mater.* **2020**, *398*, 122938. [CrossRef] [PubMed]
42. Liu, Z.; Pan, S.; Xu, F.; Wang, Z.; Zhao, C.; Xu, X.; Gao, B.; Li, Q. Revealing the fundamental role of MoO_2 in promoting efficient and stable activation of persulfate by iron carbon based catalysts: Efficient Fe^{2+}/Fe^{3+} cycling to generate reactive species. *Water Res.* **2022**, *225*, 119142. [CrossRef] [PubMed]
43. Zhu, K.; Bin, Q.; Shen, Y.; Huang, J.; He, D.; Chen, W. In-situ formed N-doped bamboo-like carbon nanotubes encapsulated with Fe nanoparticles supported by biochar as highly efficient catalyst for activation of persulfate (PS) toward degradation of organic pollutants. *Chem. Eng. J.* **2020**, *402*, 126090. [CrossRef]
44. Chen, L.; Jiang, X.; Xie, R.; Zhang, Y.; Jin, Y.; Jiang, W. A novel porous biochar-supported Fe-Mn composite as a persulfate activator for the removal of acid red 88. *Sep. Purif. Technol.* **2020**, *250*, 117232. [CrossRef]
45. Ma, D.; Yang, Y.; Liu, B.; Xie, G.; Chen, C.; Ren, N.; Xing, D. Zero-valent iron and biochar composite with high specific surface area via K_2FeO_4 fabrication enhances sulfadiazine removal by persulfate activation. *Chem. Eng. J.* **2021**, *408*, 127992. [CrossRef]
46. Yao, B.; Luo, Z.; Du, S.; Yang, J.; Zhi, D.; Zhou, Y. Sustainable biochar/ $MgFe_2O_4$ adsorbent for levofloxacin removal: Adsorption performances and mechanisms. *Bioresour. Technol.* **2021**, *340*, 125698. [CrossRef]
47. Yao, B.; Li, Y.; Zeng, W.; Yang, G.; Zeng, J.; Nie, J.; Zhou, Y. Synergistic adsorption and oxidation of trivalent antimony from groundwater using biochar supported magnesium ferrite: Performances and mechanisms. *Environ. Pollut.* **2023**, *323*, 121318. [CrossRef]
48. Ma, Y.; Li, M.; Li, P.; Yang, L.; Wu, L.; Gao, F.; Qi, X.; Zhang, Z. Hydrothermal synthesis of magnetic sludge biochar for tetracycline and ciprofloxacin adsorptive removal. *Bioresour. Technol.* **2021**, *319*, 124199. [CrossRef]
49. Ouyang, D.; Yan, J.; Qian, L.; Chen, Y.; Han, L.; Su, A.; Zhang, W.; Ni, H.; Chen, M. Degradation of 1,4-dioxane by biochar supported nano magnetite particles activating persulfate. *Chemosphere* **2017**, *184*, 609–617. [CrossRef]
50. Taheran, M.; Naghdi, M.; Brar, S.K.; Knystautas, E.J.; Verma, M.; Ramirez, A.A.; Surampalli, R.Y.; Valero, J.R. Adsorption study of environmentally relevant concentrations of chlortetracycline on pinewood biochar. *Sci. Total Environ.* **2016**, *571*, 772–777. [CrossRef]
51. Ma, Y.; Lu, T.; Tang, J.; Li, P.; Mašek, O.; Yang, L.; Wu, L.; He, L.; Ding, Y.; Gao, F.; et al. One-pot hydrothermal synthesis of magnetic N-doped sludge biochar for efficient removal of tetracycline from various environmental waters. *Sep. Purif. Technol.* **2022**, *297*, 121426. [CrossRef]

52. Xiong, W.; Zeng, Z.; Li, X.; Zeng, G.; Xiao, R.; Yang, Z.; Zhou, Y.; Zhang, C.; Cheng, M.; Hu, L.; et al. Multi-walled carbon nanotube/amino-functionalized MIL-53(Fe) composites: Remarkable adsorptive removal of antibiotics from aqueous solutions. *Chemosphere* **2018**, *210*, 1061–1069. [CrossRef]
53. Yao, B.; Luo, Z.; Zhi, D.; Hou, D.; Luo, L.; Du, S.; Zhou, Y. Current progress in degradation and removal methods of polybrominated diphenyl ethers from water and soil: A review. *J. Hazard. Mater.* **2021**, *403*, 123674. [CrossRef]
54. Luo, Z.; Yao, B.; Yang, X.; Wang, L.; Xu, Z.; Yan, X.; Tian, L.; Zhou, H.; Zhou, Y. Novel insights into the adsorption of organic contaminants by biochar: A review. *Chemosphere* **2022**, *287*, 132113. [CrossRef]
55. Su, S.; Liu, Y.; He, W.; Tang, X.; Jin, W.; Zhao, Y. A novel graphene oxide-carbon nanotubes anchored α -FeOOH hybrid activated persulfate system for enhanced degradation of Orange II. *J. Environ. Sci.* **2019**, *83*, 73–84. [CrossRef]
56. Lu, J.; Zhou, Y.; Lei, J.; Ao, Z.; Zhou, Y. Fe₃O₄/graphene aerogels: A stable and efficient persulfate activator for the rapid degradation of malachite green. *Chemosphere* **2020**, *251*, 126402. [CrossRef]
57. Xian, G.; Zhang, G.; Chang, H.; Zhang, Y.; Zou, Z.; Li, X. Heterogeneous activation of persulfate by Co₃O₄-CeO₂ catalyst for diclofenac removal. *J. Environ. Manag.* **2019**, *234*, 265–272. [CrossRef]
58. Jiang, Z.; Wei, J.; Zhang, Y.; Niu, X.; Li, J.; Li, Y.; Pan, G.; Xu, M.; Cui, X.; Cui, N.; et al. Electron transfer mechanism mediated nitrogen-enriched biochar encapsulated cobalt nanoparticles catalyst as an effective persulfate activator for doxycycline removal. *J. Clean. Prod.* **2023**, *384*, 135641. [CrossRef]

Disclaimer/Publisher’s Note: The statements, opinions and data contained in all publications are solely those of the individual author(s) and contributor(s) and not of MDPI and/or the editor(s). MDPI and/or the editor(s) disclaim responsibility for any injury to people or property resulting from any ideas, methods, instructions or products referred to in the content.

Article

Efficiency of Coagulation/Flocculation for the Removal of Complex Mixture of Textile Fibers from Water

Sanja Vasiljević¹, Maja Vujić¹, Jasmina Agbaba¹, Stefania Federici^{2,*}, Serena Ducoli², Radivoj Tomić¹ and Aleksandra Tubić^{1,*}

¹ Department of Chemistry, Biochemistry and Environmental Protection, Faculty of Sciences, University of Novi Sad, Trg Dositeja Obradovića 3, 21000 Novi Sad, Serbia

² Department of Mechanical and Industrial Engineering, University of Brescia and INSTM Unit of Brescia, via Branze, 38, 25123 Brescia, Italy

* Correspondence: stefania.federici@unibs.it (S.F.); aleksandra.tubic@dh.uns.ac.rs (A.T.)

Abstract: Synthetic fibers enter wastewater treatment plants together with natural fibers, which may affect treatment efficiency, a fact not considered in previous studies. Therefore, the aim of the present study was to evaluate the efficiency of the coagulation/flocculation process for the removal of a mixture of textile fibers from different water matrices. Natural and synthetic fibers (100 mg/L; cotton, polyacrylonitrile, and polyamide) were added to a synthetic matrix, surface water and laundry wastewater and subjected to coagulation/flocculation experiments with ferric chloride (FeCl₃) and polyaluminum chloride (PACl) under laboratory conditions. In the synthetic matrix, both coagulants were found to be effective, with FeCl₃ having a lesser advantage, removing textile fibers almost completely from the water (up to 99% at a concentration of 3.94 mM). In surface water, all dosages had approximately similar high values, with the coagulant resulting in complete removal. In laundry effluent, the presence of surfactants is thought to affect coagulation efficiency. PACl was found to be effective in removing textile fibers from laundry wastewater, with the lowest removal efficiency being 89% and all dosages having similar removal efficiencies. Natural organic matter and bicarbonates showed a positive effect on the efficiency of FeCl₃ in removing textile fibers from surface water. PACl showed better performance in coagulating laundry wastewater while surfactants had a negative effect on FeCl₃ coagulation efficiency.

Keywords: textile fibers; coagulation and flocculation; wastewater; removal of textile fibers; ferric chloride; polyaluminium chloride

Citation: Vasiljević, S.; Vujić, M.; Agbaba, J.; Federici, S.; Ducoli, S.; Tomić, R.; Tubić, A. Efficiency of Coagulation/Flocculation for the Removal of Complex Mixture of Textile Fibers from Water. *Processes* **2023**, *11*, 820. <https://doi.org/10.3390/pr11030820>

Academic Editor: Monika Wawrzekiewicz

Received: 31 January 2023

Revised: 3 March 2023

Accepted: 4 March 2023

Published: 9 March 2023



Copyright: © 2023 by the authors. Licensee MDPI, Basel, Switzerland. This article is an open access article distributed under the terms and conditions of the Creative Commons Attribution (CC BY) license (<https://creativecommons.org/licenses/by/4.0/>).

1. Introduction

In recent years, the presence of microplastic fibers (MPFs) in wastewater attracted considerable concern and attention, as synthetic fibers became one of the most commonly used materials in the manufacture of clothing, along with natural fibers [1]. Every year, more than 42 million tons of synthetic fibers are produced in the textile industry [2–4], most of which end up in the environment. In the environment, MPFs are mostly recognized as small fibers released during the production and use of textiles [5–7]. Polyester and nylon are the most common polymers used for the production of textile fibers, accounting for about 63% of the total textile materials, but also polyamide, polystyrene, polyacrylonitrile, etc. are frequently used [7]. Based on previous research, it was proved that the formation of MPFs is influenced by the type of detergent, the type of washing machine, and the program temperature, among other factors. It is assumed that parameters such as high temperature and water hardness further promote the formation of MPFs, while the addition of softeners reduces their number [8]. MPFs enter the environment through two main pathways: laundry waste that directly enters the environment or municipal wastewater in wastewater treatment plants [9–11].

Different types of microplastics (e.g., polyester, polyethylene, polypropylene, polyamide, etc.) enter wastewater treatment plants in different forms (flakes, fibers, films, and particles) and from different sources (from synthetic textile washing processes and microbeads from household products, such as cosmetics, detergents, eyeglass cleaners, etc.) [12–14]. It was found that 6 million polyester fibers and 700,000 acrylic fibers are released from one washing of textiles in the machine, which depends on the washing program, detergent, and textile properties [12]. Previous research indicated that synthetic MPF should be given special attention because they are very small and narrow and can be retained very easily in wastewater [15].

Advanced technologies for the removal of microplastics from water such as biodegradation, adsorption, catalysis, photocatalytic degradation, coagulation, filtration, and electrocoagulation are being investigated to some extent but are still considered as under-researched technologies, especially in wastewater treatment plants [16]. Coagulation and flocculation technology is considered as a typical treatment for the removal of suspended solids and colloidal particles in wastewater. Researchers focused on this treatment in recent years, mainly because of its low cost, ease of operation, and energy savings [17]. Several factors affect the efficiency of removal of synthetic fibers by coagulation/flocculation, such as pH, natural organic matter, surfactants, ions present in the matrix, coagulation conditions, etc.

The pH is a very important factor in coagulation treatment. At lower pH values, the main mechanism of coagulation is believed to be neutralization of charge between positively charged Fe/Al hydroxypolymers and negatively charged particles. The removal of particles at higher pH values is mainly due to the adsorption of particles on Fe/Al precipitates. Previous studies showed that PACl is effective at slightly acidic pH, but also at higher pH values, which depends on the properties of the matrix [18].

In surface waters, there is a large amount of natural organic matter (NOM) consisting of humic substances containing humic and fulvic acids characterized by a large molar mass. In addition, they are rich in aromatic and phenolic structures, conjugated double bonds, and hydroxyl and carboxyl groups. Therefore, NOM can change the surface properties of the fibers and thus affect the treatment [17].

The presence of surfactants in water can affect the efficiency of coagulation/flocculation treatment by altering polymer surface properties and affecting binding to coagulants. It was found that nonionic surfactants in particular can reduce coagulation efficiency [19,20].

In previous research, coagulation in wastewater treatment plants was used sparingly to remove microplastics. Most of the research in this area focused on studying the treatment of municipal wastewater, since wastewater treatment plant effluents are considered the main source of pollution of microplastics in the environment [4,8,21,22]. Available literature provides data on the coagulation/flocculation efficiency in removing different types of microplastic particles (polyethylene, polyester, polystyrene, rayon, etc.) with different sizes and shapes, untreated or aged. Common coagulants, such as iron and aluminum salts were used in the experiments. For the study of the coagulation/flocculation mechanism, synthetic matrices are usually prepared under laboratory conditions with well-defined properties in terms of pH, content of natural organic matter, metal salts, etc. [23–25]. However, the obtained results vary depending on the coagulation conditions, polymer types and properties, and matrix characteristics. Therefore, the need for studies related to more realistic matrices and different types of synthetic fibers was pointed out [7,26].

Based on these considerations, the aim of this work was to investigate the potential of coagulation/flocculation treatment in the removal of a complex mixture of textile fibers from natural and synthetic materials. Two common coagulants (ferric chloride and polyaluminum chloride) were used, as well as the potential of their combination. Wastewater from textile washing and surface water were selected as representatives of real water matrices, and the results were compared with those obtained for a synthetic matrix. In this way, we were able to evaluate the influence of natural organic matter, surfactants, and pH on the efficiency of removing complex textile fibers from real water matrices by coagulation/flocculation treatment.

2. Materials and Methods

2.1. Experimental Setup

In the present study, the efficiency of removing complex mixtures of textile fibers from water by coagulation and flocculation was investigated. Three different water matrices (synthetic water, surface water, and laundry wastewater) were used to evaluate the effects of different matrix properties. The removal of textile fibers was studied by adding 50 mg of textile fibers to the studied water matrices (0.5 L). The efficiency of the commonly used coagulants ferric chloride (FeCl_3) and polyaluminum chloride (PACl) and their combination was evaluated. The experiments were performed under laboratory conditions using the standard JAR test. Figure 1 shows a schematic diagram of the experiment.

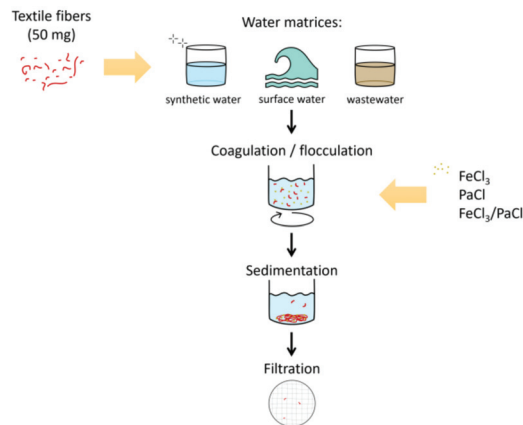


Figure 1. Schematic representation of the experiment.

2.2. Materials

Three waters were studied to have representatives of different matrix properties: laundry wastewater, surface water from the Danube River, synthetic matrix (distilled water enriched with NaHCO_3 , CaCl_2 , and MgSO_4 salts), with the properties presented in Table 1.

Mixed fibers containing cotton and synthetic polymers were used as material. A commercial detergent was used to approximate the actual washing conditions as closely as possible. A “mixed” cycle at 40 °C for 1 h and 40 min with a spin speed of 800 rpm was used as the wash program. The wastewater was collected at the outlet pipe of the machine in polyethylene terephthalate canisters. Both detergent and fabric softener were used to wash the textile garments, and the laundry was rinsed four times. It was then dried in a dryer, and the residue on the filter after the laundry was dried and used as material for further experiments. The concentration of textile fibers was 100 mg/L.

To compare the process of coagulation and flocculation with and without added textile fibers, samples without textile fibers (blank tests) were prepared.

FeCl_3 stock solution was prepared by dissolving 10 g of solid FeCl_3 (obtained from Sigma Aldrich, USA) in 50 mL of distilled water and used for dosing in water samples. The PACl stock solution was prepared by dissolving 7.7 mL of a PACl stock solution in 100 mL of distilled water. The dosage of coagulants is listed in Table S1. The stock solution of the flocculant (UNIFLOC M27, Unichem KFT, Hungary) was prepared by dissolving 0.5 g of the powdered substance in 100 mL of distilled water with stirring at 10 rpm in a JAR apparatus for 120 min. A working solution was prepared from the stock solution of the flocculant ($c = 0.05$ mL/mL) by dissolving 2.5 mL of the stock solution in 50 mL of distilled water so that the concentration in the experiment was 0.025 mL/mL.

Table 1. Characteristics of the water matrices.

Parameter	MDL	Synthetic Water	Surface Water	Laundry Wastewater
pH	/	7.90 ± 0.06	7.75 ± 0.07	8.13 ± 0.07
Electrical conductivity 25 °C (µS/cm)	/	303 ± 5	437 ± 8	578 ± 15
Turbidity (NTU)	0.01	0.3 ± 0.3	8.35 ± 0.15	149 ± 25
COD (mg/L)	15	<15 *	<15 *	920 ± 23
Total organic carbon (mg/L)	0.3	<0.3 *	2.4 ± 0.3	104 ± 1.1
Na ⁺ (mg/L)	0.1	75.7 ± 5.7	5.5 ± 0.7	2.71 ± 0.22
Mg ²⁺ (mg/L)	0.09	4.33 ± 0.41	10.4 ± 0.9	5.01 ± 0.47
K ⁺ (mg/L)	0.11	<0.11 *	2.31 ± 0.17	6.8 ± 0.6
Ca ²⁺ (mg/L)	0.11	44.0 ± 3.6	6.00 ± 0.54	7.33 ± 0.71
Cl ⁻ (mg/L)	5.0	52.1 ± 3.6	44.0 ± 1.5	3140 ± 150
SO ₄ ²⁻ (mg/L)	5.0	21.2 ± 4.9	25.5 ± 3.2	97.6 ± 27.2
HCO ₃ ⁻ (mg/L)	18.4	134 ± 6	218 ± 43	252 ± 32

* method detection limit (MDL).

2.3. Coagulation/Flocculation Experiments

The coagulation experiments were performed on the JAR apparatus under laboratory conditions. All experiments were performed in duplicate or triplicate. Before performing the JAR test, 50 mg of textile fibers were added to 0.5 L of water and allowed to stand for 24 h before the coagulation/flocculation experiments. Two common coagulants (ferric chloride and polyaluminum chloride) were used. Coagulation was performed by adding the coagulant at a mixing speed of 120 rpm for a period of 2 min, after which a flocculant was added and mixing was continued at 45 rpm for a period of 30 min. Sedimentation was performed for 30 min. After settling, the samples were filtered through a cellulose nitrate membrane filter with a pore size of 0.45 µm using a vacuum filtration device.

The dosage of coagulant followed the dosages commonly used in the literature [26] and was adjusted according to water requirements (Table S1). Therefore, lower dosages (0.72–3.95 mM Fe and 0.77–3.85 mM Al) were used in the synthetic matrix and surface water experiments, while higher dosages (7.16–21.49 mM Fe and 1.92–9.62 mM Al) were required for coagulation of laundry wastewater. The coagulant concentrations for laundry wastewater were higher due to the surfactants and other substances present in this water.

In addition, two coagulants were combined in that the dosage of FeCl₃ and PACl was lower than that which showed the best performance in removing textile fibers when used separately. Three dosing approaches were carried out: (1) FeCl₃ was added first and then PACl, (2) PACl was added first and then FeCl₃, and (3) the coagulants were added simultaneously.

The filter papers were dried in Petri dishes at room temperature for 24 h, and then their masses were measured, based on which further calculations were performed and the efficiency of removing textile fibers from water was determined.

2.4. Analytical Procedures

Textile fibers were characterized using a scanning electron microscope SEM (TM3030, Hitachi, Japan) to study their size, surface area, and shape. Chemical characterization was performed using Fourier transform infrared spectroscopy (FTIR), specifically the attenuated total reflection (ATR) technique on a FTIR Nexus 670 (Thermo Nicolet, USA) instrument in the range 4000–400 cm⁻¹ with a resolution of 4 cm⁻¹ and a speed of 60 scans per analysis at room temperature. The ATR technique was implemented using an ATR crystal of Ge on a reflective plate and a pressure clamp. In addition, characterization was also performed using micro-FTIR. FTIR measurements were performed using a Nicolet iN10MX (Thermo

Scientific, Waltham, MA, USA) microscope equipped with a cooled MCT detector and operating in transmission mode. For each sample, 20 individual fibers were isolated and placed on a BaF₂ window to collect IR spectra in transmission mode. Measurements were made with a nominal spectral resolution of 8 cm⁻¹ in the range of 4000–650 cm⁻¹. To increase the signal-to-noise ratio, 64 scans per sample were co-added without changing the position of the sample between each scan (total acquisition time: 12 s, including dead time). OMNIC™ Picta software (Thermo Scientific, Waltham, MA, USA) was used for all spectra manipulations.

The pH of the water samples was measured using a pH meter 340i, WTW, SenTix® 21 electrodes. Electrical conductivity analysis was performed using a Hanna conductometer, model HI 933000, Austria. Total organic carbon (TOC) in water samples was analyzed using an LiquiTOCII, Elementar, Germany instrument. Turbidity was determined using a WTW Austria, Cond 3210 with a Tetracon 325 WTW electrode. The chemical oxygen demand (COD) was determined according to the standard method [27].

Chloride concentration in water was determined by titration with silver nitrate using a potassium chromate indicator according to the method SRPS ISO 9297/1:2007 [28]. Sulfate was determined by iodometric titration of the excess chromate ion with sodium thiosulfate solution after precipitation of sulfate with the addition of excess barium chromate. The alkalinity of water in terms of bicarbonate and carbonate concentration was determined by the volumetric method [29].

Sodium and potassium metal ions were detected using the flame atomic emission spectroscopy (FAES) technique according to the standard method [29], and Ca and Mg metal ions were detected using the flame atomic absorption spectroscopy (FAAS) technique on a Perkin Elmer Analyst 700 atomic absorption spectrometer, according to the USEPA methods [30,31].

3. Results

3.1. Water Matrix Characterization

The characteristics of the water matrices studied are shown in Table 1. All three waters have similar pH values in the slightly alkaline range (pH = 7.75 ± 0.07–8.13 ± 0.07) to evaluate the efficiency of the coagulation/flocculation process under the conditions of the real pH of the water matrices.

The obtained results show that, as expected, laundry wastewater has the highest organic matter load, with a TOC content about 50 times higher than in surface waters and a COD of 920 ± 23 mg/L. The synthetic matrix is characterized by TOC and COD values lower than the detection limit of the method. This is followed by a high turbidity of the effluent and a very low (<1 NTU) for the other two matrices. As expected, the electrical conductivity shows the highest ion content in laundry wastewater, followed by surface water and synthetic matrix. When evaluating the influence on textile fiber behavior during coagulation/flocculation treatment, pH, TOC, and COD are the most important water quality parameters, as are Cl⁻, SO₄²⁻, and HCO₃⁻ [25,26].

3.2. Textile Fibers Characterization

3.2.1. SEM Characterization

The different appearance of textile fibers in SEM micrographs indicates the presence of fibers of both natural and synthetic origin. A detailed visual characterization was performed using SEM and the results are shown in Figure 2. SEM microscopic images showed differences in the diameter of isolated textile fibers, ranging from 8.28 µm to 19.00 µm. Moreover, the different fiber structure in the samples is visible on the images obtained by SEM, indicating irregular, uneven, and heterogeneous fiber shapes. Fibers with a heterogeneous shape are usually of natural organic origin, such as cotton and wool, while fibers with a smooth structure are of synthetic, typically polymeric, origin [32]. A wide diameter range also indicates presence of different types of fibers in the selected sample [33].

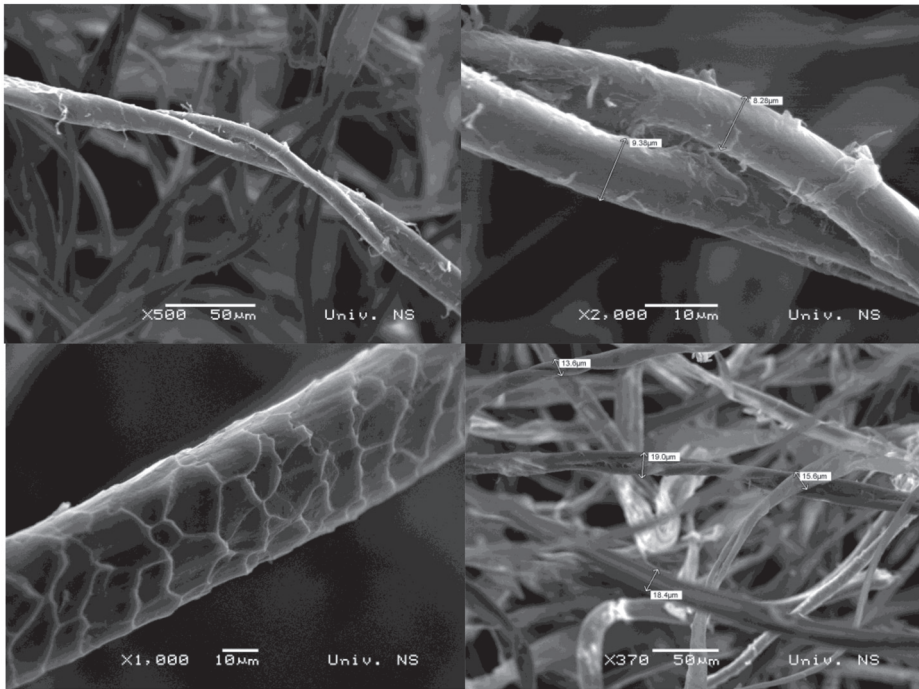


Figure 2. SEM microscopic images of textile fibers.

The SEM results also indicate that there is a wide range of fiber diameters that can enter the water matrix, which means that this is one of the parameters that can affect the efficiency of removal processes, such as coagulation/flocculation [33].

3.2.2. FTIR

To determine the functional groups present in the textile fibers, the FTIR spectra were recorded in the range of $4000\text{--}400\text{ cm}^{-1}$ (Figure 3). Based on the FTIR technical library “Synthetic fibers under the microscope”, 51% of the isolated fiber sample analyzed was identified with rayon. Considering that the specific rayon/viscose peaks are 2917.4 cm^{-1} associated with an aldehyde functional group (C-H , weak bond), 1093.9 cm^{-1} aliphatic amines (C-N stretch, strong bond) and 1017 cm^{-1} alkyl fluoride (C-F stretch, strong bond), it is possible that other types of textile fibers were also part of the selected sample [34].

The main differences between the spectral data of the microscopic library and the obtained spectrum of the synthetic fibers are 1467 , 1198 , and 1155 cm^{-1} in viscose. Moreover, the FTIR spectra of the analyzed isolated sample indicate the presence of a large amount of organic components in the analyzed sample. The presence of organic components, presumably derived from cotton, in the analyzed samples can be confirmed by the specific vibrations at the wavelengths $3250\text{--}4000\text{ cm}^{-1}$, as suggested by Geminiani et al. (2022) [35].

3.2.3. Micro-FTIR

To further improve the characterization of the chemical composition of the textile fibers, additional analyses were performed using micro-FTIR. Furthermore, sample purification was performed according to the methods described in the literature [36–38]. Figures 4 and 5 show representative FTIR spectra and images of textile fibers.

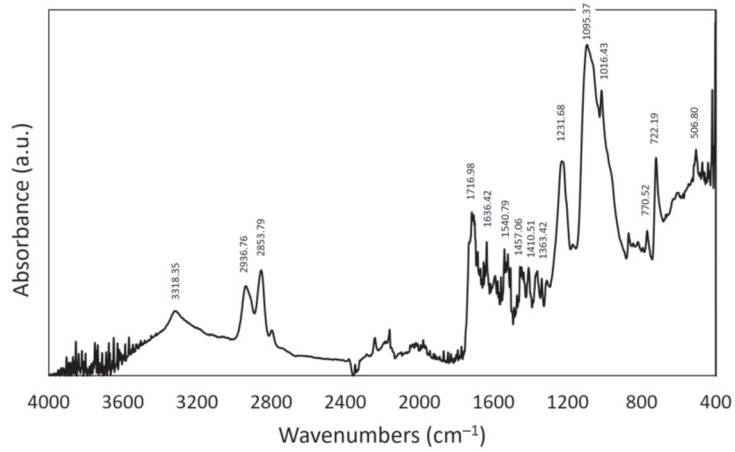


Figure 3. FTIR spectrum of textile fibers.

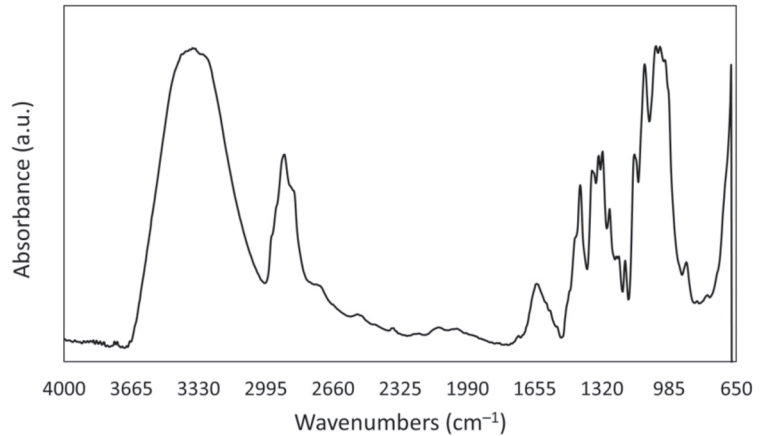


Figure 4. Representative FTIR spectrum of complex textile fibers (a total of 20 randomly selected fibers were analyzed).

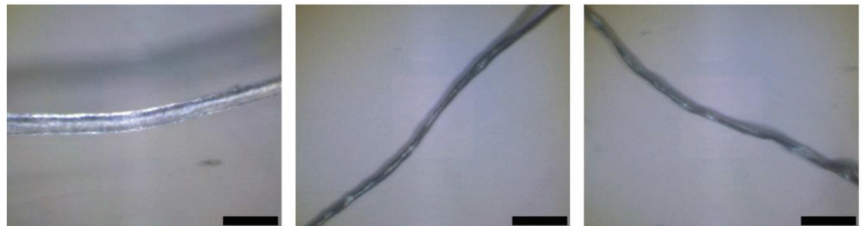


Figure 5. Images of a representative fiber mixture analyzed with an FTIR spectrometer.

The spectrum shown in Figure 4 shows characteristic absorption bands matching to the characteristics of cotton fibers: peak at 3360 cm^{-1} corresponding to intramolecular and intermolecular hydrogen bond (O-H) stretching vibrations; peaks at 2900 cm^{-1} and 2860 cm^{-1} corresponding to asymmetric and symmetric $-\text{CH}_2$ stretching vibrations; peak at 1740 cm^{-1} corresponding to carbonyl group (C=O) stretching vibrations; peak at 1650 cm^{-1} corresponding to O-H bending vibrations of adsorbed water; peak at 1433 cm^{-1}

corresponding to -CH_2 in-plane bending vibrations; peaks at 1370 cm^{-1} , 1339 cm^{-1} , and 1322 cm^{-1} corresponding to C-H bending vibrations, O-H in-plane bending vibrations, and C-H out-of-plane bending vibrations, respectively; peak at 1284 cm^{-1} corresponding to C-H deformation stretching vibrations; peak at 1208 cm^{-1} corresponding to O-H in-plane bending vibrations; peaks at 1160 cm^{-1} and 1109 cm^{-1} corresponding to asymmetrical bridge C-O-C stretching vibrations; peaks at 1054 cm^{-1} , 1034 cm^{-1} , and 1008 cm^{-1} corresponding to C-O stretching vibrations; peak at 905 cm^{-1} corresponding to asymmetric out-of-plane ring stretching vibrations and β -glucoside bond vibrations [39,40]. All 20 fibers analyzed in the sample had the same spectral profile, indicating that natural fibers (cotton) predominate and synthetic fibers are difficult to identify.

Due to the limited ability to distinguish synthetic fibers in the mixture of textile fibers, sample purification and re-characterization was required. The sample was purified with 100 mL of 30% hydrogen peroxide and dried for 24h, after which it was re-characterized (Figures 6 and 7).

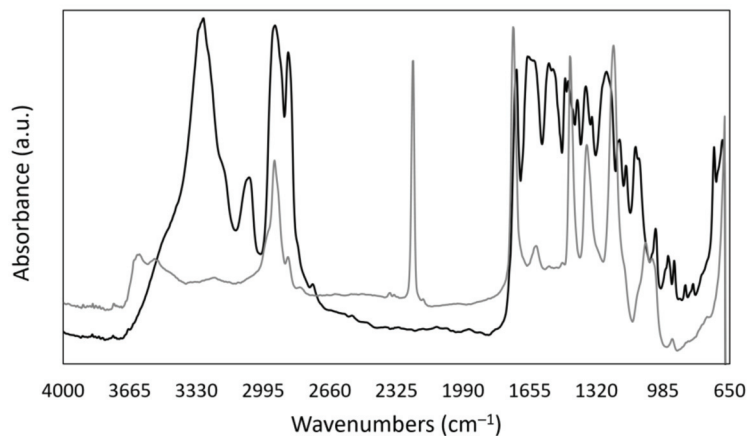


Figure 6. Representative FTIR spectrum of synthetic fibers (black spectrum: polyamide; grey spectrum: polyacrylonitrile). A total of 20 randomly selected fibers from a purified sample were analyzed.

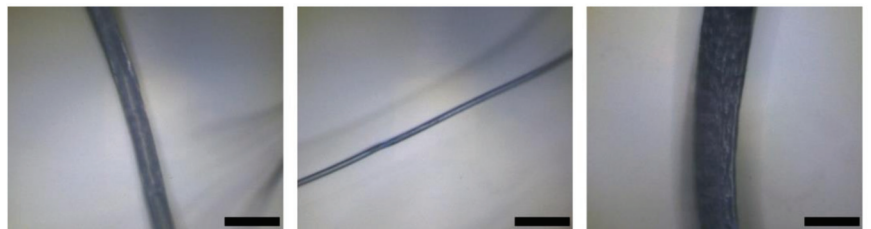


Figure 7. Images of representative synthetic fibers analyzed by FTIR spectrometer.

The black spectrum in Figure 6 shows characteristic absorption bands corresponding to the features of polyamide polymer: peak at 3300 cm^{-1} corresponding to N-H stretching vibrations; peak at 3080 cm^{-1} corresponding to N-H bending vibrations; peaks at 2931 cm^{-1} and 2861 cm^{-1} corresponding to stretching vibrations of methylene groups (-CH_2); peak at 1635 cm^{-1} corresponding to stretching vibrations of carbonyl groups (C=O) (amide I); peak at 1535 cm^{-1} corresponding to N-H bending vibrations and C-N stretching vibrations (amide II); peak at 1370 cm^{-1} corresponding to C-N stretching vibrations; peak at 1141 cm^{-1} corresponding to out of plane bending vibrations of carbonyl (C=O) groups; and peaks at 933 cm^{-1} and 906 cm^{-1} corresponding to N-H stretching vibrations [41–43].

The grey spectrum presented in Figure 7 shows characteristic absorption bands matching the characteristics of the polyacrylonitrile polymer: namely, peaks at 3626 cm^{-1} and 3545 cm^{-1} corresponding to asymmetric and symmetric O-H stretching vibrations, respectively; peaks at 2944 cm^{-1} and 2875 cm^{-1} corresponding to asymmetric and symmetric $-\text{CH}_2$ stretching vibrations; peak at 2245 cm^{-1} correlating with $\text{C}\equiv\text{N}$ stretching vibrations; peaks at 1740 cm^{-1} and 1630 cm^{-1} corresponding to $\text{C}=\text{O}$ stretching vibrations (attributed to a small amount of vinyl acetate monomers in the polyacrylonitrile structure); peaks at 1458 cm^{-1} and 1375 cm^{-1} corresponding to $-\text{CH}_2$ and C-H bending vibrations; peak at 1240 cm^{-1} corresponding to C-O stretching vibrations (vinyl acetate); and peak at 1074 cm^{-1} corresponding to $-\text{CH}_2$ stretching vibrations [44,45].

Of the 20 randomly analyzed fibers in purified textile fibers, the spectra match corresponded to about 20% polyamide and about 80% polyacrylonitrile, reflecting the composition of the original synthetic compounds. A fiber with a high match to polyester was also discovered. This type of fiber is one of the most frequently documented sources of microplastic contamination in textiles, which consist of about 60% synthetic fibers [46].

3.3. Effects of Coagulation on Textile Fibers Removal Efficiency

To evaluate the efficiency of coagulation/flocculation for removing complex textile fiber mixtures from water, different dosages of coagulants were tested. The optimal dosage for the selected coagulants was determined by comparing the removal efficiency.

Figure 8 and Table S2 show the removal efficiency as a function of coagulant concentration in the synthetic matrix.

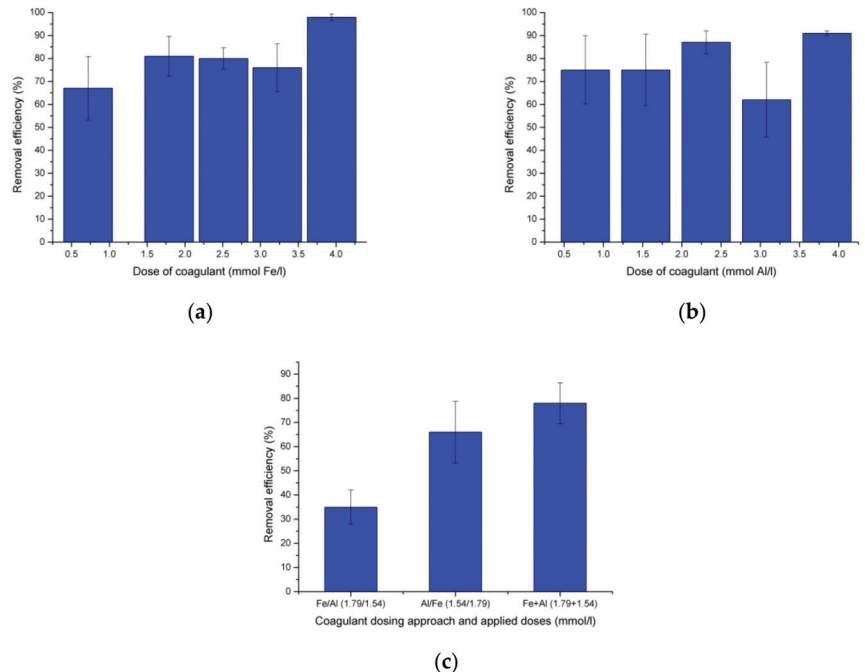


Figure 8. Efficiency of removal of textile fibers from a synthetic matrix by coagulation with (a) FeCl_3 , (b) PACl, and (c) a combination of FeCl_3 and PACl (error bars show standard deviation of duplicates).

From the results shown in Figure 8, coagulation and flocculation with the application of FeCl_3 in the synthetic matrix 67–99% removal of textile fibers can be achieved, compared to the initial concentration. The highest removal efficiency was achieved at a FeCl_3 concentration of 3.94 mM, while the lowest was at a FeCl_3 concentration of 0.72 mM. It can be observed that all applied doses showed similar values for removal efficiency, except for the highest dose, indicating a complete removal. The use of PACl as a coagulant allowed a slightly lower removal efficiency with values in the range of 57–91% compared to coagulation with FeCl_3 . The removal efficiencies for the combination of coagulants in this treatment were 35%, 66%, and 78% for Fe/Al, Al/Fe, and Fe+Al dosages, respectively. These values indicate that the combination of coagulants has no effect on improving the removal efficiency of textile fibers compared to single coagulants.

In the results obtained with both coagulants, it can be noted that when a dose of 3.22 mM is applied, the efficiency of coagulation begins to decrease significantly. This can be explained by the fact that the micro flakes of the coagulant tend to loosen and break when a large amount of coagulant is used, reducing the performance of the process, which was also confirmed by Zhou et al. 2021 [25].

Figure 9 and Table S2 show the efficiency of the removal of textile fibers from surface water using two separate coagulants and their combination.

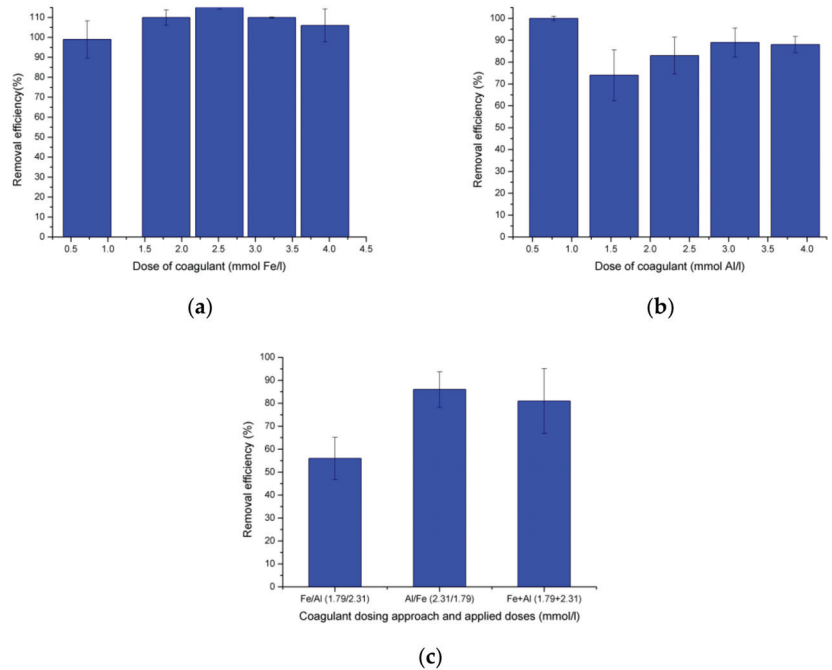


Figure 9. Efficiency of the removal of textile fibers from a surface water by coagulation with (a) FeCl_3 , (b) PACl, and (c) a combination of FeCl_3 and PACl (error bars show standard deviation of duplicates).

Removal of textile fibers from surface water with FeCl_3 proved to be effective, as shown by the values in the plot (Figure 9a). All dosages had approximately similar high values, with the coagulant resulting in complete removal. Coagulation with FeCl_3 resulted in additional precipitation of particles from the water, as in this case the calculated amounts of material removed were higher than the amounts of textile fibers added to the matrix. The removal of textile fibers with PACl also proved to be an effective treatment, as shown by the values of more than 74% compared to the initial concentrations. The combination of FeCl_3 and PACl did not significantly improve the removal of textile fibers compared to the use of

the individual coagulants. The removal values for the combination of these two coagulants were 56%, 86%, and 81% for the dosages of Fe/Al, Al/Fe, and Fe+Al, respectively. For both the two coagulants used and their combination, the removal efficiency of textile fibers is higher than that of the synthetic matrix (Figure 8). It can be assumed that the natural organic matrix and the HCO_3^- present in natural water contribute to a higher removal efficiency compared to the results obtained in synthetic matrix, which is also pointed out by other authors [25].

Coagulation and flocculation treatment of laundry wastewater required higher dosages of coagulants compared to synthetic matrix and surface water due to the presence of surfactants in the water (Table 1). Lower dosages were also investigated, but since no precipitation occurred, the results are not presented. The coagulation/flocculation efficiency of textile fibers in wastewater treatment is shown in Figure 10 and Table S3.

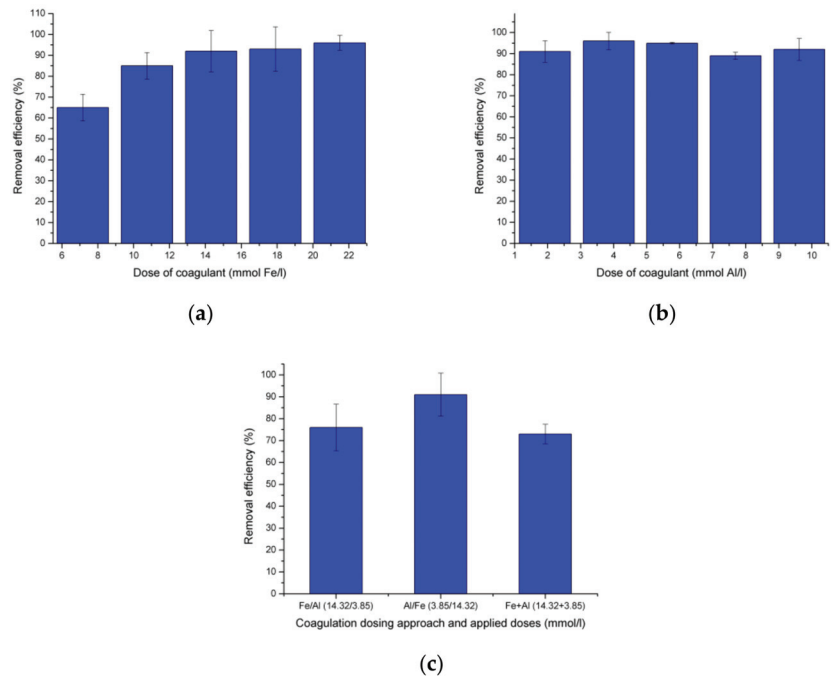


Figure 10. Efficiency of removal of textile fibers from a laundry wastewater by coagulation with (a) FeCl_3 , (b) PACl, and (c) a combination of FeCl_3 and PACl (error bars show standard deviation of duplicates).

The results presented in Figure 10 show that as the FeCl_3 dosage increases, the removal efficiency also increases, with the highest applied doses completely removing the textile fibers from the wastewater. Doses higher than 9.62 mM were also used, but were not found to be effective. This can be explained by the fact that at a high coagulant dosage, saturation occurs where the particles no longer form flocs and therefore sink to the bottom along with the textile fibers [18].

PACl was also shown to be an effective coagulant in the removal of textile fibers from laundry effluents, as evidenced by the fact that the lowest removal efficiency was as high as 89% compared to initial values. All coagulant concentrations achieved similar removal efficiencies. When both coagulants were used in combination, the values were found to be slightly lower, but still considered effective for the removal of textile fibers.

The lower removal rates obtained in laundry wastewater compared to those in surface water can be explained by the presence of surfactants in this mixture. This is in agreement

with the results of Li et al. (2022) [47], who demonstrated a low efficiency of FeCl_3 in removing MPFs from surfactant-rich laundry wastewater. Moreover, these studies indicated the lower effect of surfactants on PACl performance during coagulation compared to FeCl_3 , which is also confirmed by our results (Figure 10b).

Using a combination of coagulants, for both surfaces and wastewater, the best combination was when PACl was added first followed by FeCl_3 , with removal rates of 86% for surfaces and 91% for wastewater. For the synthetic matrix, the best result was obtained with the simultaneous addition of both coagulants, with a removal rate of 78% compared to the initial concentration.

According to the literature data, the removal efficiency depends on the type of material to be removed, i.e., its properties. From the literature data [25,48], it can be concluded that microplastics, such as polyethylene, polystyrene, and polypropylene are removed more efficiently by using PACl in deionized water and drinking water, while the results of this study show a better removal rate when FeCl_3 was applied in similar water matrices. Moreover, according to the literature [24,49–51], it is clear that the effectiveness of the coagulant also depends on the characteristics of the water matrix, which was also confirmed by this work, as much higher coagulant dosages were required to effectively remove textile fibers from laundry wastewater compared to surface water and synthetic matrix. The type and dosage of coagulant is another factor affecting the treatment efficiency, where PACl was more effective on laundry wastewater, while Fe-based coagulants were more effective at removing textile fibers from synthetic matrix and surface water. Therefore, future studies should focus on optimizing the coagulation–flocculation treatment (e.g., by adding activated carbon) to reduce the coagulant dose required for efficient treatment and better removal of textile fibers from water.

4. Conclusions

As a contribution to a better understanding of the behavior of this type of pollution in wastewater treatment, the coagulation/flocculation treatment of different types of water containing a complex mixture of textile fibers was studied. It was found that a mixture of textile fibers containing natural and synthetic microfibers can be effectively removed from different water matrices with different compositions by using FeCl_3 and PACl as coagulants and their combination under near neutral pH conditions. The results show that high dosages of coagulants (>0.7 mmol/L for synthetic and surface waters; >7 mmol Fe/L and >1.9 mmol Al/L for laundry wastewater) are required to achieve efficient removal of textile fibers. Natural organic matter enhance textile fiber removal during coagulation/flocculation treatment. The highest removal efficiency of both coagulants was demonstrated in surface water, where complete removal was achieved by the application of FeCl_3 and almost complete removal was achieved by the application of PACl. Surfactants can reduce the efficiency of coagulation/flocculation in removing textile fibers from water when FeCl_3 is used as a coagulant, while the efficiency of PACl is actually increased. Natural fibers make it difficult to identify synthetic fibers in the mixture, which can lead to an underestimation of the amount present in the water, and thus the treatment efficiency.

Supplementary Materials: The following supporting information can be downloaded at: <https://www.mdpi.com/article/10.3390/pr11030820/s1>, Table S1: Doses of coagulants used in experiments; Table S2: Concentration of textile fibers in synthetic water after coagulation/flocculation; Table S3: Concentration of textile fibers in surface water after coagulation/flocculation; Table S4: Concentration of textile fibers in laundry wastewater after coagulation/flocculation.

Author Contributions: Conceptualization, J.A.; methodology, M.V., J.A., S.F., A.T.; formal analysis, S.F., R.T.; investigation, S.V., M.V., S.F., S.D.; resources, J.A.; data curation, S.V., R.T.; writing—original draft preparation, S.V.; writing—review and editing, M.V., J.A., S.F., S.D., A.T.; visualization, S.V., S.D.; supervision, A.T.; project administration, A.T. All authors have read and agreed to the published version of the manuscript.

Funding: Provincial Secretariat for Higher Education and Scientific Research: 142-451-3182/2022-01/2; European Cooperation in Science and Technology: CA20101.

Data Availability Statement: The data presented in this study are available on request from the corresponding author.

Acknowledgments: The authors gratefully acknowledge the support of the Provincial Secretariat for Higher Education and Scientific Research (Project No. 142-451-3182/2022-01/2). This article is based upon work from COST Action Plastics monitoRIng detectiOn RemediaTion recovery—PRIORITY, CA20101, supported by COST (European Cooperation in Science and Technology).

Conflicts of Interest: The authors declare no conflict of interest.

References

1. Radhakrishnan, S. 2—Sustainable cotton production. In *Sustainable Fibres and Textiles*; Woodhead Publishing: Coimbatore, India, 2017; pp. 21–67.
2. Krifa, M.; Stewart, S.S. Cotton utilization in conventional and non-conventional textiles—A statistical review. *Agric. Sci.* **2016**, *7*, 747–758. [CrossRef]
3. L'Abbate, P.; Dassisti, M.; Cappelletti, G.M.; Nicoletti, G.M.; Russo, C.; Ioppolo, G. Environmental analysis of polyester fabric for ticking. *J. Clean. Prod.* **2018**, *172*, 735–742. [CrossRef]
4. Napper, I.E.; Parker-Jurd, F.N.F.; Wright, S.L.; Thompson, R.C. Examining the release of synthetic microfibres to the environment via two major pathways: Atmospheric deposition and treated wastewater effluent. *Sci. Total Environ.* **2023**, *857*, 159317. [CrossRef]
5. Zambrano, M.C.; Pawlak, J.J.; Daystar, J.; Ankeny, M.; Venditti, R.A. Impact of dyes and finishes on the aquatic biodegradability of cotton textile fibers and microfibers released on laundering clothes: Correlations between enzyme adsorption and activity and biodegradation rates. *Mar. Pollut. Bull.* **2021**, *165*, 112030. [CrossRef]
6. Pedrotti, M.L.; Petit, S.; Eyheraguibel, B.; Kerros, M.E.; Elineau, A.; Ghiglione, J.F. Pollution by anthropogenic microfibers in North-West Mediterranean Sea and efficiency of microfiber removal by a wastewater treatment plant. *Sci. Total Environ.* **2021**, *758*, 144195. [CrossRef] [PubMed]
7. Li, Y.; Lu, Q.; Xing, Y.; Liu, K.; Ling, W.; Yang, J.; Yang, Q.; Wu, T.; Zhang, J.; Pei, Z.; et al. Review of research on migration, distribution, biological effects, and analytical methods of microfibers in the environment. *Sci. Total Environ.* **2023**, *855*, 158922. [CrossRef] [PubMed]
8. De Falco, F.; Gullo, M.P.; Gentile, G.; Di Pace, E.; Cocca, M.; Gelabert, L.; Brouta-Agnésa, M.; Rovira, A.; Escudero, R.; Villalba, R.; et al. Evaluation of microplastic release caused by textile washing processes of synthetic fabrics. *Environ. Pollut.* **2018**, *236*, 916–925. [CrossRef] [PubMed]
9. Leslie, H.A.; Brandsma, S.H.; van Velzen, M.J.M.; Vethaak, A.D. Microplastics en route: Field measurements in the dutch river delta and Amsterdam canals, wastewater treatment plants, North Sea sediments and biota. *Environ. Int.* **2017**, *101*, 133–142. [CrossRef]
10. Gies, E.A.; LeNoble, J.L.; Noël, M.; Etemadifar, A.; Bishay, F.; Hall, E.R.; Ross, P.S. Retention of microplastics in a major secondary wastewater treatment plant in Vancouver, Canada. *Mar. Pollut. Bull.* **2018**, *133*, 553–561. [CrossRef]
11. Gündoğdu, S.; Çevik, C.; Güzel, E.; Kilercioğlu, S. Microplastics in municipal wastewater treatment plants in Turkey: A comparison of the influent and secondary effluent concentrations. *Environ. Monit. Assess.* **2018**, *190*, 626. [CrossRef]
12. Napper, I.E.; Thompson, R.C. Release of synthetic microplastic plastic fibres from domestic washing machines: Effects of fabric type and washing conditions. *Mar. Pollut. Bull.* **2016**, *112*, 39–45. [CrossRef]
13. Mintenig, S.M.; Int-Veen, I.; Löder, M.G.J.; Primpke, S.; Gerdts, G. Identification of microplastic in effluents of waste water treatment plants using focal plane arraybased micro-fourier-transform infrared imaging. *Water Res.* **2017**, *108*, 365–372. [CrossRef] [PubMed]
14. Franco, A.A.; Arellano, J.M.; Albendín, G.; Rodríguez-Barroso, R.; Quiroga, J.M.; Coello, M.D. Microplastic pollution in wastewater treatment plants in the city of c'adiz: Abundance, removal efficiency and presence in receiving water body. *Sci. Total Environ.* **2021**, *776*, 145795. [CrossRef]
15. Tian, W.; Song, P.; Zhang, H.; Duan, X.; Wei, Y.; Wang, H.; Wang, S. Microplastic materials in the environment: Problem and strategical solutions. *Prog. Mater. Sci.* **2023**, *132*, 101035. [CrossRef]
16. Pivokonský, M.; Pivokonská, L.; Novotná, K.; Čermáková, L.; Klimtová, M. Occurrence and fate of microplastics at two different drinking water treatment plants within a river catchment. *Sci. Total Environ.* **2020**, *741*, 140236. [CrossRef]
17. Xue, J.; Peldszus, S.; Van Dyke, M.I.; Huck, P. Removal of polystyrene microplastic spheres by alum-based coagulation-flocculation-sedimentation (CFS) treatment of surface waters. *J. Chem. Eng.* **2021**, *422*, 130023. [CrossRef]
18. Pivokonsky, M.; Novotna, K.; Čermakova, L.; Petriček, R. *Jar Tests for Water Treatment Optimisation, How to Perform Jar Tests—A handbook*; IWA Publishing: London, UK, 2022.
19. Li, J.; Green, C.; Reynolds, A.; Shi, H.; Rotchell, J.M. Microplastics in mussels sampled from coastal waters and supermarkets in the United Kingdom. *Environ. Pollut.* **2018**, *241*, 35–44. [CrossRef]

20. Xia, Y.; Xiang, X.M.; Dong, K.Y.; Gong, Y.Y.; Li, Z.J. Surfactant stealth effect of microplastics in traditional coagulation process observed via 3-D fluorescence imaging. *Sci. Total Environ.* **2020**, *729*, 138783. [CrossRef]
21. Belzagui, F.; Crespi, M.; Álvarez, A.; Gutiérrez-Bouzán, C.; Vilaseca, M. Microplastics' emissions: Microfibers' detachment from textile garments. *Environ. Pollut.* **2019**, *248*, 1028–1035. [CrossRef] [PubMed]
22. Cesa, F.S.; Turra, A.; Checon, H.H.; Leonardi, B.; Baruche-Ramos, J. Laundering and textile parameters influence fibers release in household washings. *Environ. Pollut.* **2020**, *257*, 113553. [CrossRef]
23. Ma, B.; Xue, W.; Ding, Y.; Hu, C.; Liu, H. Removal characteristics of microplastics by Fe-based coagulants during drinking water treatment. *J. Environ. Sci.* **2019**, *78*, 267–275. [CrossRef]
24. Skaf, D.W.; Punzi, V.L.; Rolle, J.T.; Kleinberg, K.A. Removal of micron-sized microplastic particles from simulated drinking water via alum coagulation. *J. Chem. Eng.* **2019**, *386*, 123807. [CrossRef]
25. Zhou, G.; Wang, Q.; Li, J.; Li, Q.; Xu, H.; Ye, Q.; Wang, Y.; Shu, S.; Zhang, J. Removal of polystyrene and polyethylene microplastics using PAC and FeCl₃ coagulation: Performance and mechanism. *Sci. Total Environ.* **2021**, *752*, 141837. [CrossRef] [PubMed]
26. Tang, W.; Li, H.; Fei, L.; Wei, B.; Zhou, T.; Zhang, H. The removal of microplastics from water by coagulation: A comprehensive review. *Sci. Total Environ.* **2022**, *851*, 158224. [CrossRef] [PubMed]
27. SRPS ISO 6060:1994; Water Quality—Determination of Chemical Consumption of Oxygen. Institute for Standardization of Serbia: Belgrade, Serbia, 1994.
28. SRPS ISO 9297-1:2007; Water Quality—Determination of Chloride Content—Silver-Nitrate Titration with Chromate Indicator (Mor's Method). Institute for Standardization of Serbia: Belgrade, Serbia, 2007.
29. APHA-AWWA-WEF. *Standard Methods for the Examination of Water and Waste Water*, 23th ed.; Eaton, A.D., Clesceri, L.S., Greenberg, A.E., Eds.; American Public Health Association: Washington, DC, USA, 2017.
30. EPA 7000 B:2007; Flame Atomic Absorption Spectrophotometry. Institute for Standardization of Serbia: Belgrade, Serbia, 2007.
31. EPA 3015 A:2007; Microwave Assisted Acid Digestion of Aqueous Samples and Extracts. Institute for Standardization of Serbia: Belgrade, Serbia, 2007.
32. Dalla Fontana, G.; Mossotti, R.; Montarsolo, A. Assessment of microplastics release from polyester fabrics: The impact of different washing conditions. *Environ. Pollut.* **2020**, *264*, 113960. [CrossRef]
33. Dalla Fontana, G.; Mossotti, R.; Montarsolo, A. Influence of sewing on microplastic release from textiles during washing. *Water Air Soil Pollut.* **2021**, *232*, 50. [CrossRef]
34. Mishra, S.; Dash, D.; Prasad Das, A. Detection, characterization and possible biofragmentation of synthetic microfibers released from domestic laundering wastewater as an emerging source of marine pollution. *Mar. Pollut. Bull.* **2022**, *185*, 114254. [CrossRef]
35. Geminiani, L.; Campione, F.P.; Corti, C.; Luraschi, M.; Motella, S.; Recchia, S.; Rampazzi, L. Differentiating between Natural and Modified Cellulosic Fibres Using ATR-FTIR Spectroscopy. *Heritage* **2022**, *5*, 4114–4139. [CrossRef]
36. Nuelle, M.T.; Dekiff, J.H.; Remy, D.; Fries, E. A new analytical approach for monitoring microplastics in marine sediments. *Environ. Pollut.* **2014**, *184*, 161–169. [CrossRef]
37. Napper, I.E.; Bakir, A.; Rowland, S.J.; Thompson, R.C. Characterisation, quantity and sorptive properties of microplastics extracted from cosmetics. *Mar. Pollut. Bull.* **2015**, *99*, 178–185. [CrossRef]
38. Monteiro, S.S.; Rocha-Santos, T.; Prata, J.C.; Duarte, A.C.; Girão, A.V.; Lopes, P.; Cristovão, T.; Pinto Da Costa, J. A straightforward method for microplastic extraction from organic-rich freshwater samples. *Sci. Total Environ.* **2022**, *815*, 152941. [CrossRef] [PubMed]
39. Chung, C.; Lee, M.; Choe, E.K. Characterization of cotton fabric scouring by FT-IR ATR spectroscopy. *Carbohydr. Polym.* **2004**, *58*, 417–420. [CrossRef]
40. Abidi, N.; Cabrales, L.; Haigler, C.H. Changes in the cell wall and cellulose content of developing cotton fibers investigated by FTIR spectroscopy. *Carbohydr. Polym.* **2014**, *100*, 9–16. [CrossRef] [PubMed]
41. Vasanthan, N.; Salem, D.R. Infrared Spectroscopic Characterization of Oriented Polyamide 66: Band Assignment and Crystallinity Measurement. *J. Polym. Sci. B Polym. Phys.* **2000**, *38*, 516–524. [CrossRef]
42. Sengupta, R.; Tikku, V.K.; Somani, A.K.; Chaki, T.K.; Bhowmick, A.K. Electron beam irradiated polyamide-6,6 films—I: Characterization by wide angle X-ray scattering and infrared spectroscopy. *Radiat. Phys. Chem.* **2005**, *72*, 625–633. [CrossRef]
43. Navarro-Pardo, F.; Martínez-Barrera, G.; Martínez-Hernández, A.; Castaño, V.; Rivera-Armenta, J.; Medellín-Rodríguez, F.; Velasco-Santos, C. Effects on the Thermo-Mechanical and Crystallinity Properties of Nylon 6,6 Electrospun Fibres Reinforced with One Dimensional (1D) and Two Dimensional (2D) Carbon. *Materials* **2013**, *6*, 3494–3513. [CrossRef]
44. Tadokoro, H.; Murahashi, S.; Yamadera, R.; Kamei, T.-I. Infrared absorption spectra of polyacrylonitrile and deuterated polyacrylonitriles. *J. Polym. Sci. A Gen. Pap.* **1963**, *1*, 3029–3042. [CrossRef]
45. Karacan, I.; Erdogan, G. The influence of thermal stabilization stage on the molecular structure of polyacrylonitrile fibers prior to the carbonization stage. *Fibers Polym.* **2012**, *13*, 295–302. [CrossRef]
46. Barrows, A.P.W.; Cathey, S.E.; Petersen, C.W. Marine environment microfiber contamination: Global patterns and the diversity of microplastic origins. *Environ. Pollut.* **2018**, *237*, 275–284. [CrossRef] [PubMed]
47. Li, J.; Dagniew, M.; Ray, M.B. Effect of coagulation on microfibers in laundry wastewater. *Environ. Res.* **2022**, *212*, 113401. [CrossRef]

48. Tabatabaei, F.; Mafigholami, R.; Moghimi, H.; Khoramipoor, S. Effect of Fe and Al based coagulants and disinfectants on polyethylene microplastics removal in coagulation process through response surface methodology. *Water Sci. Technol.* **2022**, *87*, 99–114. [CrossRef]
49. Lapointe, M.; Farner, J.M.; Hernandez, L.M.; Tufenkji, N. Understanding and improving microplastic removal during water treatment: Impact of coagulation and flocculation. *Environ. Sci. Technol.* **2020**, *54*, 8719–8727. [CrossRef] [PubMed]
50. Cherniak, S.L.; Almuhtaram, H.; McKie, M.J.; Hermabessiere, L.; Yuan, C.; Rochman, C.M.; Andrews, R.C. Conventional and biological treatment for the removal of microplastics from drinking water. *Chemosphere* **2022**, *288*, 132587. [CrossRef] [PubMed]
51. Wang, Z.; Lin, T.; Chen, W. Occurrence and removal of microplastics in an advanced drinking water treatment plant (ADWTP). *Sci. Total Environ.* **2020**, *700*, 134520. [CrossRef] [PubMed]

Disclaimer/Publisher’s Note: The statements, opinions and data contained in all publications are solely those of the individual author(s) and contributor(s) and not of MDPI and/or the editor(s). MDPI and/or the editor(s) disclaim responsibility for any injury to people or property resulting from any ideas, methods, instructions or products referred to in the content.

MDPI AG
Grosspeteranlage 5
4052 Basel
Switzerland
Tel.: +41 61 683 77 34

MDPI Books Editorial Office
E-mail: books@mdpi.com
www.mdpi.com/books



Disclaimer/Publisher's Note: The statements, opinions and data contained in all publications are solely those of the individual author(s) and contributor(s) and not of MDPI and/or the editor(s). MDPI and/or the editor(s) disclaim responsibility for any injury to people or property resulting from any ideas, methods, instructions or products referred to in the content.



Academic Open
Access Publishing

[mdpi.com](https://www.mdpi.com)

ISBN 978-3-7258-2200-3